AD-A047 161 NONCONTACT NONDESTRUCTIVE DETERMINATION OF PAVEMENT DEFLECTION UNDER MOVING LOADS(U) PURDUE RESEARCH FOUNDATION LAFAYETTE IN M E HARR ET AL. AUG 77 1/4

UNCLASSIFIED FAA-RD-77-127 DOT-FA73WAI-361 F/G 13/2 NL

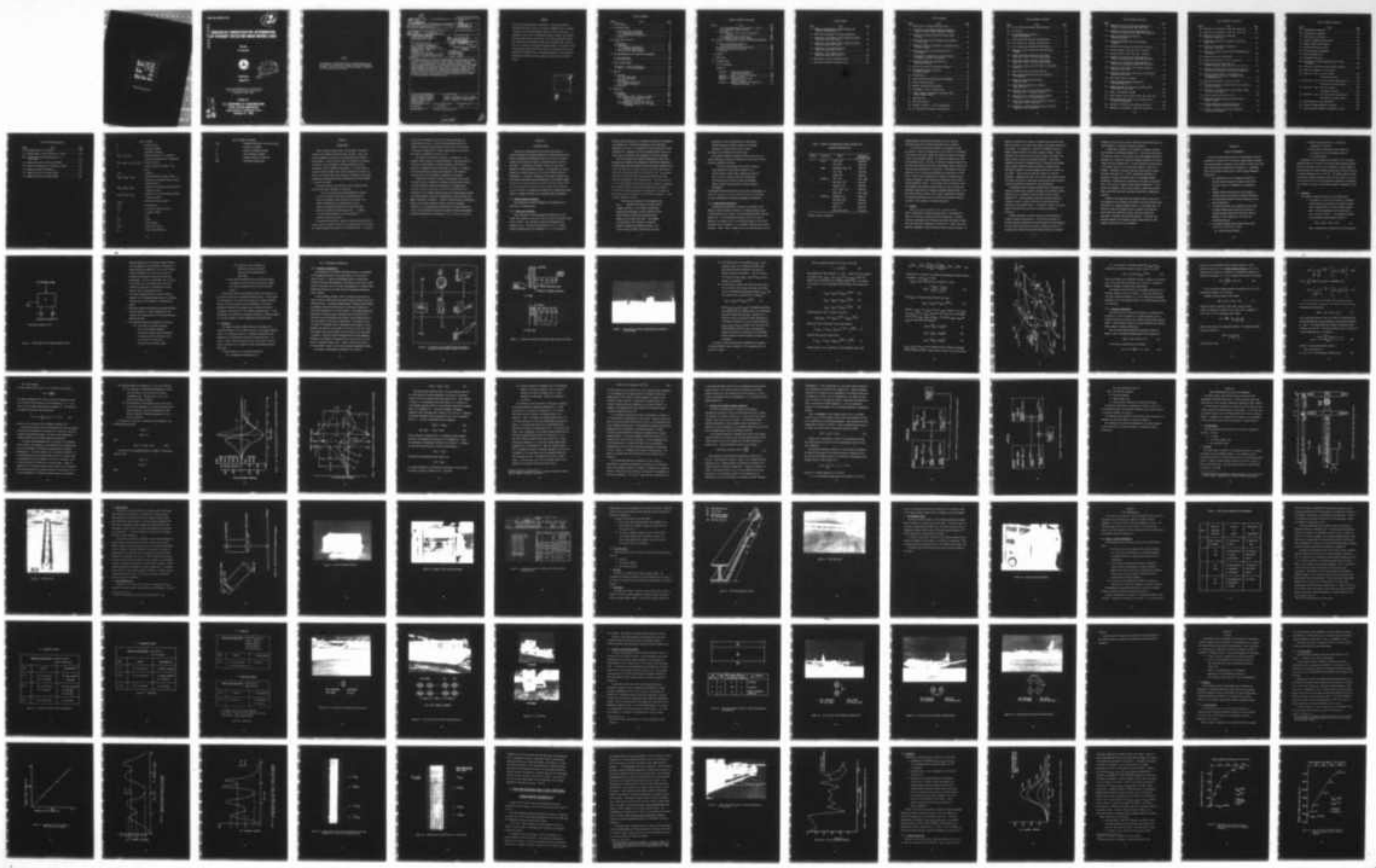

MICROCOPY RESOLUTION TEST CHART
NATIONAL BUREAU OF STANDARDS-1963-A

Report No. FAA-RD-77-127

12

AD A047161

NONCONTACT NONDESTRUCTIVE DETERMINATION OF PAVEMENT DEFLECTION UNDER MOVING LOADS

M.E. Harr

N.T. Ng-A-Qui

DDC
RECEIVED
NOV 28 1977
F

Final Report

August 1977

Document is available to the U.S. public through
the National Technical Information Service,
Springfield, Virginia 22161.

Prepared for

U.S. DEPARTMENT OF TRANSPORTATION
FEDERAL AVIATION ADMINISTRATION
Systems Research & Development Service
Washington, D.C. 20590

AD No.
DDC FILE COPY

NOTICE

This document is disseminated under the sponsorship of the Department of Transportation in the interest of information exchange. The United States Government assumes no liability for its contents or use thereof.

19

Technical Report Documentation Page

1. Report No.	2. Government Accession No.	3. Recipient's Catalog No.
18 FAA-RD-77-127		11

4. Title and Subtitle	5. Report Date
6 Noncontact Nondestructive Determination of Pavement Deflection Under Moving Loads	August 1977
	6. Performing Organization Code
7. Author(s) 10 M. E. Harr N. T. Ng-A-Qui	8. Performing Organization Report No.
9. Performing Organization Name and Address: Purdue Research Foundation, Division of Sponsored Research, West Lafayette, IN 47907	10. Work Unit No. (TRAIS)
	11. Contract or Grant No. 15 DOT-FA73WAI-361
12. Sponsoring Agency Name and Address: U. S. Department of Transportation, Federal Aviation Administration, Systems Research and Development Service, Washington, D.C. 20590	13. Type of Report and Period Covered: 9 Final Report, Dec 1974 - Dec 1976
	14. Sponsoring Agency Code: ARD-430

15. Supplementary Notes

Department of the Air Force
Air Force Civil Engineering Center (AFSC)
Tyndall Air Force Base, Florida 32403

12 327p.

16. Abstract

This report presents a procedure for nondestructively evaluating and predicting the deflection response of various flexible pavements to loads imposed by different aircraft. Transfer function theory is used to form the basis of a pavement evaluation and response scheme. Two mobile systems were developed for the measurement of pavement deflections; the Light Emitting Diode (LED) system and the Linear Variable Differential Transformer (LVDT) system. The report concludes that the rapid nondestructive measurement of pavement deflections due to moving prototype loads is feasible and that a total nondestructive evaluation scheme based entirely on the use of prototype loads and measured deflections can be fabricated to evaluate and predict instantaneous response and cumulative effects of loads of various magnitudes and configurations.

17. Key Words	18. Distribution Statement
Civil engineering Airfield pavement performance Airfield pavement evaluation Pavement deflection response Transfer function theory Energy concepts	Document is available to the U.S. public through the National Technical Information Service, Springfield, Virginia 22161.

19. Security Classif. (of this report)	20. Security Classif. (of this page)	21. No. of Pages	22. Price
unclassified	unclassified	327	

Form DOT F 1700.7 (8-72) Reproduction of completed page authorized

390 985

1B

PREFACE

This work was conducted under sponsorship of the Federal Aviation Administration (FAA) as part of the runway roughness study to determine the effect of the loaded pavement profile on aircraft operations. An outgrowth of this study is a noncontact system to measure the pavement deflection basin under a moving load. This report describes the hardware developed and associated transfer function theory which forms the basis for a pavement evaluation and response scheme. (The effect of the loaded pavement profile will be the subject of a separate report to be published in September 1977.) Continued development of the noncontact system reported herein is being sponsored by the FAA under separate contract.

ACCESSION for
NTIS White Section
DDC Buff Section
UNANNOUNCED
JUSTIFICATION
BY
DISTRIBUTION/AVAILABILITY CODES
SPECIAL
A

TABLE OF CONTENTS

TABLE OF CONTENTS (Continued)

LIST OF TABLES

LIST OF FIGURES

LIST OF FIGURES (Continued)

LIST OF FIGURES (Continued)

LIST OF FIGURES (Continued)

LIST OF FIGURES (Continued)

LIST OF FIGURES (Concluded)

LIST OF SYMBOLS

m	- equivalent mass
c	- equivalent damping
k	- equivalent stiffness
$z(t)$, $\dot{z}(t)$, $\ddot{z}(t)$	- pavement deflection (or signature), velocity and acceleration, respectively
$F(t)$, $F_{sn}(t)$, $F_x(t)$, $F_{ln}(t)$	- loading function
x	- lateral distance from edge of tire print
$A(t)$	- signature
A'_{peak}, A''_{peak}, A_{peak}	- maximum deflection at edge of wheel, parameter of the maximum lateral dynamic deflection basin
β'_{peak}, β''_{peak}, β_{peak}	- parameter of the maximum lateral dynamic deflection profile
r'_{peak}, r''_{peak}, r_{peak}	- parameter of the maximum lateral dynamic deflection profile
z_{max_j}	- maximum deflection at gage j
$I(t)$	- modified input
$G(t)$	- the reduced transfer function
s	- a complex variable
t	- time
$O(t)$	- output
ΔT	- time increment
$EF(t)$	- equivalency function
T_p	- time to peak deflection

LIST OF SYMBOLS (Concluded)

$W(X)$	- subgrade deflection at x from tire print
p	- pressure on subgrade
$\bar{k}$	- modulus of subgrade reaction
CH	- shear stiffness parameter
E_s	- subgrade modulus of elasticity
CBR	- California Bearing Ratio

SECTION I

INTRODUCTION

Today, personnel concerned with the evaluation of airfield pavements are confronted with three major problems. First, many primary pavements are old and/or are approaching early stages of deterioration. Second, the gross weight of aircraft is increasing continually, thus the demands on airfield pavements are also increasing. Third, procedures (References 1, 2, 3 and 4) used to evaluate airfield pavements are; either, destructive in nature, or, apply to only small areas of the pavement: in addition, they require considerable performance time and are therefore costly with respect to the flow of traffic.

The problem faced by the Air Force in this context has been stated by one author (Reference 5) who wrote,

> "The Air Force alone owns enough pavement to be able to provide a 200-foot wide runway stretching from the state of Washington to the Southern tip of Florida. The problem of maintenance and rehabilitation of this inventory becomes more complex and critical each year. Most of the systems are over 20 years old . . . coupled with these aging pavements is the rapid growth of aircraft traffic and weights."

The need exists today for a method of pavement evaluation which would be able to quantify the stage of the aging process of a pavement and provide guidance with respect to its rehabilitation. It should be

able to do so considering the action of varying magnitudes and configurations of loads, and under varying ambient conditions. Ideally, it should be nondestructive, rapid, permit the evaluation of the entire pavement with a minimum interruption to air traffic, and should be inexpensive and easy to use.

The problem of evaluating a pavement is a complex one. The pavement section consists of various materials. These materials are far from the ideal models of classical mechanics; and they vary diurnally, seasonally and with repetitions of loading. In addition, both vehicular and non-vehicular loads applied to the pavement-subgrade system vary in magnitude, intensity, and frequency.

Recognizing the nature and scope of the problem, and the need that exists today to overcome it, research activities were initiated at Purdue University toward the development of a nondestructive pavement evaluation capability to account for the complexity and variability of the pavement-subgrade system, and simultaneously satisfy the demands imposed by practical considerations; such as mobility and ease of operation of equipment. Research in this endeavor is predicated on the use of transfer function theory as the key to pavement evaluation. This methodology has evolved over a 15 year period from concept, through theory and laboratory studies to field investigations using fixed installations (References 6, 7, 8, 9, 10, 11, 12 and 13).

SECTION II

LITERATURE REVIEW

The need for improving methods and developing theories to quantify adequately the complex mechanism of pavement-subgrade interaction has generated considerable activity in the area of pavement analysis and evaluation in general, and nondestructive testing in particular. In evaluation procedures, efforts are being made to eliminate or reduce destructive testing. In nondestructive testing emphasis is currently being put on the use of surface deflection measurements. In analysis, attempts are being made to deviate from the classical approaches and use probabilistic and stochastic models. Because in the recently published literature several excellent state of the art papers and literature reviews already exist (References 14, 15, 16 and 17), no attempt will be made here to repeat these works, however, a synoptic overview of the principal works is presented.

2.1 Airfield Pavement Evaluation

The evaluation of airfield pavements can be categorized as destructive or nondestructive.

2.1.1 Destructive Evaluation

These procedures, as the name implies, destroy parts of the system; and, generally, involve the use of test pits, laboratory and/or in situ testing. Five procedures, with minor modifications are currently in use. These are the procedures of the U. S. Federal Aviation Administration (FAA) (Reference 1); U. S. Navy Bureau of

Yards and Docks (Reference 2); the Canadian Department of Transportation (Reference 3); the British Department of the Environment (Reference 4) and the U. S. Department of the Army and the Air Force (Reference 18). Basically, the five procedures involve the use of field tests in conjunction with sampling and laboratory testing.

The FAA procedure uses California Bearing Ratio (CBR) tests conducted in accordance with procedures in MIL-STD 621A Method 101. The Navy method uses non-repetitive plate load tests conducted according to specifications of American Society for Testing and Materials (ASTM) Test Method-Designation D-1196 (Reference 19). The Canadian practice uses repetitive plate bearing tests specified in ASTM Test Method Designation D-1195 (Reference 20). The British procedure also uses repetitive plate bearing tests but these are conducted in a slightly different manner from the ASTM D-1195 Test Method. The Air Force evaluation procedure is summarized in the report of the testing program conducted in a recent (1975) evaluation. It was reported (Reference 21) that,

> "Field testing consisted of 28 exploratory test pits . . . Thickness measurements were made on each pavement component, in situ density and moisture contents were determined, values of Modulus of Subgrade Reaction and CBRs were obtained and bulk samples of soil layers were taken. Core samples were extracted at 184 locations to ascertain pavement thickness and subsurface profile. Laboratory testing included classification of soils;

development of soil moisture-density relationships; Marshall testing of asphaltic concrete; and tensile splitting of Portland cement concrete cores."

The period of the evaluation was about 8 days.

The prevalent feeling concerning the use of test pits, and current destructive evaluation procedures was quite aptly put when one author (Reference 22) wrote,

> "Yet most civil engineers still cannot scientifically evaluate the load carrying capacity of an airport pavement without first rendering it unserviceable in a way no aircraft could have accomplished. The resulting test pits when filled and resurfaced remain as abrupt discontinuities to uniform pavement performance."

This general feeling coupled with the many other disadvantages of destructive testing has directed research towards the development of rapid, nondestructive evaluation equipment and procedures.

2.1.2 Nondestructive Evaluation

Nondestructive procedures are based on the analysis of the measured surface deflection response of a pavement-subgrade system to loads applied at the surface. The main differences among existing methods are: (1) the magnitude and manner in which the load is applied to the surface, and (2) the particular aspect of the surface disturbance that is measured, i.e., deflection magnitude, wave length, frequency. Table 1 shows a summary of the major load classes and their

TABLE 1 SUMMARY OF NONDESTRUCTIVE TESTING EQUIPMENT AND PERTINENT CHARACTERISTICS

Category	Load Class	Device	Deflection Measurement Made
1	Static	Plate (19)[a]	Magnitude
		Plate (20)	Magnitude
2	Impact	Washington State (58)	Magnitude
		Paris (58)	Magnitude
		German (58)	Magnitude
3	Vibratory	Shell (23)	Wave Length
		Road Rater (25)	Magnitude
		Dynaflect (23)	Magnitude
		Corp of Engr. (25)	Magnitude
		AFCEL (68)	Wave Length
4	Vehicular	Benkleman (69)	Magnitude
		California (55)	Magnitude
		Lacroix (70)	Magnitude
		TRRL (71)	Magnitude
		South Africa (23)	Curvature

[a]Numbers refer to references

characteristics, devices being developed and in use, and the particular aspect of the surface disturbance that is measured.

In the static load class repetitive or non-repetitive loads are applied to plates of varying sizes on the surface of the pavement. In the impact load class, weights are allowed to free-fall and impact a plate on the pavement surface. The weights may range in size from 20 lbs (Reference 23) to 500 lbs, as was used by Isaada (Reference 24). The vibratory procedures also show a considerable range in magnitude of vibratory loads and frequency of vibration. Peak vibratory loads may range from 0.75 to 25 kips and frequencies may range from 1 to 5000 hertz. Green and Hall (Reference 25) conducted a thorough study of vibratory equipment. Their work and the references cited in Table 1 provide additional details. Of the devices that use vehicular loads, the Benkleman beam measures rebound deflection, and the LaCroix and California deflectometer are somewhat automated Benkleman beams. The TRRL device employs an optical (non contact) displacement transducer for measuring deflections, and the South African apparatus measures curvature of the pavement as the wheel approaches.

2.2 Analysis

Numerous analytical solutions exist, employing various models, representing a pavement-subgrade system. These models are based on the theories of elasticity and viscoelasticity. Numerous equations representing their behavior under static and dynamic loading have also been solved (References 26 through 40). In 1972, Boyer (Reference 11) presented a rather definitive review of these solutions. In

addition, he employed the concept of transfer function theory along with the results of full scale field testing, using gages installed in the pavement. He proposed an "a posteriori" modelling concept to develop transfer functions and predict pavement response. Highter (Reference 13) reviewed the use of energy concepts and methods, and failure criteria relative to pavement evaluation. Using energy concepts he was able to substantiate that "a functional relationship exists between cumulative energy as measured by cumulative peak deflections imparted to a given pavement system and the condition of the system". Three sources of data were studied to verify his hypothesis. AASHO Road Test data, the Air Force base traffic records from Pease and Castle Air Force Bases, and data from field testing of overlays specifically constructed for his investigation.

A theoretical study of dynamic stiffness and its application to vibratory nondestructive testing of pavements was conducted by Weiss (Reference 41) in conjunction with the study by Green and Hall (Reference 25). Weiss developed a nonlinear vibration theory for pavements and gave a method of obtaining the shear modulus and thickness of each pavement layer. In this work a vibrator is used to generate the deflections from which the dynamic stiffness is calculated.

Wiseman (Reference 42) used the Hogg and the Hertz models to estimate pavement characteristics. The Hogg model provided the required pavement stiffness for full-depth asphalt airfield pavements. He then related the computed stiffness to projected traffic and a characteristic length using published Asphalt Institute procedures.

Wiseman also used the Hertz model to compute the single wheel load on a rigid pavement as a function of measured stiffness.

A probabilistic analysis of the response of pavement structures was undertaken by McCullough (Reference 17). He cited the application of stochastic process, in this regard by the Texas Highway Department (Reference 43), California Division of Highways (Reference 44) and the Asphalt Institute (Reference 45). He also illustrated the application of the Markov process and its theoretical relation to states of a pavement. Reliability techniques have also been reported by Darter and Hudson (Reference 46). In 1976, Moavenzadeh (Reference 47) presented a stochastic simulation model for predicting pavement performance. Recognizing the limitations of his model, he concluded that it can be used to compare various design alternatives. It also accounts for geometry, load area and intensity, random inter-arrival times, statistical variation in material properties and temperature histories.

Inherent in all analytical and stochastic models is the notion that parameters can be obtained that reflect the actual vehicular load experienced by a pavement subgrade system. At the present time, the literature shows that parameters used in analysis are obtained by static field test, laboratory testing, vibrations, impact and measurement of pavement rebound characteristics. The actual time dependent response of the pavement-subgrade system subject to one complete vehicular pass is not considered.

SECTION III

THEORY AND METHODOLOGY

There exist today numerous elastic and viscoelastic solutions (References 26 through 40) to the overall vehicle-pavement-subgrade interaction problem, in addition to the results of several full scale field testing programs (References 48 through 50). Accumulated theory and prototype testing point to the following fundamental observations:

1. The characteristics of the component materials of a pavement-subgrade system vary locally, even within the small volume of a representative "homogeneous" sample.
2. Pavement-subgrade characteristics and response to loadings change with seasonal and ambient conditions.
3. Load repetitions affect the various components of the system differently.
4. A nondestructive field test conducted in situ using prototype loading better reflects the action of a pavement-subgrade system than destructive tests on samples, or tests conducted in situ using non-representative loads.
5. The pavement subgrade system exhibits three basic behavioral characteristics; namely,
   (a) inertial characteristics,

(b) elastic characteristics, i.e. linear and independent of time, and

(c) viscoelastic characteristics that account for the memory and the time dependent nature of the system response.

Recognition of the complexity and variability of the pavement-subgrade system and the nature of the wheel loading-pavement-subgrade interaction problem, has led to the development of global methods of characterizing the pavement-subgrade system under prototype conditions of loadings (References 38, 51, and 52). The global concept provides a quantitative spatial evaluation rather than one limited to the very near vicinity of a point and the subsequent assumptions of homogeneity and isotropy in the case of the classical theories (References 11 and 12).

3.1 Hypotheses

The principal hypotheses embodied in this research are:

1. The response of a point on the surface of a pavement-subgrade system when subjected to vehicular loadings can be characterized by a (Kelvin) lumped parameter model. The three parameters of the model are m, c, and k, as shown in Figure 1. The equation describing the hypothesized lumped parameter system is

$$m\ddot{z}(t) + c\dot{z}(t) + kz(t) = F(t) \qquad (1)$$

where m represents the equivalent mass (the interacting

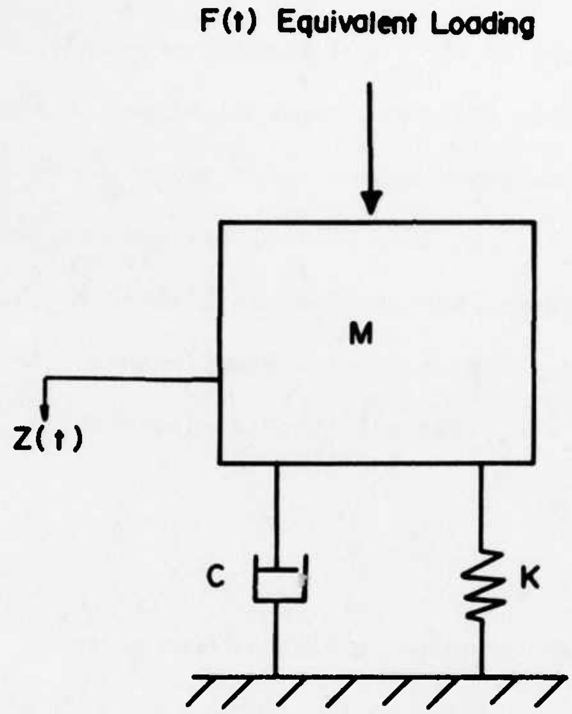

$$m\ddot{z}(t) + c\dot{z}(t) + kz(t) = F(t)$$

Figure 1. Kelvin Model of the Pavement Subgrade System

inertial components of the pavement-subgrade system), c is the damping (the time dependent viscoelastic or energy dissipating component), and k is the stiffness (elastic component); $z(t)$, $z(t)$ and $z(t)$ are the equivalent acceleration, velocity and deflection, respectively. $F(t)$ is the equivalent input force due to the wheel load, (its maximum value for the F-4 aircraft, for example, is approximately 25 kips). Figure 1 shows the hypothesized model.

2. The salient characteristics of the time dependent response of the pavement-subgrade system to a complete vehicular pass can be obtained in a nondestructive manner.

3. Equivalent parameters describing the pavement-subgrade system stiffness (k), energy dissipation (c) and inertial (m) characteristics can be extracted from the measured response.

4. The extracted parameters accomplish the following:

    (a) they reflect the global structural state of the pavement-subgrade system and; whereas, they are responsive to seasonal and local variations, they can be used as the basis of a nondestructive evaluation scheme.

(b) they can be used to predict the deflection response to varying magnitudes and configurations of wheel loads.

5. Many current parameters used in conventional design and analysis can be obtained from the noted response of a pavement-subgrade system to actual vehicular loading.

The developed theory and methodology provide the following: (1) the theoretical basis of a pavement evaluation scheme. This includes the determination of the deflection response of a pavement-subgrade system to prototype loading, and the methodology of extracting parameters describing the equivalent mass, stiffness and energy dissipation characteristics of the pavement-subgrade system. (2) The methodology for predicting the deflection response of flexible pavements to prototype loadings of varying magnitudes and configurations.

3.2 Evaluation

The pavement evaluation scheme consists of determining the parameters inherent in the transfer function of the pavement-subgrade system. The transfer function is a mathematical expression which represents the mechanism that converts the equivalent input to an output. Figure 2 shows an overview of the input-transfer function-output interrelation as it applies to wheel load-pavement-subgrade interaction.

The basic elements of the evaluation scheme are:

(a) the signature determination, and

(b) the parameter determination.

3.2.1 Signature Determination

The signature is the pavement deflection-time plot corresponding to the pavement deflection at the outer edge of the tire print as shown in Figure 3. Because the mechanical setup of the measuring equipment precludes the measurement of deflections closer than 3 inches from the outer edge of the tire print, the signature is calculated from deflections measured in the field using the "stationary beam-moving load" procedure.

In this procedure (Figures 3 and 4) a cantilever beam with its pivot outside the deflection basin supports sensing elements within the deflection basin. The sensing elements measure relative motion between the pavement surface and the beam as the load vehicle travels in a direction perpendicular to the beam position. The sensing elements are positioned at different lateral distances from the load wheel and therefore record the deflection time history for one complete pass of the load vehicle at the points of measurement. The location of the tire print is determined from the impression the tire makes on silver adhesive tape placed on the pavement in its path in front of the beam. The distance from the outer edge of the tire print to the first gage is measured. From this initial measurement and the fixed intergage distances, the distance of each gage from the outer edge of the tire print is calculated [Figure 3(b)]. Figure 4 shows an Air Force P-2 fire truck about to make a pass by two stationary measurement systems.

The method of calculating the signature is as follows:

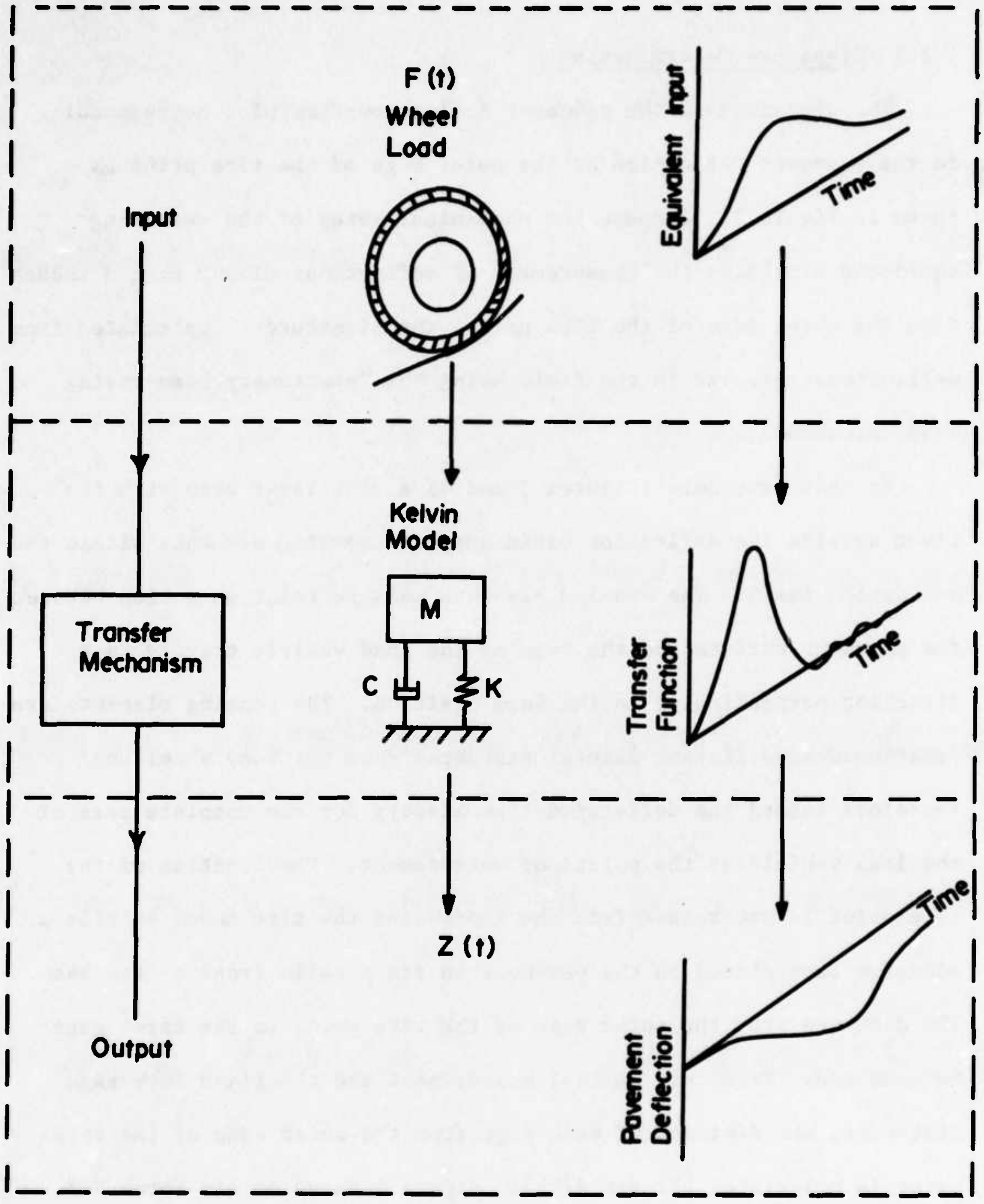

Figure 2. An Overview of the Transfer Function Concept as Applied to Wheel-Pavement Subgrade Interaction

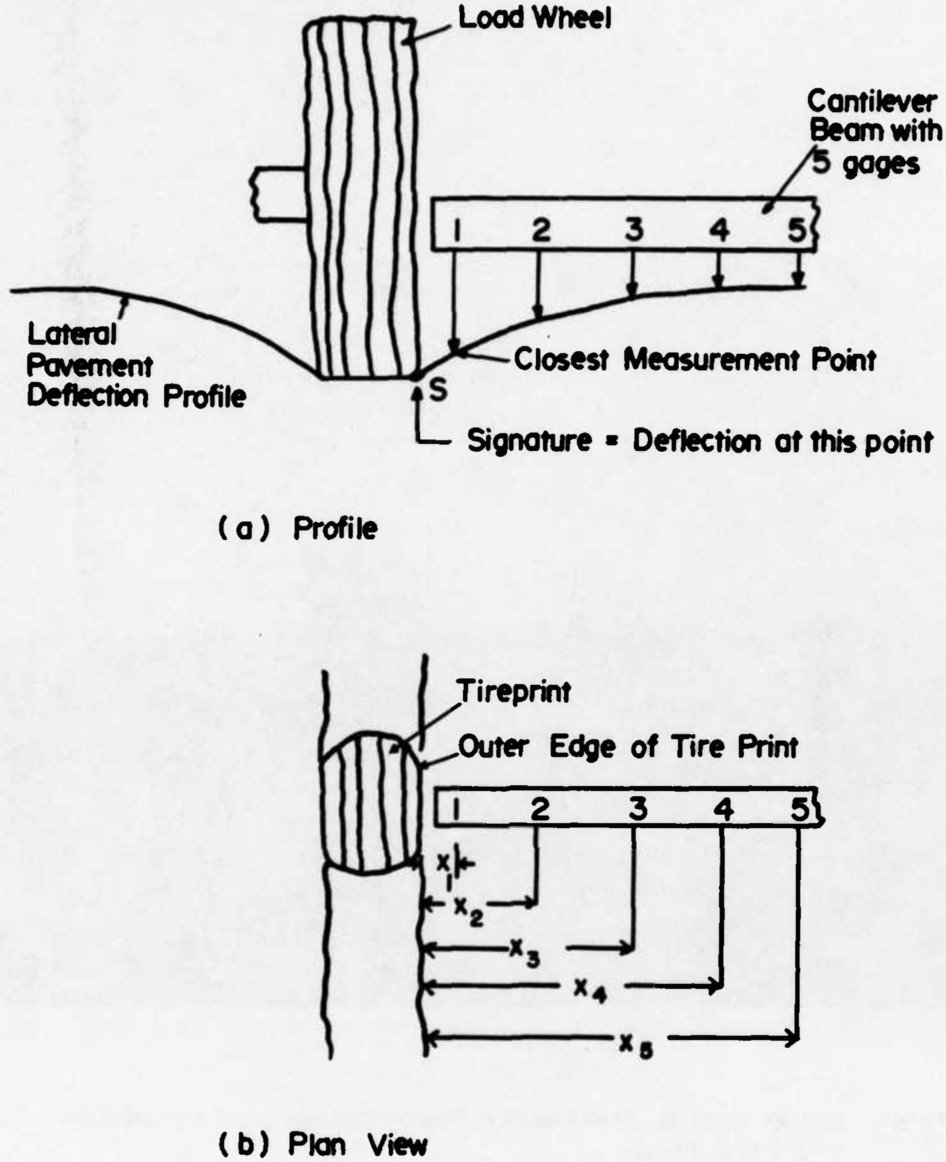

Figure 3. Location of Signature and Relative Gage Location and Setup

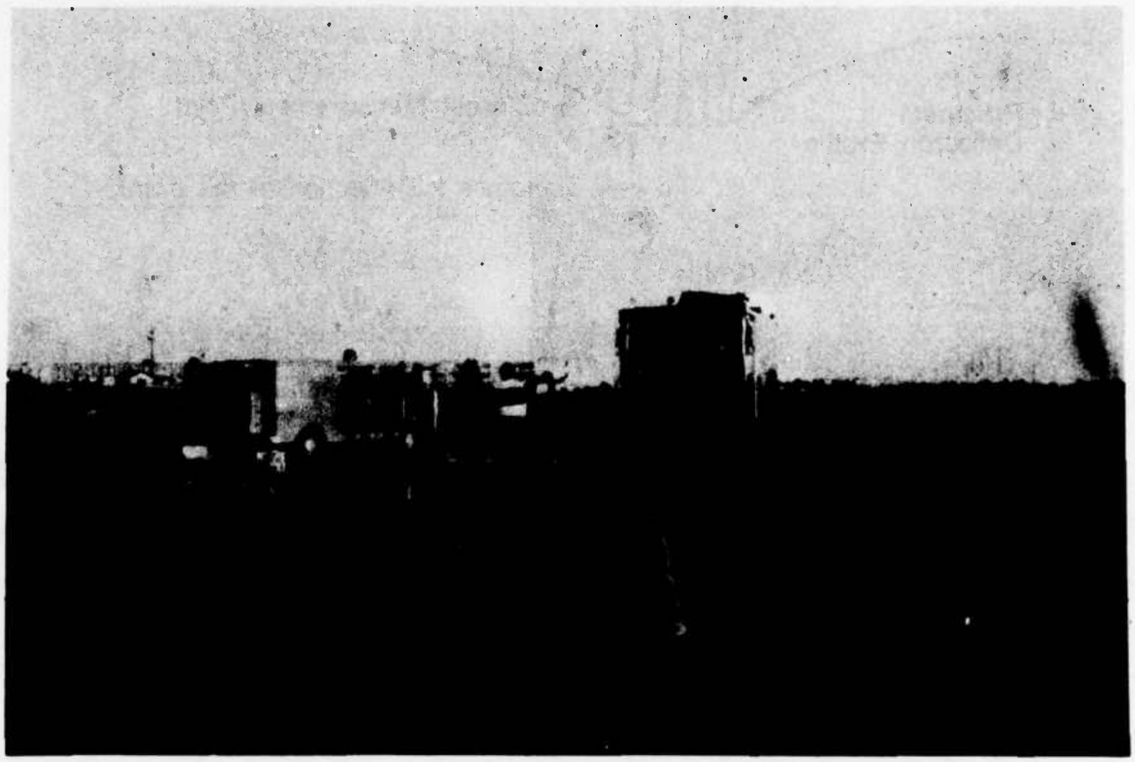

Figure 4. Setup During Stationary Beam-Moving Load Operation - P-2 Fire Truck

(a) The maximum value of the deflection, z_{max}, at each particular gage (j) is obtained from each of the deflection-time plots recorded at said gage (j) during one pass of the vehicle. V and W of Figure 5 show z_{max_1} and z_{max_2} (z_{max_3}, z_{max_4} and z_{max_5} are not shown), in perspective.

(b) The distances x_j [Figure 3(b)] from the outer edge of the tire print to each gage as recorded in the field, and the corresponding maximum gage readings, z_{max_j}, are then fitted with a curve given by the equation

$$z_{max_j} = A_{peak} \exp (\beta_{peak}\, x_j^{\,r_{peak}}) \qquad (2)$$

where A_{peak}, β_{peak} and r_{peak} are parameters describing the attenuation of the maximum values of the deflection-time plots recorded on each gage. Equation (2) is similar in form to those used by Boyer (Reference 11) and Highter (Reference 12), but has three parameters, A_{peak}, β_{peak} and r_{peak}, instead of two that they used. Baladi (Reference 52) also uses a three-parameter equation to describe the attenuation of the maximum lateral deflection profile caused by vehicular loads on highways.

The curve fitting calculations are performed by the computer subroutine EXACFIT listed in Appendix C. The equations used are derived as follows:

Given the general equation of the curve in the form

$$z = A \exp (\beta x^{r}) \tag{2a}$$

This equation has three unknowns, A, β and r. Using this basic equation and values of (x_1, z_{max_1}), (x_2, z_{max_2}) and (x_3, z_{max_3}), (where the numbers in the subscripts refer to gages numbered from 1, the closest to the wheel, to 5 the farthermost from the wheel), the following are had:

$$z_{max_1} = A'_{peak} \exp (\beta'_{peak}\, x_1^{\,r_{peak}}) \tag{3a}$$

$$z_{max_2} = A'_{peak} \exp (\beta'_{peak}\, x_2^{\,r_{peak}}) \tag{3b}$$

$$z_{max_3} = A'_{peak} \exp (\beta'_{peak}\, x_3^{\,r_{peak}}) \tag{3c}$$

Dividing equation (3a) by equation (3b) gives

$$z_{max_1}/z_{max_2} = \exp (\beta'_{peak}\, x_1^{\,r'_{peak}} - \beta'_{peak}\, x_2^{\,r'_{peak}})$$

Taking the natural logarithm of both sides produces

$$\ell n\, z_{max_1} - \ell n\, z_{max_2} = \beta'_{peak} (x_1^{\,r'_{peak}} - x_2^{\,r'_{peak}}) \tag{4}$$

Similarly from equation (3a) and (3c)

$$\ell n\, z_{max_1} - \ell n\, z_{max_3} = \beta'_{peak} (x_1^{\,r'_{peak}} - x_3^{\,r'_{peak}}) \tag{5}$$

Dividing equation (4) by equation (5) and rearranging terms gives

$$\left(x_1^{r'_{peak}} - x_3^{r'_{peak}}\right)\left(\frac{\ln z_{max_1} - \ln z_{max_2}}{\ln z_{max_1} - \ln z_{max_3}}\right) = x_1^{r'_{peak}} - x_2^{r'_{peak}} \qquad (6a)$$

Equation (6a) is solved by an iteration-interpolation procedure detailed in Appendix C, and r'_{peak} is found.

β'_{peak} is then calculated using equation (5), where

$$\beta'_{peak} = \frac{\ln z_{max_1} - \ln z_{max_3}}{x_1^{r'_{peak}} - x_3^{r'_{peak}}} \qquad (5a)$$

Then A'_{peak} is calculated using equation (3a) where

$$A'_{peak} = z_{max_1} / \exp\left(\beta'_{peak}\, x_1^{r'_{peak}}\right) \ . \qquad (3a)$$

Using (x_1, z_{max_1}), (x_3, z_{max_3}) and (x_5, z_{max_5}) instead of (x_1, z_{max_1}), (x_2, z_{max_2}) and (x_3, z_{max_3}), equations (3a), (3b) and (3c) are again solved to find r''_{peak}, β''_{peak} and A''_{peak}. The desired r_{peak}, β_{peak} and A_{peak} are found using the equations

$$r_{peak} = \left(r'_{peak} + r''_{peak}\right)/2 \qquad (7)$$

$$\beta_{peak} = \left(\beta'_{peak} + \beta''_{peak}\right)/2 \qquad (8)$$

$$A_{peak} = \left(A'_{peak} + A''_{peak}\right)/2 \qquad (9)$$

r_{peak}, β_{peak} and A_{peak} are the parameters which describe the maximum lateral deflection profile, partly shown in Figure 5 as the curve V'VW.

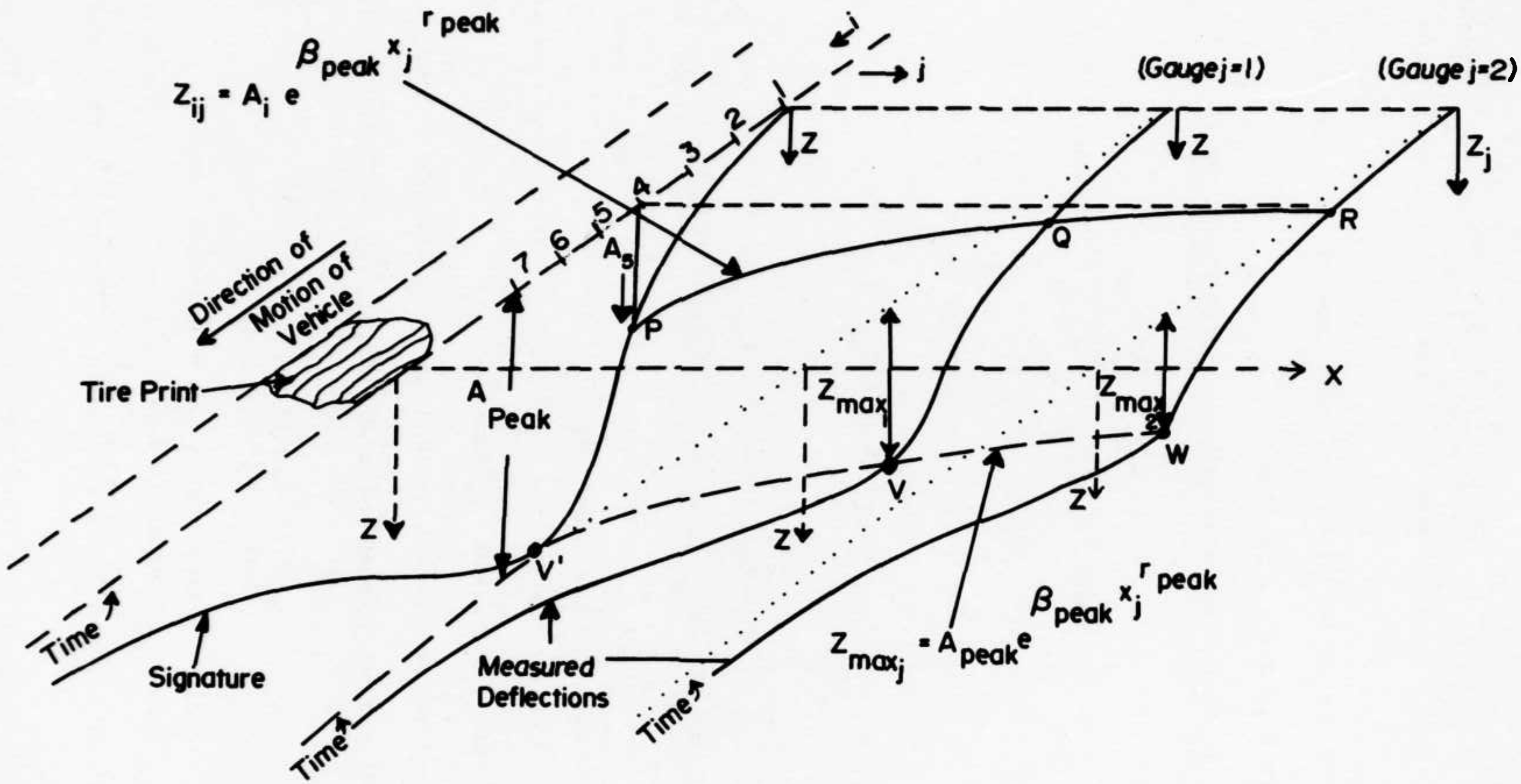

Figure 5. Overview of Method of Calculation of Signature Due to Prototype Loading

(c) The signature is calculated using the r_{peak} and β_{peak} parameters and the basic equation, equation (2a), in the form

$$A(t) = z_1(t)/\exp\,(\beta_{peak}\; x^{r_{peak}}) \qquad (10)$$

where $z_1(t)$ refers to the deflection at gage 1 (closest to the wheel), and t is the time shown discretized as i in Figure 5. Subroutine SIGNTR in Appendix C performs these computations.

The signature thus calculated is the pavement deflection due to prototype loading at point S in Figure 3. Using this signature as the output (Figure 2), parameters k, c, and m describing the transfer mechanism of the three-parameter model of the pavement-subgrade system, are calculated.

3.2.2 Parameter Determination

The objective of the theoretical procedure is to determine the equivalent m, c and k parameters of a pavement-subgrade from the signature obtained from actual field loadings using transfer function theory. These parameters define the transfer mechanism that converts wheel loadings to pavement deflections.

The wheel load-pavement-subgrade interaction, as shown in Figure 2, can be represented mathematically by the equation (1):

$$m\ddot{z}(t) + c\dot{z}(t) + kz(t) = F(t) \qquad (1)$$

It can also be represented by the equation

$$I(t) * G(t) = \frac{F(t)}{m} * G(t) = z(t) \qquad (11)$$

where $F(t)$ is the equivalent loading (input) function, m is the equivalent mass, $G(t)$ is the <u>reduced transfer function</u>, $z(t)$ is the response and the symbol (*) represents the mathematical operation of convolution (Reference 53). In its integral form equation (11) becomes

$$z(t) = \int_0^t \frac{F(t)}{m} \cdot G(t-\tau)\, d\tau \qquad (12)$$

$G(t)$, the reduced transfer function in equations (11) and (12) is obtained from equation (1) as follows:

Consider the basic equation of the model:

$$m\ddot{z}(t) + c\dot{z}(t) + kz(t) = F(t) \qquad (1)$$

taking the Laplace transform of both sides, imposing initial conditions (pavement is assumed to be at rest prior to loading) of $z(0) = z(0) = 0$, and transposing terms, yields:

$$\bar{z}(s) = \frac{\bar{f}(s)}{m} \cdot \left(\frac{1}{s^2 + \frac{c}{m} s + \frac{k}{m}}\right)$$

where the bars denote the transformed function. The reduced transfer function is defined as

$$\bar{G}(s) = \frac{1}{s^2 + \frac{c}{m} s + \frac{k}{m}}$$

Inverting $\bar{G}(s)$ gives,

$$G(t) = \left[\frac{1}{\dfrac{k}{m} - \dfrac{c^2}{4m^2}} e^{-\frac{c}{2m} \cdot t} \right] \left[\sin \frac{k}{m} - \frac{c^2}{4m^2} t \right] \tag{13a}$$

if $k/m < \dfrac{c^2}{4m^2}$, namely, the system is overdamped, then

$$G(t) = \left[\frac{1}{\dfrac{c^2}{4m^2} - \dfrac{k}{m}} e^{-\frac{c}{2m} \cdot t} \right] \left[\sinh \frac{c^2}{4m^2} - \frac{k}{m} t \right] \tag{13b}$$

Two ways to obtain the equivalent input (loading function) $F(t)$ will be pursued in this work. The first way is by the direct substitution in the equation

$$m\ddot{z}(t) + c\dot{z}(t) + kz(t) = F(t) \tag{1}$$

of the calculated values of $z(t)$, $z(t)$ and $z(t)$ obtained from the measured deflections, and the parameters of the transfer mechanism m, c and k. The second method is by implicit convolution using equations (11) and (12). The implicit discrete form of equation (12) is given (Reference 53) by the equation

$$I(i) = \frac{O(i)/\Delta T - \sum_{m=1}^{k=i-1} I(m) \cdot G(k + 2 - m)}{I(1)} \tag{14}$$

where $G()$ = the reduced transfer function

$O(i)$ = the output $z(i)$

$m \times I(i) = F(i)$ = the equivalent loading function (15)

ΔT = time increment

and, the initial value of $I(i) = I(1)$ is given by the equation

$$I(1) = \frac{O(1)}{G(1) \cdot \Delta T}$$

The same two arguments above lead to two ways of finding the output $z(t)$, given the forcing function and the parameters m, c, k. The first is by the closed form solution of equation (1). The second is by explicit convolution using the equation

$$O(i) = z(i) = \sum_{j=1}^{i} G(i) \cdot I(i - j + 1)\ \Delta T \qquad (16)$$

where z(), G(), I() and ΔT are as defined in equation (14).

During field testing, only the deflections with time are measured, and from these deflections the signature A(t) in equation (10) can be obtained as discussed previously. How then are the parameters of transfer frunction and the loading functions determined?

In concept, the methodology used is as follows: The signature A(t) is taken to be equivalent to the response z(t) in equations (11) to (16) as discussed in the previous section entitled "Signature Determination". The input function F(t) is now known initially. It is assumed however that the maximum value of F(t) is the wheel load, or approximately 25 kips (Reference 54) for the F-4 aircraft, which is the main vehicle of interest in the present study. Using the signature z(t), the maximum assumed value (25 kips) of the equivalent input, and the equations developed previously in this section, the k, c, and m parameters of the pavement-subgrade system are determined.

The detailed procedure for finding k, c, and m is as follows:

(1) The signature is differentiated numerically to yield the time history of the velocity $z(t)$ and the acceleration $z(t)$. Typical plots of $z(t)$, $z(t)$, and $z(t)$ are shown in Figure 6.

(2) The components of the equivalent force, due to each of the three parameters, on the left hand side of the basic equation (1), are then considered for three special conditions, labelled as sections (1), (2), and (3) in Figure 7.

At section (1), the point of inflection of the signature, the following equations hold:

$$\ddot{z}(t_1) = 0$$

$$m\ddot{z}(t_1) = 0$$

hence,

$$c\dot{z}(t_1) + k\,z(t_1) = F(t_1) \qquad (17a)$$

At section (3), the maximum deflection response, the following equations hold:

$$\dot{z}(t_3) = 0$$

$$c\dot{z}(t_3) = 0$$

hence,

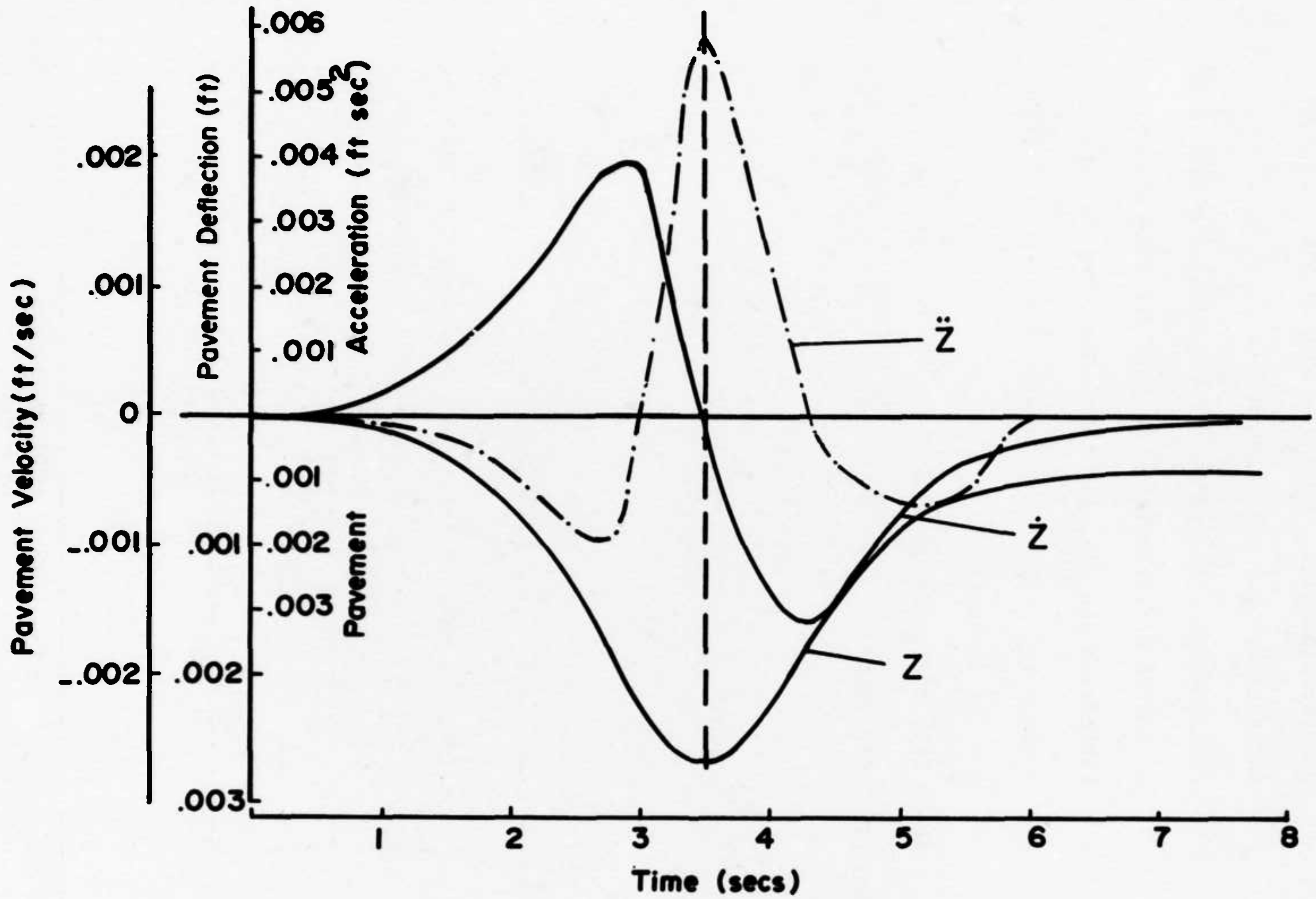

Figure 6. Zero, First and Second Derivatives of the Measured Displacement Function (Typical)

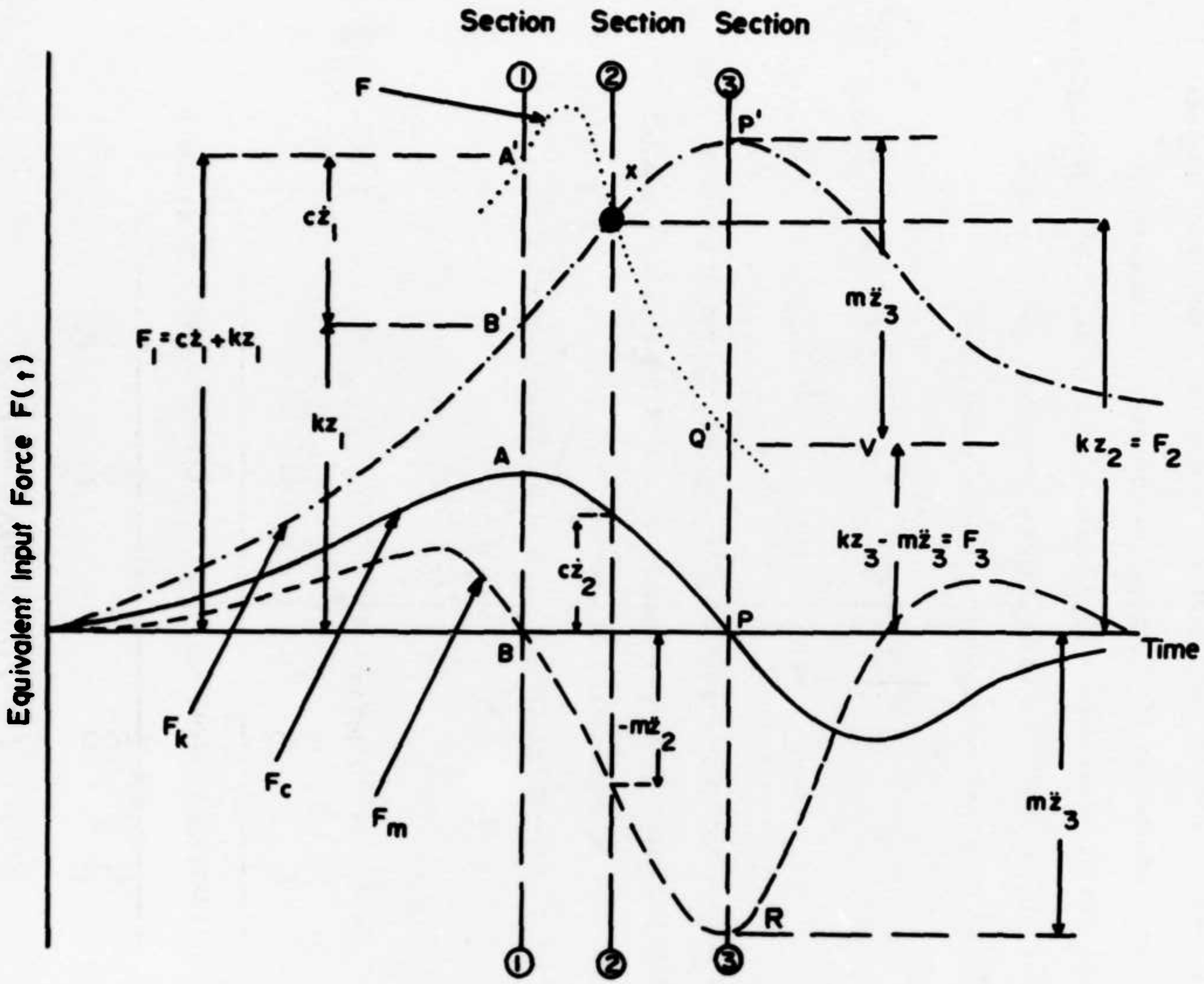

Figure 7. Determination of Parameters of Transfer Function - A Graphical Overview of Methodology

$$m\ddot{z}(t_3) + kz(t_3) = F(t_3) \tag{17}$$

The third special condition occurs, for each deflection data set, at a time between the time corresponding to the point of inflection [section (1)] and the maximum deflection [section (3)]. With reference to Figure 7, with increasing times from section (1) to section (3), the stiffness component [kz(t)] of the equivalent input force increases from B' to a maximum at P'. During this passage, the damping component [cz(t)] decreases from a maximum of A to zero (P). Similarly, the inertial component [mz(t)] decreases from zero (B) to a negative value of R. The time corresponding to the conditions,

$$c\dot{z}(t_2) = - m\ddot{z}(t_2) \tag{18}$$

$$\text{and, hence,} \quad kz(t_2) = F(t_2) \tag{19}$$

will be called the crossing point. It provides the final special condition for determining the measure of the parameters m, c and k. This condition is represented as section (2) of Figure 7. It should be noted that between section (1) and the crossing point,

$$kz(t) \leq F(t_2)$$

and between the crossing point and section (3)

$$kz(t) > F(t_2)$$

In concept, therefore, the crossing point represents the time at which the Winkler hypothesis (Reference 55) is satisfied.

(3) Using the equation in paragraph (2) and the developed method, an iterative procedure, given in detail in Appendix C was used to determine the k, c and m parameters in this study. Briefly the procedure is as follows:

The signature of the load vehicle is obtained as described in the section entitled "Signature Determination". A first trial value of k is taken as a fraction (AA1 < 1.0)[1] of the wheel load (25 kips) divided by the maximum value of the signature. Then it is assumed that another fraction (AA2 < 1) of the wheel load acts at the time corresponding to section (3) Figure 7. The first trial value of m is calculated for the conditions at section (3) using equation (17). The initial trial value of the c parameters is then computed using equation (18) at the first estimated crossing point in the data set, i.e., at the first discrete interval of time after section (1). Using these first estimates of k, c and m the transfer function G(t) [equation (13)] is had [EXACT 1][1]. Next the loading function F(t) is obtained by implicit convolution [equations (14) and (15) and NWCONV] in the time domain using the signature deflection z(t) is output and G(t). The maximum value of F(t) is then found. A check is made to see if this (maximum) value of F(t) satisfies the necessary (500 pound) criterion that,

[1]Capital letters in parentheses refer to computer programs or symbols used in computer programs in Appendix C.

$$24{,}500 \text{ lb} \leq F(t) \text{ maximum} < 25{,}500 \text{ lb} \tag{20}$$

If this criterion is not satisfied, the next crossing point is selected, c is recalculated and the same procedure is followed to obtain the maximum value of F(t), which is again examined with respect to the previously stated criterion. This process is repeated until the possible crossing points are exhausted i.e. section (3) Figure 7 is reached, or the maximum value F(t) satisfies the previously stated criterion, whichever occurs first.

If all possible crossing point times are exhausted a new value of m is calculated by incrementing the value of AA2. Using the first trial value of k and the second trial value of m a new c is calculated for the first estimated crossing point. The procedure is repeated, checking the maximum value of F(t) against the 500 pound criterion. If this criterion is not satisfied the sequence of crossing points is again stepped through. If these are exhausted a next trial value of m is assumed and the entire process is repeated. If the incremented value of AA2 reaches unity, a second trial value of k is calculated by incrementing AA1, and the entire procedure, including a new sequence of m and c values, is examined at all possible crossing points. This process is repeated until the 500 pound criterion (equation 20) is satisfied.

If the 500 pound criterion is satisfied, a new c value is calculated for conditions corresponding to the time at the inflection point of the signature (section (1), Figure 7, equation 17a); using the current k value and the force obtained by convolution, corresponding to the time of inflection. If this new c value does not correspond to the

c value which satisfied conditions at the crossing point and the 500 pound criterion, the iteration process is continued by selecting another crossing point and repeating the entire procedure. If the c values do correspond then the corresponding k, c, and m values are the desired parameters.

3.3 Prediction of Pavement Response (Signature)

The theory and methodology for signature and parameter determination developed in the previous sections were used to predict the signature of a vehicle (vehicle A) at a site prior to the actual passage of the vehicle at that location. This was done by first obtaining signatures of both a standard vehicle and vehicle A at another site, and the signature of the standard vehicle at the new site. This is accomplished by using an equivalency function.

The equivalency function is defined as the ratio of the loading (input) function of a vehicle, $F_1(t)$, and the loading function of the standard vehicle, $F_2(t)$, both obtained at the same location (at a standard site). This relationship is given by the equation.

$$\text{Equivalency Function} = EF(t) = \frac{F_1(t)}{F_2(t)} \tag{21}$$

The procedure for determining the equivalency function is as follows: with reference to Figure 8, Block I, at a standard site the signature due to a standard vehicle is obtained as discussed in the section entitled "Signature Determination". Using this signature as output, the transfer function, $G_2(t)$, of the standard site and the loading $F_2(t)$ of the standard vehicle at the standard site are determined as previously discussed in the section entitled "Parameter

Determination". Next the signature of A (the vehicle whose response is to be predicted) is obtained at the standard site. Using the transfer function of the standard site as determined by the standard vehicle and the signature of vehicle A at the standard site, the loading function $F_1(t)$ of vehicle A is obtained by implicit convolution using equation 14 and 15, and subroutine NWCONV (Appendix C). Once the equivalency function is had from equation 21, the predicted signature is obtained as follows:

First, the signature of the standard vehicle, $z(t)$, its loading function $F_{sA}(t)$ and the transfer function $G_A(t)$ are obtained at the new site as discussed in the preceding paragraph. These functions are shown schematically in Block III Figure 9. Next the loading function $F_{1A}(t)$, of vehicle A at the new site is calculated using the equation

$$EF(t) \times F_{sA}(t) = F_{1A}(t) \tag{22}$$

Equation 22 is represented in Figure 9 as the connection between the loading function of Block III and the equivalency function at the point labelled β.

The predicted signature of vehicle A at the new site is computed by the explicit convolution of the loading function of vehicle A at the new site and the transfer function of the new site as determined by the standard vehicle, using equation (16),

$$z(i) = \sum_{j=1}^{i} G(i) \cdot I\,(i - j + 1)\,\Delta T$$

where $G(i)$ = transfer function of the new site

$I(\ )$ = the equivalent loading function of vehicle A at the new

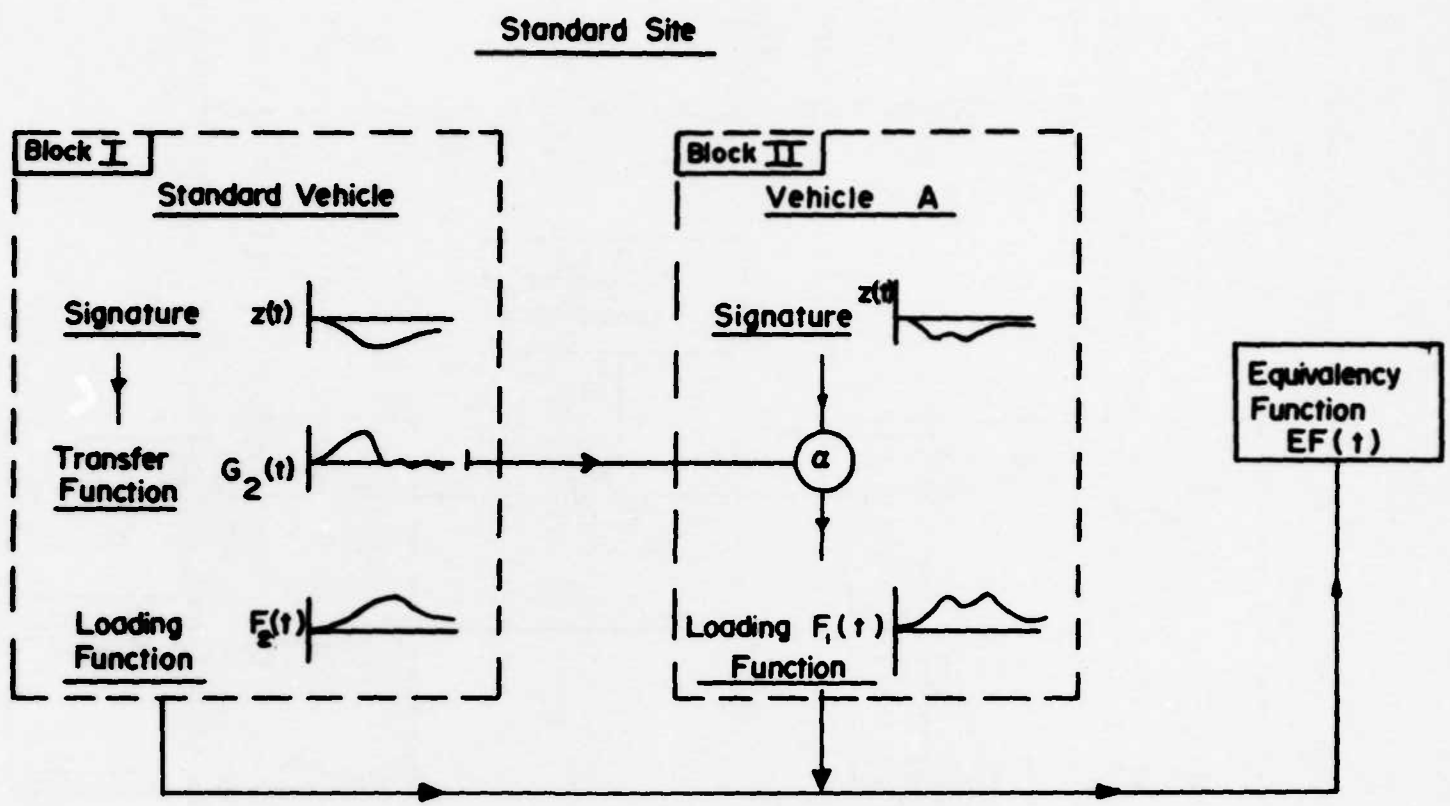

Figure 8. Overview of Scheme for Determining the Equivalency Function

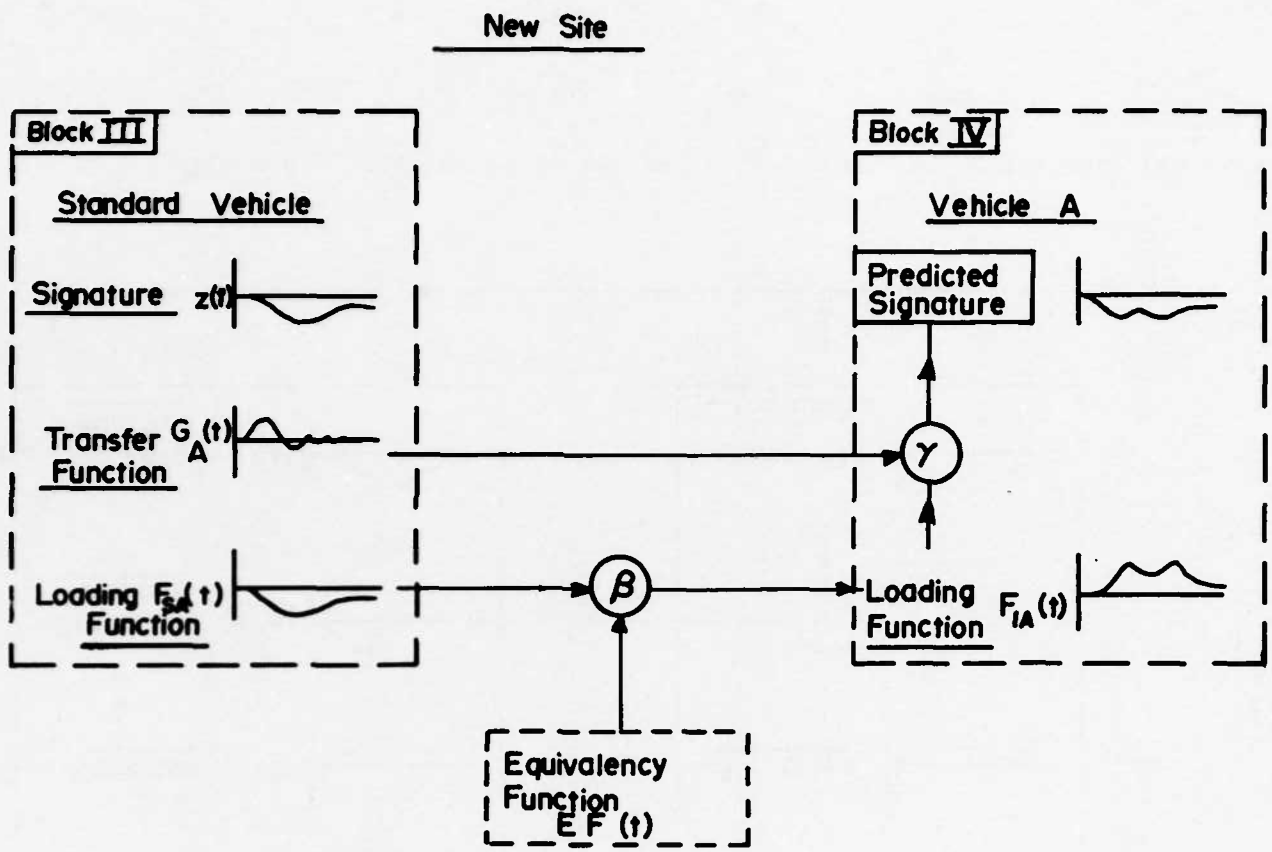

Figure 9. Overview of Scheme for Predicting the Signature

site (see equations 11 and 15)

$z(i)$ = the predicted signature

ΔT = the time increment

j = dummy variable, and

i = dummy variable indicating the time interval number

The explicit convolution is represented in Figure 9, Block IV as the connection between the equivalent loading and the transfer function at the point labelled γ of Figure 9.

The computer program PREDCT that performs the noted calculations to generate the predicted signature is given in Appendix C.

The evaluation and prediction methodologies are clearly dependent on the availability of reliable equipment for measuring pavement deflections.

SECTION IV

NEW INSTRUMENTATION FOR DEFLECTION MEASUREMENT

Two mobile systems were developed during this study for the measurement of pavement deflections: the Light Emitting Diode (LED) system and the Linear Variable Differential Transformer (LVDT) system.[3]

The LED system is essentially an optical system which does not make contact within the deflection basin of the pavement. On the other hand the sensing elements of the LVDT system make contact with the pavement surface. A summary of the research effort expended in the development of these systems and their basic developments is presented below.

4.1 The LED System

The LED measurement system consists of three major operational sections: they are,

a. the beam

b. the sensor modules, and

c. the recording system

a. The Beam

The beam is made of aluminum. Its principal function is to support the sensors above the pavement surface. It is designed so that a 20-mile-per-hour gust of wind will deflect the end of the beam less than 0.004 in. Figure 10 shows schematic details of the beam. Figure 11 shows the LED beam setup. Seven LED sensor modules are shown between the channel of the beam.

---

[3] The LVDT system was developed by Baladi (Reference 52) as part of his research effort, sponsored by the Federal Highway Administration.

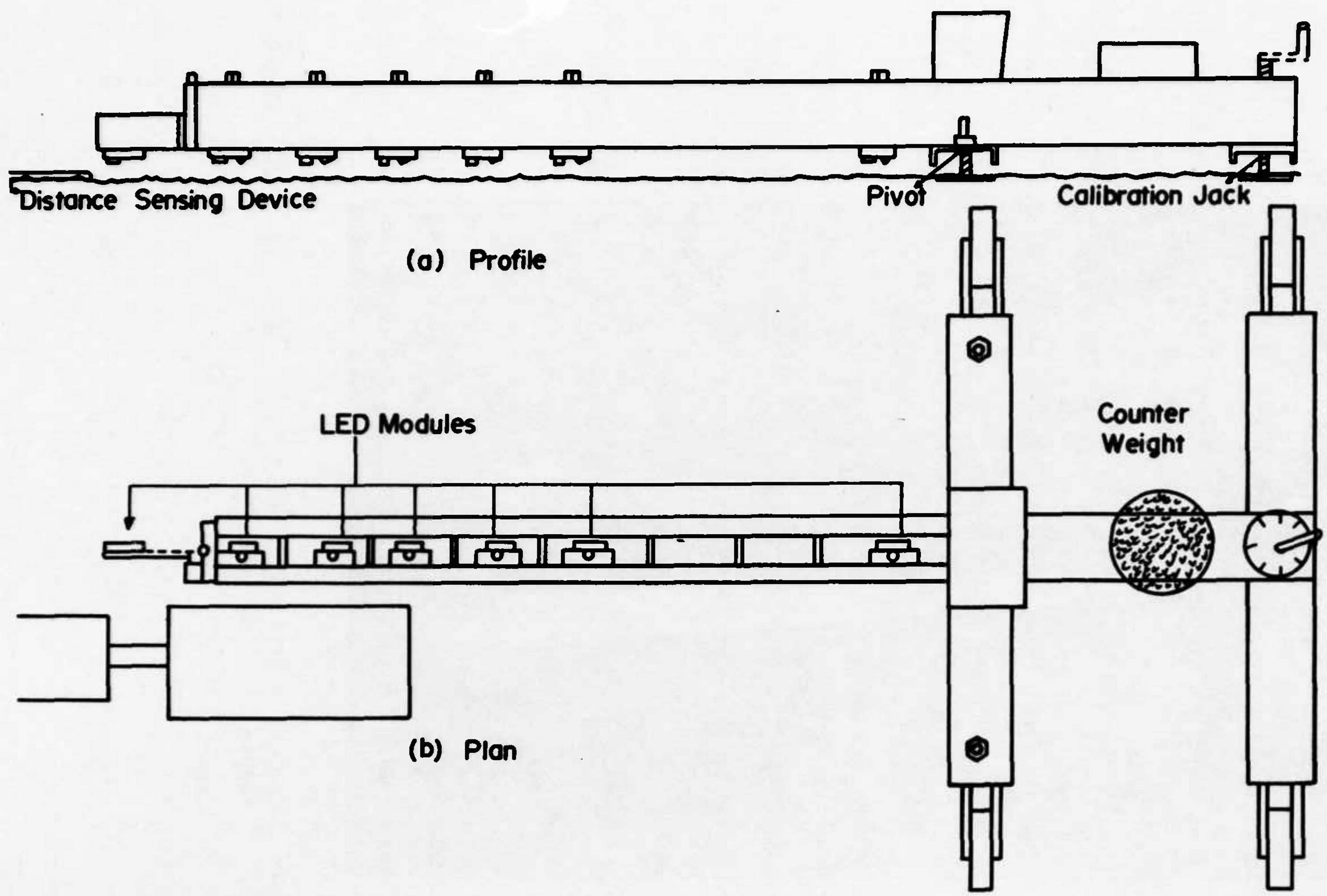

Figure 10. Light Emitting Diode (LED) Beam Schematic Details

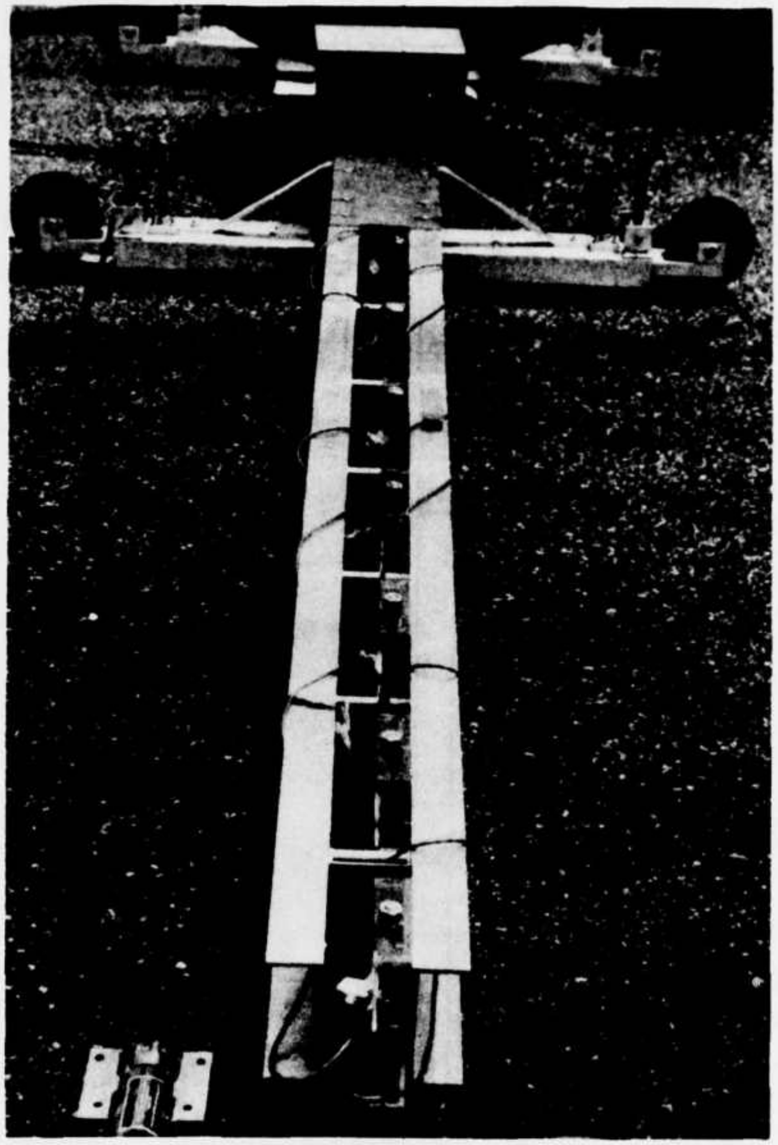

Figure 11. LED Beam Setup

b. Sensor Modules

Several ways of obtaining deflections using optical, non-contact techniques were considered prior to selection of the final sensor. These methods can be categorized under two general classes; namely, point methods and global methods. The point methods considered were focal point displacement, beam triangulation, retro-reflector beam displacement methods, diffraction gages, interferometers, Moire gages and grating gages. The global techniques considered were holography and Moire contour techniques.

The technique selected for development was the beam triangulation method, using a light emitting diode as the coherent light source. Figure 12 shows the basic geometrical optics of the beam triangulation method. Basically, pavement deflection is measured by the amount of displacement of the reflected light impinging on the collector lens. Research has established that a line of light impinging on the surface of small chips of various materials, asphalt, concrete, and sand paper, produces a reflected signal that can be normalized to produce a linear position measurement independent of surface reflectivity. The sensors have a range of 0.2 in and an accuracy of 0.0005 in. Figure 13 shows a complete sensor module ready for mounting on the beam. Additional details are given in Appendix A.

c. The Recording System

Signals from the sensors are collected on a magnetic tape unit. Figure 14 shows the recorder[4] used during this investigation. Figure 15

[4]A light beam recorder was also used in some special tests.

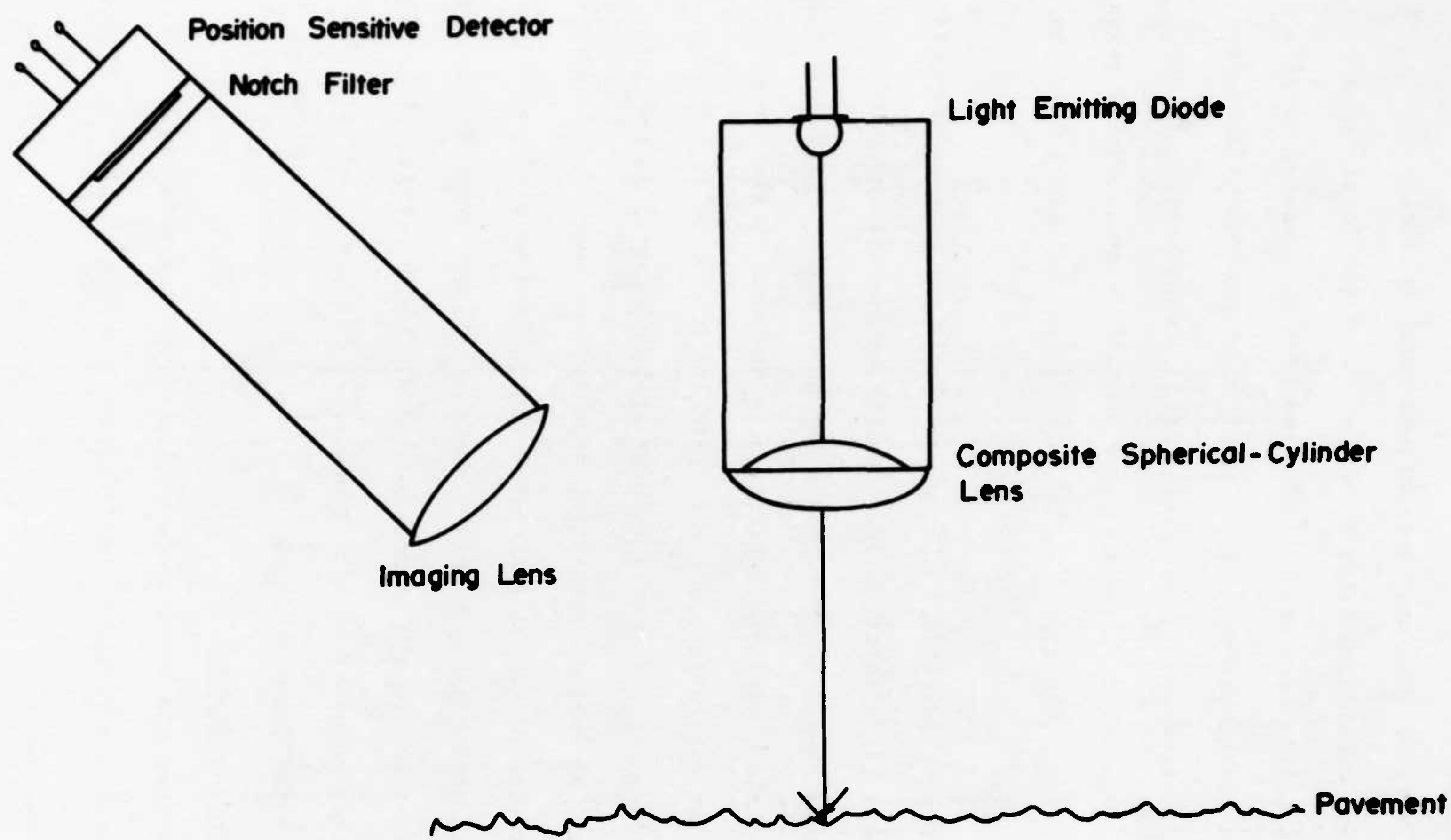

Figure 12. Light Emitting Diode Triangulation Arrangement

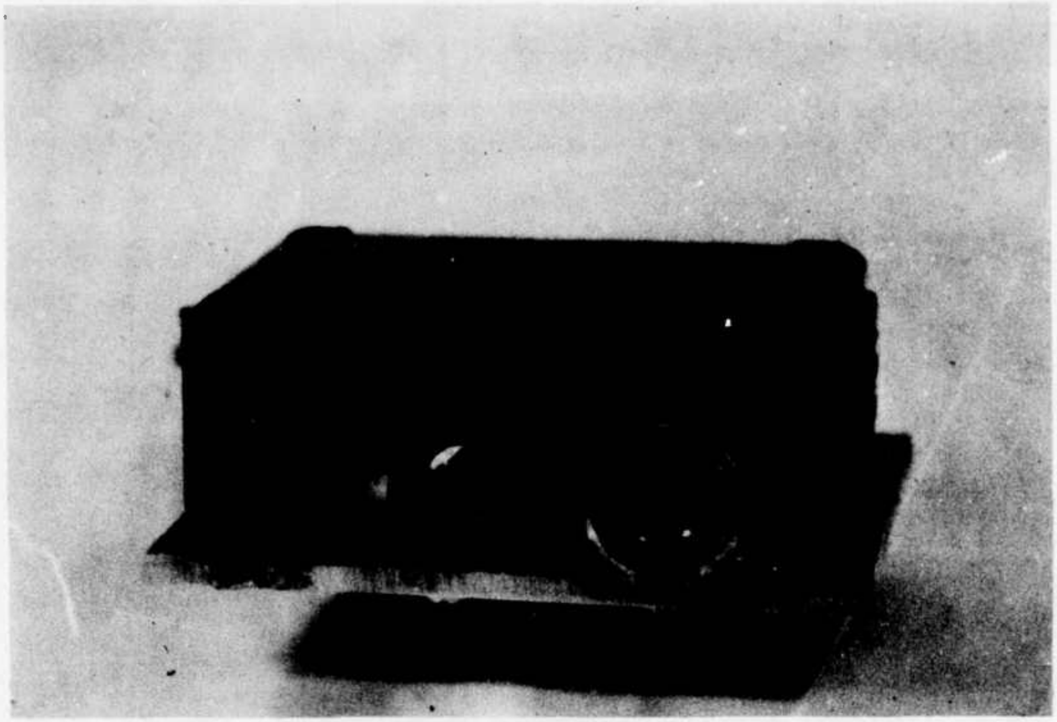

Figure 13. Typical LED Sensor Module

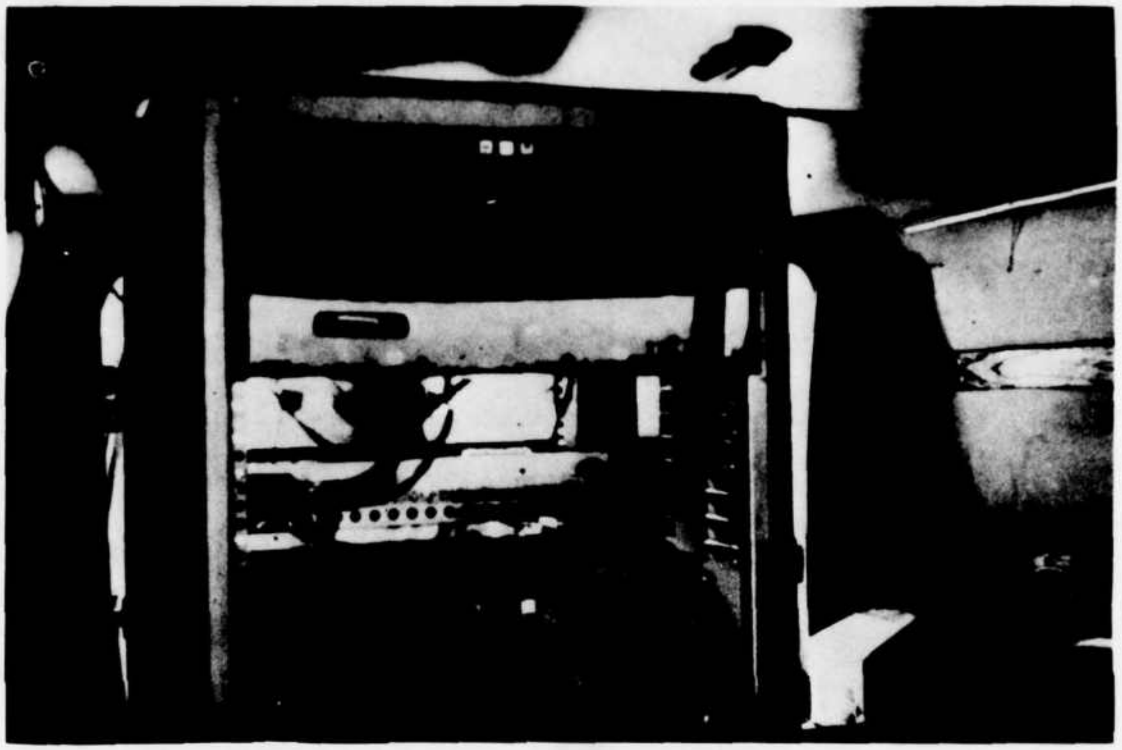

Figure 14. Magnetic Tape Recording Equipment

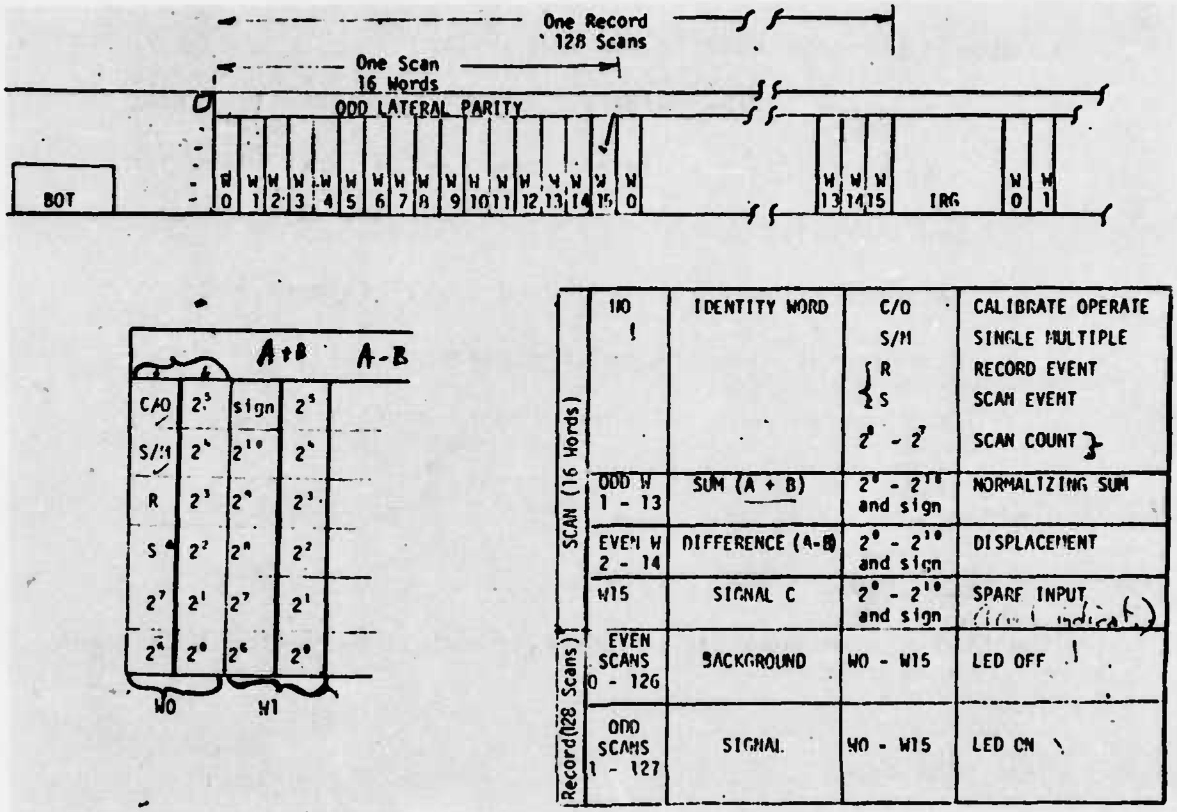

SCAN (16 Words)	W0	IDENTITY WORD	C/O S/M R S $2^0 - 2^7$	CALIBRATE OPERATE SINGLE MULTIPLE RECORD EVENT SCAN EVENT SCAN COUNT
	ODD W 1 - 13	SUM (A + B)	$2^0 - 2^{10}$ and sign	NORMALIZING SUM
	EVEN W 2 - 14	DIFFERENCE (A-B)	$2^0 - 2^{10}$ and sign	DISPLACEMENT
	W15	SIGNAL C	$2^0 - 2^{10}$ and sign	SPARE INPUT [illegible]
Record (128 Scans)	EVEN SCANS 0 - 126	BACKGROUND	W0 - W15	LED OFF
	ODD SCANS 1 - 127	SIGNAL	W0 - W15	LED ON

Figure 15. Arrangement of Data on Magnetic Tape (After Murphy [Reference 56])

demonstrates the basic arrangement of the data on the tape. Additional details on the tape decoding and data reduction computer programs are presented in Appendix C.

It should be noted that in the LED system:

1. The output, after being recorded on the magnetic tape, must be fed into a digital computer for data reduction and analysis, and
2. No contact (excepting infrared light) is made between the sensing elements and the pavement surface. The LVDT system required some (minor) contact within the deflection basin of the pavement.

4.2 The LVDT System

The LVDT system consists of three principal operational sections. They are:

a. the beam
b. the sensor elements
c. the recording system

a. The Beam

The beam is a modified wide flange aluminum I-beam. Its dimensions and principal features are shown schematically in Figure 16. A picture of the beam, set up in position for measurements, is shown in Figure 17.

b. The Sensors

The sensors are LVDT's. These are fixed on the beam as shown in Figure 17, with the sensing elements in contact, through adjustable jacks, with the pavement surface. The relative movement between the

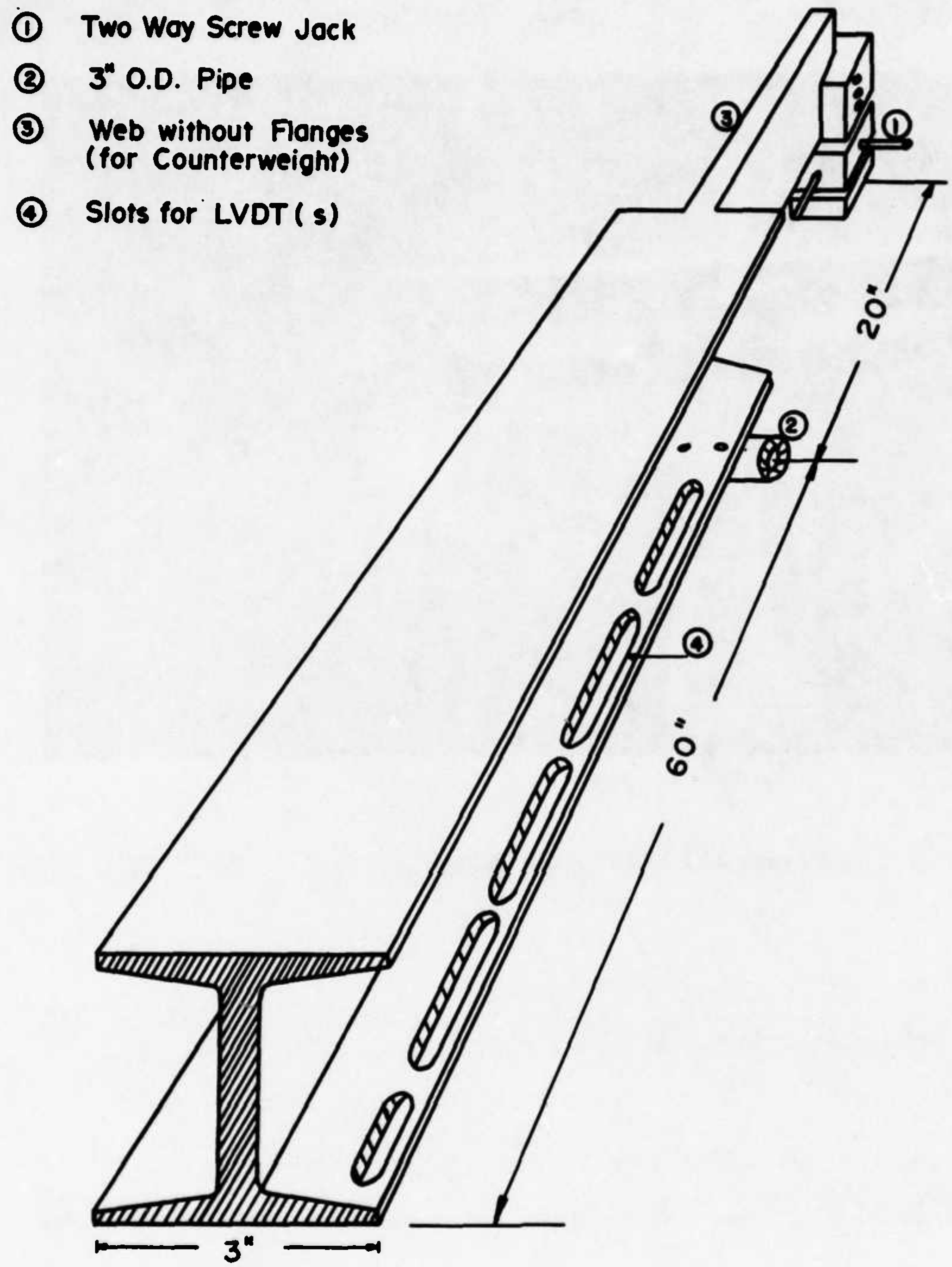

Figure 16. LVDT Beam Schematic Details

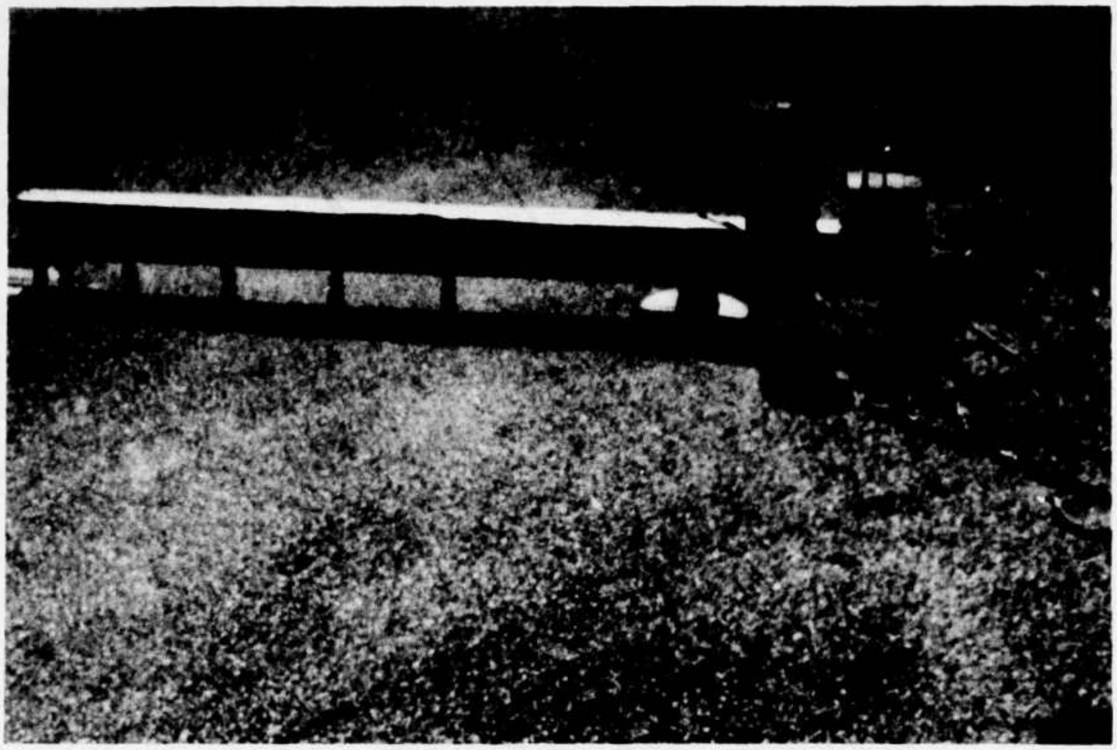

Figure 17. LVDT Beam Setup

core of the sensing element and the induction coil of the LVDT, fixed on the beam, produces a signal which is a measure of the displacement.

c. The Recording System

The LVDT recording system is a six channelled light beam recorder. Figure 18 shows the recorder used in this study. An analogue signal is recorded on light sensitive paper tape. The paper tape output can be converted to digital data by using a digitizing system (Reference 57) which automatically provides punch data cards.

It should be noted that, although the LVDT system requires contact between the pavement and the sensor, its simplicity, directness of data collection and ease of operation make it very adaptable for general use.

The LVDT and the LED systems were both used at various stages of this study.

//

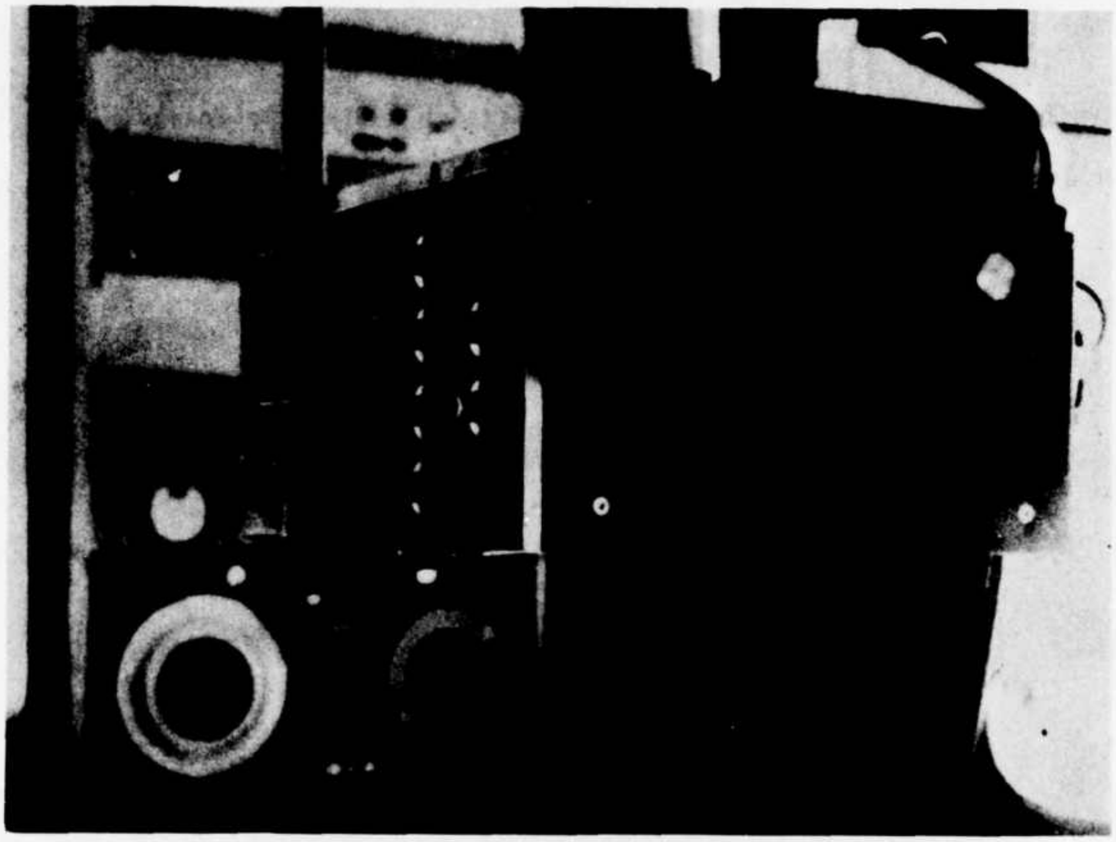

Figure 18. Project Light Beam Recorder

SECTION V

FIELD INVESTIGATIONS

The results of two series of field investigations were used in the validation of the evaluation and prediction schemes discussed previously. The first series of field investigations, Series A, was conducted during the course of this project. The second series, Series B, had been conducted in 1972 at Kirtland AFB and the basic data were reported by Boyer (Reference 11).

5.1 Series A Field Investigations

The principal objectives of this series of field investigations were:

1. To verify that the new nondestructive testing equipment, i.e., LED beam (and LVDT beam), can provide measurements of pavement deflection consistent with destructive test measurements.
2. To use the NDT (nondestructive testing) equipment to obtain deflection measurements for several different vehicles at different sites, for the purposes of providing initial input into the evaluation scheme developed in conjunction with the NDT equipment.
3. To show that the evaluation and prediction schemes are consistent with the factual information currently available.

The methodology evolved over the period of this study therefore reflects the need to satisfy the principal objectives.

The basic methodology with respect to equipment development, shown in Table 2, evolved over the period of this study. As can be seen from

TABLE 2. FIELD TESTING METHODOLOGY OF DEVELOPMENT

Stage	Method of Measuring Deflections	Features of Method	Distribution of Measurements
1.	Gages Installed in Pavement	(a) Destructive (b) Fixed	(a) Along one line
2.	LVDT Beam	(a) Nondestructive (b) Contact (c) Stationary	(a) Along one line and/or Global
3.	LED Beam	(a) Nondestructive (b) Noncontact (c) Stationary	(a) Along one line and/or Global
4.	LED Beam	(a) Nondestructive (b) Noncontact (c) Moving	(a) Global

Table 2 the method of measurement of deflections progressed in four steps from destructive fixed instrumentation, namely gages installed in the pavement, to noncontact, nondestructive instrumentation. Details of the gage installations, LVDT beam and the LED measurement systems are presented in Appendices A and B.

Deflection measurements were obtained during each step using different vehicles at different sites. The developed instrumentation was used as available for measurement purposes as shown in Figure 19. Figure 19 also shows a synopsis of the observed characteristics of the test sites, instrumentation and loading vehicles used in the Series A field investigation. Details of the sites and testing program conducted at each site during each phase are presented in Appendix B.

It should be recognized that the sites selected reflect reasonably well the extremes of the range of the airfield pavement conditions. Site 1 at Eglin AFB is a functionally failed flexible pavement and Site 2 is an in-service taxiway. The loading vehicles used also reflect a range of tire pressures using airfield pavements. The F-4 aircraft and the P-2 fire truck have tire pressures of 255 psi and 55 psi, respectively. The contrast in gross static wheel load also spans a reasonable range. The F-4 aircraft and the P-2 fire truck have gross single wheel[5] loads of approximately 25 kips and 8 kips, respectively. Figures 20 and 21 show the F-4 aircraft and the P-2 fire truck, respectively, and their pertinent characteristics. Figure 22 shows the F-4 load-cart loaded and unloaded. When loaded the central load wheel exerts a load on the pavement equivalent to a single main gear of the

[5] For the F-4, this refers to the main gear.

(a) EGLIN AFB: SITE 1

General Site Description: Severely Cracked: used as parking area.		
Date	Loading	Instrumentation
5-75	(a) P-2 Fire truck (b) F-4 Aircraft	(a) Gages installed in pavement
11-75	(a) P-2 Fire truck (b) F-4 Aircraft	(a) Gages installed (b) LVDT Beam (c) LED Beam[a]
3-76	(a) F-4 Load Cart	(a) LVDT Beam

Figure 19. Synopsis of Series A Field Investigation

(b) EGLIN AFB: SITE 2

General Site Description: Few cracks: in use as a taxiway		
Date	Loading	Instrumentation
5-75	(a) P-2 Fire truck	(a) Gages installed
11-75	(a) P-2 Fire truck	(a) Gages installed (b) LVDT Beam
3-76	(a) F-4 Load Cart	(a) LVDT Beam

Figure 19. (Continued)

(c) PEASE AFB

General Site Description: Uncracked in-service runway: Rutted by several passes of KC-135A Aircraft and P-2 Fire truck		
Date	Loading	Instrumentation
7-75	(a) P-2 Fire truck (b) KC-135A Aircraft	LVDT Beam

(d) EGLIN AFB: TAXIWAY

General Site Description: Cracked not-in service taxiway		
Date	Loading	Instrumentation
6-76[b]	F-4 Load Cart	(a) LED Beam[c] (b) LVDT Beam

a Stationary Beam - Moving Load operation

b 6000 feet of runway were also tested on this date.

c Moving Beam - Moving Load operation

Figure 19. (Concluded)

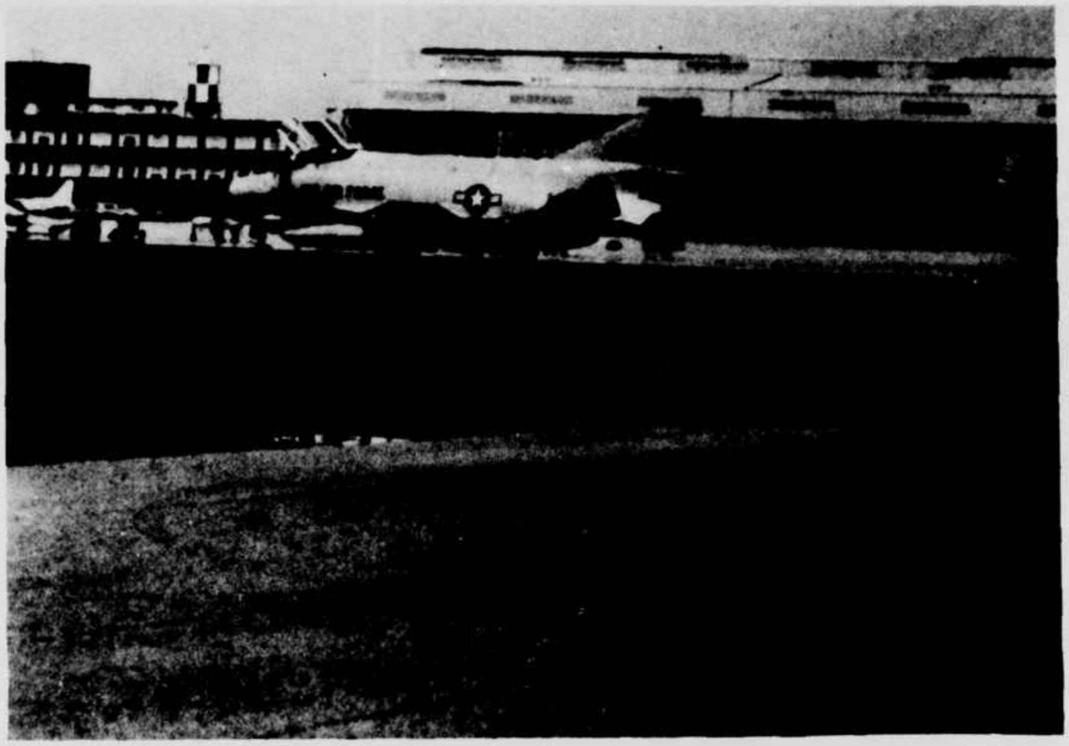

Gear Configuration	Single Wheel
Test Weight	25 Kips

Figure 20. F-4 Aircraft and Pertinent Characteristics

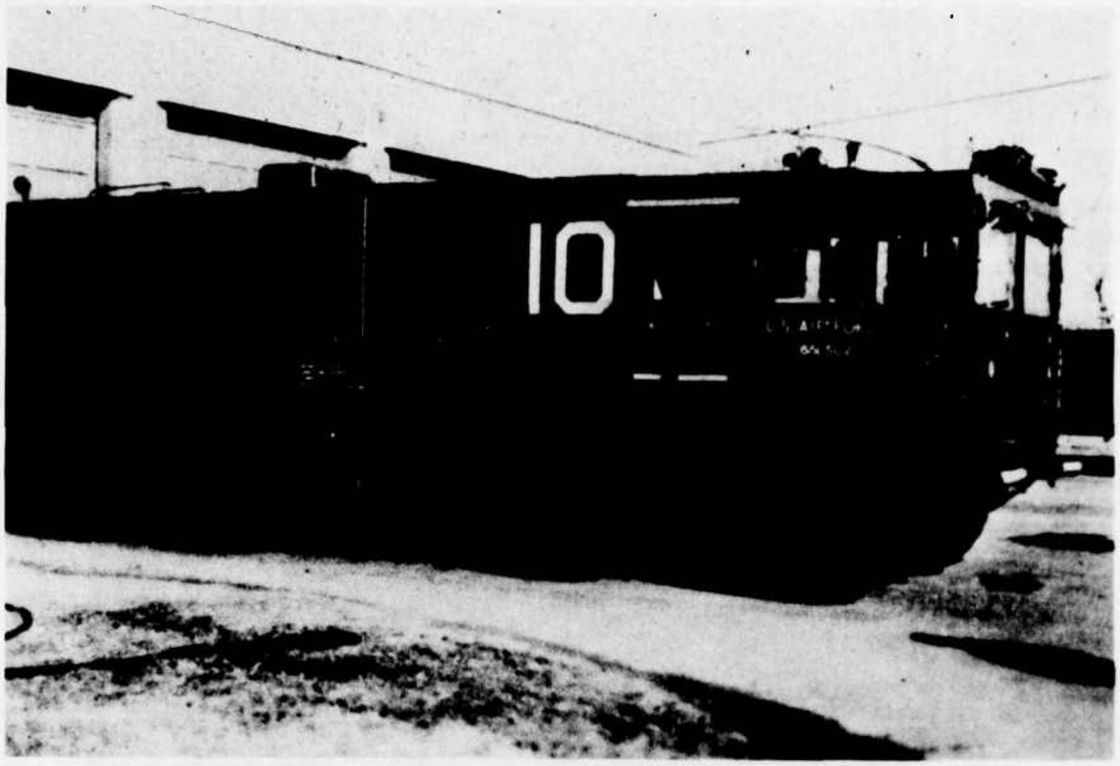

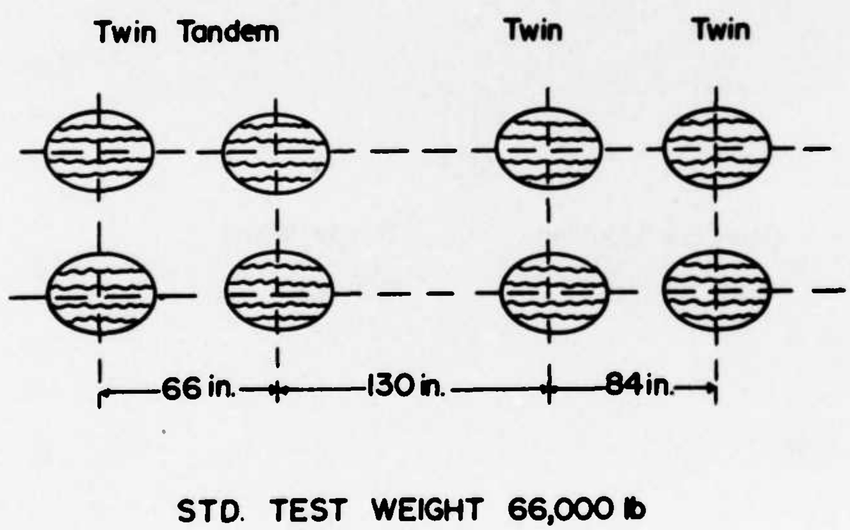

Figure 21. P-2 Fire Truck and Pertinent Characteristics

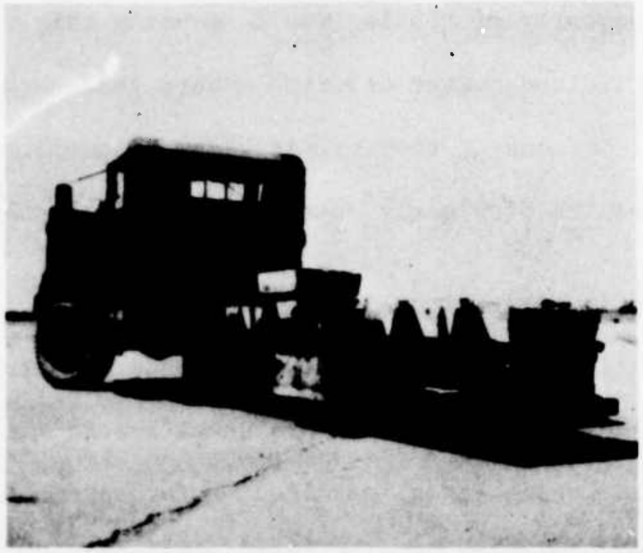

(a) Loaded

(b) Unloaded

Figure 22. F-4 Load Cart

F-4 aircraft. The majority of testing was done using this vehicle.

Because of the limited number of prime movers that were made available during the periods of testing, it became necessary to utilize some test results previously reported by Boyer (Reference 11).

5.2 Series B Field Investigations

The field investigations in Series B were conducted by Boyer at Kirtland AFB in New Mexico in 1972. In his investigation deflection measurements were made using gages installed in the pavement in a manner similar to the procedure used in the Series A field investigations. For details on his instrumentation and methodology the reader should refer to the original reference (Reference 11). The pavement characteristics at the three sites reported are shown in Figure 23. The prime movers and their characteristics are shown in Figures 24 through 26.

As previously stated the series B data provide additional information required to test the evaluation and prediction schemes. The gear configuration of the C-130, C-135 and C-131 provide, in addition to a variation in gross load and tire pressures, a loading function due to multiple and sequential wheel loads, and combinations thereof. The C-131 (single-twin) is an example of a multiple but not sequential loading function. The C-130 (single-tandem) is an example of a sequential[6] but partially multiple, loading function. The C-135 (twin-tandem) is an example of sequential and a multiple loading

---

[6] The P-2 fire truck is an example of a purely sequential loading function.

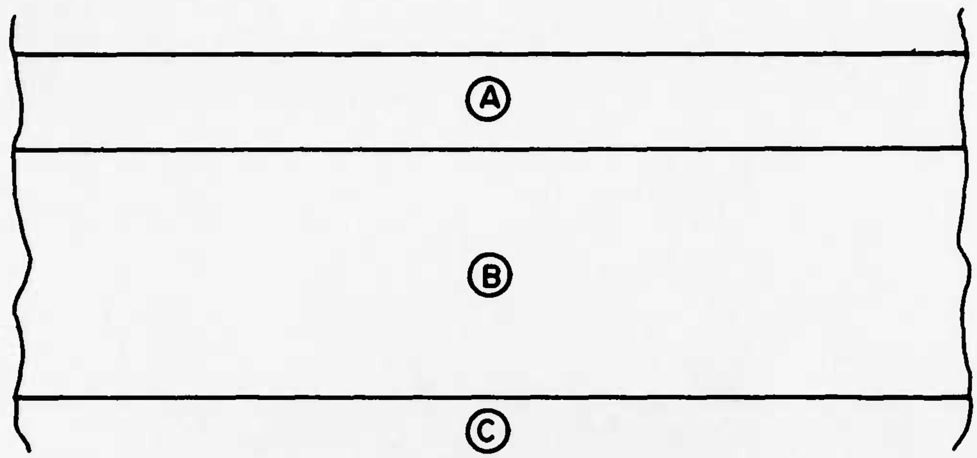

Test Site No.	Taxiway No.	A Asphaltic Concrete (in)	B Base Course (in)	C Subgrade
1	6	3	9	Silt/Sand
2	2	6.5	8	Silt/Sand
3	8	10	6	Highly Compacted Silt/Sand

Figure 23. Site Characteristics Series B Field Investigations (Reference 11)

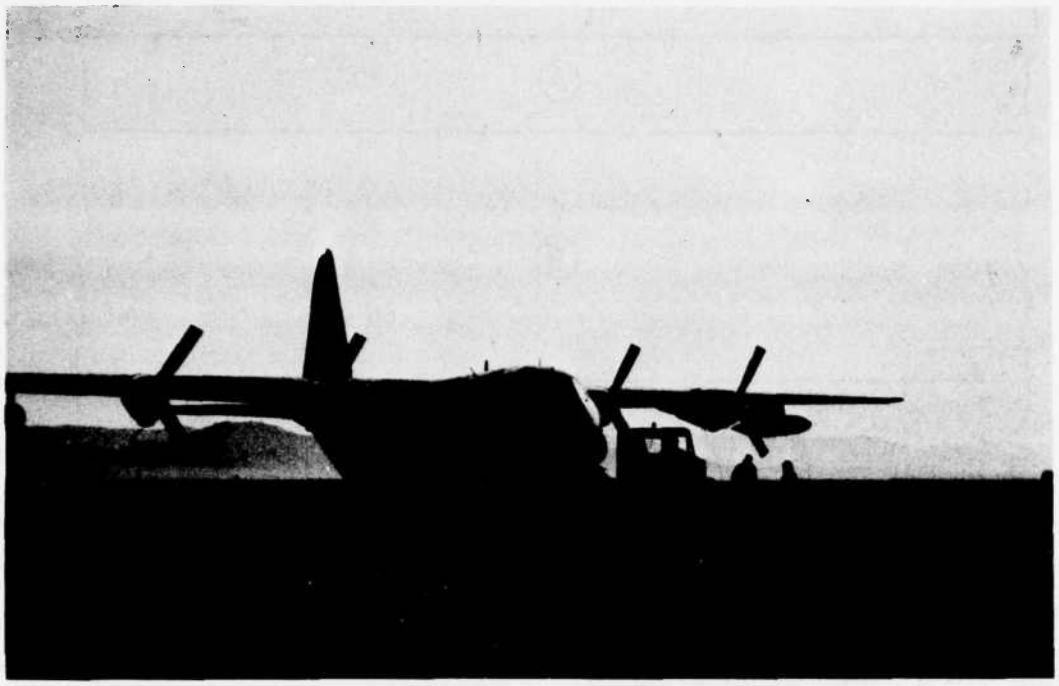

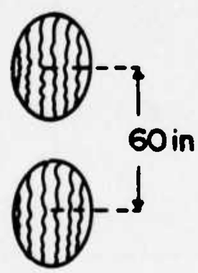

Gear Configuration	Single Tandem
STD. Test Weight	90 Kips (Gear load)

Figure 24. C-130 Aircraft and Pertinent Characteristics

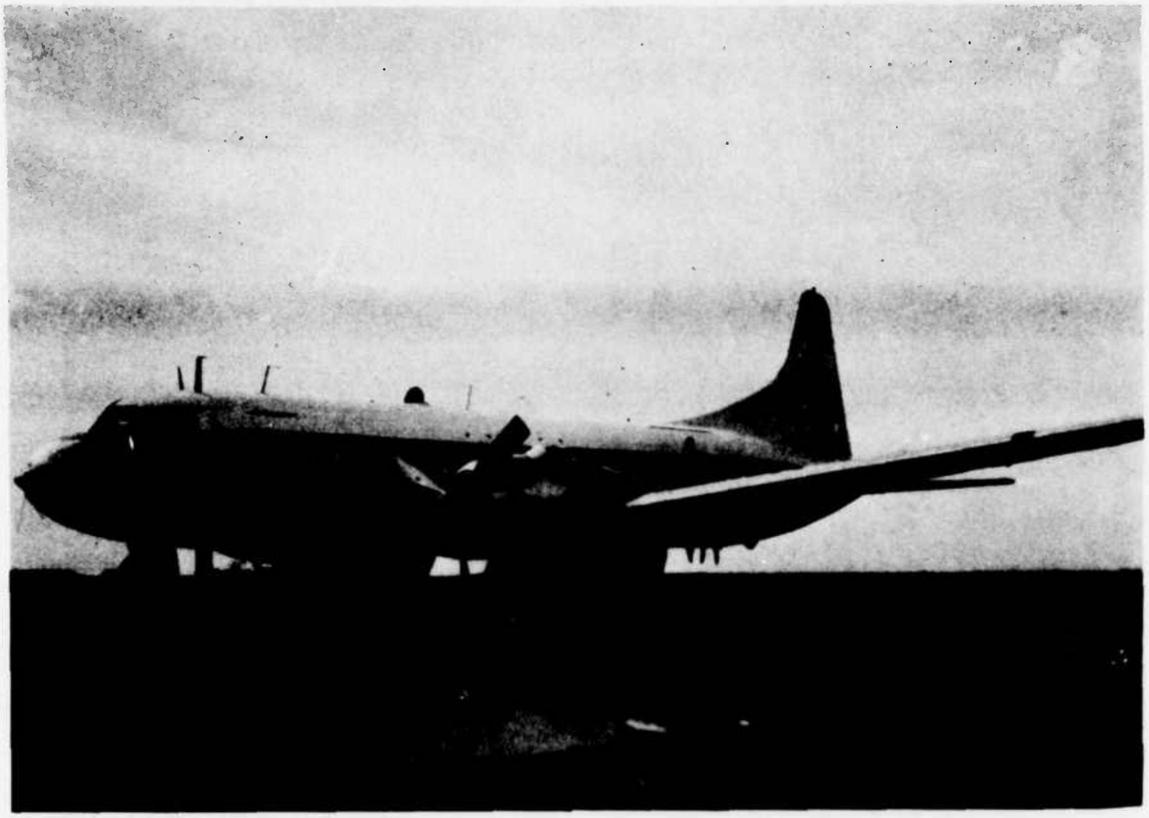

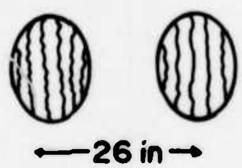

Gear Configuration	Single Twin
STD. Test Weight	20 Kips (Gear load)

Figure 25. C-131 Aircraft and Pertinent Characteristics

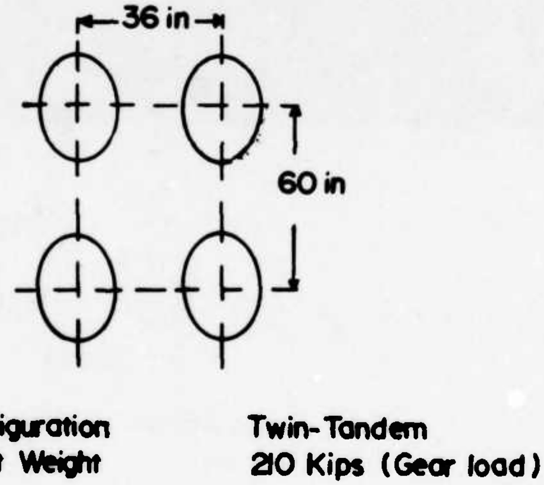

Figure 26. C-135 Aircraft and Pertinent Characteristics

function.

The data from the Series A and the Series B Field investigations were analyzed using the evaluation and prediction schemes previously presented.

SECTION VI

RESULTS

This research effort encompasses a broad spectrum of engineering activity ranging from the development of NDT equipment and a procedure for nondestructively evaluating flexible pavements, to the development of a methodology for predicting the deflection response of various pavements to different aircraft. This section presents the following:

1. typical results of equipment field verification tests,
2. results of the evaluation of the two sites (Series A: Field Investigations) using the developed evaluation scheme, and,
3. results of the application of the prediction methodology to three different aircrafts at three different sites (Series B: Field Investigations).

6.1 Equipment

It is necessary during the development of new equipment for measurement of pavement deflections to show that the new equipment provides measurements which are consistent with those obtained using established measurement systems. It is assumed that the LVDTs installed in the pavement comprise the absolute measurement system.

6.1.1 The LVDT System

The verification check of the LVDT system consisted of a comparison between pavement deflections measured by an LVDT mounted on the beam and an LVDT installed in the pavement as shown in Appendix B of this report.

Figure 27 shows a comparison of the pavement deflection measured

by an LVDT installed in the pavement and an LVDT mounted on the beam, and produced by the same pass of a P-2 fire truck during the testing sequence conducted at Eglin AFB, at Site 1 on November 17, 1975.

The results show that the installed LVDT and the LVDT mounted on the beam give basically the same measurements.

6.1.2 The LED System

The verification checking of the LED system consisted of two phases: a laboratory and a field testing phase.

The laboratory phase was conducted by Science Applications Incorporated, and is summarized in Appendix A of this report. The principal field checkout consisted of a comparison between the output[7] from an LED on the LED beam and the output from an LVDT mounted on the LVDT beam.

Figures 28 and 29 show the pavement deflections measured by the LED system and the LVDT system, respectively, and produced by one pass of a P-2 fire truck (Figure 21), during the testing sequence at Eglin AFB, Site 1, on November 19, 1975. Figures 30 and 31 show the actual digital output from the LED system and the analog output from the LVDT system as recorded by the light beam recorder. Since the deflections shown were measured for two separate passes of the P-2 fire truck, a direct comparison of measured deflections can not be made.

As stated previously a direct comparison of the measurements made by the two beams (LED and LVDT) could not be made since it is

---

[7] Due to persistent problems of compatibility between the LED modules and the magnetic tape recording unit, the LED output was recorded on a light beam recorder.

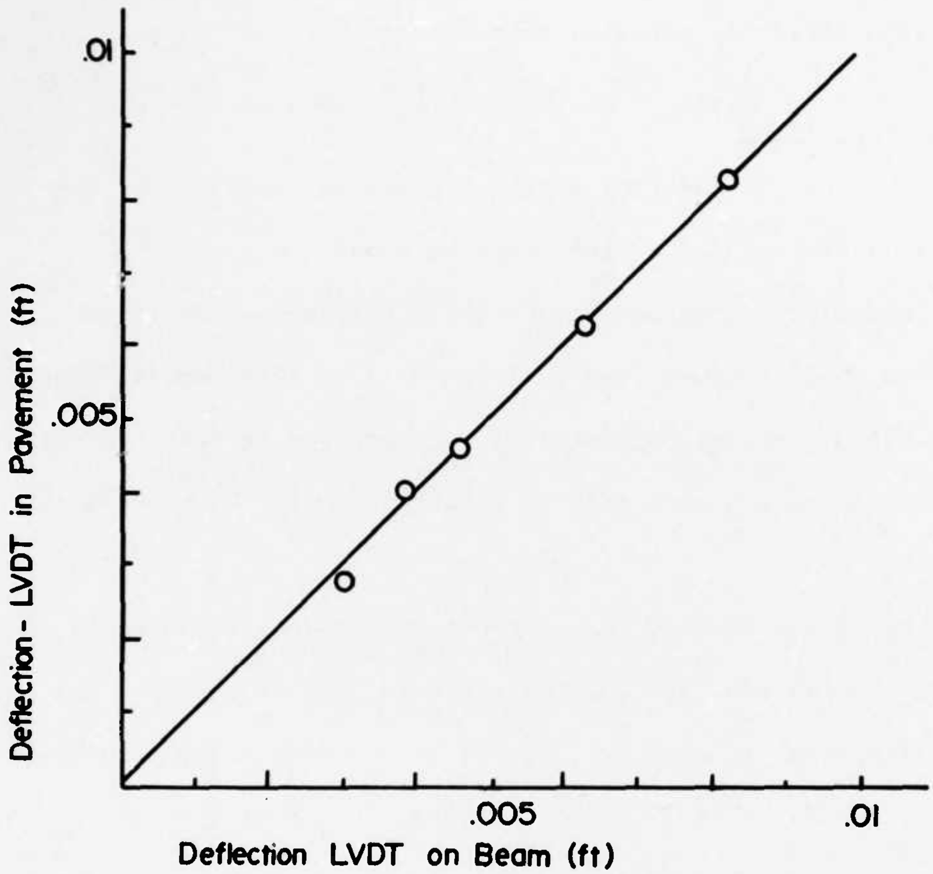

Figure 27. Comparison of LVDT on Beam and LVDT Installed in Pavement

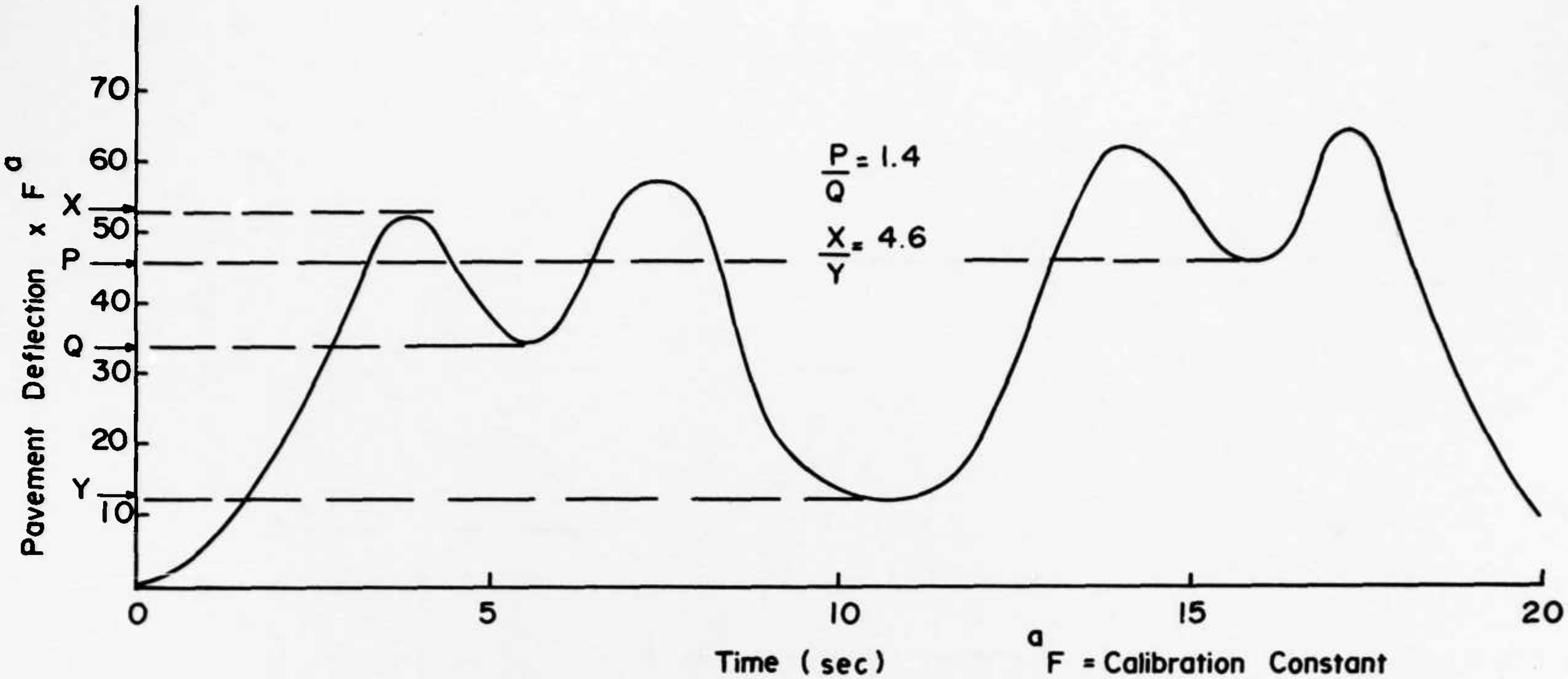

Figure 28. Pavement Deflections Measured by LED System: Eglin AFB - Site 1: P-2 Fire Truck Loading

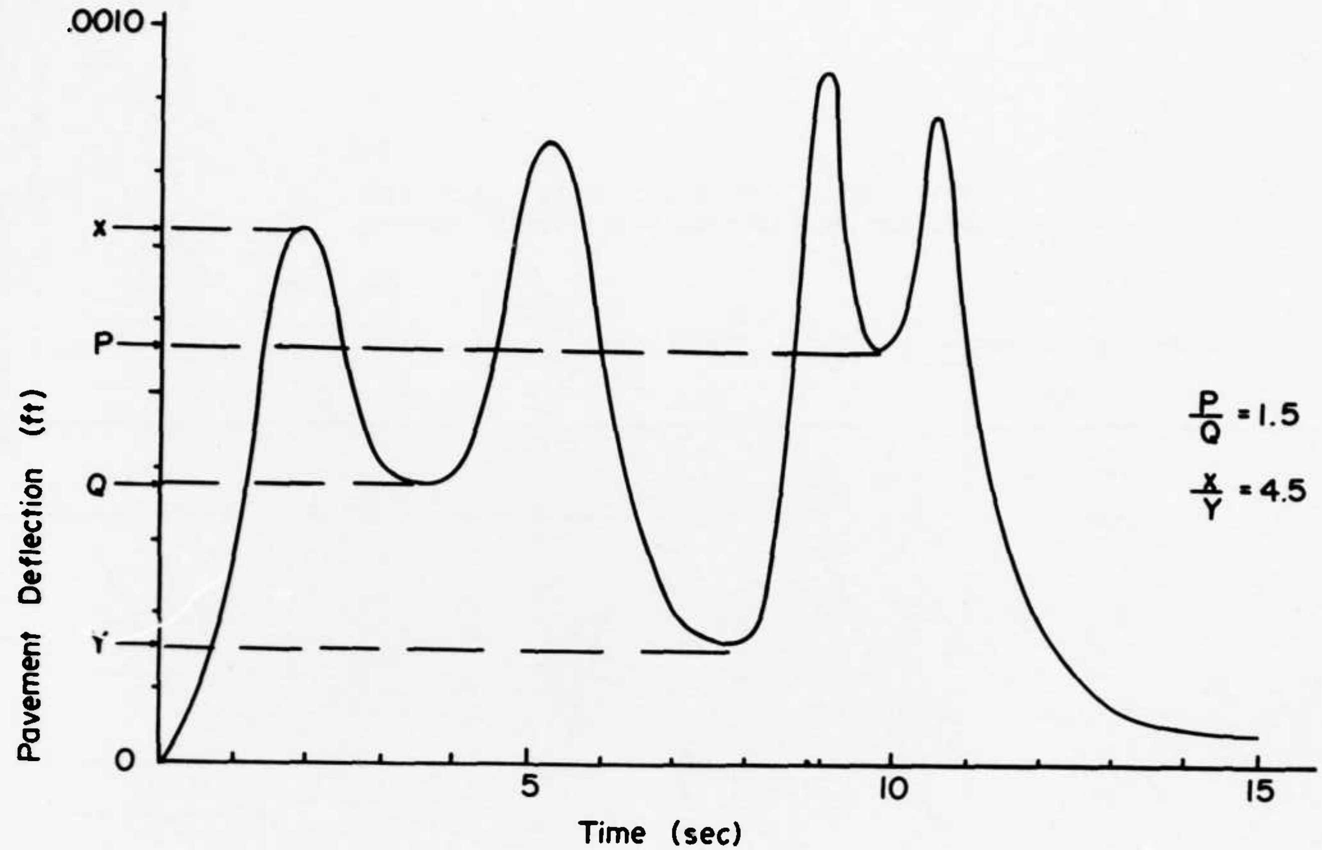

Figure 29. Pavement Deflection of Gage Closest to Edge of Wheel Measured by LVDT System: Eglin AFB - Site 1: P-2 Fire Truck Loading

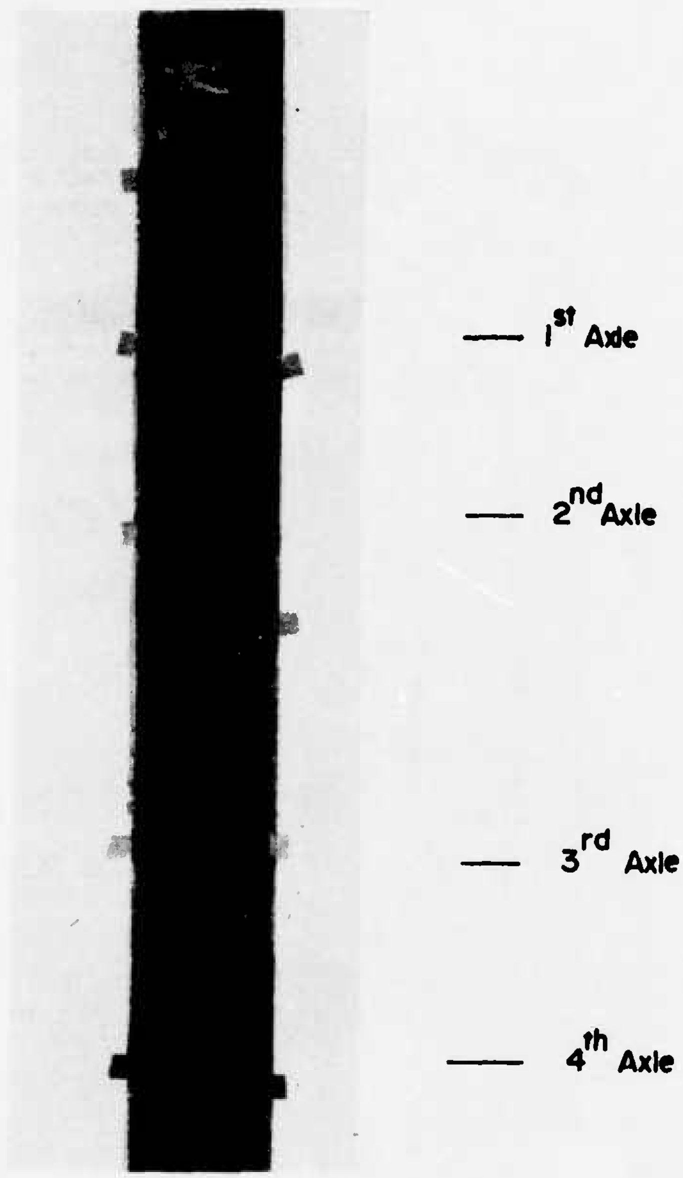

Figure 30. Actual Digital Output From LED System On Light Beam Recorder: P-2 Fire Truck Is Loading Vehicle

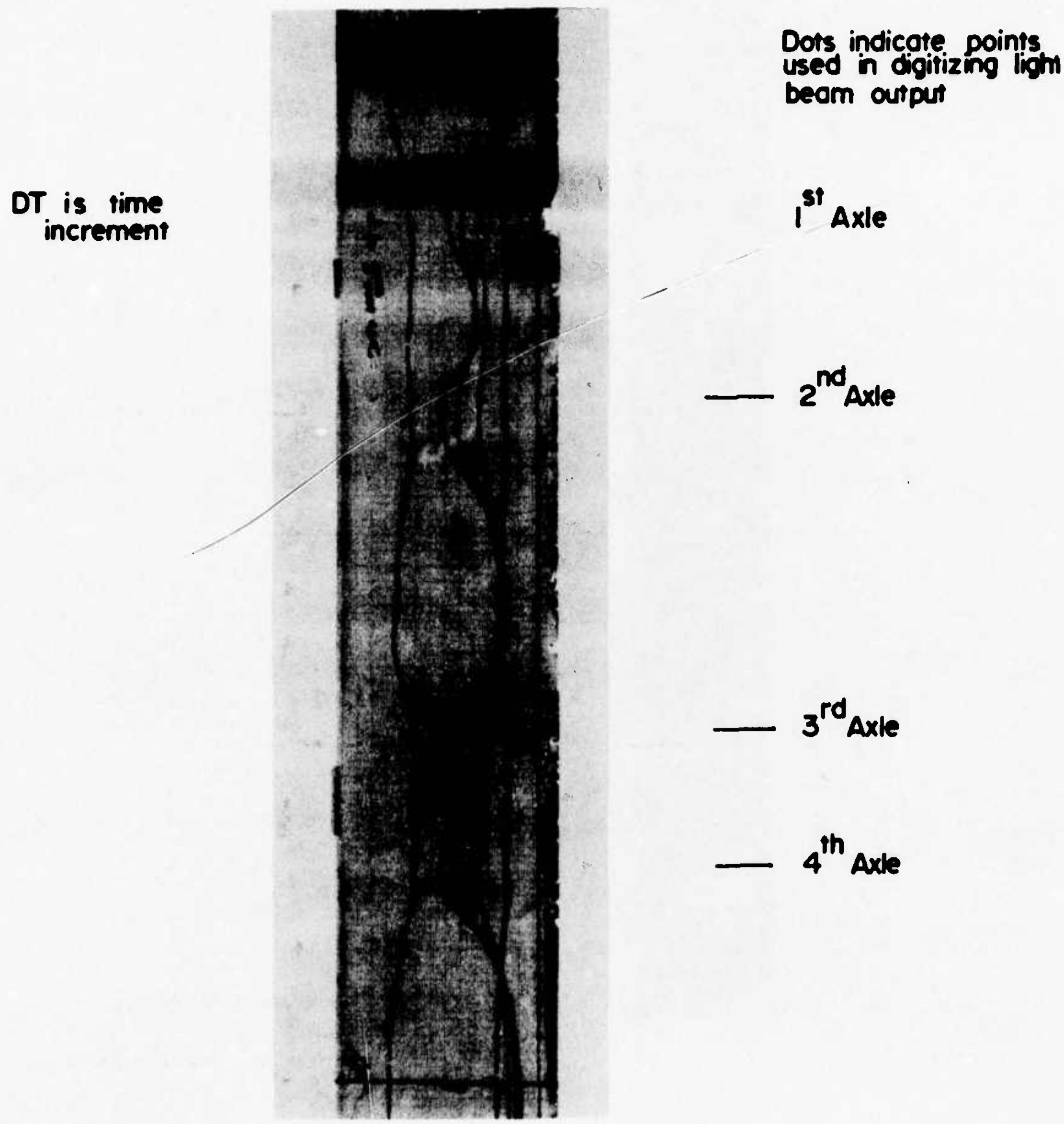

Figure 31. Analog Output From LVDT System: P-2 Fire Truck

impossible to get the two beams over the same point at the same time. Thus, a comparison was made of significant points on the measured deflection plots; e.g., peaks and troughs. The points P, Q, X and Y were selected, where P is the minimum deflection between the second two peaks of the deflection time plot; Q is the minimum deflection between the first two peaks; X is the first peak and Y is the minimum between the first two peaks and the last two peaks. The ratios P/Q and X/Y are thus dimensionless, and are independent of the system (dependent) calibration constants. That is,

$$\frac{X}{Y} = \frac{\text{Actual Light Beam Recorder Output at point X times Constant}}{\text{Actual Light Beam Recorder Output at point Y times Constant}}$$

$$= \frac{\text{Pavement Deflection corresponding to X}}{\text{Pavement Deflection corresponding to Y}}$$

Figures 28 and 29 show that the corresponding ratios have essentially the same values. Both the P/Q and the X/Y ratios differ by only 0.1.

From the discernable deflection observable at point Y in Figure 28 and Figure 29, it can be seen that measurements of less than 0.0001 feet are obtainable by both the LED and LVDT systems.

In June 1976, both the LVDT and the LED systems were used in connection with a study to investigate the difference in the dynamic response of aircraft.

A mechanical system was designed to allow the LED beam to be rigidly mounted on the F-4 load cart. The system was fabricated at Tyndall Air Force Base by Air Force personnel and was then transported to Eglin AFB. At Eglin, 2000 feet of taxiway and 1 1/4 miles of runway

were tested using the LED system attached to the F-4 load cart as shown in Figure 32. The LED measured deflections due to the load wheel of the F-4 load cart as the load cart moved at creep speeds over the pavement. LED measurements were made continuously. The LVDT system was used to make deflection measurements at stations 100 feet apart as the load cart passed in front of the stationary beam. The continuous measurements made by the LED were synchronized with the LVDT stations by the use of an electronic event marker of the LED system. The synchronization allowed the time at which the load wheel passed the LVDT stations to be recorded on the magnetic tape to within 0.25 sec as follows. At the instant the load wheel passed the LVDT station marked on the taxiway, a button was depressed on the control panel of the LED system. This caused a digital record to be made on magnetic tape. Since the scan rate was four scans per second, an event marker could be recorded to within 0.25 seconds, which constituted one scan. Figure 33 shows a summary of the taxiway deflection data. The deflections on the dashed line in Figure 33 were measured at locations offset by about 20 feet from the previous measurement locations. Listing of typical measurements[8] made by the LED system is given in Appendix D.

The results shown on Figures 28 and 29 indicate that the pavement deflection measurements with the LED system are consistent with those of the LVDT system, in form; and the LED can measure deflections with the desired accuracy in a field environment.

---

[8] The LED system data reduction software, a complete listing of all the taxiway data, and a copy of the data (on magnetic tape) has previously been supplied to the Civil Engineering Center, Tyndall AFB, Florida.

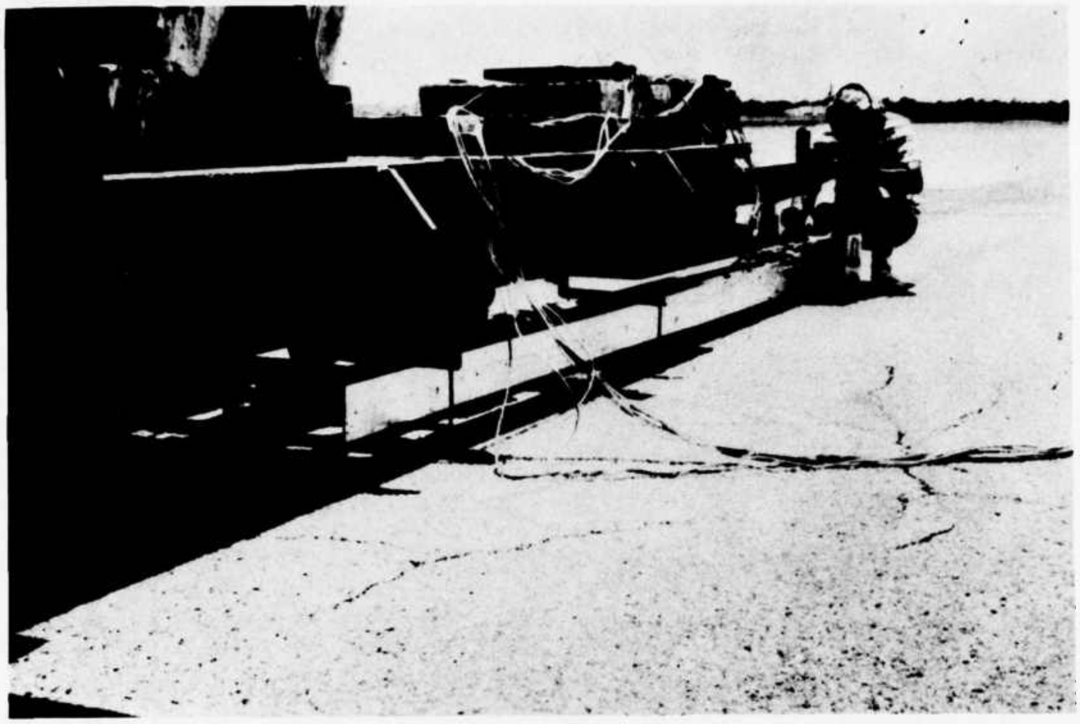

Figure 32. Setup During Moving Beam - Moving Load Operation: F-4 Load Cart

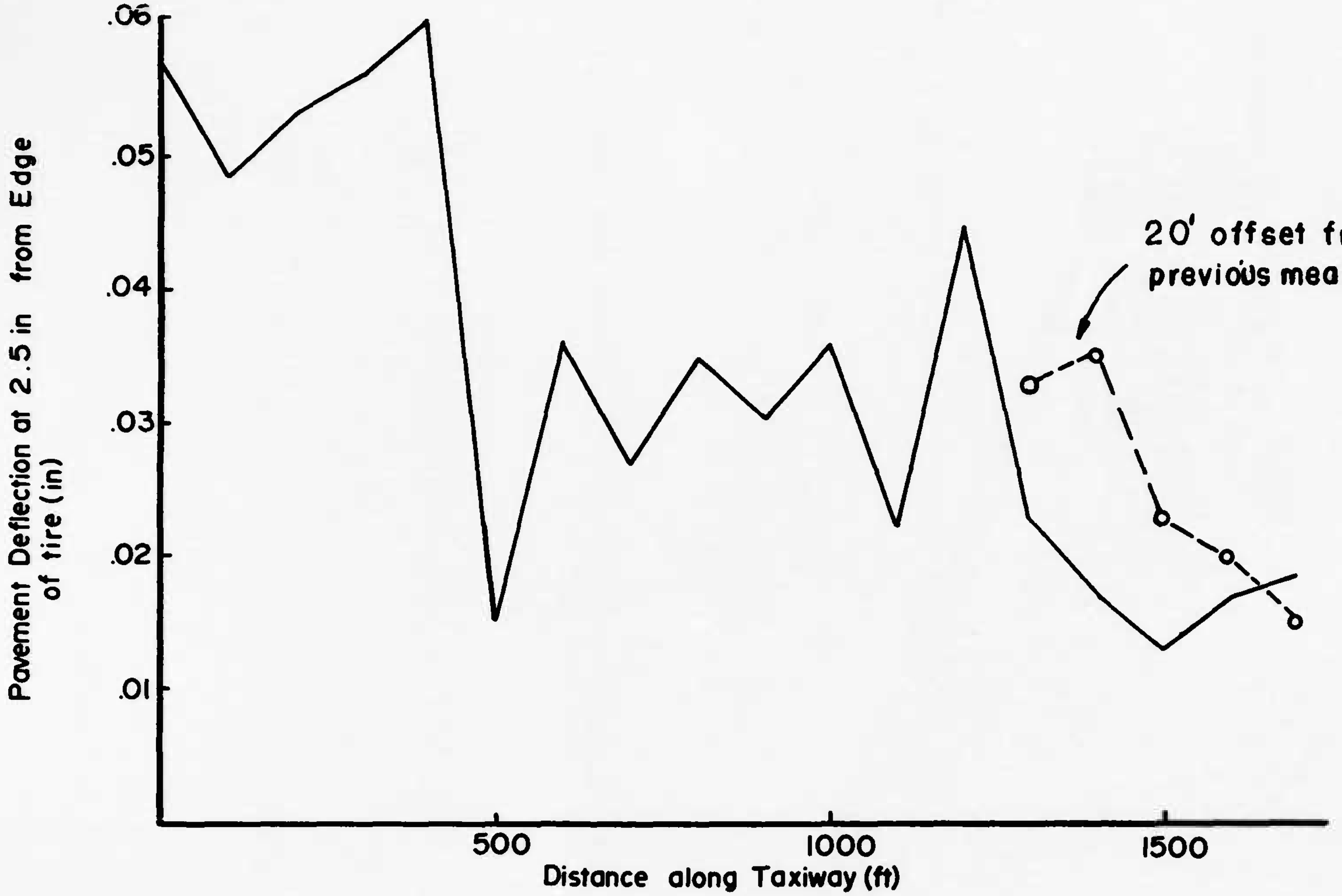

Figure 33. Summary of Taxiway Deflection Measurements-Eglin AFB 1976

6.2 Evaluation

Evaluation, as presented here, consists of the following:

1. determining the parameters A_{peak}, β_{peak}, and r_{peak} of the maximum lateral deflection profile due to F-4 loadings,
2. obtaining the k, c, and m parameters of the transfer function, and
3. relating the determined parameters to performance.

   The two sites in Series A field investigation are compared using the data obtained during the field testing program conducted at Eglin AFB in March 1976. As the F-4 aircraft is the vehicle of primary interest in this study only the results obtained using the F-4 load cart are presented in this section. A more complete listing of the data base and results is given in Appendix D.

Briefly, the evaluation procedure consisted of measuring pavement deflections using the LVDT beam as the F-4 load cart passed in a direction perpendicular to the stationary LVDT beam. From these deflections, the parameters A_{peak}, β_{peak}, and r_{peak} of the maximum lateral deflection profile, and the signature were determined as discussed in detail in paragraph 3.2.1. The k, c, and m parameters at each site were then obtained using the methodology of paragraph 3.2.2.

6.2.1 Pavement Deflections

Figure 34 shows a typical set of deflection functions due to the F-4 load cart as measured by the LVDT beam. Gage 1, which recorded

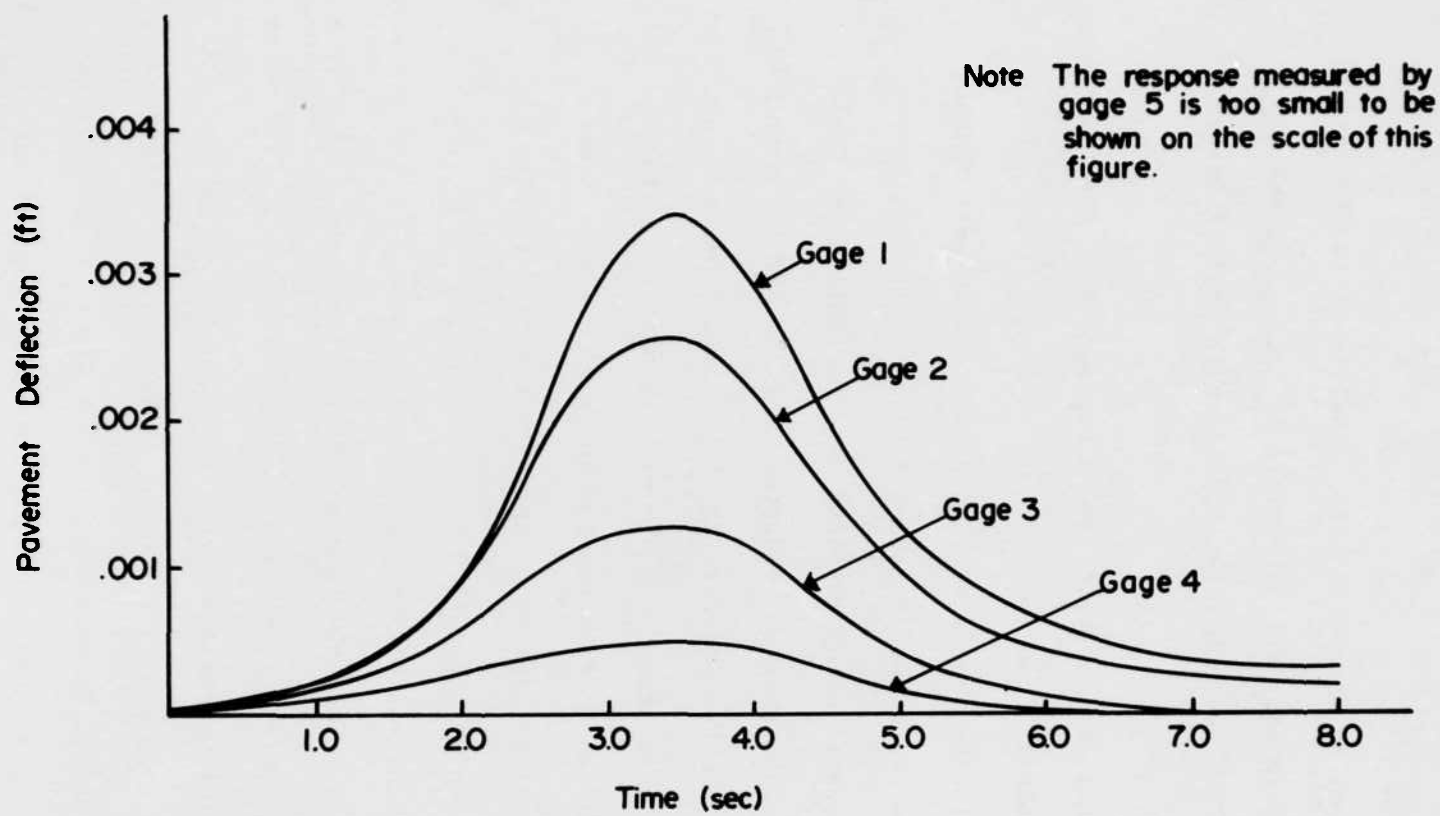

Figure 34. System Response Functions F-4 Loading: Eglin Site 1 (Typical)

the largest deflection is located closest to the wheel. Figure 35 shows the maximum deflection of each gage plotted against the distance of the gage from the edge of the tire print. The dashed line through the points G-1 through G-5 is the lateral profile of maximum deflections at Site[9] 1 for one pass of the F-4 load cart. Figure 35 also shows the A_{peak}, β_{peak}, and r_{peak} parameters determined as discussed in paragraph 3.2.1 and the maximum deflections at each gage calculated by equation 2. Figure 36 shows a similar plot for one pass of the F-4 load cart at Site 2. Tables 3 and 4 give the stations[10] and values of the A_{peak}, β_{peak}, and r_{peak} value for Sites 1 and 2, respectively. Figures 37 and 38 show the variability in the measured maximum lateral deflection values for Sites 1 and 2, respectively. Figures 39 and 40 show a comparison of the local and site characteristics at the two sites as given by the A_{peak}, β_{peak}, and r_{peak} values. "Local" refers to a station or location at a "site". The lines in these figures are drawn for convenience and do not represent continuity of parameter values. Figure 41 shows the typical effects of two consecutive passes on the maximum lateral pavement deflection profiles.

These results show the following:

1. The gage (Gage 1, Figure 34) closest to the wheel records the maximum deflection and retains the most permanent set after the wheel load has passed. The gage (Gage 4, Figure 34) farthest from the wheel does the opposite; namely,

---

[9] Sites are indicated in Figures B-1(a) and B-3(a).

[10] Stations are given in Appendix B, Figures B-1(b) and B-3(b).

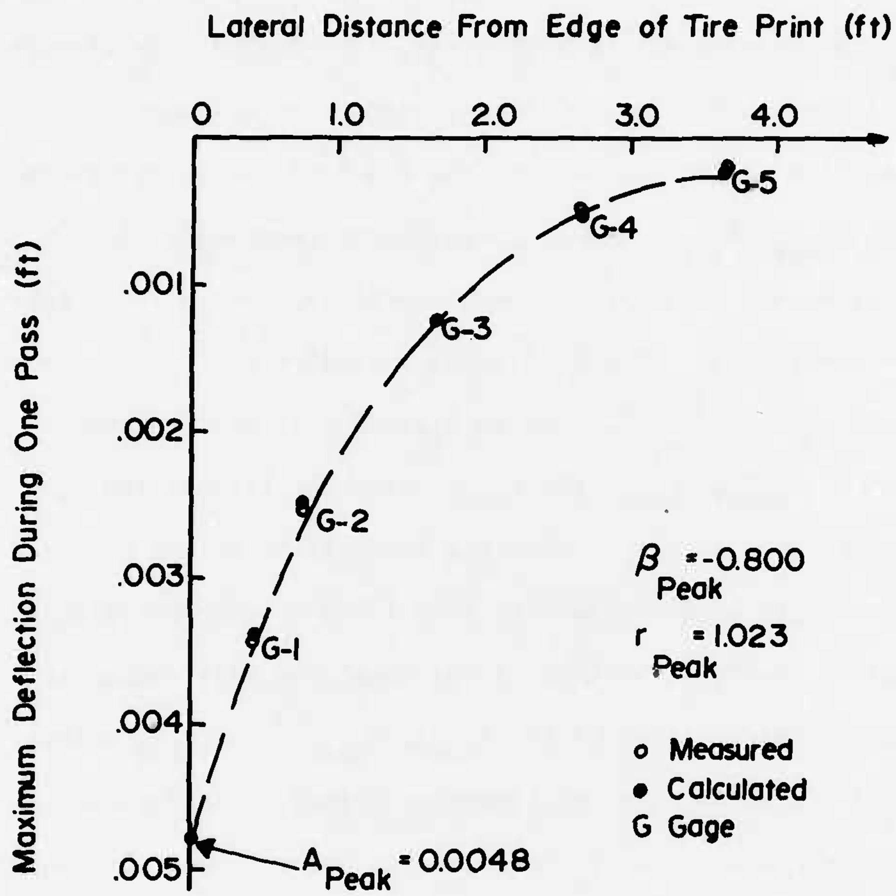

Figure 35. Eglin AFB: Site 1 Lateral Profile of Maximum Deflections for F-4 Loading (Typical)

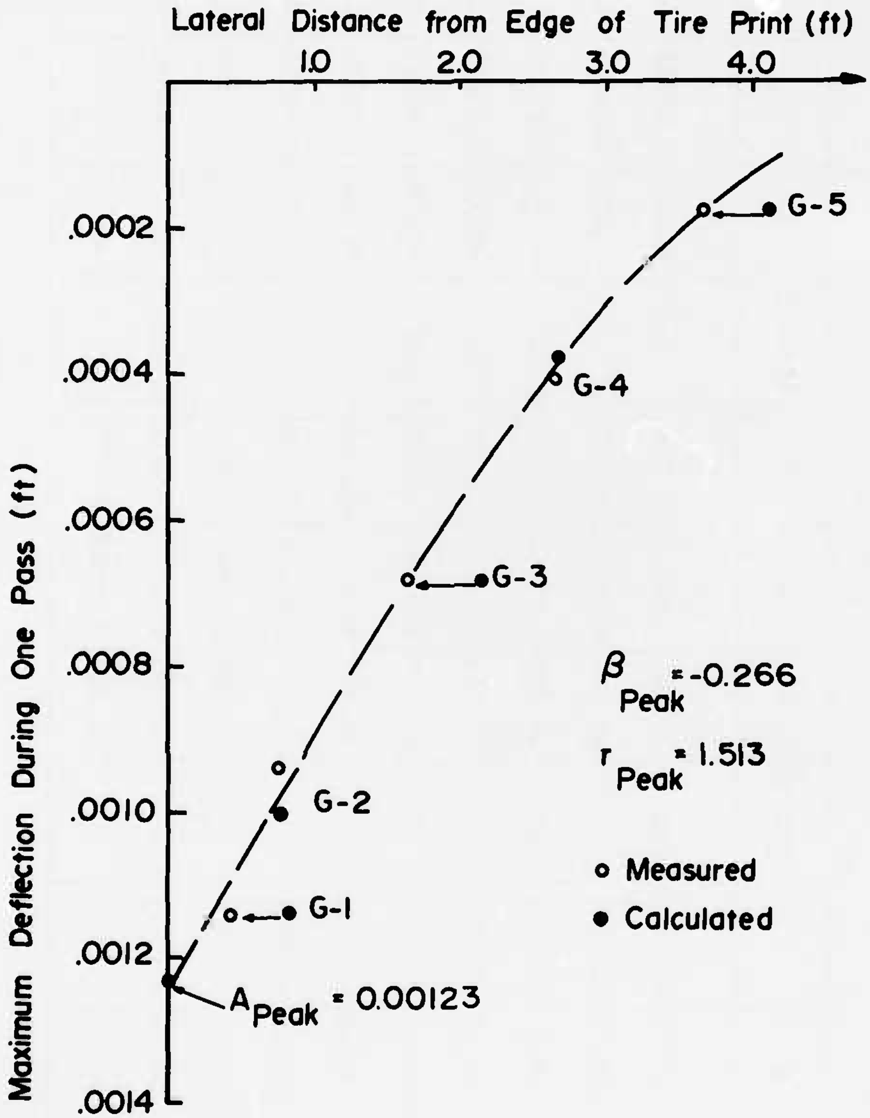

Figure 36. Eglin AFB: Site 2 Lateral Profile of Maximum Deflection for F-4 Loading (Typical)

AD-A047 161 NONCONTACT NONDESTRUCTIVE DETERMINATION OF PAVEMENT DEFLECTION UNDER MOVING LOADS(U) PURDUE RESEARCH FOUNDATION LAFAYETTE IN M E HARR ET AL AUG 77 2/4

UNCLASSIFIED FAA-RD-77-127 DOT-FA73WAI-361 F/G 13/2 NL

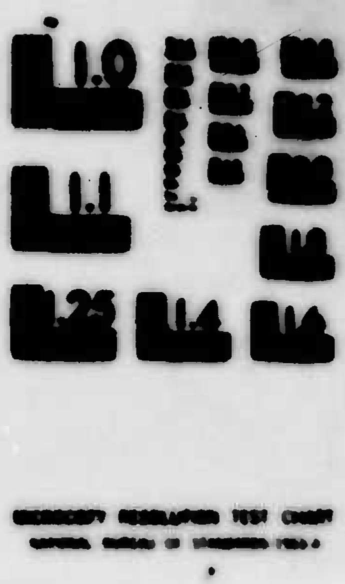
1.0
1.1
1.25
1.4
1.6

TABLE 3. PARAMETERS[a] OF THE [illegible] LATERAL [illegible] PROFILES, [illegible], MARCH 1976, SITE 1

Station	[illegible]	[illegible]	[illegible]	Station	[illegible]	[illegible]	[illegible]	Station	[illegible]	[illegible]	[illegible]
A1	[illegible]	[illegible]	[illegible]	B1	[illegible]	[illegible]	[illegible]	C1	[illegible]	[illegible]	[illegible]
	[illegible]	[illegible]	[illegible]		[illegible]	[illegible]	[illegible]		[illegible]	[illegible]	[illegible]
A2	[illegible]	[illegible]	[illegible]	B2	[illegible]	[illegible]	[illegible]	C2	[illegible]	[illegible]	[illegible]
	[illegible]	[illegible]	[illegible]		[illegible]	[illegible]	[illegible]		[illegible]	[illegible]	[illegible]
	[illegible]	[illegible]	[illegible]	B3	[illegible]	[illegible]	[illegible]	C3	[illegible]	[illegible]	[illegible]
A3	[illegible]	[illegible]	[illegible]		[illegible]	[illegible]	[illegible]		[illegible]	[illegible]	[illegible]
A4	[illegible]	[illegible]	[illegible]	B4	[illegible]	[illegible]	[illegible]	C4	[illegible]	[illegible]	[illegible]
	[illegible]	[illegible]	[illegible]		[illegible]	[illegible]	[illegible]		[illegible]	[illegible]	[illegible]
A5	[illegible]	[illegible]	[illegible]	B5	[illegible]	[illegible]	[illegible]	C5	[illegible]	[illegible]	[illegible]
	[illegible]	[illegible]	[illegible]		[illegible]	[illegible]	[illegible]		[illegible]	[illegible]	[illegible]

a) [illegible], respectively.

TABLE 4. PARAMETERS[a] OF THE MAXIMUM LATERAL DEFLECTION PROFILE, [illegible] AFB, MARCH 1976, TEST 2

Station	[illegible]	A	B	Station	[illegible]	A	B	Station	[illegible]	A	B
A1	-0.440	[illegible]	-0.445	B1	-0.472	0.00253	-0.265	C1	[illegible]	0.00272	[illegible]
A2	-0.342	[illegible]	[illegible]		-0.470	0.00239	-0.270		-0.958	[illegible]	[illegible]
	-0.343	[illegible]	[illegible]	B2	-0.477	0.00212	[illegible]	C2	[illegible]	[illegible]	[illegible]
A3	[illegible]	[illegible]	[illegible]		[illegible]	[illegible]	-0.476		[illegible]	[illegible]	[illegible]
A4	-0.374	[illegible]	[illegible]	B3	[illegible]	[illegible]	-0.473	C3	[illegible]	[illegible]	[illegible]
	-0.370	[illegible]	[illegible]		-0.475	[illegible]	[illegible]		[illegible]	[illegible]	[illegible]
A5	-0.379	[illegible]	[illegible]	B4	-0.393	[illegible]	[illegible]	C4	[illegible]	[illegible]	[illegible]
	[illegible]	[illegible]	[illegible]	B5	[illegible]	[illegible]	[illegible]	C5	-0.727	[illegible]	[illegible]
	0.777	[illegible]	[illegible]		[illegible]	[illegible]	[illegible]		[illegible]	[illegible]	[illegible]

a) See footnote Table 3.

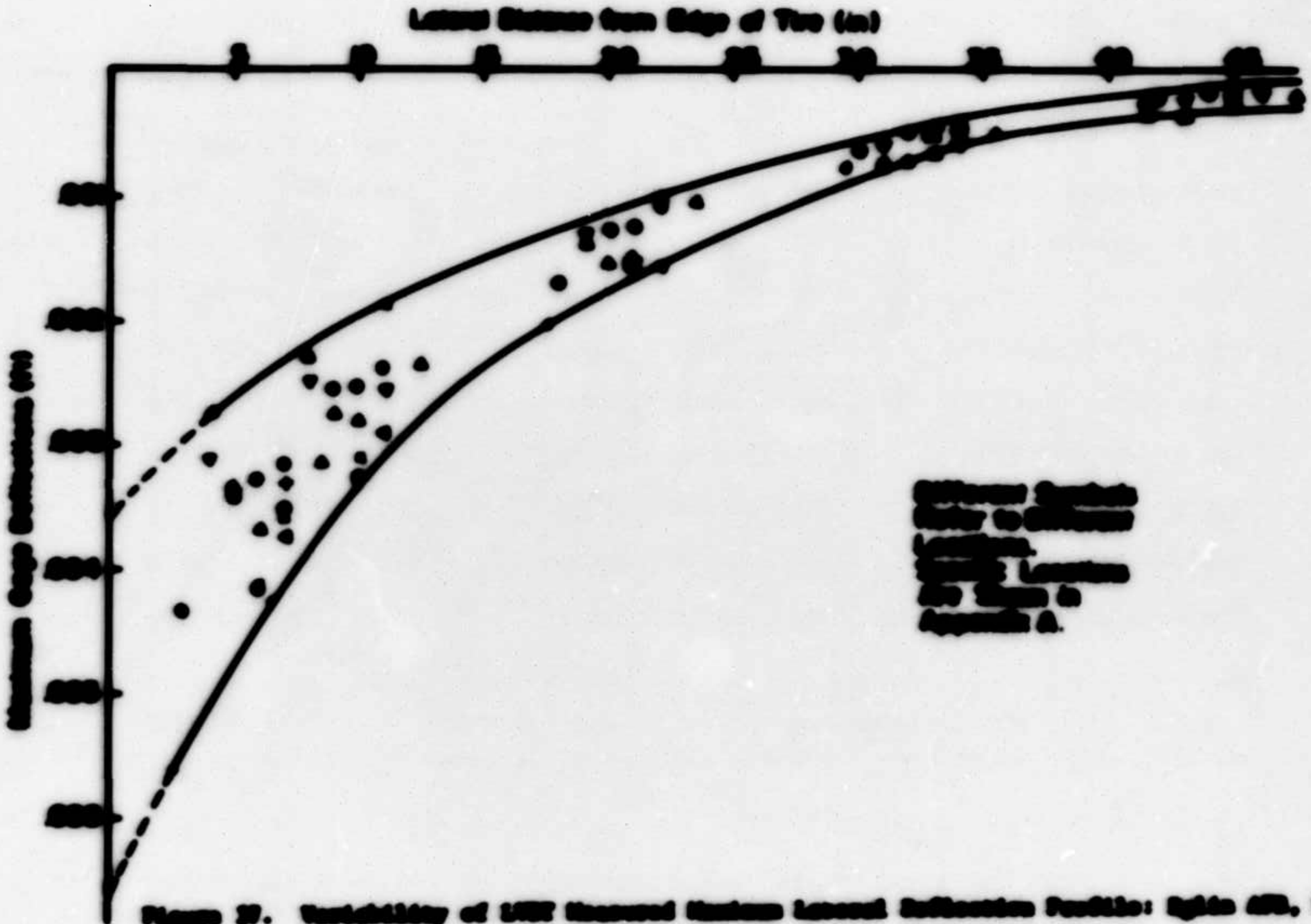

Figure 37. Variability of [illegible] Measured Maximum Lateral Deflection Profile: [illegible], Site 1
March [illegible]

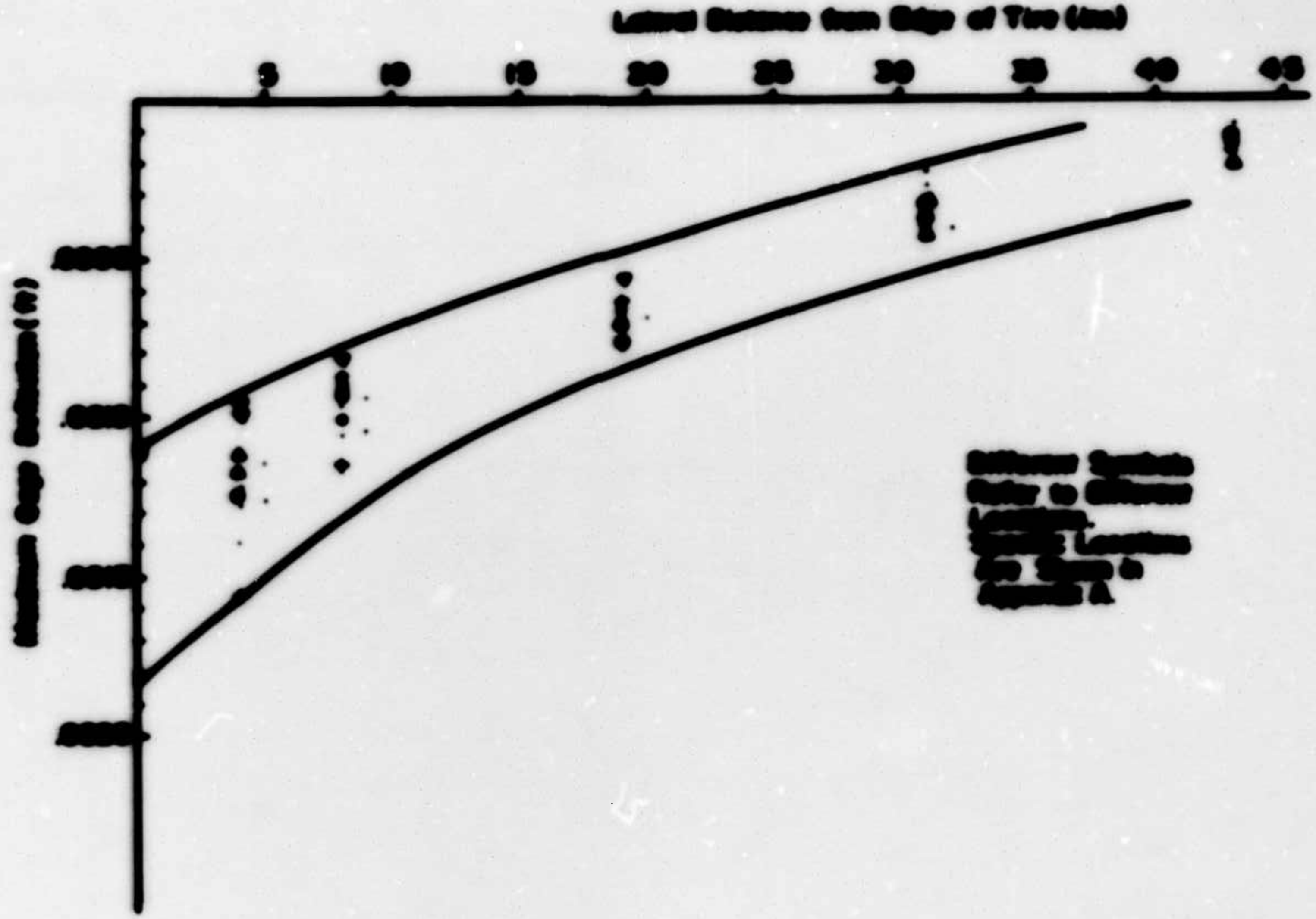

Figure [illegible]. Variability of Maximum Lateral Deflection Profiles: [illegible], Site 2, [illegible]

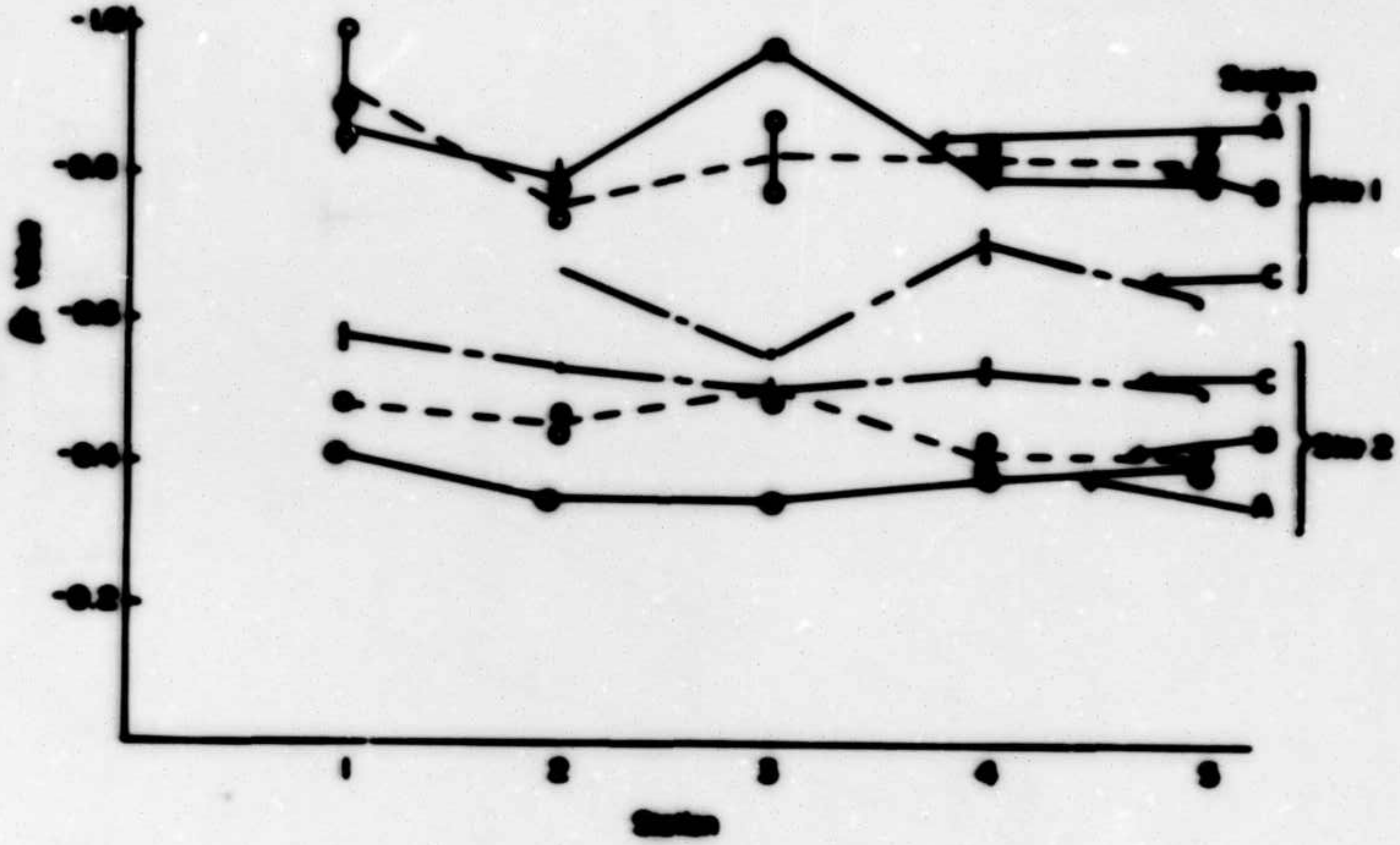

Figure 39. Comparison of Local and Site Characteristics as Shown by Δr values: Eglin AFB, March 1976

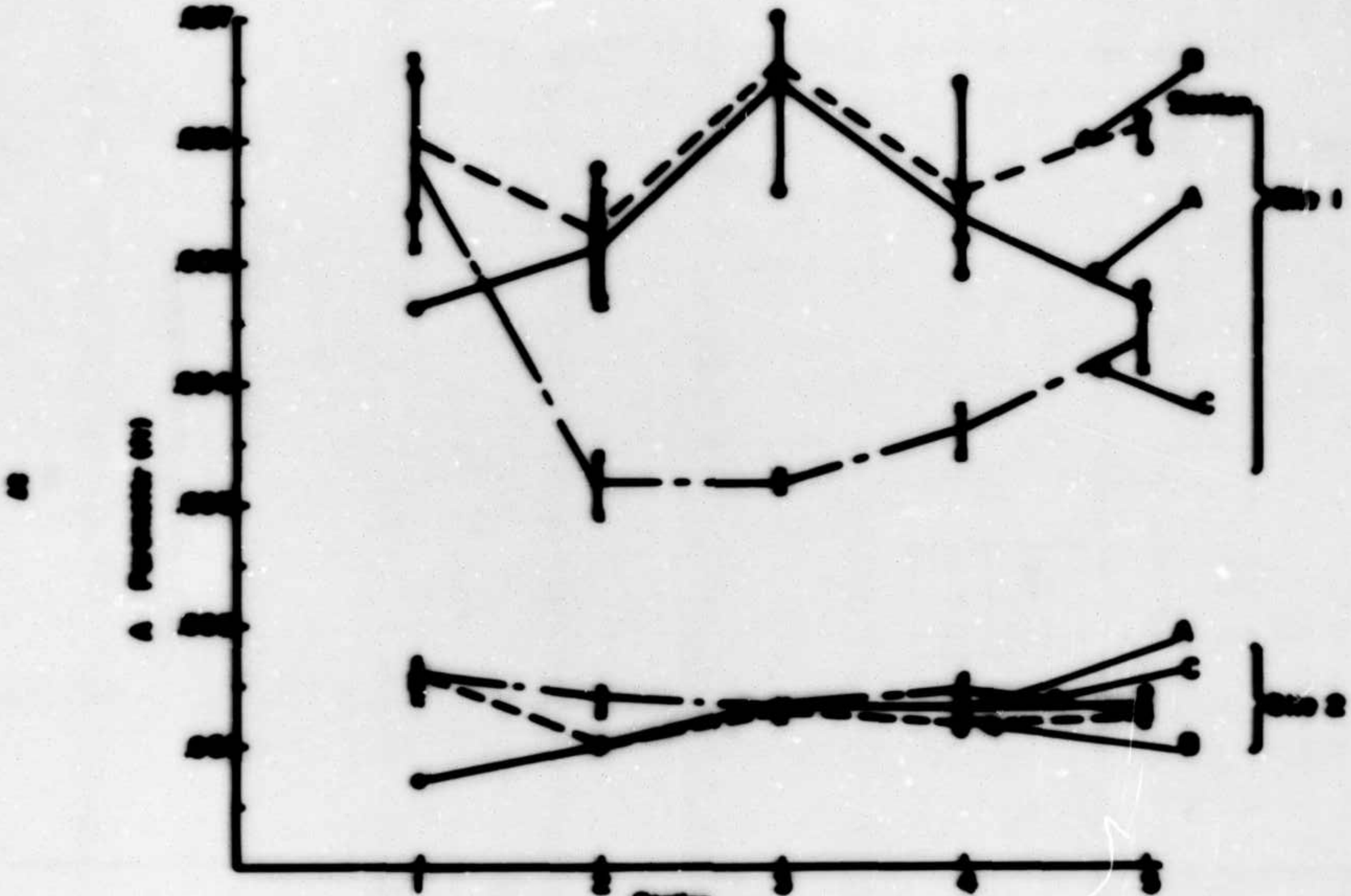

Figure 41. Effect of Two Consecutive Passes on Measured Deflection

records the smallest deflection and shows no permanent set. The amount of permanent set increases as distance from the wheel decreases.

2. The peakedness of deflection-time plots decreases as the distance from the wheel increases (Figure 34).
3. The width of the measured maximum lateral deflection basin is about 4 feet to 5 feet for both Site 1 (Figure 35) and Site 2 (Figure 36).
4. The maximum measured deflection at Site 1 is about three to four times the maximum deflection at Site 2.
5. There is a close fit between the calculated and measured maximum lateral deflection profiles.
6. There is considerable variability in the measured maximum lateral deflection profile at both Site 1 and Site 2, over the areas tested (Figures 37 and 38).
7. The absolute values of τ_{peak} and β_{peak} are consistently larger for Site 2 than Site 1, and the A_{peak} values are smaller for Site 2 than Site 1.
8. Short term repetition of load decreases the measured deflection i.e. the second pass of the F-4 load cart produced less deflections than the first pass (Figure 41).

6.2.2 Transfer Functions

Transfer functions were calculated using the theory and methodology presented in paragraph 3.2.2. Briefly, the procedure involved finding the transfer function which, when convoluted implicitly with the signature yielded an equivalent input, which satisfied certain

specified conditions.

Figure 42 shows the calculated equivalent force and the components of the force on the left hand side of equation 1. Figure 43 shows a comparison of the equivalent force calculated by implicit convolution (equation 15) and by direct substitution in equation 1. Figures 44 and 45 show typical transfer functions for Sites 1 and 2, respectively. Tables 5 and 6 list the parameters of the transfer function for the two sites tested. Station labels (A1, A2 etc) correspond to station locations shown in Appendix B. The k, c, and m parameters were obtained from deflections measured at each location. Where two values are given at the same station, the first listed value corresponds to a forward pass and the second, to a backward pass of the F-4 load cart. Additional entries designate the repetition of the cycle. Figures 46 and 47 show a comparison of the local and site characteristics as given by the equivalent stiffness (k) and damping (c) parameters. Figures 48 (TDT is time dependent transfer) and 49 show a comparison of the magnitude of the first peaks and the time to the first peak of the transfer functions having the parameters listed in Tables 5 and 6, respectively. Figure 50 shows the input force, F(t), and the signature s(t) for one pass of the F-4 load cart. These results show the following:

1. the numerical procedure used to find the transfer function is consistent with the developed theory, both in the determination of the force components (Figure 42), and implicit convolution techniques to obtain the equivalent force (Figure 43).

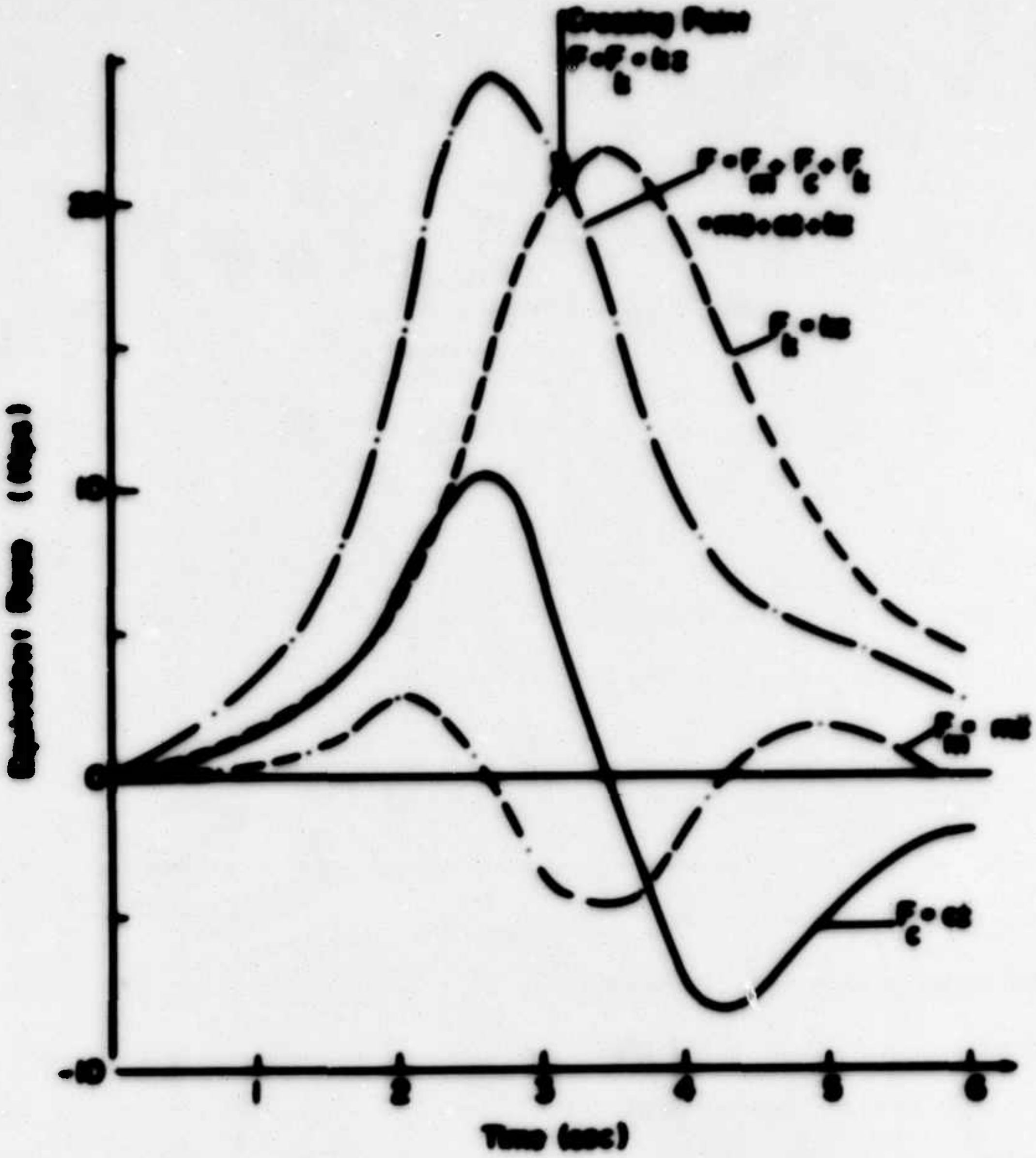

Figure 42. Calculated Equivalent Force and Components (Typical)

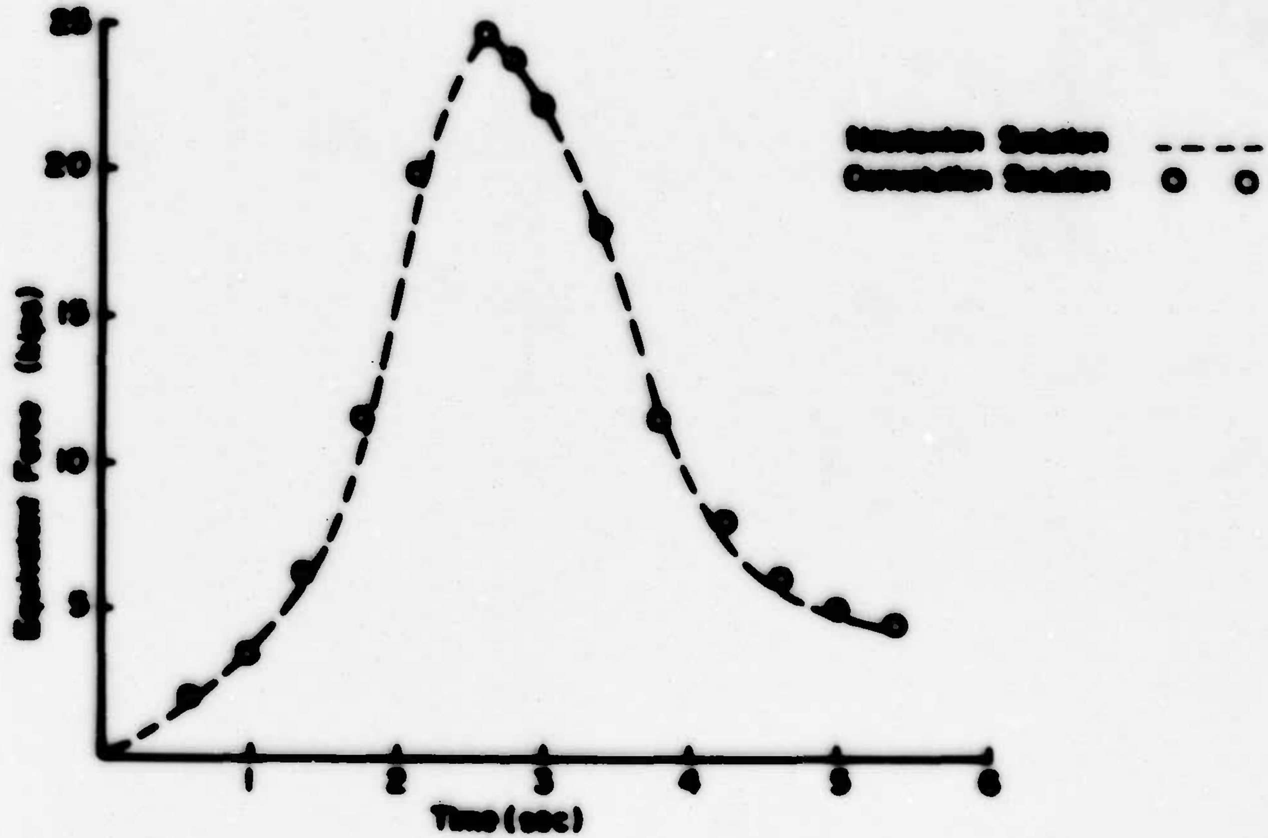

Figure 43. Comparison of Newtonian and Convolution Solutions (Typical)

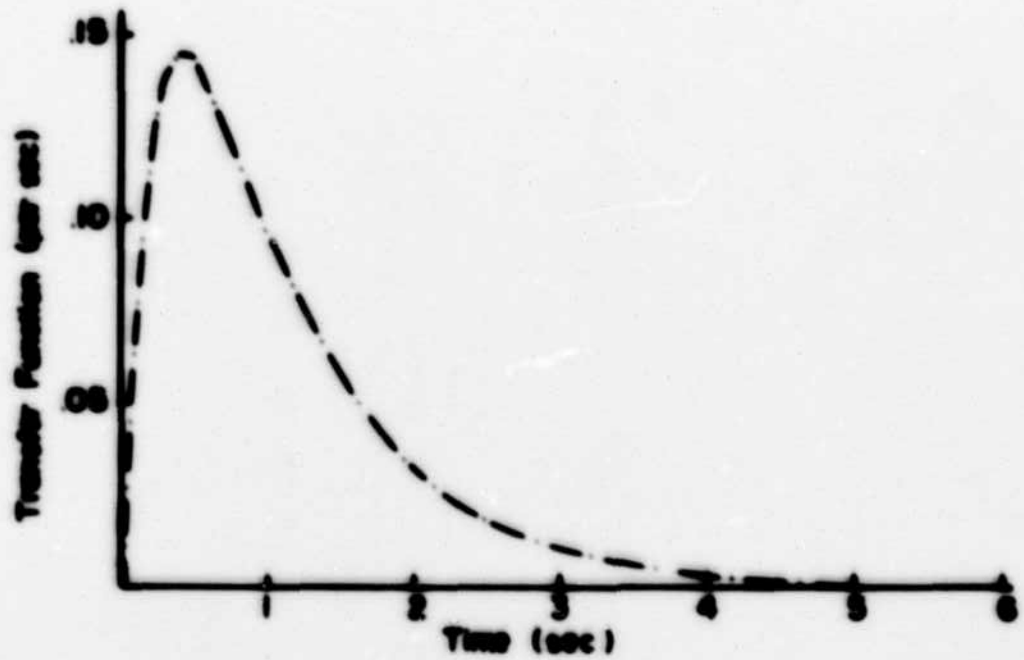

Figure 44. Transfer Function: Eglin AFB Site 1 (Typical)

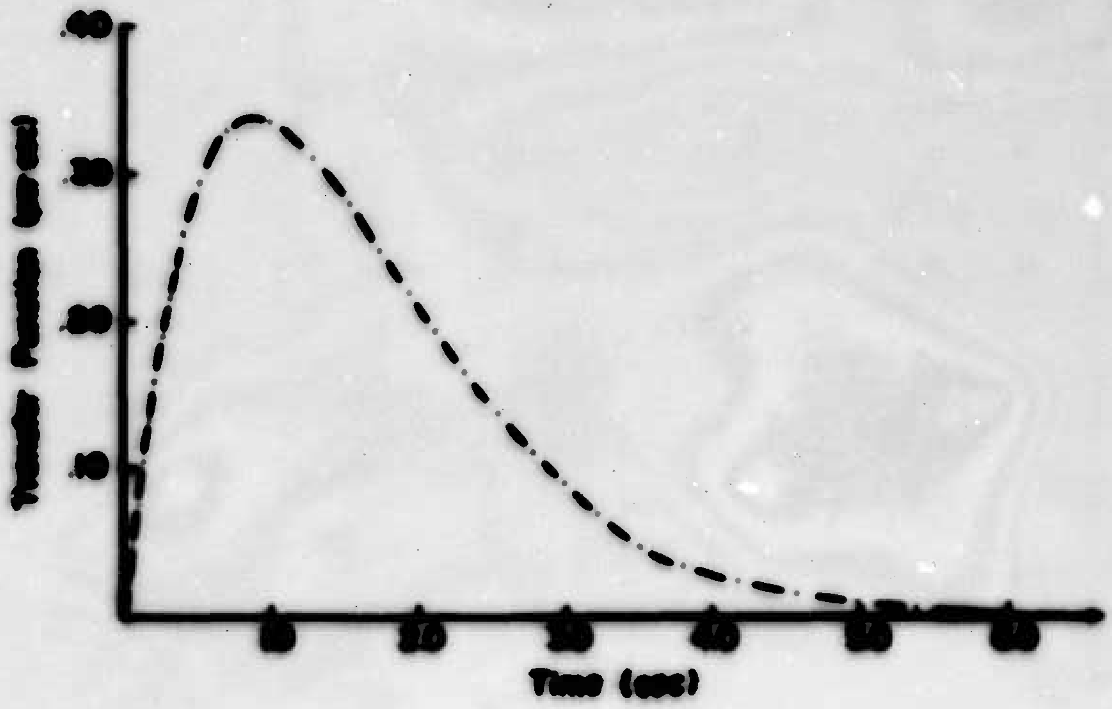

Figure 45. Transfer Function: Eglin AFB Site 2 (Typical)

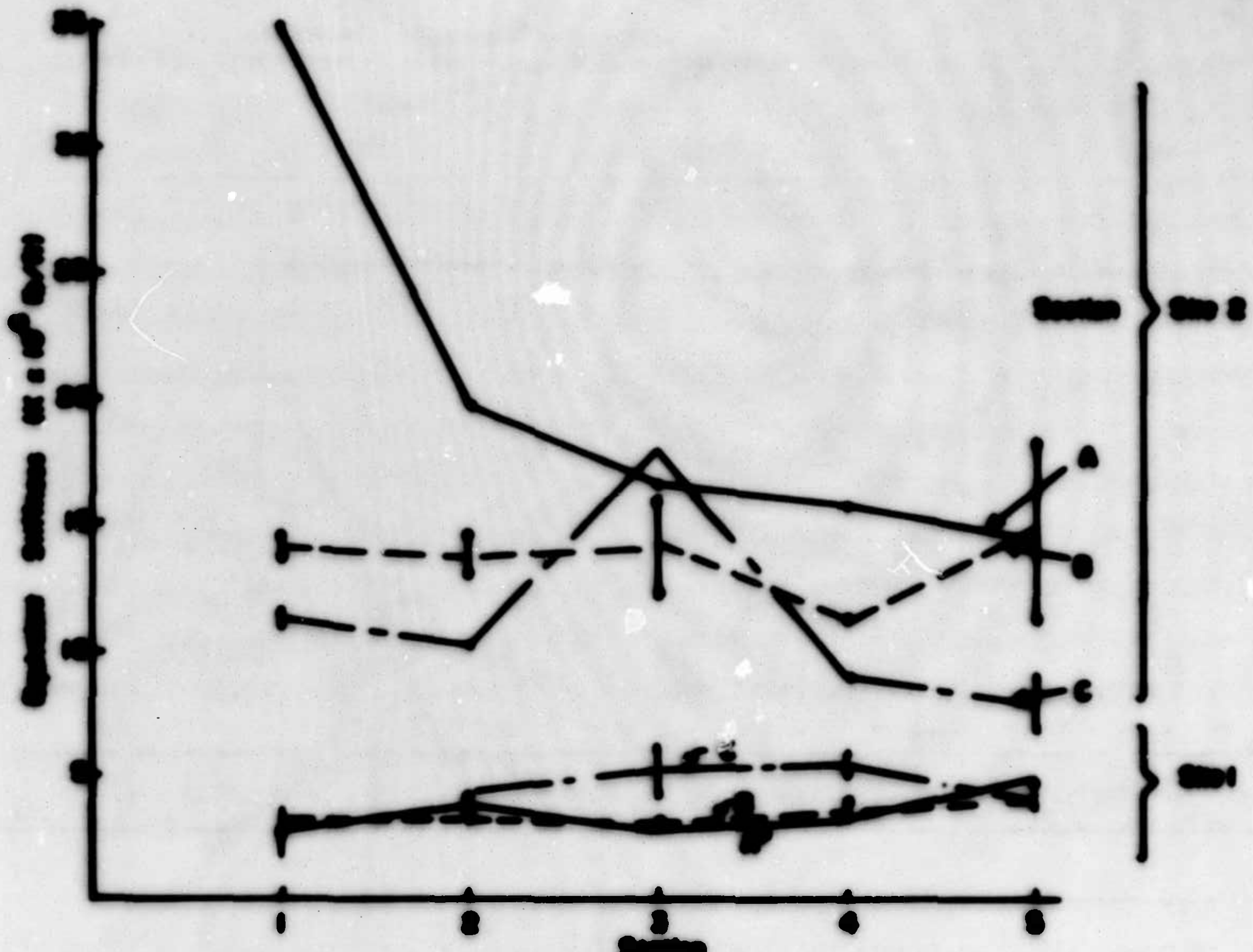

Figure 46. Comparison of Local and Site Characteristics as Shown by E-Parameter: Eglin AFB, March 1976

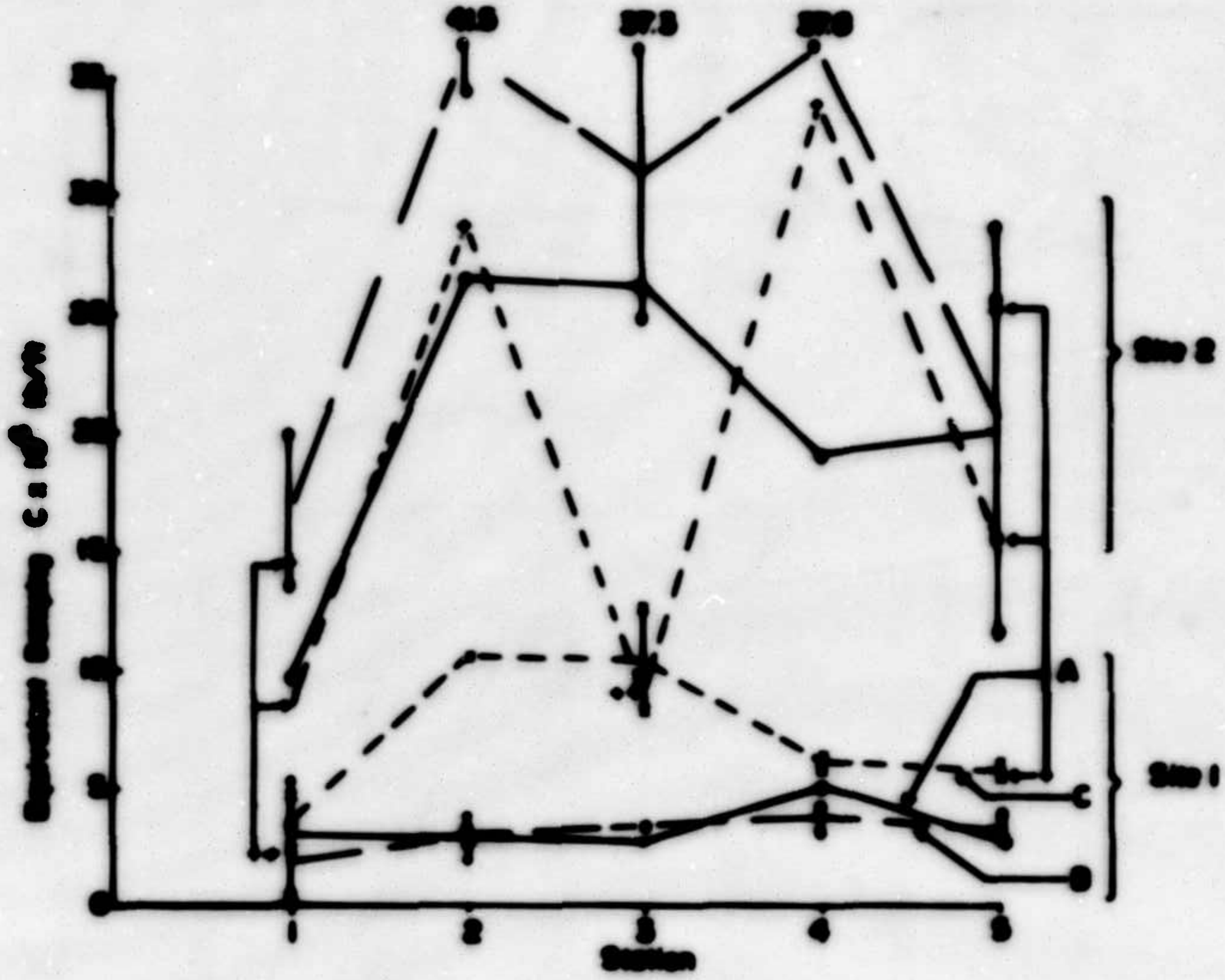

Figure 47. Comparison of Local and Site Characteristics as shown by C-Parameter: Eglin AFB, March 1976

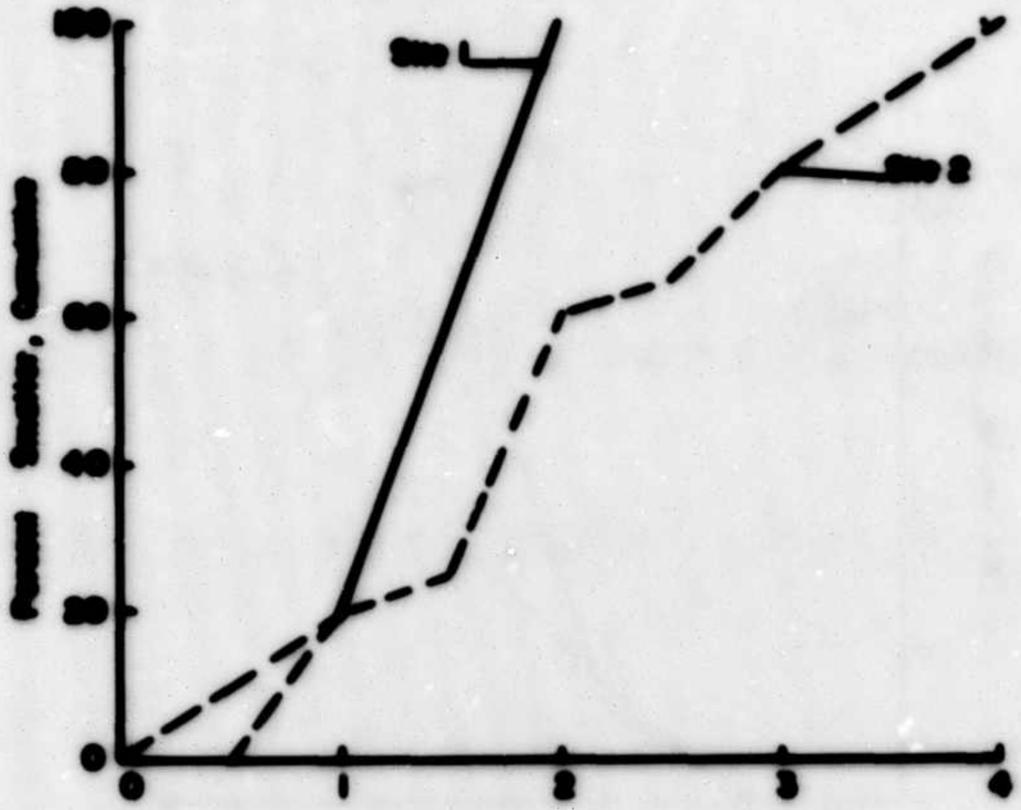

Figure 40. Comparison of The Peaks of The Transfer Functions: Eglin AFB March 1976

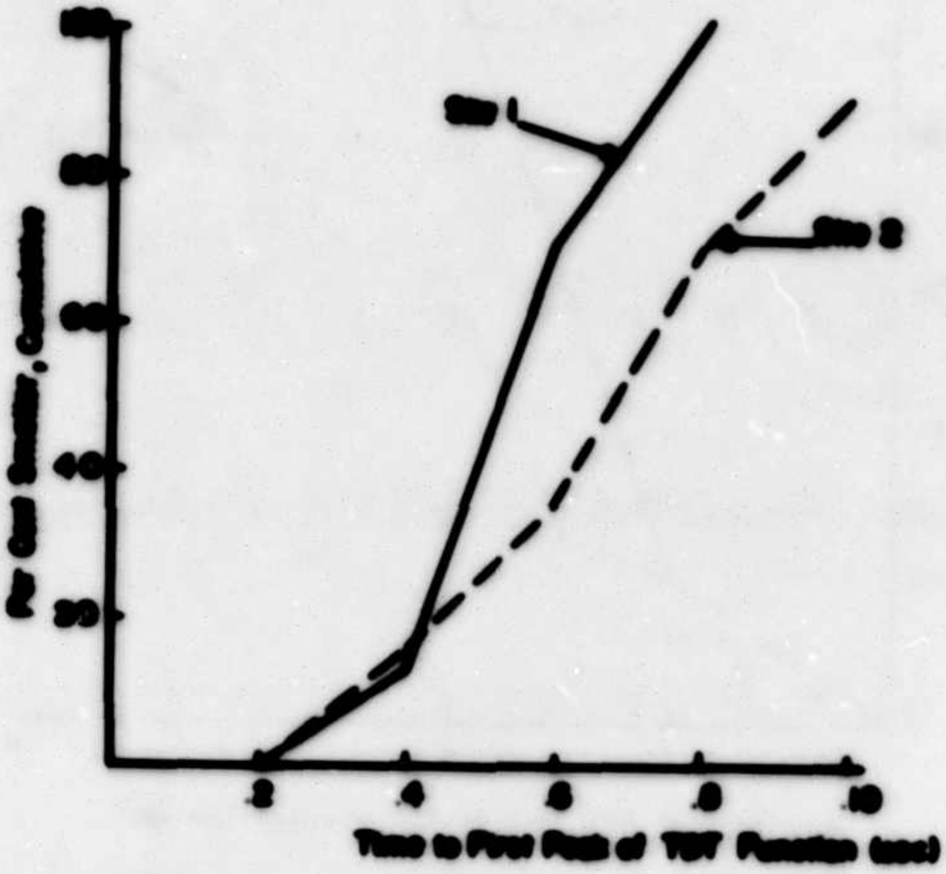

Figure 40. Comparison of Time to First Peak of TBF Function: Eglin AFB, March 1976

TABLE 5. PARAMETERS OF THE [illegible] FUNCTION, [illegible] AFB, MARCH 1976, SITE 1

Station	$k \times 10^6$ lb/ft	$c \times 10^6$ lb-sec/ft	$m \times 10^5$ slugs	Station	$k \times 10^6$ lb/ft	$c \times 10^6$ lb-sec/ft	$m \times 10^5$ slugs	Station	$k \times 10^6$ lb/ft	$c \times 10^6$ lb-sec/ft	$m \times 10^5$ slugs
A1	3.485	5.250	9.343	B1	3.251	0.289	2.473	C1	3.985	2.358	1.994
	1.744	0.468	130.0		2.600	3.387	7.296		1.664	4.707	5.081
A2	4.166	2.330	4.997	B2	3.987	2.827	1.878	C2	4.246	10.408	8.350
	3.250	3.440	8.932		4.084	3.437	8.988		-	-	-
	4.052	3.934	6.496	B3	2.582	3.358	2.078	C3	4.057	12.571	11.790
A3	2.731	2.758	3.828		2.365	3.344	4.284		6.289	8.289	19.886
A4	3.094	5.082	20.720	B4	3.726	4.089	5.389	C4	4.828	6.373	7.553
	-	-	-		2.986	3.887	5.889		5.636	5.669	12.790
A5	4.616	3.212	9.284	B5	3.985	2.686	4.530	C5	3.581	5.966	12.770
	4.670	2.088	8.151		3.728	3.824	7.687		3.942	5.075	7.247

TABLE 6. PARAMETERS OF THE TRANSFER FUNCTION, KELLY AFB, MARCH 1976, TEST 2

Station	$k \times 10^6$ lb/ft	$c \times 10^6$ lb-sec/ft	$m \times 10^3$ slugs	Station	$k \times 10^6$ lb/ft	$c \times 10^6$ lb-sec/ft	$m \times 10^3$ slugs	Station	$k \times 10^6$ lb/ft	$c \times 10^6$ lb-sec/ft	$m \times 10^3$ slugs
A1	12.20	9.035	146.0	B1	13.46	20.00	42.65	C1	10.96	2.21	153.8
A2	-	-	-		14.94	13.65	35.95		7.84	14.60	22.05
	10.73	16.90	120.1	B2	11.5	14.26	128.0	C2	-	-	-
A3	16.90	16.25	124.1		13.1	42.90	67.9		10.25	18.75	57.91
A4	-	-	-	B3	15.92	14.85	86.25	C3	27.97	9.277	14.47
	15.80	10.05	18.66		12.40	37.33	10.91		-	-	-
A5	8.88	18.51	45.63	B4	-	-	-	C4	-	-	-
	13.1	11.46	14.27		11.41	37.84	66.40		0.880	33.81	79.94
				B5	17.20	13.40	63.37	C5	16.76	5.44	12.27
					10.90	15.94	126.4		0.244	15.21	10.96

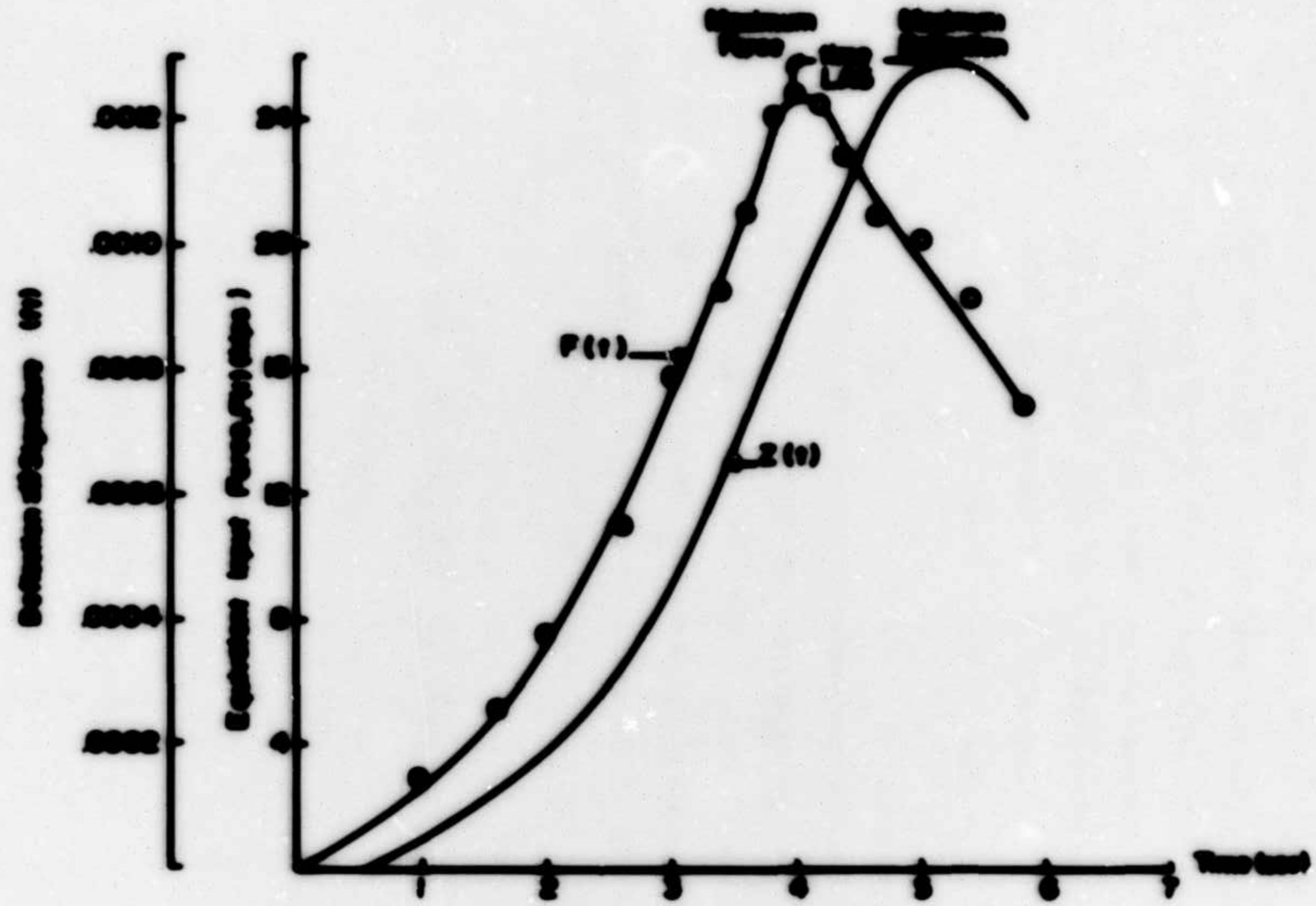

Figure 20. Input-Output Relation (Typical)

2. Both sites are over critically damped (Figures 44 and 45).

3. Site 2 has consistently larger b, c, and n parameters than Site 1 (Tables 5 and 6 and Figures 46 and 47).

4. Minor differences occur between the peaks of the transfer functions and the time to first peak for the two sites tested (Figures 48 and 49).

5. The maximum deflection lags behind the maximum input force by about 1.0 second (Figure 50).

6.3 Prediction

The methodology developed previously was used to predict the peak deflection response of the C-130 and the C-135 at Sites 2 and 3 (paragraph 5.2, Series B Field Investigation). The C-131 and Site 1 were the standard vehicle and site, respectively. Figure 51 shows a typical plot of the predicted and measured signature. Figure 52 shows a summary plot of the measured and predicted peak dynamic deflections.

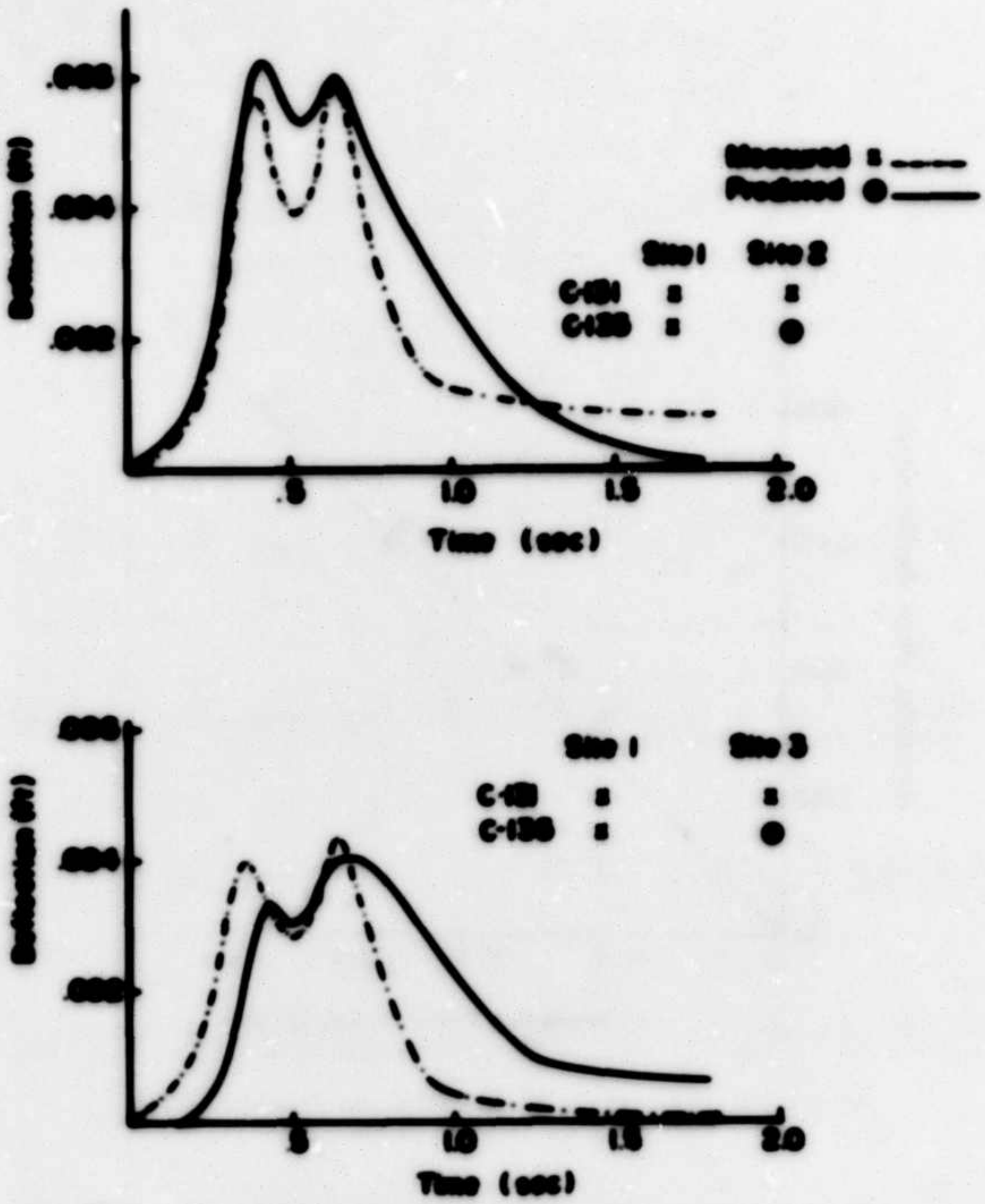

Figure 31. Typical Comparison Between Measured and Predicted Signature

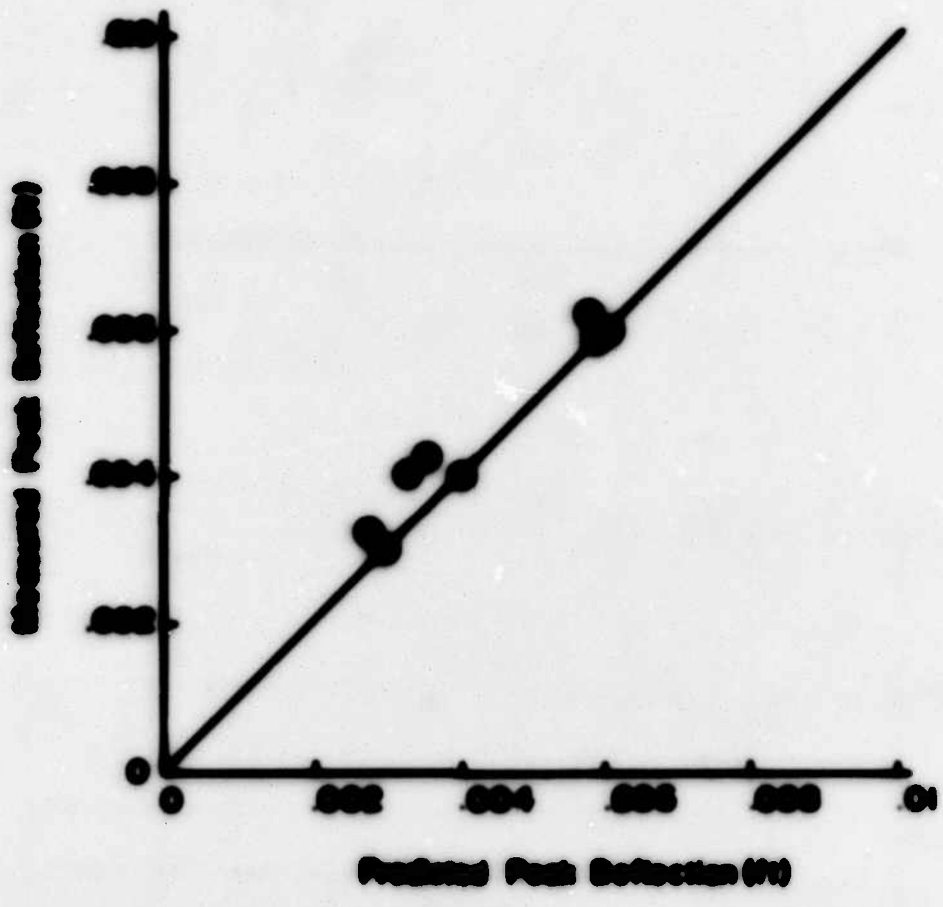

Figure 32. Comparison of Measured and Predicted Peak Deflections for Two Sites

SECTION VII

DISCUSSION

The scope of this work includes equipment development, pavement evaluation, and prediction of pavement response. The significance of the results and the reliability and practical applicability of the equipment are discussed in this section.

7.1 Equipment

Several optical systems were considered during the initial stages of the development of this study. The first system used a laser as a coherent light source. The initial concept was that the laser would be positioned off the pavement and shoot at either the moving load vehicles or reflectors on the pavement surface. Changes in the position of the reflected light beam impinging on a fixed surface would indicate deflections.

It was next thought that, rather than having a laser fixed at a particular location off the pavement, a cantilever beam with its pivot outside the deflection basin would yield a more versatile and mobile system. The beam would support lasers which would shoot down on the pavement surface. Changes in the light beam reflected from the surface and impinging on collector lens on the beam would indicate pavement deflections. Several lasers would have to be purchased and mounted on a cantilever beam. The expense and bulkiness of the lasers prompted a search for a more compact, inexpensive coherent light source. Light emitting diodes on a cantilever beam were finally selected as the breadboard noncontact system for measuring pavement deflections.

The deflection measuring equipment (LED beam) developed in this

work has a demonstrated capability of measuring pavement deflections on the order of 0.001 inch in a field environment. The companion LVDT beam[11] was found to be more rugged, reasonably simple to use, and very reliable. The breadboard LED system is somewhat more delicate. Special care had to be taken when in the moving mode, to ensure the safety of the lenses of the LEDs. Considerable problems also arose with the compatibility of the LED module and the magnetic tape recording system. These may be a result of the fact that the magnetic tape recording system was designed for use with another system, and thus the finer variations in the electronics which may not have affected the operation of the original design, may have been amplified when the system was used in conjunction with the LED modules. Although efforts were made to reduce these problems at Purdue University other still undiscovered incompatibilities between the LED sensor modules and the magnetic tape recording system may still exist.

Figure 33 shows a summary of measurement systems available today. It can be seen that actual vehicular loads are applied only in the procedures using the Benkleman beam, and the California and LaCroix deflectometer. It should be noted however that for these only the rebound deflections are measured. The total time response for one complete pass of a vehicle is not measured by any current device excepting those reported in this study. Under normal operating conditions a vehicle passes over a pavement without pause. This situation is very different from the conditions modelled by the Benkleman beam or the California or LaCroix deflectometers. For

[11]Developed under contract with the Federal Highway Administration.

[illegible]	[illegible]	[illegible]	[illegible]	[illegible]		[illegible]	[illegible]	[illegible]	[illegible]
				[illegible]	[illegible]				
[illegible]	[illegible]	[illegible]	[illegible]		[illegible]	[illegible]	[illegible]	[illegible]	[illegible]
[illegible]	[illegible]	[illegible]	[illegible]	[illegible]	[illegible]	[illegible]	[illegible]		[illegible]
		[illegible]	[illegible]	[illegible]	[illegible]	[illegible]	[illegible]		[illegible]
		[illegible]	[illegible]	[illegible]	[illegible]	[illegible]	[illegible]		[illegible]
[illegible]	[illegible]	[illegible]	[illegible]	[illegible]	[illegible]	[illegible]	[illegible]		[illegible]
[illegible]	[illegible]	[illegible]	[illegible]	[illegible]					
		[illegible]		[illegible]					
		[illegible]		[illegible]					
[illegible]	[illegible]	[illegible]	[illegible]		[illegible]	[illegible]	[illegible]		[illegible]
		[illegible]	[illegible]	[illegible]		[illegible]	[illegible]	[illegible]	[illegible]
		[illegible]	[illegible]	[illegible]		[illegible]			[illegible]
		[illegible]		[illegible]					
[illegible]	[illegible]	[illegible]	[illegible]	[illegible]	[illegible]	[illegible]	[illegible]		[illegible]
		[illegible]	[illegible]	[illegible]	[illegible]	[illegible]	[illegible]		

Figure 53. Summary of Measurement Systems (After Yoder and Crumline [Reference 58])

these the testing procedure starts at a maximum deflection under static loading. The vehicle then moves away and the residual deflection is recorded. The complete load cycle is not recorded by this stopping and starting procedure even though an actual vehicle is used.

Vibratory techniques also model a situation which is not representative of prototype vehicular loading on a pavement-subgrade system. The procedure for conducting vibratory tests generally consists of preloading a pavement-subgrade system by applying a static preload to the pavement surface through a plate of a specified size. At a certain preload level the steady state vibratory load is then applied at a designated frequency. Pavement deflection or a certain aspect thereof is then measured. There are significant differences between this procedure and the prototype loading of a pavement-subgrade system. First, a vehicle does not apply a static preload to the pavement-subgrade system. As previously mentioned, vehicular loading under normal operating conditions is applied to the system without pause. Second, a steady state vibratory force applied vertically dissipates approximately 67 percent of its total energy as Raleigh waves, 26 percent as shear waves and 7 percent as compression waves (Reference 39). The bulk (67 percent) of the energy is therefore dissipated by generating surface disturbance at distances in excess of 20 feet from the vibratory load as evidenced by ground motion at these distances. Prototype loading, however, generally dissipates its energy at distances of less than 5 feet. For the F-4 aircraft the surface effect of the prototype load only extended between 4 to 5 feet from the wheel.

Impact and quasi-static loading likewise do not model prototype

vehicular loading. The time of impact loading is extremely small compared with the time a pavement section actually feels vehicular loads. On the other hand for quasi-static loading, the time of loading is very large compared with that of prototype vehicular loading. In addition, for impact loading, a major portion of the input energy is used to generate surface disturbances similar to steady state vibratory loading. Prototype loading, however, generates little lateral surface disturbance but effects of prototype surface loading are felt at depths of greater than 10 feet (Reference 60). Another important aspect of prototype loadings will be illustrated by an actual example.

During the March field investigation a request was made by the Air Force officials at Eglin AFB that a runway overrun area be evaluated to determine whether it was adequate for use by F-4 aircraft. Figure 34(a) shows the area before prototype loading. Figure 34(b) shows the section after the first passage of the F-4 load cart. The test vehicle punched through the pavement. It is doubtful that any available steady state vibratory loading testing apparatus (that dissipates a large measure of its energy as Raleigh waves) would have demonstrated the discovered inadequacy. The significance of this experience may be summarized as follows: An evaluation scheme that uses prototype loading in conjunction with nondestructive measurements of pavement-subgrade response provides, not only measurements of its response, but more importantly a test of necessity.

The speed of operation or the number of tests per day shown in Figure 33 indicate results vary from very slow to 3000 per day. The literature (Reference 23), however, shows the upper limit to be overly

(a) Before

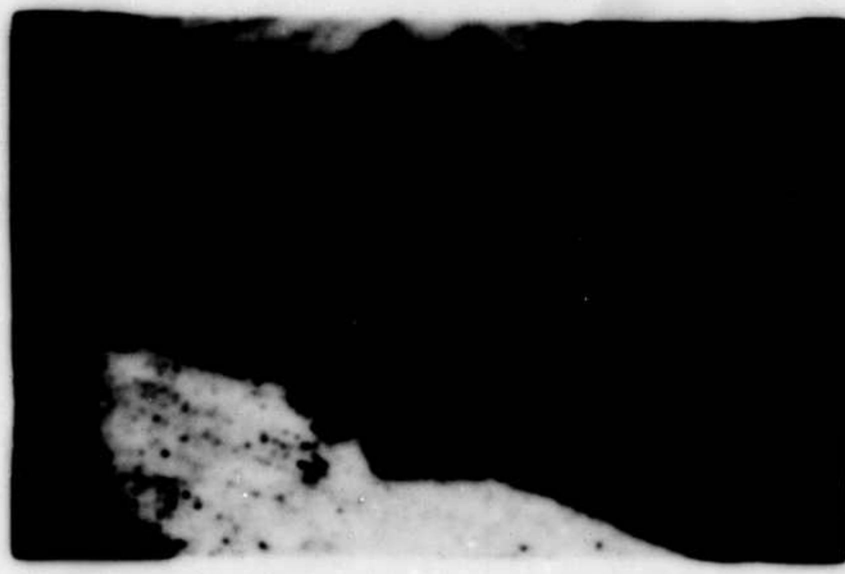

(b) After

Figure 34. Runway Overrun Test - Eglin AFB: March 1976

optimistic. On the other hand, the operational speed of the [illegible] LVDT and LID systems are indisputable.

In June 1976, both the LVDT and the LID systems were used at Eglin Air Force Base to help investigate the difference between loaded and unloaded profiles. Measurements were made on 2,000 feet of taxiway using both systems. The LVDT stationary beam-moving load operation was used to measure the system response at 100-foot intervals. The LID beam was fixed to the F-4 load cart and was used in conjunction with the LVDT measurements to provide an estimate of deflections between the 100-foot LVDT stations. The average time for setup, including manually moving the LVDT beam between locations and positioning the load cart, was 7 to 10 minutes. In addition to the 2000 feet of taxiway, the LID system mounted to the load cart was used to test 1 1/4 miles of runway. The runway testing took less than 1 hour after initial setup.

It is important to note also that in the stationary beam-moving load mode the LID and LVDT beams both provide the complete deflection-time response of a pavement-subgrade due to prototype loading, that is, the entire dynamic deflection basin is obtained. No other instrumentation system currently available has demonstrated this capability. Furthermore, the LID system does it without making mechanical contact with the pavement surface.

7.2 Evaluation

The evaluation procedure consists of measuring pavement deflections due to prototype loadings. From these deflections the signature and parameters of the maximum lateral dynamic deflection profile and the transfer function are obtained using the computer program detailed in

Appendix C. The parameters of the maximum lateral dynamic deflection profile and the transfer function are then related to performance.

7.2.1 <u>Concepts Used in Computer Program</u>

The developed computer program determines the m, c, and k parameters of the equation that describes the behavior of the hypothesized model of vehicle-pavement-subgrade interaction. The equation of the model,

$$m\ddot{x}(t) + c\dot{x}(t) + kx(t) = F(t)$$

describes at best an approximation to physical reality. The lumped parameters represent average measures of the actual inertial (m), damping (c), and stiffness (k) characteristics of the real system. F(t) represents an input force at time t, and $x(t)$, $\dot{x}(t)$, and $\ddot{x}(t)$ represent the signature and its first and second derivatives.

Research (Reference 64) has shown that when a vehicle is in motion, F(t) may have instantaneous values varying from 50 percent greater to 50 percent less than the static wheel load. The wide range is caused by many factors including both pavement and vehicle characteristics. The maximum F(t) of 25 kips used to establish the 300-pound criterion (see pages   through   ) in the computer program is thus simply a convenient approximation to actual maximum values which may range from 12.5 kips to 37.5 kips. The 300-pound criterion then serves as a normalizing function and in effect has little physical significance, except in the sense that 25 kips is close to the static wheel load.

The lumped parameters of the transfer function represent measures of the inertial (m), stiffness (k), and damping (c) characteristics of

the pavement-subgrade system. Local[12] characteristics may vary significantly; however, when the overall interaction mechanism is translated to surface deflections, local variations lose their significance.

In the computer program, three parameters of the transfer function were obtained using an iteration-interpolation procedure detailed in paragraph 3.2.2. Conditions at times corresponding to the maximum deflection, the crossing point, and the point of inflection had to be satisfied. Two criteria were used. The first criterion was that the input load obtained by implicit convolution had to be between 24,500 and 25,500 pounds. The second and final criterion was that the c value satisfied the conditions at the crossing point and simultaneously satisfied conditions at the point of inflection. All forces were obtained by implicit convolution of the signature s(t) and the transfer function using a series of trial values of h, c, and m.

With reference to Figure 33, in concept the first criterion ensures that the maximum force lies within the crosshatched area. The second criterion ensures that the convolution and Newtonian solutions are very close. For example, consider the curves labelled A, B, D, C, and E in Figure 33. Suppose that the curve labelled E is the true but unknown (Newtonian) solution. Curve B satisfies neither criterion as (1) its peak value is outside the specified (shaded) band width, and (2) the computed c-value would be too large. The failure of the latter criterion is demonstrated when the force $F(t_1)$ (obtained by convolution)

---

[12] Local, as used here refers to dimensions of the size of a typical laboratory specimen.

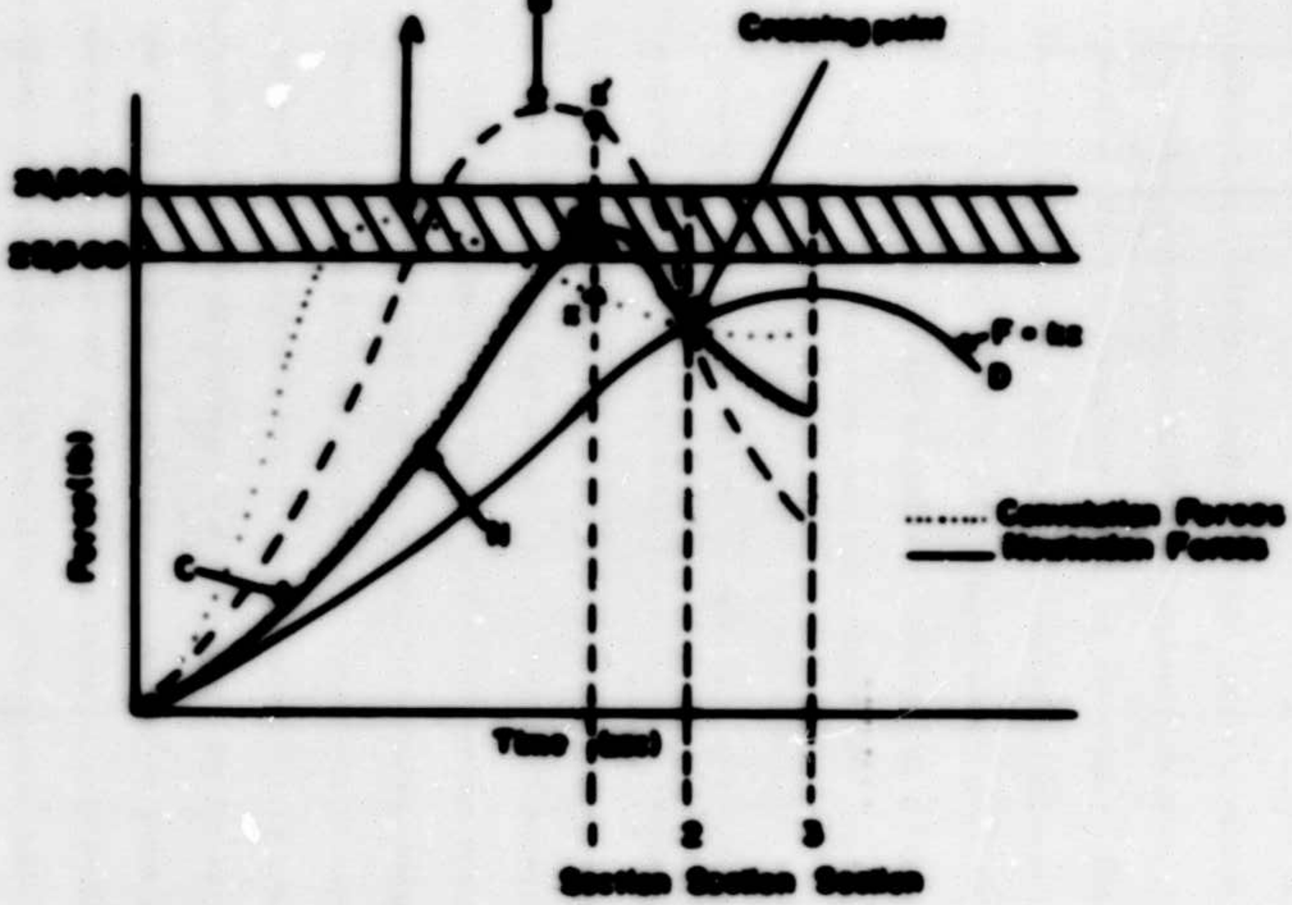

Figure 35. Sketch Showing the Concept of the Criteria Used in Parameter Identification

of X' (Figure 36) is used instead of R to calculate the c parameter at the point of inflection (section (1), Figure 33), using equation (17a). Curve A satisfies the 300-pound criterion but does not satisfy the c-parameter criterion, since the value of the force X at the point of inflection is less than R. Substitution of X for F(t) in equation (17a) would yield a value of c which would be less than the desired value. Curve C would satisfy both criteria. For this curve the convolution and Newtonian solutions are essentially the same. The fact that the two solutions are the same ensures that a standard point of convergence is used for all calculations. It does not mean that the k, c, and m parameters are absolute values since as previously cited, the parameters are average values, and are influenced by the approximation [F(t)] to reality inherent in the hypothesized model.

Since measurements could not be made exactly at the edge of the tire print, it was necessary to calculate the signature (the deflection at the edge of the tire print) using the characteristics of the lateral dynamic deflection profile. It was assumed, and subsequently verified (Figures 35 and 36), that the deflections under the wheel and at its edge are essentially equal. In calculating the signature the three parameters A_{peak}, B_{peak}, and C_{peak} were used to provide a scaling of the lateral attenuation of the peak deflections with time. Figure 36 shows a comparison of a typical measured and calculated signature. The signature (curve A) was measured as the F-4 passed over a gage embedded in the pavement. The other embedded gages measured points on the deflection basin which provided the inputs to the calculations. The closest gage was 18 inches from the center of the load wheel. The difference between the maximum calculated curve (B)

and measured deflections is about 5 percent. Since all field measurements analyzed in this work were made with the LVDT beam at distances closer than 18 inches from the edge of the tire, the correspondence between the calculated and the measured signatures in Figure 36 indicates the upper bound of the differences between calculated and measured signature. Using linear interpolation, the dotted curve (C) in Figure 36 corresponds more closely to typical calculated signatures used in the data analyzed herein since the LVDT beam permitted measurements to be made as close as 3 inches from the edge of the tire print.

7.2.2 Parameters of the Maximum Lateral Deflection Profile

Pavement deflection has been used as an indicator of the support condition of a pavement-subgrade system for some time. Methods of evaluation have been developed that are based on (a) magnitude of deflection (Reference 62), (b) bending index (Reference 63), (c) radius of curvature (Reference 23), and (d) the "slope of deflection" (Reference 64). These methods in general have used static or quasi-static loadings. For the reasons discussed previously in paragraph 7.1, these deflection measurements are not true indicators of the dynamic response of a pavement-subgrade system subject to vehicular loads.

The dynamic lateral deflection profile defined by equation 2 has three parameters A_{peak}, B_{peak}, and r_{peak} which together account for both the magnitude and the curvature of the lateral deflection basin. Since the deflection measurements were made during a nonstop passage of the F-4 load cart in front of the LVDT beam, the three parameters are representative of the actual maximum dynamic lateral deflection basin due to prototype loads.

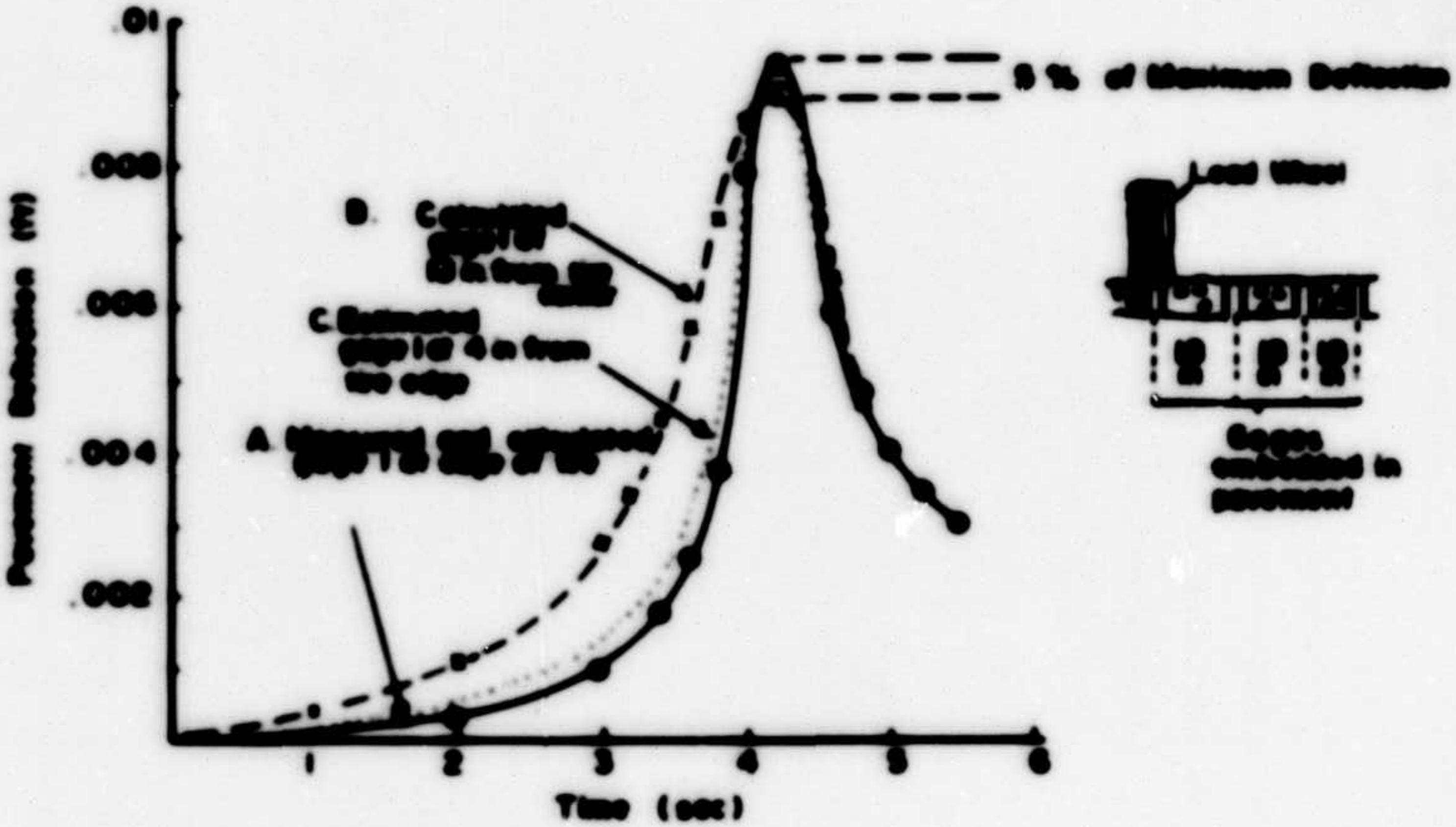

Figure 36. Comparison of Signatures

The results presented in paragraph 6.2.1 showed some variation in the parameters A_{peak}, B_{peak}, τ_{peak} at each site, and there were distinct differences between Sites 1 and 2. In order to better characterize the two sites and give due consideration to the parameter variability at the sites, plots of cumulative percent smaller versus each parameter were prepared from the results in paragraph 6.2.1. Figures 57 through 59 show these plots. The distinct differences between the two sites are displayed as a shift of the individual site characterization plots.

The U. S. Air Force in recognition of the structural inadequacy of Site 1[13] uses the area as a parking area. Site 2 on the other hand is an in-service taxiway. If the lower 10 percent of the Site 2 parameters is arbitrarily selected as the line denoting failure, criterion based on the correlation of parameters with performance is established. This is shown in Figures 57 through 59. The lower 10 percent as used here means that 10 percent of the values do not meet the criterion. Thus, in Figure 59, the line denoting failure intersects the Site 2 cumulative percent smaller curve at the 10 percent smaller value whereas in Figures 57 and 58, the 90 percent smaller value of the cumulative percent smaller plot is intersected by the criterion line.

7.2.3 Parameters of the Transfer Function

The results given in paragraph 6.2.2 showed that there is some variation in the parameters k, c, and n of the transfer function over

---

[13] See Appendix B, Figure B-1(a)

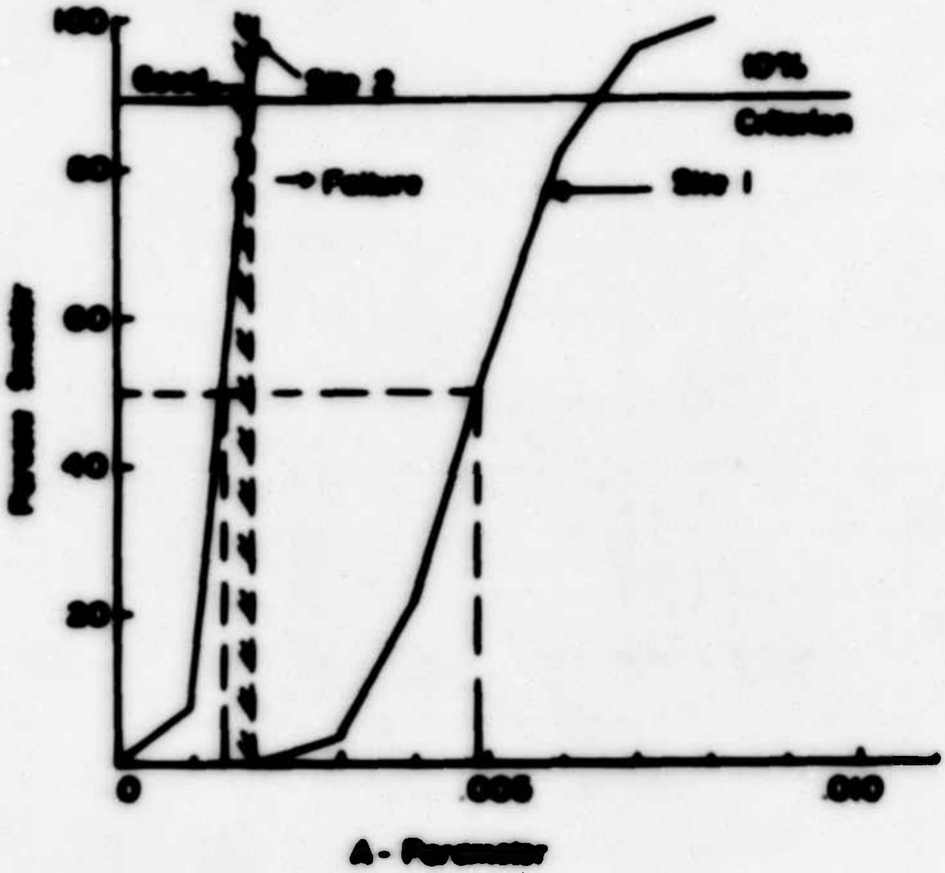

Figure 37. Comparison of A Parameters: Eglin AFB March 1976

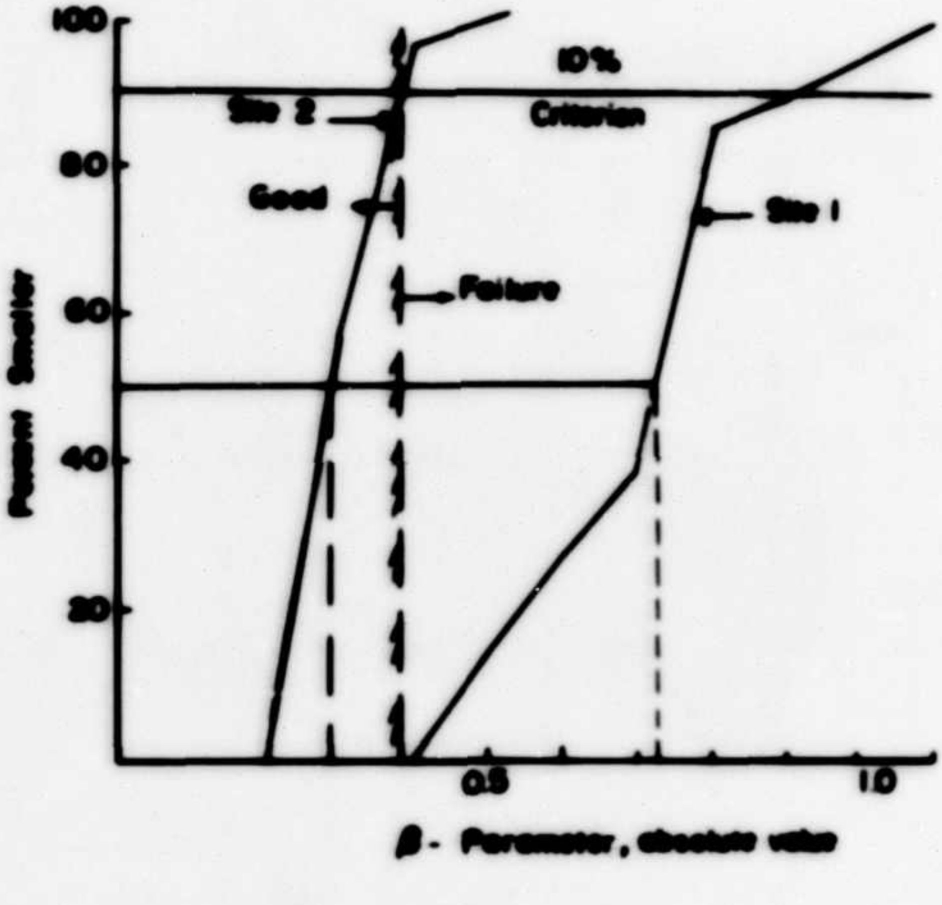

Figure 38. Comparison of the β-Parameters: Eglin AFB, March 1976

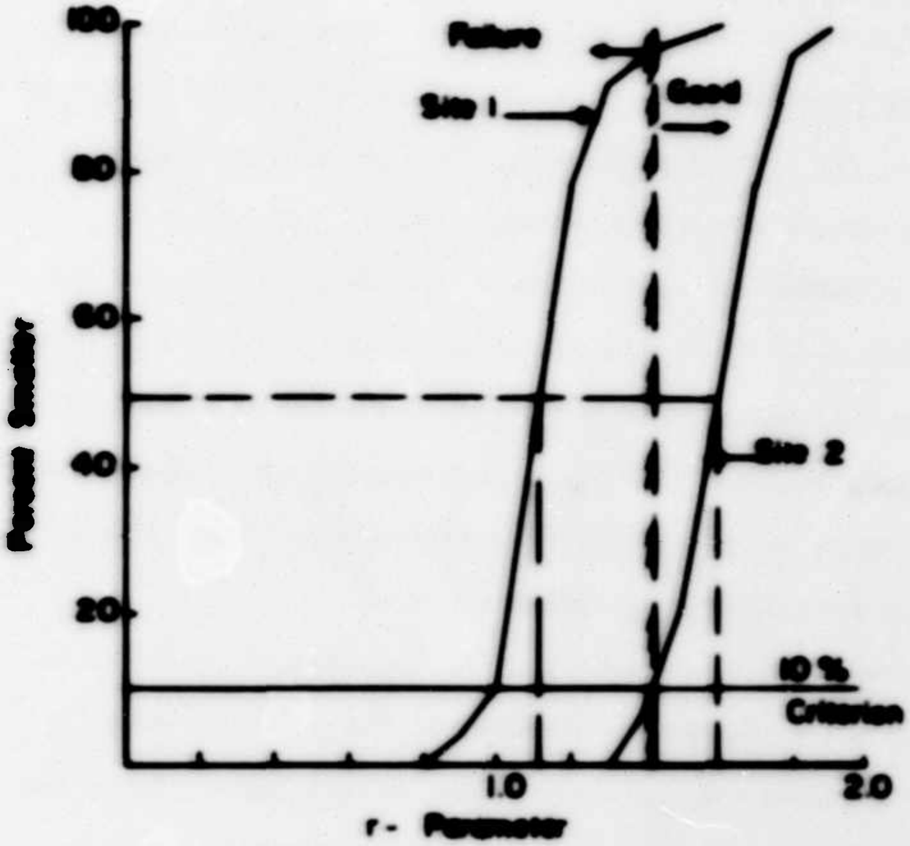

Figure 59. Comparison of r Parameters: Eglin AFB March 1976

each of the two sites. Plots of cumulative percent smaller versus each parameter have been prepared for each site. Figures 60 through 62 show these plots. It can be seen that Site 1 exhibits more uniformity and considerably smaller values of all three parameters than Site 2. With reference to Figure 60 the fact that the entire curve of "cumulative percent smaller" is shifted towards higher stiffnesses for Site 2 indicates that the stiffnesses determined in the evaluation procedure are not local hard spots, but represent the variability in the stiffness characteristics of the area tested.

If the arbitrary 10 percent criterion shown in Figures 57 through 59, is applied to each of the parameters k, c, and n of the transfer function, a criterion based on performance can be had. The line denoting failure is shown on Figures 60 through 62. The performance based criteria shown in Figures 60 through 62 can then be used in the same manner as was presented in the discussion of the parameters of the maximum lateral dynamic deflection basin.

It is interesting to compare the k parameters with stiffness as determined in a 1973 evaluation (Reference 28) by the Air Force, in which an F-4 aircraft was used as the load vehicle and the Benkelman beam was used to measure rebound deflections. Figure 63 shows the locations where relative stiffnesses were determined. Figure 64 shows a histogram on the relative stiffnesses calculated by their procedure. Figure 64 also shows the mean k parameters for Sites 1 and 2 as calculated by the procedure developed in this research effort. Site 1 is shown to have a smaller mean stiffness than all the sections evaluated, while Site 2 is in the range that occurs with about 9

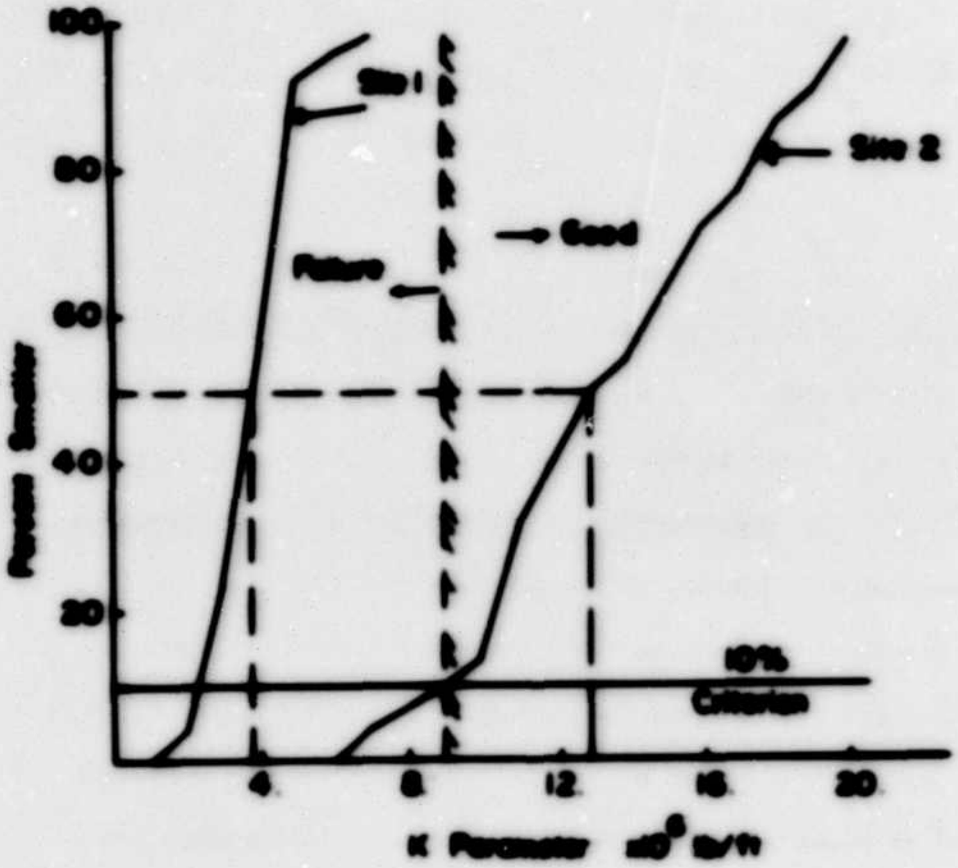

Figure 60. Comparison of Equivalent k Parameters: Eglin AFB March 1976

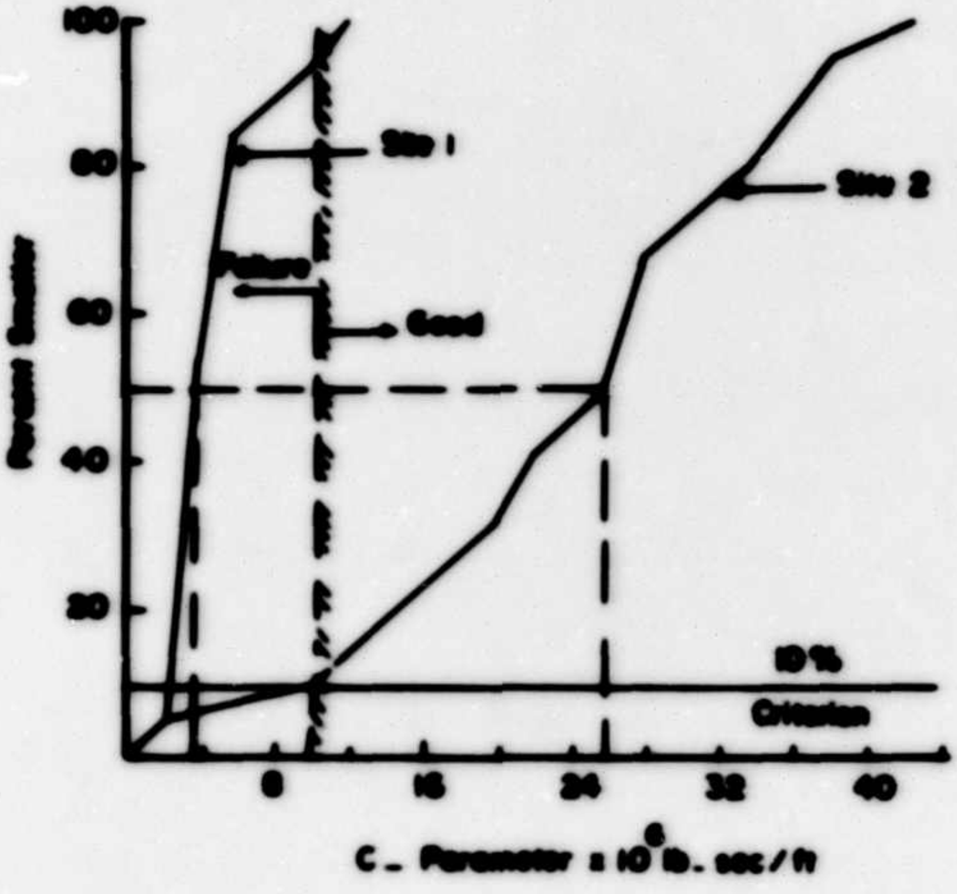

Figure 61. Comparison of Equivalent c Parameters: Eglin AFB March 1976

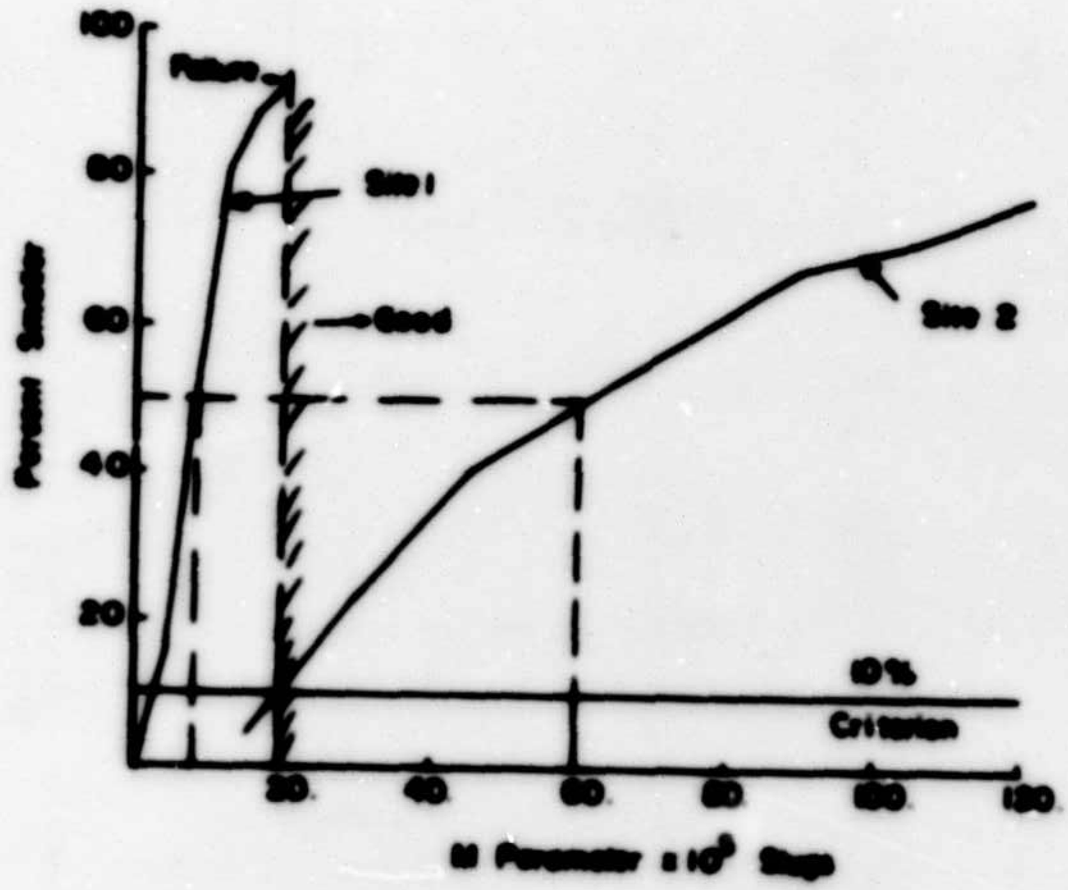

Figure 62. Comparison of the Equivalent n Parameters: Eglin AFB, March 1976

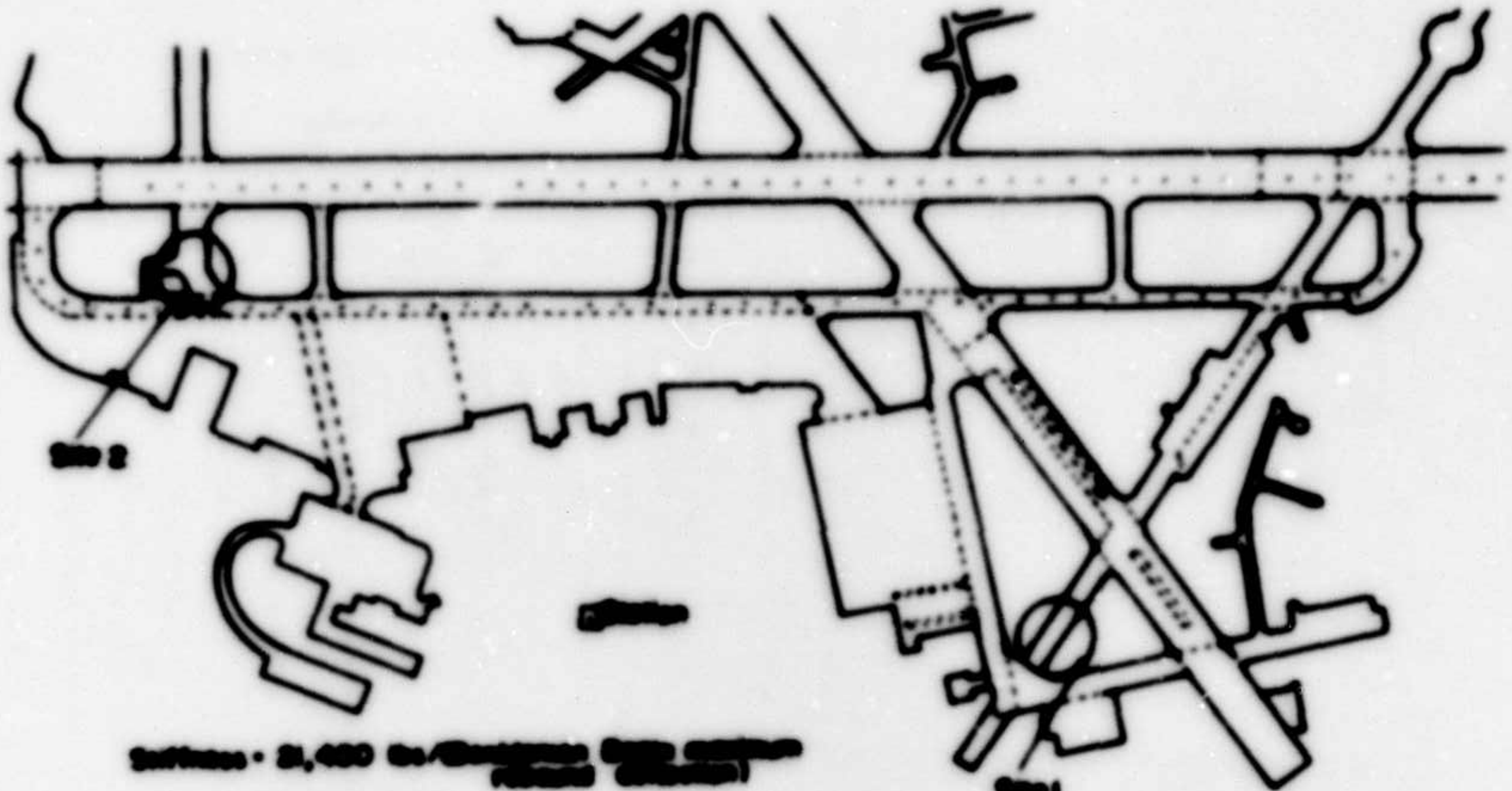

Figure 61. Locations of Stations Where Relative Stiffnesses Were Determined (after AFCEC, Tyndall AFB)

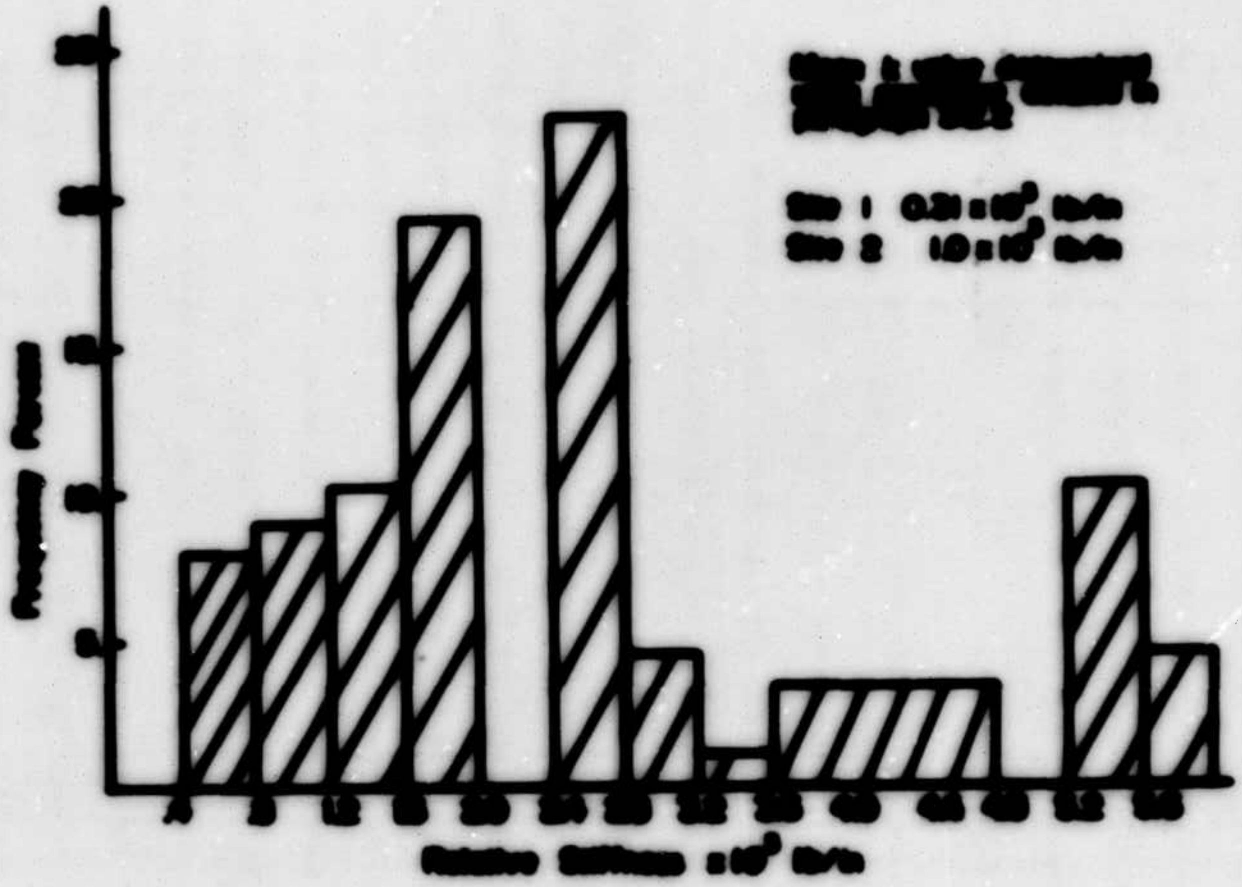

Figure 64. Histogram of Relative Stiffness (Based on AFWL Report)

percent frequency.

It appears then that field performance and comparison of stiffness both substantiate the lower limit of the k parameter. A reasonable lower bound of an acceptable k value of about 9.0×10^6 lb/ft (750 kips/in) is suggested by the Site 2 curve in Figure 60. This is the lower 10 percent value.

7.2.4 Relationship between the k and A_{peak} parameters

The A_{peak} parameter defined in this study is basically the maximum deflection under the load wheel. The k parameter, on the other hand, represents an equivalent stiffness. This stiffness reflects the complicated unknown interaction of all the materials in the zone of influence of the wheel load. The k parameter is thus a measure of the stiffness resulting from this interaction. Figure 65 shows a plot of the A_{peak} and corresponding k parameters from the two sites as given in the results in Tables 5 and 6. The dashed line represents a limiting envelope. There appears to be two linear sections to this envelope. If the straight line portions are extended, the A and k parameters corresponding to their point of intersection are 0.0026 ft (0.0312 in) and 6×10^6 lb/ft (500 kips/in) respectively. It is interesting to note that the Site 2 (active taxiway) (k, A) parameters fall below the line PQ (0.0312 in) and the Site 1 (parking area) (k, A) parameters lie above the PQ line. It is also interesting to note where the k coordinate of this point (Q) lies, if plotted on Figure 66. The curves in Figure 66 were developed by the Corps of Engineers using vibratory techniques and correlations with actual

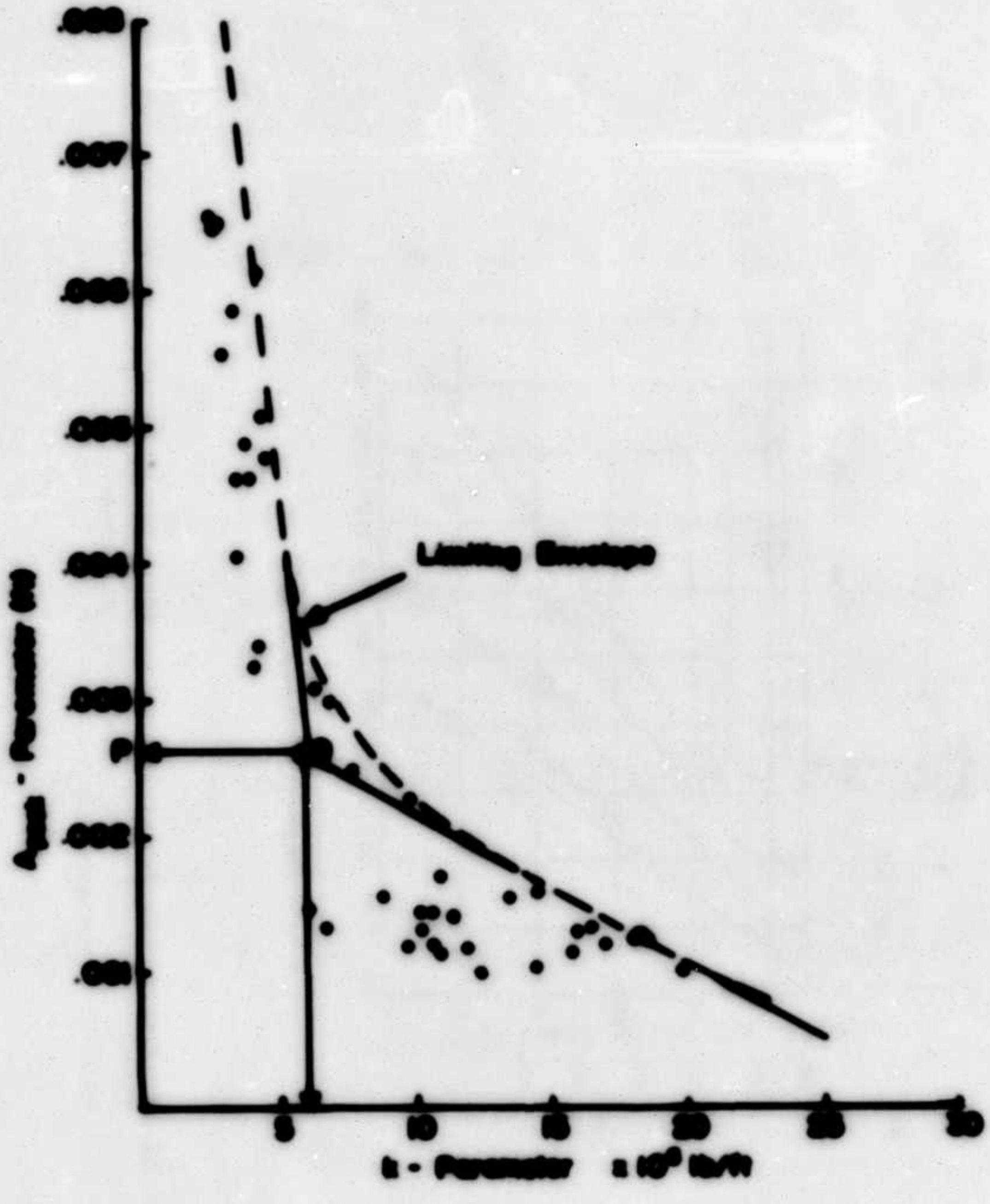

Figure 65. Relationship Between A_{peak} and k Parameters

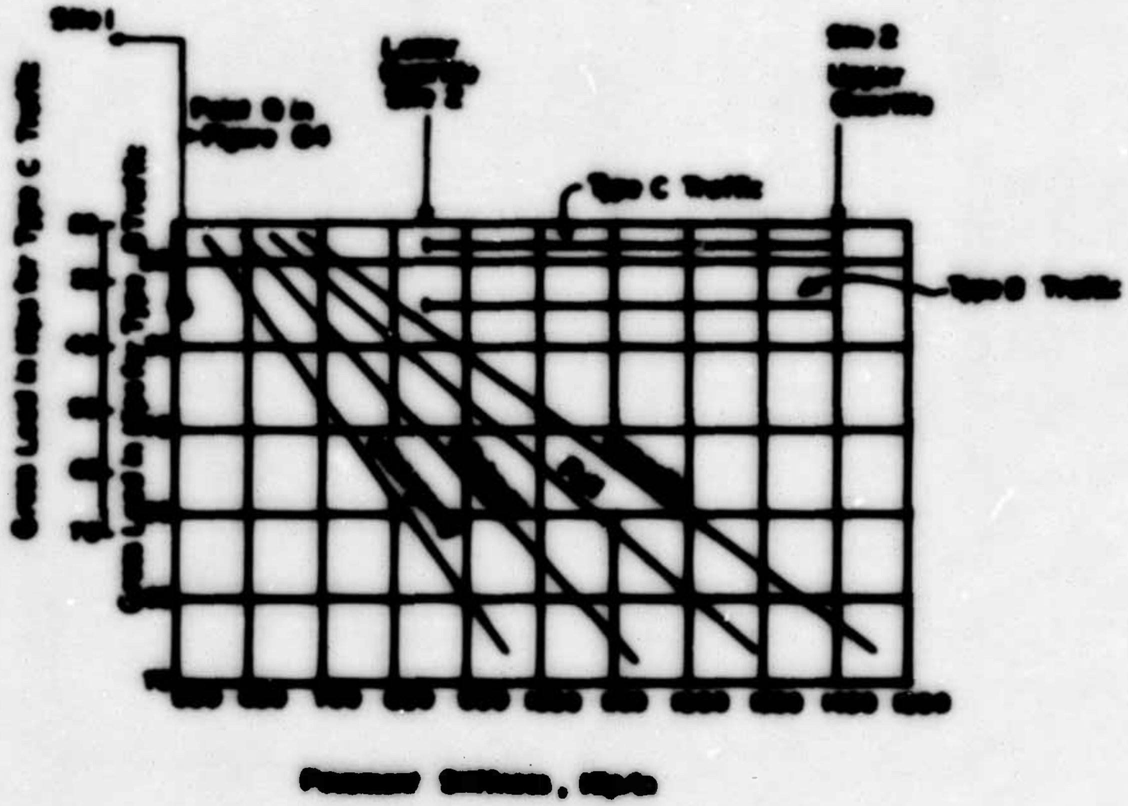

Figure 46. Nondestructive Evaluation Curves for Flexible Pavement, Single Wheel Load, 100 in.² after Wiseman (Reference 16)

aircraft loads. Since the F-4 aircraft gear is a single wheel of contact area 102 in.^{2} loaded to about 25 kips (Reference 56), the h value of the point Q (Figure 65) can be plotted directly on Figure 66 for C type or B type traffic. Figure 66 also shows h-parameters corresponding to the lower and upper quartile values at Site 2 (active taxiway). Site 2 lies above the capacity line and Site 1 lies below the emergency line. This estimation appears to confirm the known status of Sites 1 and 2.

The limiting envelope in Figure 65, therefore, appears to provide an additional evaluation tool. Since deflections alone are measured, the limiting h values can be estimated from Figure 65, and compared with available correlations as shown, to estimate load rating.

7.2.3 <u>Approximate Method for Estimating h, c and n for F-4 Loading</u>

Figure 50 showed the typical relationship between the input force F(t) and the output s(t). Figure 67 shows the frequency characteristics of F(t) normalized by the maximum assumed wheel load (25 kips) at three sections corresponding to sections 1, 2 and 3 of Figure 7. Sixty data sets were used to develop the frequency curves.

With reference to Figure 67, at the point of inflection (section 1), the normalized force ratio has a mean value of approximately 0.9. This suggests that the maximum applied force occurs at a time close to maximum pavement velocity. Similarly at maximum deflection (section 3), 0.5 of the maximum force is the mean value of normalized force ratio. This indicates that at the time the measured deflection is a maximum the wheel has already passed the point under consideration. At the

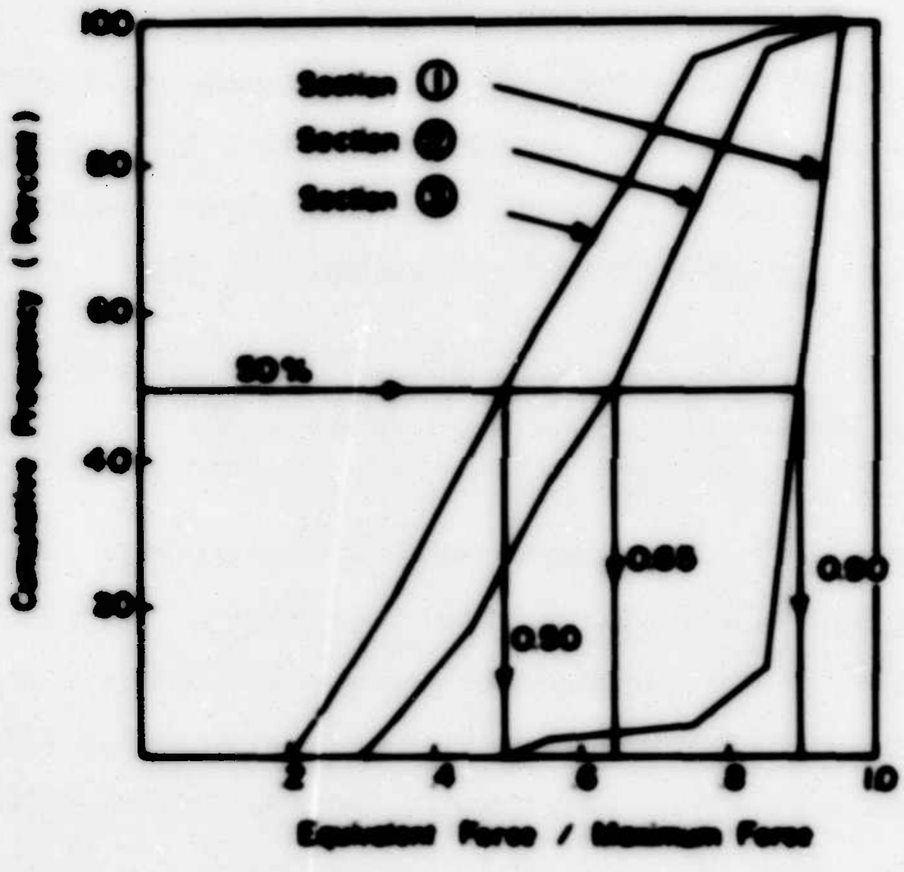

Figure 67. Frequency Characteristics of Forces at the Point of Inflection, Crossing Point and Maximum Deflection

crossing point (section 2), approximately 0.65 of the maximum load is the mean value of the force ratio.

Figure 68 shows the frequency characteristics of the time normalized by the time to peak deflection corresponding to the point of inflection (section 1) and the crossing point (section 2) respectively. At the 50 percent level the normalized time ratio is seen to be 0.72 and 0.90 for the point of inflection (section 1) and the crossing point (section 2) respectively.

Figures 67 and 68 suggest a simplified approximate method for determining the transfer function parameters from the deflection-time history of one pass of a vehicle. In order to determine k from the signature $z(t)$, the deflection $z(t_2)$[14] is found at 0.9 T_p, where T_p is the time to the peak deflection (Figure 68). The force $F(t_2)$ applied at the time (t_2) is approximately 0.65 F_{max} (Figure 67) where F_{max} is 25 kips for the F-4 loading. As was noted in paragraph 3.2.2 at the crossing point,

$$F(t_2) = k \cdot z(t_2)$$

hence, using the approximate values,

$$k = \frac{F(t_2)}{z(t_2)} = \frac{(0.65)(25000)}{z_{0.9\,T_p}}$$

---

[14] For the sake of clarity, the subscript of "t", such as in t_2, will be retained to describe the corresponding section in Figures 67 and 68.

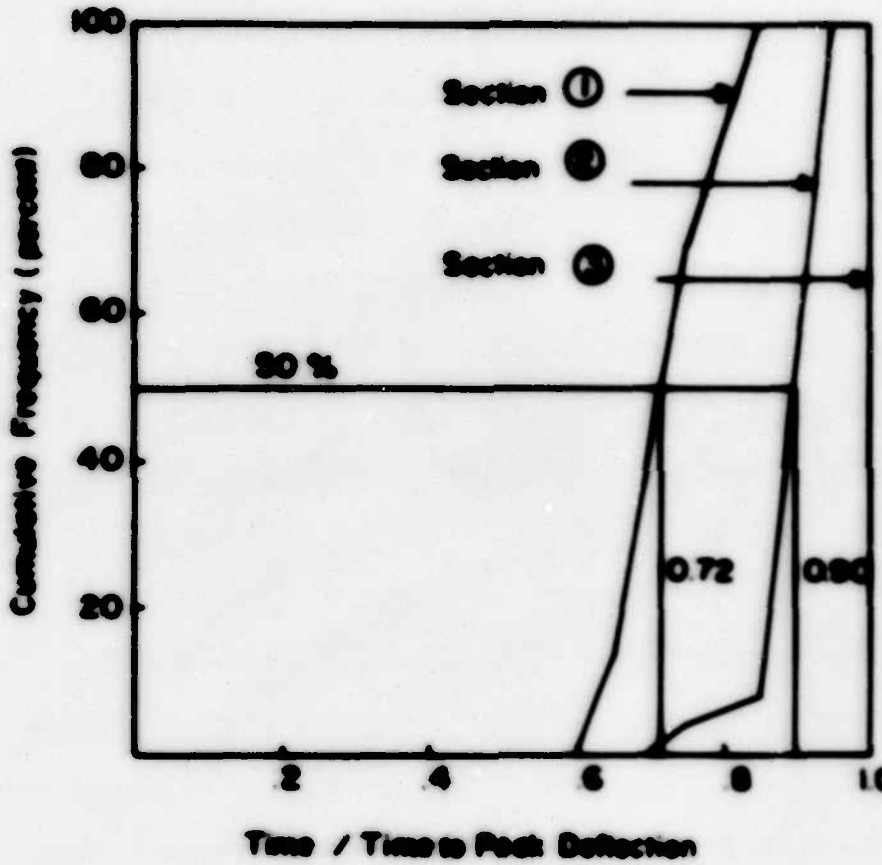

Figure 68. Frequency Characteristics of Time at the Point of Inflection, Crossing Point and Maximum Deflection

Once k is known, the c parameter can be obtained by applying the same reasoning to the point of inflection (section 1, Figure 67); namely,

$$c = [F(t_1) - kz(t_1)]/\dot{z}(t_1)$$

where $F(t_1)$ is 0.9 F_{max} (Figure 67) and $z(t_1)$ and $\dot{z}(t_1)$ are the deflection and numerical approximation of the velocity, respectively, at the time corresponding to 0.72 T_p (Figure 68).

The parameters m can then be estimated using the equation for conditions at the crossing point, where

$$m = - \frac{c \times \dot{z}(t_2)}{\ddot{z}(t_2)}$$

and $\dot{z}(t_2)$ and $\ddot{z}(t_2)$ are the numerical values for the velocity and acceleration at the time 0.9 T_p.

The developed approximate procedure for estimating k, c and m was examined with respect to 38 data sets from both Sites 1 and 2 at Eglin AFB[15]. The normalized forces at the crossing point and the point of inflection were taken to be 0.65 and 0.85[16], respectively. The normalized times at the crossing point and the point of inflection were taken to be 0.72 and 0.9, respectively. The k, c and m parameters obtained using the simplified procedure were then compared with their computer solutions. Correlation coefficients of 0.93, 0.93 and 0.90

[15] See Appendix B

[16] 0.9 was tried initially but 0.85 yielded c values which correlated more closely with the computer solutions.

were obtained from the linear least squares correlation study for the h, c and m parameters, respectively. The advantage of the simplified procedure is that it allows reasonably reliable estimates to be made of parameters without the need of a digital computer.

7.2.6 Estimating Design Parameters

The modulus of subgrade reaction ($\bar{k}$) and CBR of the subgrade can be estimated from the A_{peak} parameter of the peak deflection profile.

Using the assumption of a Kelvin model, Pister and William (Reference 26) developed the following relation between the subgrade deflection W(x), pressure on the subgrade (p), modulus of subgrade reaction ($\bar{k}$) and a shear stiffness parameter (CH) as the distance from the edge of the loaded area (x):

$$W(x) = \frac{p}{2\bar{k}} \exp(-x/CH)$$

This expression is similar in form to equation (2),

$$\delta_{max_j} = A_{peak} \exp(\beta_{peak} x_j^{\gamma_{peak}})$$

which was found to describe the maximum lateral dynamic deflection profile. If it is assumed that the two relations correspond at their maximum values (for x = 0), it follows that

$$A_{peak} = \frac{p}{2\bar{k}}$$

Hence, this suggests that the modulus of subgrade reaction can be obtained as,

$$\bar{k} = \frac{p}{2A_{peak}} \tag{23a}$$

Using a 1:1 simplifying assumption [cf. Yoder (Reference 33)] to calculate the attenuation of the wheel load, P_{max}, through the pavement section of thickness D, the contact pressure, p, equals $P_{max}/(3.64 + D)^2\pi$; where 3.64 is the radius of the equivalent circular contact area due to the F-4 aircraft with tire pressure 250 psi and a P_{max} of 25,000 pounds. Substituting in equation (23a) gives

$$\bar{k} = \frac{P_{max}}{2.0(3.64 + D)^2 \pi A_{peak}} \tag{23b}$$

CBR values can then be estimated using established correlations (Reference 65) between $\bar{k}$ and CBR. One such correlation given by the Portland Cement Association (Reference 65) is shown in Figure 69.

Using equation (23b) and the maximum, median and minimum values of A_{peak} calculated at site 2, and a D of 17 inches, $\bar{k}$ values of 323, 462 and 646 pounds per cubic inch were obtained. The same calculation for site 1 (with D = 9 in) gave $\bar{k}$ values of 237, 316 and 515. The correlation chart shown in Figure 69 gave the range of CBR value for site 2 from 28 to 73, and for site 1 from 18 to 52.

Moduli of subgrade reaction were not determined under asphaltic concrete pavement sections at Eglin Air Force Base by the Air Force Civil Engineering Center during the 1974 Survey (Reference 21): subgrade CBRs were obtained for these sections and those only at a few locations (about 10 in number). In the area of site 2, a CBR

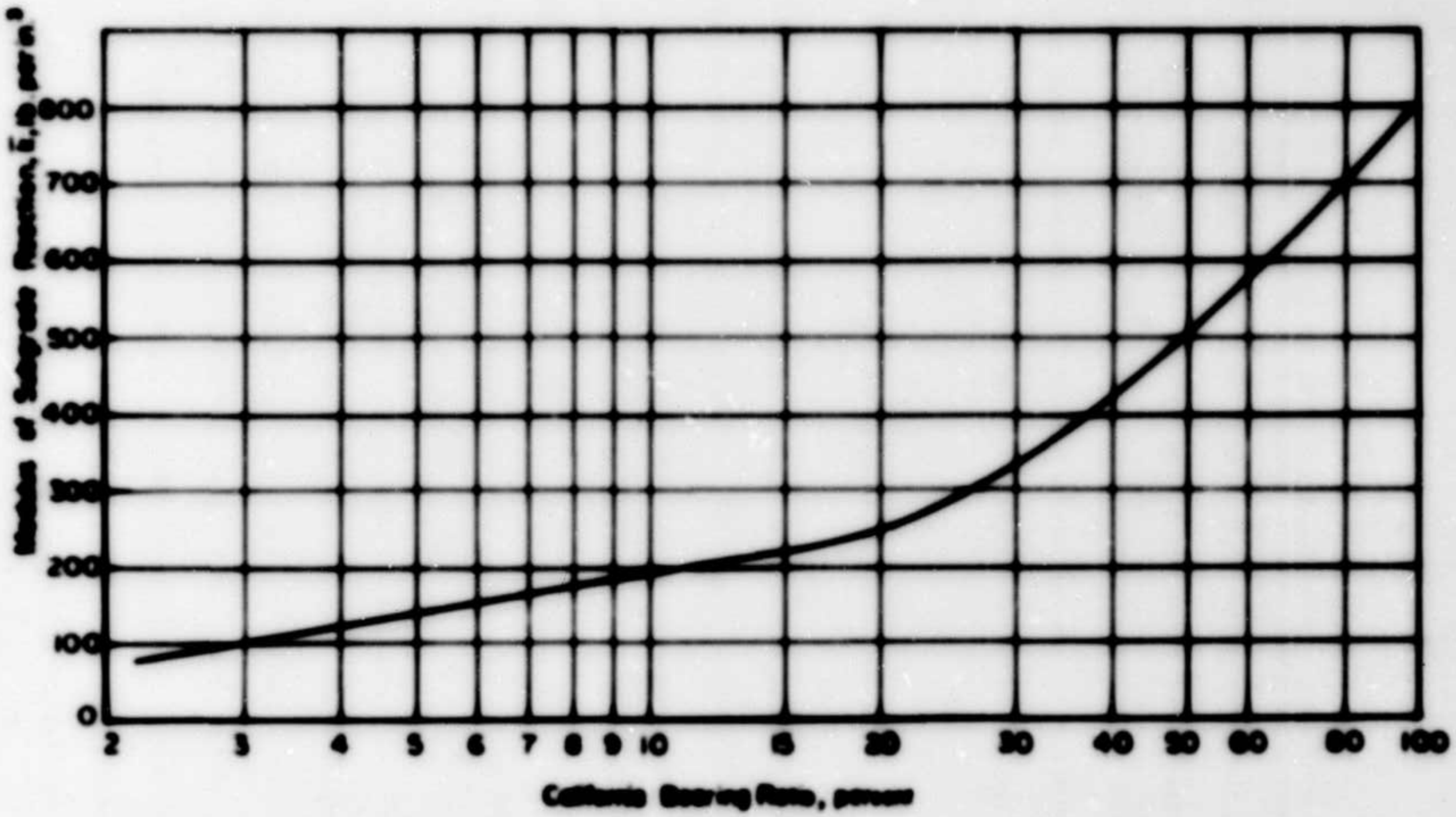

Figure 69. Relationship Between California Bearing Ratio and Modulus of Subgrade Reaction (after PCA [Reference 65])

value of 75 was reported. As noted above, this corresponds quite closely to the maximum calculated value of 73. The range of subgrade CBRs throughout the pavement sections varied from 10 to 85 percent. Reported $\bar{k}$ values, under the Portland Cement concrete sections, ranged from 220 to 520 psi.

It is interesting to note that the lower value of the range of CBRs for site 1 was about 18 while the low value for all the results was 10. Even though no CBR values were available in the vicinity of site 1, a comparison of its corresponding CBR and $\bar{k}$ values with those at site 2 indicate it to be an inferior pavement. This had been recognized by the Air Force as it is used only as a parking area; whereas, site 2 is an in-service taxiway.

In summary, the recommended procedure for estimating the $\bar{k}$ and CBR values from prototype F-4 loadings is as follows:

1. Estimate A_{peak} from an arithmetic plot of distance (x_j) from edge of the tire print versus peak deflections at each gage (x_j). A_{peak} is the intercept at $x = 0$.

2. Use equation (23b) to estimate $\bar{k}$, the modulus of subgrade reaction, and, if desired,

3. Find CBR value from established correlation charts such as Figure 69.

A worked example is shown in Appendix E.

7.3 Prediction

The prediction methodology consisted of (1) determining the relationship between the inputs of two vehicles at a standard site,

and (2) using this relationship to predict the response of one of the vehicles at another site, if only the response of that site to the other vehicle is measured.

7.3.1 <u>Validity of the Concept of the "Equivalency Function"</u>

The concept of the equivalency function has been used in many areas of engineering. In foundation engineering it has many names, some of which are "shape factor", "depth factor", and "inclination factor". In highway and airfield work it is known as "the equivalent single wheel load" or the "equivalent single axle load" or "layer equivalency factor". The basic underlying concept of "equivalency" is that two different entities can be related by a multiplier. In this work, the multiplier is a function of time - the equivalency function - and not a number.

The question arises as to whether the equivalency function defined at one site is applicable at another site where another set of conditions prevails. The results, Figure 52, showed that the equivalency function is indeed applicable under sets of conditions different from those under which it was first determined.

The equivalency function as defined in equation 21 is essentially a linear ratio of inputs of two vehicles at the same site. In reality the relationship between inputs is probably not linear; however, three factors seem to combine to make the effects of nonlinearity negligible.

First, consider the strain induced in the system due to prototype loading. Measured peak deflections are of the order of 0.05 inch,

whereas the depth of influence of the wheel load is of the order of 12 feet or 144 inches (Reference 60). Small strains, in general of about 0.0003, are thus induced in the system as a result of prototype loading. The linear approximation is valid because strains are small.

The linear approximation to actual nonlinear material behavior at small strains has been used in mechanics for years. Harr (Reference 66) has shown that if the functional relationship (F_1) between stress (σ) and strain (ϵ_x, ϵ_y, ϵ_z, $\cdots$ γ_{xz}), given by the equation

$$\sigma_x = F_1 \left(\epsilon_x, \epsilon_y, \epsilon_z, \gamma_{yz}, \gamma_{xz}, \gamma_{xy}\right)$$

is expanded in Maclaurin series, the equation

$$\sigma_x = (F_1)_o + \left(\frac{\partial F_1}{\partial \epsilon_x}\right)_o \epsilon_x + \left(\frac{\partial F_1}{\partial \epsilon_y}\right)_o \epsilon_y + \cdots + \left(\frac{\partial F_1}{\partial \gamma_{xy}}\right)_o \gamma_{xy}$$

results, if the higher order terms in the Maclaurin series are eliminated. The zero subscripts denote the value of the function F_1 relationship and its derivatives at zero strain. From this relation it can be seen that if strains are small a linear relationship exists between σ_x and ϵ_x, ϵ_y, ϵ_z, etc. Applying this same reasoning to the equivalency functions, the linear approximation between equivalent inputs works, because of the strains induced in pavement-subgrade systems due to prototype loads are, in general, small at all sites. The equivalency function at one site is thus the same equivalency function at another site where strains are small and of the same order of magnitude.

The second factor, which contributes to the validity of the

linear equivalency function, is inherent in the flexible pavement design procedures, that have evolved, and supports the "small strain" concept previously cited.

Pavements are designed, basically, to limit subgrade deflections. This can be inferred from the fact that conventionally, thick sections are constructed over weak subgrades, while on the other hand, thinner sections are built over strong subgrades. The net effect is that deflections and thus strains are forced to stay within the same order of magnitude of small strains by the design procedures. Since pavement sections are generally designed using conventional procedures, the "small strain" concept previously discussed should be valid for most pavements. Thus, the equivalency function between two such sites would be valid if strains at the two sites are of the same order of magnitude and small.

The third and final factor concerns the time the maximum load is actually applied at a point on the pavements. The time period that the wheel load is over a point is very small. Authors (References 40 and 47) have used Dirac Delta (impulse) functions to represent vehicular loads. Since the time is small, factors such as settlement, which normally are amplified in static cases, are of minimal importance in the dynamic mode.

7.3.2 Effects of Gear Configuration

The C-135, C-131 and C-130 aircraft have different gear configurations as shown in Figures 24 through 26. The prediction methodology permitted a vehicle having a single-twin gear configuration

(C-131) to be used as a standard vehicle to predict the response of a twin-tandem gear (C-135) and a single tandem gear (C-130). This implies that any vehicle in the inventory can be used as a standard vehicle. The combination of evaluation and prediction can thus be performed simultaneously by the selected vehicle. Thus, at each site evaluated, the response of all vehicles in the inventory can be predicted as a part of the evaluation.

7.3.3 Relative Effects of k, c and m Parameters

Figure 42 showed a typical plot of the calculated equivalent total force and of its force components with respect to the parameters k, c and m. The maximum resisting force due to the k parameter is seen to be about twice that of the resisting force due to the c parameter, and about 7 times greater than that of the m parameter. If design procedures could be directed toward greater mobilization of the k parameter it appears that a more logical basis for design could be had.

SECTION VIII

EFFECTS OF DISTRIBUTION OF PASSES ON RUNWAY PERFORMANCE

It is generally accepted by personnel concerned with airfield pavements that the response of the pavement-subgrade system is a function of the number of wheels on an aircraft gear, its gross load, tire pressures, width of tire print, ambient conditions and the lateral distribution of passes (References 1, 2, 3 and 4).

A method for quantifying the cumulative effect of the lateral distribution of passes, type of aircraft and ambient conditions in the context of pavement evaluation is presented. This method expands the concept of cumulative total pavement deflection presented by Highter and Harr (Reference 12). They found that a pavement could only accommodate a certain number of feet of cumulative total deflection prior to the onset of distress. Their data base consisted of AASHO Road Test data, data collected from Pease and Castle Air Force Bases and from prototype testing on specially designed test sections at Kirtland Air Force Base. Analysis of the data showed that a threshold cumulative total peak pavement deflection, at which severe distress occurs in asphaltic airfield pavements, was about 2000 feet. For asphaltic highway pavements the threshold, was about 1200 feet.

8.1 Pass to Coverage (p/c) Ratio Based on Tire-Contact Area Width

The pass to coverage (p/c) ratio, in concept, relates the number of passes made by a vehicle across a pavement-section to the number of passes over a selected point on the pavement. This ratio has been

related conventionally to the number of wheels on an aircraft landing gear, the width of the tire print and the lateral distribution of the aircraft wheel paths.

Two procedures (References 1 and 37) have been used to define the p/c ratio. Both of these procedures use as principal parameters the width of the tire print and the lateral distribution characteristics of the passes over a particular pavement section. The FAA procedure (Reference 1) defines p/c using the relationship

$$c = \frac{0.75\ D\ N\ W}{12T} \qquad (24)$$

where

c = coverages

N = Number of wheels of gear of aircraft

T = Traffic width in feet (generally, 7.5)

W = Width of tire contact area of one tire in inches, and

D = Cycles of operation (one cycle consists of one landing and one takeoff)

The constant, 0.75, is based on the assumption that the lateral distribution of aircraft can be approximated by a uniform distribution as shown in Figure 70(a). In concept, one cycle of operation is essentially two passes. Hence using D = p/2, equation (24) becomes,

$$c = \frac{(p/2)\ (0.75\ N\ W)}{12T}$$

$$= \frac{0.75\ p\ N\ W}{24T}$$

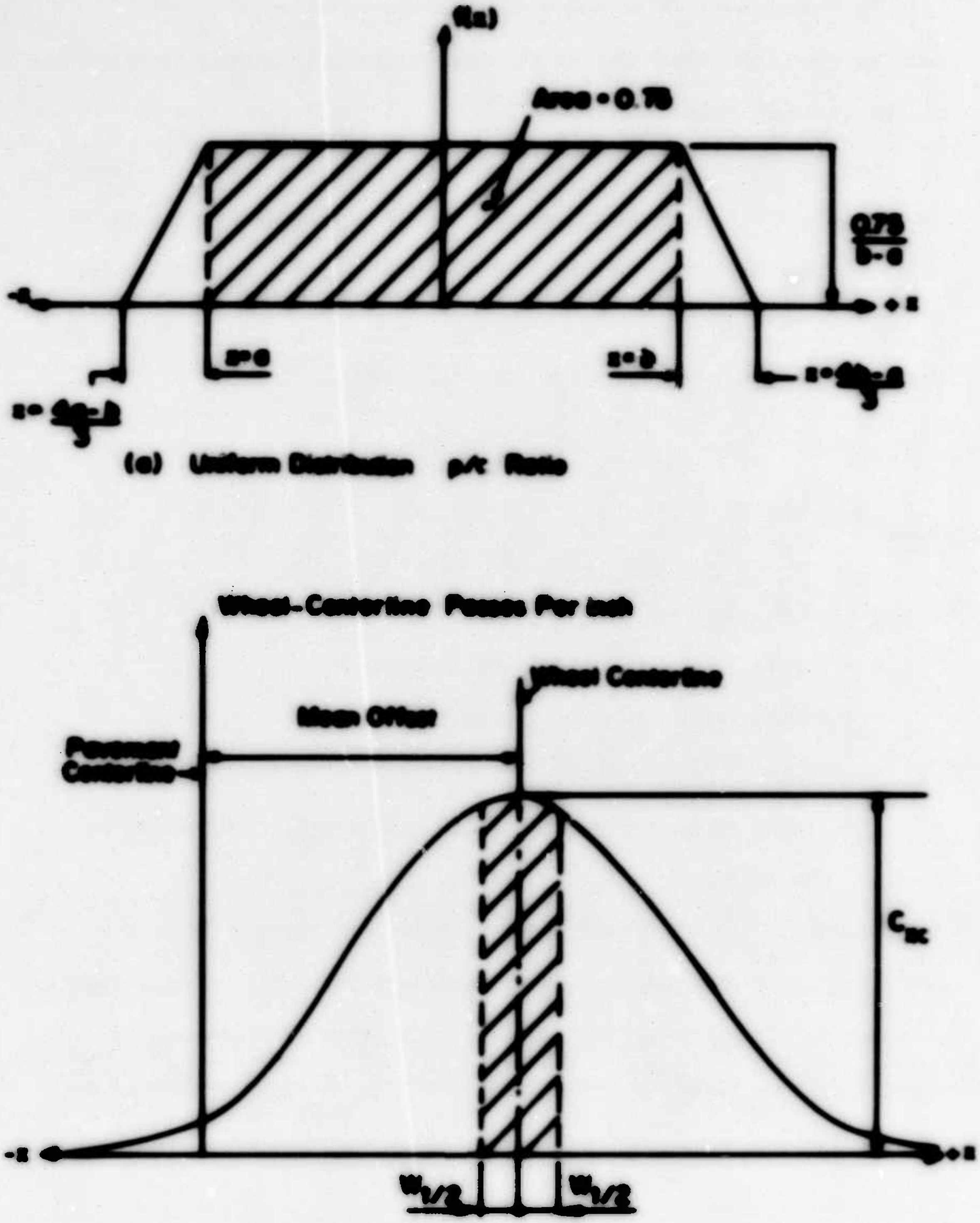

(b) Theoretical Normal Distribution

Figure 70. Lateral Distribution of Aircraft Used in Design of Airfield Pavement (after Hwang [Reference 37])

Thus

$$\frac{p}{c} = \frac{327}{N\ W}$$

Based on measurements of the lateral distribution of aircraft on various runways and taxiways, HoSang (Reference 57), proposed the use of a normal distribution instead of the uniform distribution, to describe the lateral distribution of aircraft. He gave the following expression for the p/c ratio:

$$p/c = \frac{1}{C_{wc}\ W_t}$$

where W_t is the width of the tire contact area. "C_{wc} represents the number of wheel-centerline passes per inch of width, per aircraft pass, which accumulate at the point where maximum accumulation occurs". Coverage c is defined as the maximum number of wheel passes at the point of maximum accumulation. Figure 70(b) illustrates the p/c ratio concept as applied to a single wheel. In concept, with reference to Figure 70(b), only the effects of tire prints or partial tire prints applied to the surface within the width W_t are considered in this method.

The current FAA procedure and HoSang's proposed method both use the tire print (contact area width) as a key parameter in the definition of the p/c ratio. The method developed here uses the measured dynamic lateral deflection profile, due to the prototype load, to define pass to coverage; and relates this ratio to performance extending the peak cumulative deflection concept introduced by Highter

and Kerr (Reference 12).

8.2 Deflection-Based p/c Ratio

The fundamental concept underlying the deflection-based p/c ratio is founded on the following reasoning. The level of significance of a loaded wheel during one pass over a pavement section is indicated by the measured lateral dynamic deflection basin. As the lateral distance from the load wheel increases, the work done by the load decreases. Hence, immediately under the wheel the influence is greatest; whereas, at a point where the measured deflection is zero, the influence is negligible.

As one pass, in effect, produces deflections from a maximum under the wheel to zero at some distance from the wheel; for a p/c ratio to be meaningful, it should account not only for the induced energy level corresponding to the maximum deflection but for all the levels in the range. The principal reasoning here is that the pavement-subgrade system "remembers" not only the maximum deflection but all load induced deflections. Hence, in general, large load induced deflections at a point result in greater work done and remembrances of it, than do smaller load induced deflections.

With reference to Figure 71, each of the curves labelled P, Q, R, S represents a series of peak lateral deflections. If one pass of a load wheel is applied at a point corresponding to $x = 0$, the maximum deflection (at $x = 0$) would be $A = \Delta_0$. If the same load had been applied at $x = 1$, a maximum deflection of Δ_1 would have been measured at $x = 0$. If the load had been applied at $x = 2$, then Δ_2

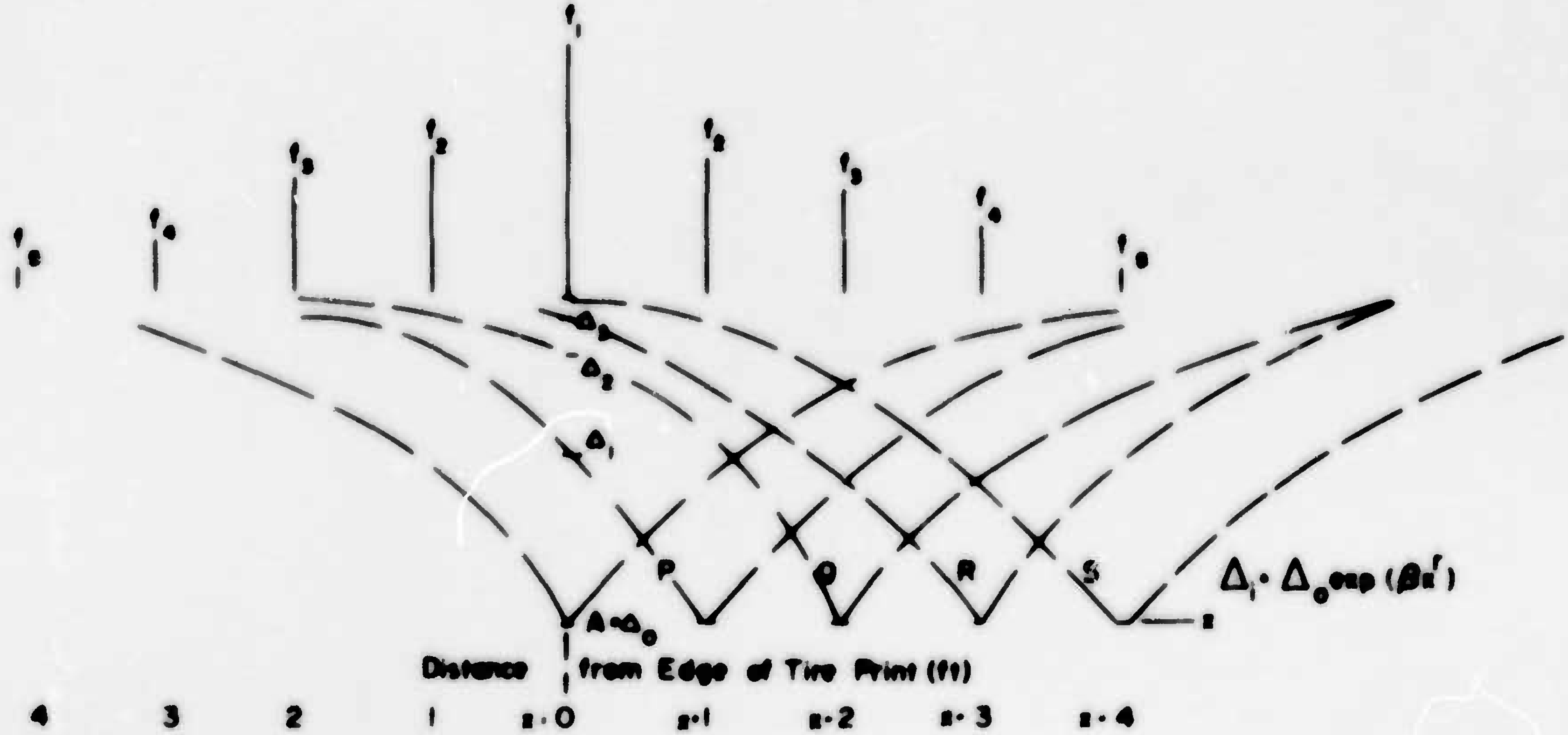

Figure 71. Overview of the Concept Used in the Deflection Based p/c Ratio Calculations

would have been measured at $x = 0$; similarly for a load at $x = 3$, etc.

One coverage then, in concept, is the cumulative peak deflection at the point in question that corresponds to maximum deflection A under the wheel. For example, if one pass of a load wheel is made at $x = 0$, then one coverage results at that point. On the other hand, one pass made at $x = 3$ corresponds to the fractional coverage Δ_3/A at $x = 0$.

Suppose that f_o through f_n are the discrete frequencies at $x = 0$, 1, 2, 3, ..., n, of the distribution of passes of aircraft laterally about $x = 0$. Then the cumulative peak deflection at $x = 0$ due to this frequency distribution becomes

$$\text{Cumulative Peak Deflection} = N_p \sum_{i=o}^{n} \Delta_i \, f_i$$

where N_p is the number of passes and Δ_i are the peak deflections corresponding to the points in question. The coverages N_c due to the N_p passes is then,

$$N_c = \frac{\text{Cumulative Peak Deflection}}{\text{Maximum Deflection under the Wheel}}$$

$$= N_p \sum_{i=o}^{n} \Delta_i \, f_i/\Delta_o$$

Therefore,

$$\frac{N_p}{N_c} = \frac{p}{c} = \frac{\Delta_o}{\sum_{i=o}^{n} \Delta_i \, f_i}$$

Equation (24) is seen to have the same form as the expression for the equivalent permeability of a layered system (Reference 67)

$$k_y = \frac{d}{\sum_{\bar{m}=1}^{n} d_{\bar{m}}/k_{\bar{m}}} \tag{25}$$

where k_y is the equivalent vertical permeability, $d_{\bar{m}}$ and $k_{\bar{m}}$ are the thickness and coefficient of permeability respectively of layer $\bar{m}$, and d is the sum of all the thicknesses.

8.3 Effects of Lateral Distribution

The effects of the frequency and of the lateral distributions of aircraft on the cumulative peak deflection and the deflection-based p/c ratio were studied.

Equation (2) in the form,

$$\Delta_j = \Delta_o \exp (\beta x_j^{r})$$

was used to calculate the lateral dynamic deflection profile, where Δ_j and x_j are the deflections and distances from the edge of the tire print at measurement points j in a direction perpendicular to the direction of motion of the wheel. Δ_o, β, and r are the parameters describing the maximum dynamic lateral deflection basin as discussed in paragraph 3.2.1. The numerical values, shown in Table 7, will be used to illustrate the procedure. These values were obtained from data collected at Site 1, Eglin AFB, in March 1976.

Table 7

Δ_o = 0.00479	
β = -0.001	
r = 1.021	
x_j (ft)	Δ_j (ft)
0	0.00479
1	0.00215
2	0.00094
3	0.00041
4	0.00018

Four discrete distributions are shown in Figure 72 for an assumed single wheel load. Figure 73 shows the effect of the four assumed lateral distributions (keyed by number to Figure 72) on the cumulative deflection. Figure 74 shows the effect of the scatter of the frequency distribution, as given by its standard deviation based p/c ratio. These results show that,

1. the assumption of a uniform distribution of passes (distribution 1 on Figure 72) yields the least cumulative peak deflection per pass and,
2. as would be expected, the distribution with the smallest scatter yields the greatest cumulative peak deflections.

8.4 Discussion

The results showed the dependence of cumulative peak deflection

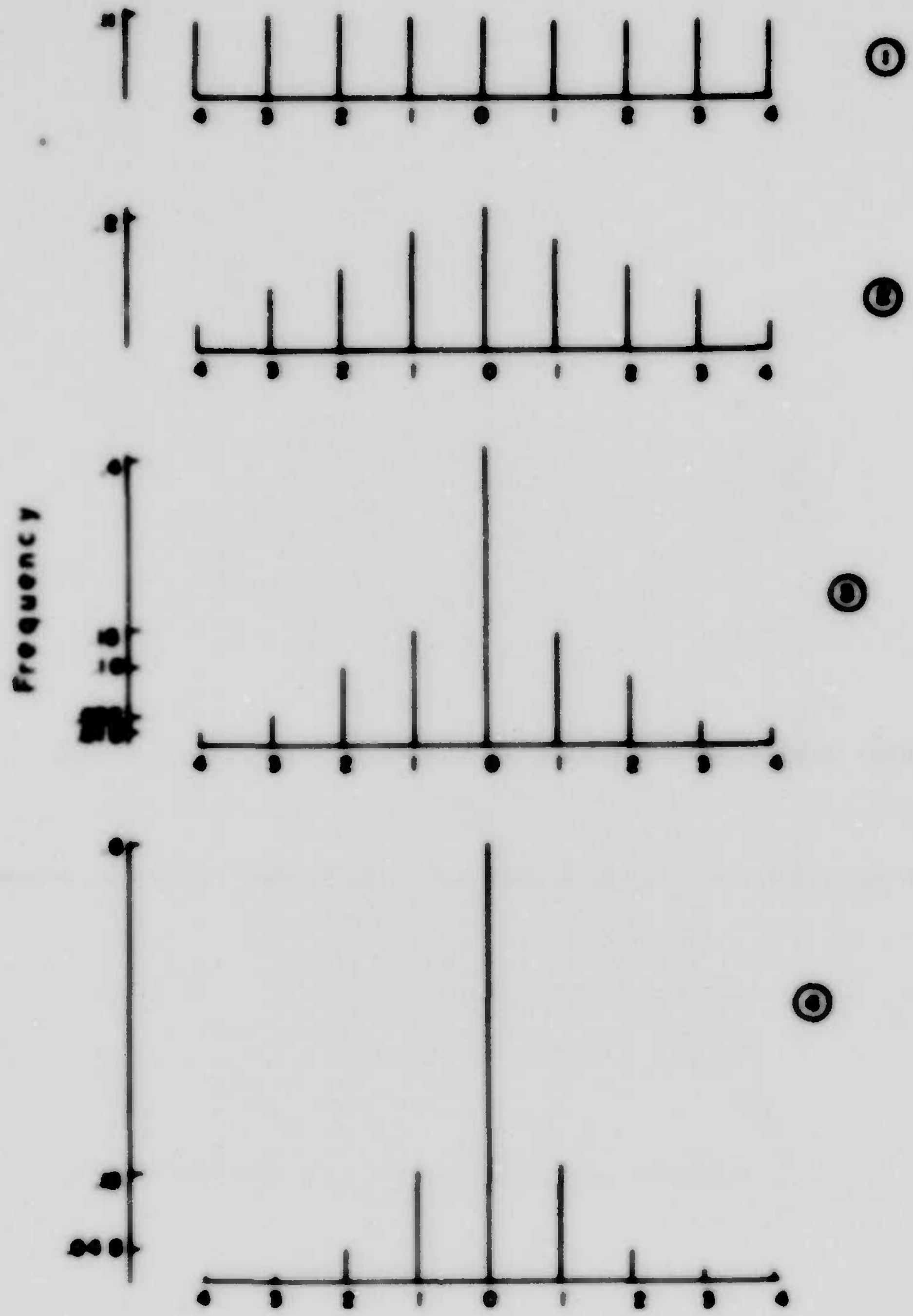

Figure 72. Discrete Distributions Used in Study

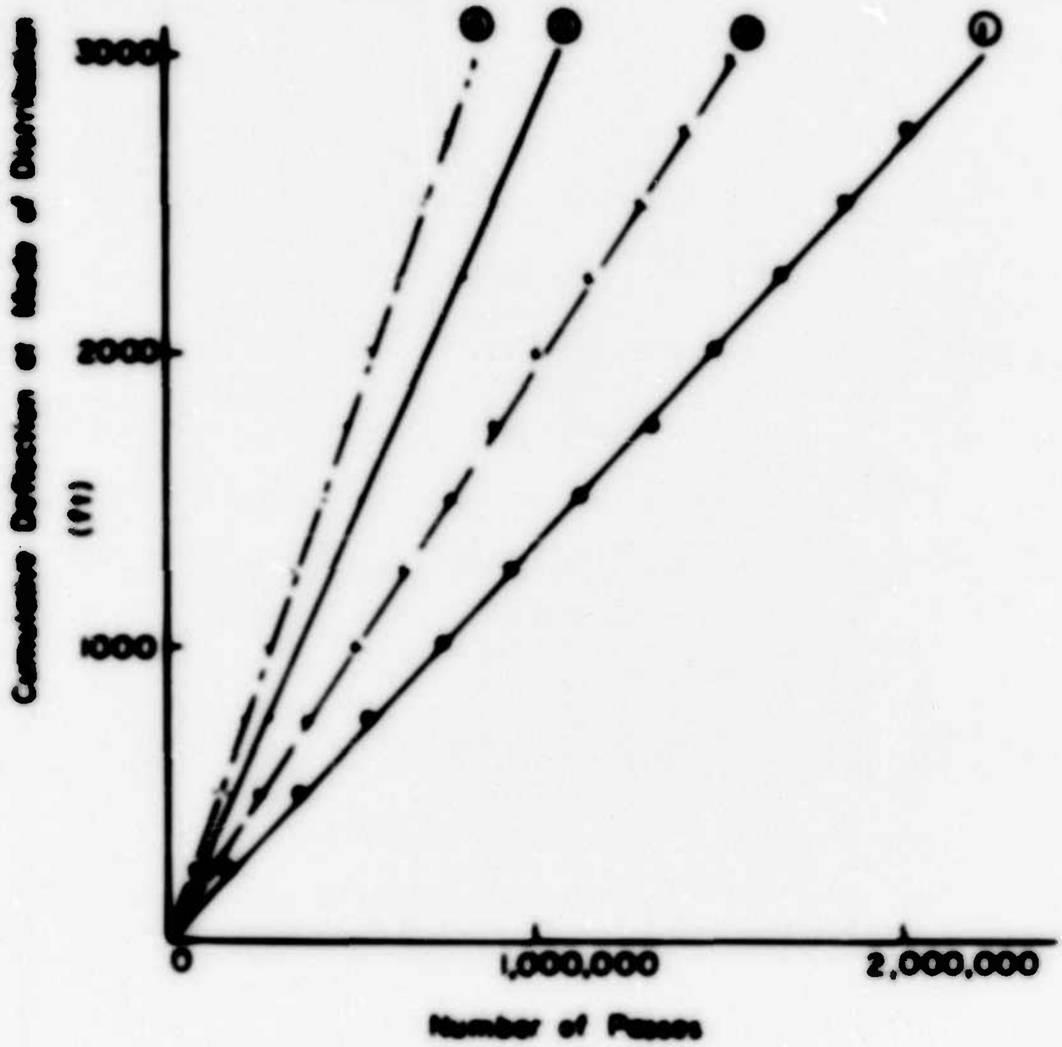

Figure 73. Cumulative Deflection vs. Passes for Four Discrete Distributions of Passes

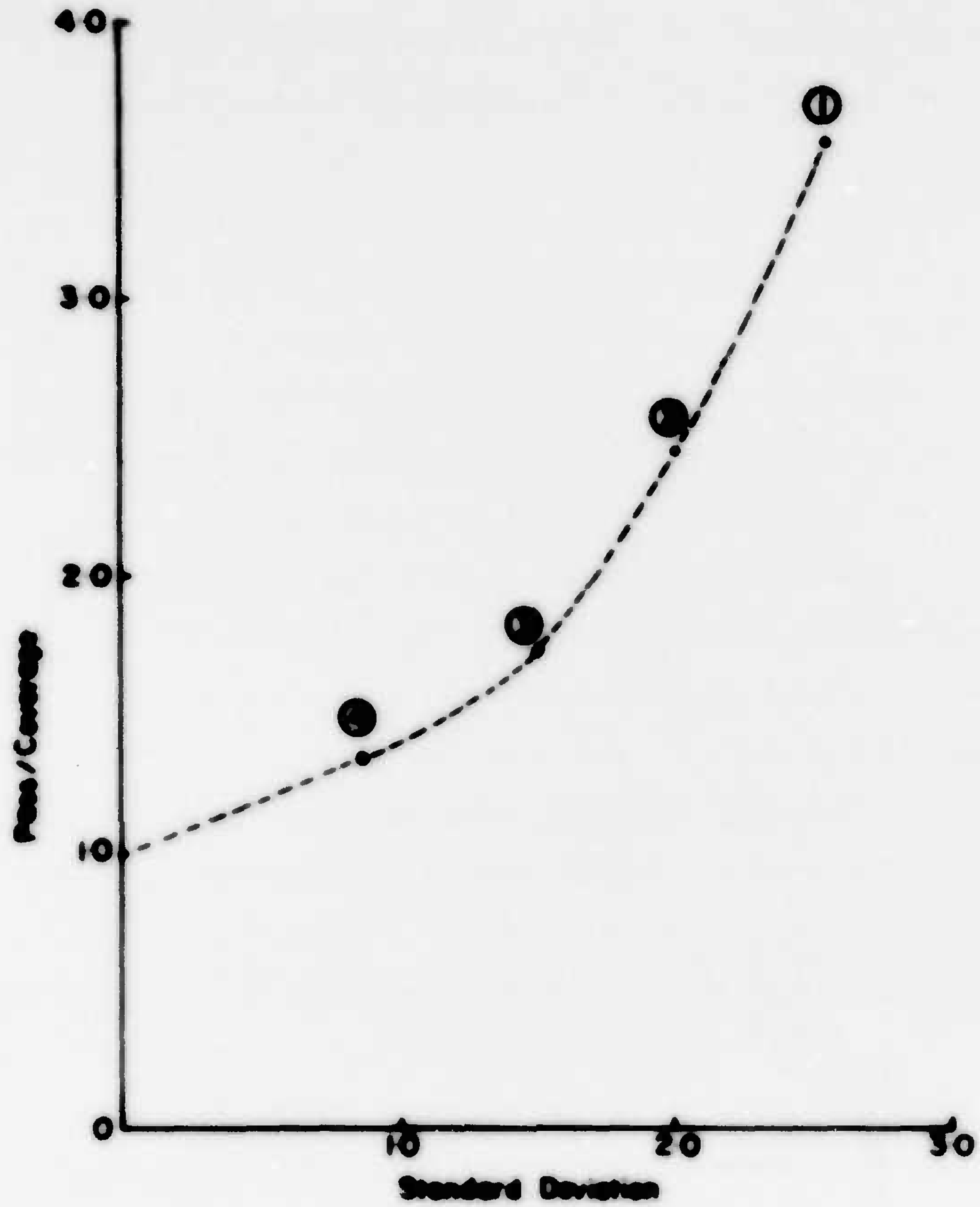

Figure 74. Effects of Standard Deviation on Deflection-Based p/c Ratio

on the lateral distribution of passes and the peak deflection profile. The p/c ratio thus provides a means of quantifying the variability of the input (aircraft loads) characteristics and pavement-subgrade system response (output).

With reference to Figure 75, input variables consist of aircraft loads and lateral distribution characteristics of loads. These can include wind effects, surface condition, type of aircraft, and quantity of fuel aboard. The main output variable is the peak pavement deflection profile. Inherent in this measurement are temperature effects and other ambient conditions. Figure 75 shows how the p/c ratio can be utilized to estimate the amount of energy imparted to a pavement-subgrade system due to variable inputs and also how to estimate the number of passes required to induce a certain energy input as given by the total cumulative peak deflections.

For example, assuming that the lateral distribution of passes has a standard deviation of 2.0 (distribution 2 in Figure 73), the number of passes required to reach the threshold[13] total cumulative peak deflection value of 2200 feet is 1,160,000 passes or 580,000 cycles of operation.

On the other hand, if the assumed lateral distribution of passes has a standard deviation of 2.66, then 580,000 cycles of operation would yield a cumulative peak deflection value of about 1500 feet, which is well below the threshold[13] value for that distribution. For this case 850,000 cycles of operation could be tolerated before severe

[13] The threshold value of 2200 feet was given by Highter (Reference 12) without due regard to the lateral positioning of traffic. Lacking additional information at this time the same value was used in the present study.

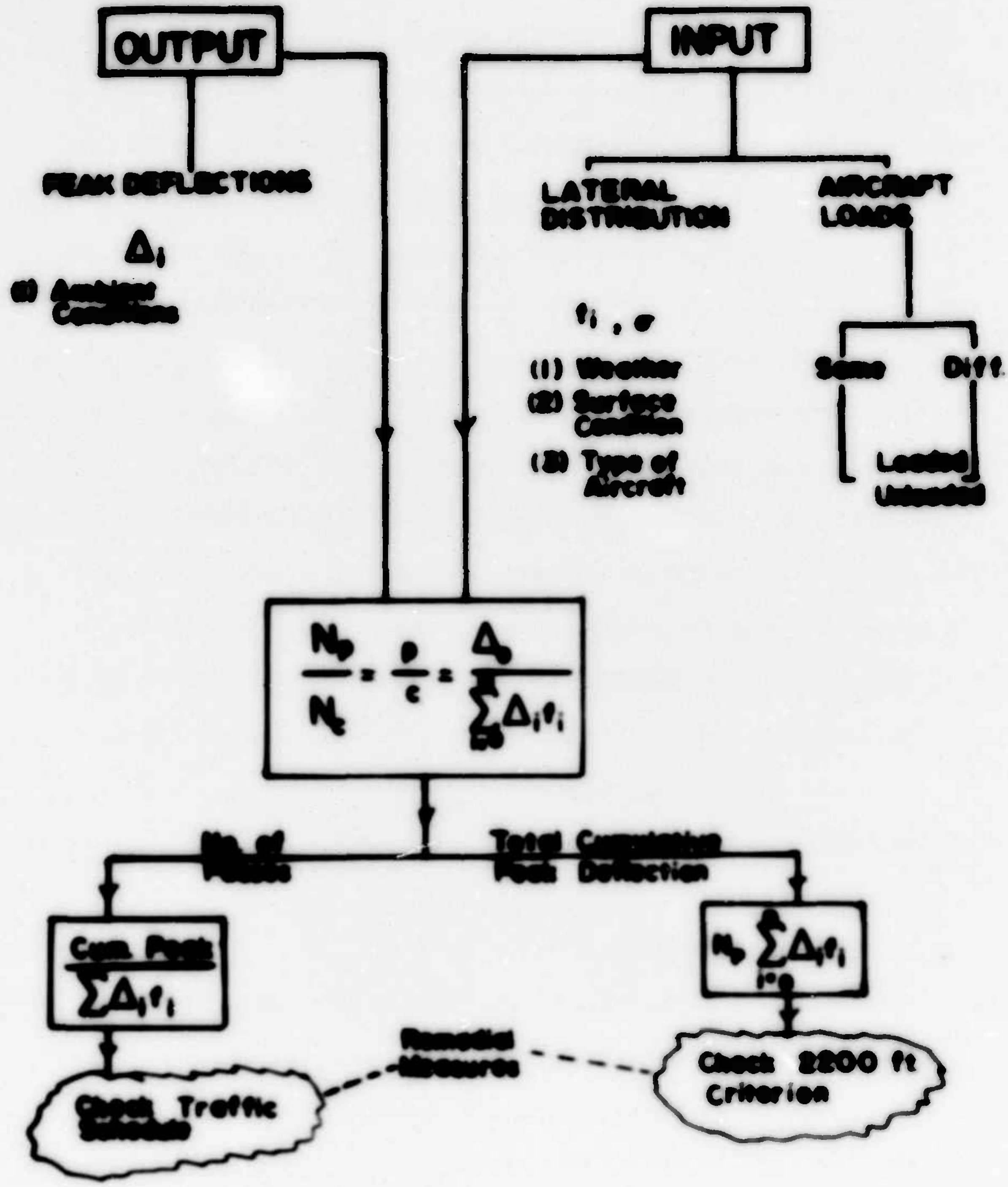

Figure 75. Overview of Evaluation Scheme Using Deflection Frequency Relationship

distress might be expected.

As another example, suppose that due to overlay or resurfacing of pavement, parameters and peak deflections change to those given in Table 8 after 290,000 cycles of operation, then 700,000 cycles of operations (rather than 290,000) would now be required to attain the threshold[14] value of 2200 feet. This assumes that the section "remembers" the loading prior to resurfacing. If resurfacing had not taken place,only 290,000 cycles of operation would have been required to show effects of distress.

The above examples have attempted to show that actual measured distribution data such as that provided by HoSang (Reference 57), and actual measured deflections (which account for ambient seasonal effects) can be combined to estimate the cumulative damage effects due to prototype loads. Once a standard site and standard vehicle have been selected, the damage effects of various magnitudes of loads

Table 8

$\Delta_o = 0.0012$

$\beta = -0.2256$

$r = 1.7770$

x_j (ft)	Δ_j (ft)
0	0.00120
1	0.00096
2	0.00055
3	0.00026
4	0.00005

[14] See Footnote 13.

and gear configurations and their distributions can be estimated. By monitoring the effects of specific pavement sections, the direction which remedial measures should take could be established [see Highter and Harr (Reference 12)].

SECTION IX

SUMMARY

The findings of the present research effort can be summarized under three basic categories, namely:

1. nondestructive pavement testing equipment development,
2. nondestructive pavement evaluation and behavior prediction, and
3. extension of cumulative peak deflection-damage-energy related concepts.

Two equipment systems for use in the nondestructive evaluation of flexible pavements have been developed. They are the LED system and the LVDT system. The feasibility of rapidly measuring pavement deflections caused by moving loads using the developed equipment has been investigated. Field testing of the developed systems using prototype loads was conducted.

A nondestructive pavement evaluation methodology using transfer function theory has been developed. Parameters of the transfer function which reflect site characteristics have been isolated and related to performance of two sites. Parameters of the lateral peak deflection profiles have been investigated. Simplified procedures for estimating the parameters of the transfer function and parameters (CBR, etc.) used in design have been suggested.

A methodology has been presented for predicting the deflection if the response at a standard site to a standard load vehicle and another vehicle, and the response of the other sites to the standard vehicle are known. The same transfer function parameters that are used in the

evaluation phase are used in the prediction scheme.

A method of accounting for the lateral distribution of aircraft on a pavement, and variability of input and output to the pavement-subgrade system has been presented. The interrelationship among the components of NDT pavement evaluation-response prediction-cumulative damage prediction based on deflections caused by prototype loading has been discussed. The deflection based pass to coverage ratio was shown to be a vital link in the scheme.

SECTION X

CONCLUSIONS

This research effort has attempted to cover a spectrum of activities that comprise nondestructive testing and evaluation of flexible airfield pavements. The following conclusions have been reached as a result of this study.

1. Rapid nondestructive measurements of pavement deflections due to moving prototype loads can be obtained in the field using the LED system "breadboarded" in this research effort and the companion LVDT system.
2. The parameters of both the transfer function and the peak lateral deflection profile reflect characteristics of the pavement-subgrade systems and can be used as the basis of a nondestructive pavement evaluation scheme. Some common parameters such as CBR and modulus of subgrade reaction can be obtained from those defined in this study.
3. The developed methodology, using the same parameters of the transfer function that are used to evaluate a pavement system, can be used to predict the deflection response function of a site to different magnitudes and configurations of loadings.
4. The concept of cumulative peak deflection (Reference 12) as it relates to energy induced in a pavement-subgrade-system due to load repetition, was extended to account for the lateral distribution of aircraft. The frequency characteristics and the number of passes of aircraft are shown to

effect, significantly, the amount of distress a pavement might evidence in time.

SECTION XI

RECOMMENDATIONS

This work has afforded the opportunity to consider in some depth a significant portion of the current state of the art of nondestructive testing theory and methods used on airfield pavements. Based on the findings of this work the following recommendations are forwarded:

1. The use of prototype loadings in evaluation should be encouraged.
2. The development of a scheme, based on the use of nondestructively measured pavement deflections due to prototype loads, similar to that briefly discussed in paragraph 8.4 of this work should be pursued.
3. The prototype of noncontact measuring equipment shown to be feasible in this investigation should be developed. This development should take advantage of the current state of the art in optical design.
4. A thorough study of the lateral distribution of aircraft has recently been made (Reference 57). A similar information gathering study should be initiated to collect data on numbers and types of aircraft using specified pavements at both commercial and military installations. Pavement deflections should be obtained regularly at the sections being monitored. This data base is necessary if the concepts and the preliminary conclusions reached at this time are to be validated and generalized.
5. The speedy development of a prototype device to move over the

pavement sections and simultaneously measure its own dynamic deflection basin without significantly interrupting traffic would greatly facilitate the information gathering phase. This would simultaneously provide a common denominator or standard vehicle.

6. Research should be directed towards determining the influences of the components of a pavement-subgrade system on the k, c, and m parameters. The success of this endeavor would be a step towards optimizing design procedures and the use of paving materials.

LIST OF REFERENCES

1. Federal Aviation Administration, Advisory Circular AC 150/53206A, Airport Paving, U. S. Department of Transportation, May 1967.

2. Design Manual - Airfield Pavements, Department of the Navy, NAVFAC - DM-21, June 1973.

3. Design and Evaluation of Flexible and Rigid Pavements, Department of Transportation, Ottawa, Canada, June 1962.

4. Design and Evaluation of Aircraft Pavements, 1971, Directorate of Civil Engineering Development, Department of the Environment, London, 1971.

5. Hanson, D., I., "Special Problems with Airfield Pavement Maintenance," Proceedings of a Workshop on Pavement Rehabilitation, Transportation Research Board, Report No. FHWA-RD-74-60, Washington, D.C., June 1974.

6. Busching, H. W., Goetz, W. H., and Harr, M. E., "Stress-Deformation Behavior of Anisotropic Bituminous Mixtures," Proceedings, Assn. Asphalt Paving Technology, Vol. 36, 1967.

7. Goetz, W. H., Harr, M. E., and Lal, N. B., "Invarient Properties of a Sheet-Asphalt Mixture," Highway Research Record No. 158, 1967.

8. Swami, S. A., Goetz, W. H., Harr, M. E., "Time and Load Independent Properties of Bituminous Mixtures," Highway Research Board, Record No. 313, 1970.

9. Ali, G. A., "A Laboratory Investigation of the Application of Transfer Functions to Flexible Pavements," Ph.D. Thesis, Purdue University, August 1972.

10. Harr, M. E., Boyer, R. E., "Predicting Pavement Performance Using Time-Dependent Transfer Functions," AFWL-TR-72-204, Kirtland Air Force Base, New Mexico, January 1973.

11. Boyer, R. E., "Predicting Pavement Performance Using Time-Dependent Transfer Functions," Ph.D. Thesis, Purdue University, August 1972.

12. Highter, W. H., and Harr, M. E., "Application of Energy Concepts to the Performance of Airfield Pavements," Tech. Rept. AFWL-TR-72-225, Kirtland Air Force Base, New Mexico, June 1973.

13. Highter, W. H. "The Application of Energy Concepts to Pavements," JHRP Rept. 38, Purdue University.

14. Haas, R., "Surface Evaluation of Pavements: State of the Art," Report No. FHWA-RD-74-60, Transportation Research Board, Washington, D. C., June 1970.

15. McComb, Richard A., and Labra, John J., "Structural Evaluation and Overlay Design for Highway Pavement," A Review Report No. FHWA-RD-74-60, Transportation Research Board, Washington, D.C.,

16. Witczak, M. W., "Structural Evaluation and Overlay Design Methodology for Airfield Pavements: State of the Art," Report No. FHWA-RD-74-60, Transportation Research Board, Washiugton, D.C., June 1970.

17. McCullough, B. Frank, "State of the Art in Predicting the Probabilistic Response of Pavement Structures." Transportation Research Record No. 575, 1976.

18. "Airfield Flexible Pavements Air Force, Departments of the Army and the Air Force," TM 5-824-2 (AFM 88-6, Chap. 2), Feb. 1969.

19. American Society for Testing and Material "Standard Method for Nonrepetitive Static Plate Load Tests on Soils and Flexible Pavement Components for Use in Evaluation and Design of Airport and Highway Pavements." ASTM Designation D1196 Vol. , 1971.

20. American Society for Testing and Materials, "Standard Method for Repetitive Static Plate Load Tests of Soils and Flexible Pavement Components, for Use in Evaluation and Design of Airport and Highway Pavements." ASTM Designation D1195, Vol. , 1971.

21. AFCEC - Tyndall AFB, "Air Field Evaluation Report - Eglin AFB, Florida," Tyndall AFB, Florida, March 1975.

22. Vittas, George P., "A User Viewpoint on Airport Design Standards Past, Present and Future." Symposium on Nondestructive Tests and Evaluation of Airport Pavements, U. S. Army Engineer Waterways Experiment Station, Vicksburg, Mississippi, November 1975.

23. Scrivner, Frank H., Peohl, Rudell, Moore, W. M., and Phillips, M. B. "Detecting Seasonal Changes in Load-Carrying Capabilities of Flexible Pavements." Highway Research Board, National Cooperative Highway Research Program Report 76, 1969.

24. Isaada, N. M., "Impulsive Load Stiffness of Flexible Pavements," Proceedings of the American Society of Civil Engineers, Journal of Soil Mechanics and Foundation Division, Vol. 96, No. SM2, March 1970.

LIST OF REFERENCES (Continued)

25. Green, J. L. and Hall, J. W., "Nondestructive Vibratory Testing of Airport Pavements, Experimental Test Results and Development of Evaluation Methodology and Procedure," Vol. 1, Report No. FAA-RD-73-205-1, U. S. D. T. - FAA, Washington, D. C., September 1975.

26. Pister, K. S., and Williams, M. L., "Bending of Plates on a Viscoelastic Foundation." Journal of the Engineering Mechanics Division, Proceedings of the ASCE, Vol. 86, No. EM5, October, 1960.

27. Pister, K. S., and Monismith, C. L., "Analysis of Viscoelastic Flexible Pavements." Flexible Pavement Design Studies 1960, Highway Research Bulletin 269, 1960.

28. Reissner, E., "A Note on Deflections of Plates on a Viscoelastic Foundation." Transactions of the ASME, Vol. 25, No. 1, March 1958.

29. Hoskin, B. C., and Lee, E. H., "Flexible Surfaces on Viscoelastic Subgrades," Journal of the Engineering Mechanics Division, Proceedings of the ASCE, Vol. 85, No. EM4, October, 1959.

30. Barksdale, R. D., and Leonards, G. A., "Predicting Performance of Bituminous Surfaced Pavements." Proceedings, International Conference on the Structural Design of Asphalt Pavements, University of Michigan, 1967.

31. Pister, K. S., and Westmann, R. A., "Analysis of Viscoelastic Pavements Subjected to Moving Loads," Proceedings, International Conference of the Structural Design of Asphalt Pavements, University of Michigan, 1963.

32. Harr, M. E., and Lewis, K. H., "Analysis of Concrete Slabs Subjected to Warping and Moving Loads," Highway Research Board Record No. 291, 1969.

33. Harr, M. E., and Leonards, G. A., "Analysis of Concrete Slabs on Ground Journal of the Soil Mechanics and Foundations Division," Proceedings of the ASCE, Vol. 85, No. SM3, June, 1959.

34. Gasi, D. C., "Analysis of Finite Beams on Elastic Foundations," Journal of the Structural Division, Proceedings of the ASCE, Vol. 84, No. ST4, July 1958.

35. Pister, K. S., "Viscoelastic Plate on a Viscoelastic Foundation." Journal of the Engineering Mechanics Division, Proceedings of the ASCE, Vol. 87 No. EM1, February 1961.

36. Hogg, A. H. A., "Equilibrium of a Thin Plate, Symmetrically Loaded, Resting on an Elastic Foundation of Infinite Depth," Philosophical Magazine, Vol. 25, 1938.

37. Terzaghi, K., "Evaluation of Coefficients of Subgrade Reaction," Geotechnique, Vol. 5, No. 4, December, 1955.

38. Harr, M. E., "Influence of Vehicle Speed on Pavement Deflection." Proceedings, Highway Research Board, Vol. 44, 1962.

39. Freudenthal, A. M., and Lorsch, H. G., "The Infinite Elastic Beam on a Linear Viscoelastic Foundation." Journal of the Engineering Mechanics Division, Proceedings of the ASCE, Vol. 83, No. EM1, January 1957.

40. Perloff, W. H., and Moavenzadeh, F., "Deflection of Viscoelastic Medium due to a Moving Load," Proceedings, International Conference on the Structural Design of Asphalt Pavements, University of Michigan, 1967.

41. Weiss, R. A., "Nondestructive Vibratory Testing of Airport Pavements." Vol. II, Report No. FAA-RD-73-205-II, U. S. D. T.-FAA, Washington, D.C., April 1975.

42. Wiseman, Gdalyah, "The Interpretation of Surface Deflection Measurements Using the Model of an Infinite Plate on an Elastic Foundation." Symposium on Nondestructive Test and Evaluation of Airport Pavements, Vicksburg, Mississippi, November 1975.

43. Orellana, J. E., "FPS-11 Flexible Pavement System Computer Program Documentation," Texas Highway Department; Texas Transportation Institute, Texas A&M University; and Center for Highway Research, University of Texas at Austin, Research Rept. 123-15, April 1972.

44. Zube, E. and R. Forsyth, "Flexible Pavement Maintenance Requirements as Determined by Deflection Measurements," Highway Research Record 129, 1966.

45. "Asphalt Overlays and Pavement Rehabilitation," The Asphalt Institute, Manual Series 17, November 1969.

46. Darter, M. I. and Hudson, W. R., "Probabilistic Design Concepts Applied to Flexible Pavement Design," Center for Highway Research, University of Texas at Austin, Research Rept. 123-18, 1973.

47. Moavenzadeh, Fred, "Stochastic Model for Prediction of Pavement Performance," Transportation Research Record 575, Washington, D.C., 1976.

48. Mignot, J. E. et al., "Aircraft Dynamic Wheel Load Effects on Airport Pavements: Final Report," Report No. FAA-RD-70-19, May 1970, Federal Aviation Administration, Washington, D.C.

49. Horn, W. J. and Ledbetter, R. H., "Pavement Response to Aircraft Dynamic Loads: Instrumentation Systems and Testing Program," Report No. FAA-RD-74-39, Vol. I, June 1975, Federal Aviation Administration, Washington, D.C., and Technical Report S-75-11, Vol. I, June 1975, U. S. Army Engineer Waterways Experiment Station, CE, Vicksburg, Miss.

50. Ledbetter, R. H., "Pavement Response to Aircraft Dynamic Loads; Presentation and Analysis of Data; Appendix B: Data," Report No. FAA-RD-74-39, Vol. II, September 1975, Federal Aviation Administration, Washington, D.C., and Technical Report S-75-11, Vol. II, September 1975, U. S. Army Engineer Waterways Experiment Station, CE, Vicksburg, Miss.

51. Szendrei, S., and Kühn, S. H., "Interpretation of Vibration Tests on Roads by the Impedance Method," Highway Research Board No. 46, 1963.

52. Baladi, G. Y., "Invariant Properties of Highway Material," Ph.D. Thesis submitted to Purdue University December 1976.

53. Harr, M. E., "Analytical and Numerical Methods in Engineering," Class Notes, Purdue University, 1975.

54. AFWL, "Aircraft Characteristics for Airfield Pavement Design and Evaluation," Technical Report No. AFWL-TR-69-54, Kirtland Air Force Base, N. M., October 1969.

55. Yoder, E. J. and Witczak, M. W., "Principles of Pavement Design," 2nd Edition, John Wiley and Sons, Inc., New York, 1975.

56. Murphy, Carl G., "Electro-Optical Pavement Deflection Measuring System," Submitted to Purdue University, W. Lafayette, Indiana, 1976.

57. HoSang, Victor A., "Field Survey and Analysis of Aircraft Distribution on Airport Pavements," Report No. FAA-RD-74-36, Federal Aviation Administration, Washington, D.C., February 1975.

58. Yoder, Eldon J. and Gramling, L. Wade., "Measurement Systems - Report of Group 2," Proceedings of a Workshop on Pavement Rehabilitation, Federal Highway Administration, Report No. FHWA-RD-74-63, Washington, D.C., June 1974.

59. Woods, R. D., "Screening of Surface Waves in Soils," Journal of Soil Mechanics and Foundations Division, Proceedings, American Society of Civil Engineers, Vol. 94, No. SM4, July 1968.

60. Ledbetter, R. H., Ulery, Jr., H. H., and Alvin, R. G., "Traffic Tests on Airfield Pavements for Jumbo Jets," Proceedings of the Third International Conference on the Structural Design of Asphalt Pavements, University of Michigan, Ann Arbor, Michigan, 1972.

61. Whittemore, Allan P., Wiley, John R., Schultz, Phillip C, and Pollock, Donald E., "Dynamic Pavement Loads of Heavy Highway Vehicles," National Cooperative Highway Research Program Report 105, Highway Research Board, 1970.

62. Nichols, Jr. F. P., "Deflections as an Indicator of Flexible Pavement Performance," Special Report, Virginia Council of Highway Investigation and Research, 1963.

63. Ford, Jr. M. C., and Bisselt, J. R., "Flexible Pavement Performance Studies in Arkansas," Highway Research Board Bulletin 321 (1962).

64. Kung, Juang-Yuan, "A New Method in Correlation Study of Pavement Deflection and Cracking," Proceedings of the Second International Conference on the Structural Design of Asphalt Pavement, University of Michigan, Ann Arbor, Michigan 1967.

65. Portland Cement Association, "The Design of Concrete Pavements for City Streets," PCA, Skokie, Illinois, 1963.

66. Harr, M. E., "Foundations of Theoretical Soil Mechanics," McGraw Hill Book Company, New York 1966.

67. Harr, M. E., "Groundwater and Seepage," McGraw Hill Book Company, New York 1962.

68. Nielsen, John P.,"Pavement Evaluation System,"AFCEC-TR-76-28, Tyndall Air Force Base, Florida, December 1976.

69. Benkelman, A. C., "Analysis of Flexible Pavement Deflection and Behaviour Data," Highway Research Board Bulletin 210, 1959.

70. Prandi, E., "LaCroix-LCPC Deflectograph," Proceedings of the Second International Conference on the Structural Design of Flexible Pavements, University of Michigan, Ann Arbor, Michigan, August 1967.

LIST OF REFERENCES (Concluded)

71. Still, P. B., and Winnett, M. A., "Development of Contactless Displacement Transducer," Transport and Road Research Laboratory TRRL Rept. 690, Department of the Environment, Crowthorne, Berkshire 1975.

APPENDIX A

RESEARCH AND DEVELOPMENT

OF

MEASUREMENT SYSTEMS

The breadboard model of the LED system was subcontracted by Purdue University to Science Applications Incorporated (SAI), New Mexico, during the period May, 1974 to December, 1975. The contents of Section a of this Appendix is based principally on SAI's Final Report (Reference 56).

During the period January 1975 to June 1976, the breadboard model electronics was upgraded at Purdue University and work was done to convert the static measurement system in order to make it more compatible with a moving beam-moving load concept. Section b of this Appendix presents a summary of this work.

Section c of this Appendix presents some details of the Linear Variable Differential Transformer System (LVDT) developed at Purdue University by G. Baladi (Reference 52) for a study sponsored by the FHWA.

a. The LED System

Several optical systems were considered during the development of the LED system. These include:

1. A retroflector module whose motion is detected by a laser beam.
2. A limited version of the global Moire method.
3. Focal point shift detection.
4. Triangulation of a light spot on a surface.

As the triangulation method was finally selected for development, only the summary details concerning this method are presented herein.

The breadboard model employing the triangulation method is shown in Figure A-1. This arrangement has an image shift δ_2 (Figure A-2) perpendicular to the line of view which is related to the pavement deformation by the equation,

$$\delta_2 = m \frac{\sin (\gamma + \beta)}{\sin \gamma} \cdot \frac{\delta}{\tan (90 - \gamma)}$$

where m is the magnification of the deformation. Other symbols are designated in Figure A-2. The pavement "roughness" function is represented by f(x).

The straight line of the input center ray is given by

$$y = (x-b) \tan (90 - \gamma)$$

or

$$y = x \tan (90 - \gamma) + a$$

The intersection of the input ray with f(x) is at x_o, giving

$$f(x_o) = x_o \tan (90 - \gamma) + a$$

and the intersection with the displaced f(x) is at x_1, giving

$$\delta + f(x_1) = x_1 \tan (90 - \gamma) + a$$

Using a Taylor expansion near x_o to get $f(x_1)$ and dropping higher orders gives

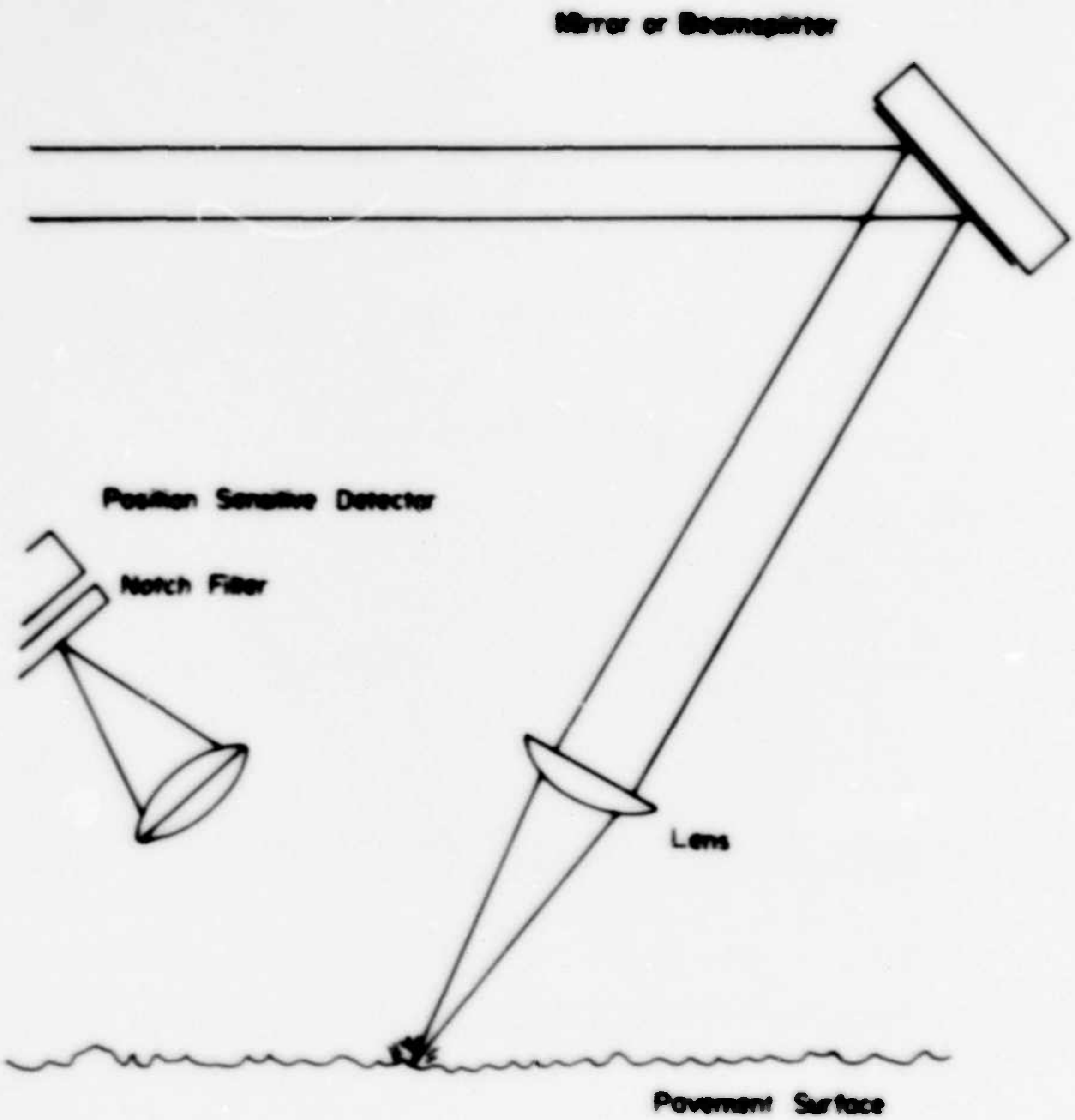

Figure A-1. Triangulation Arrangement

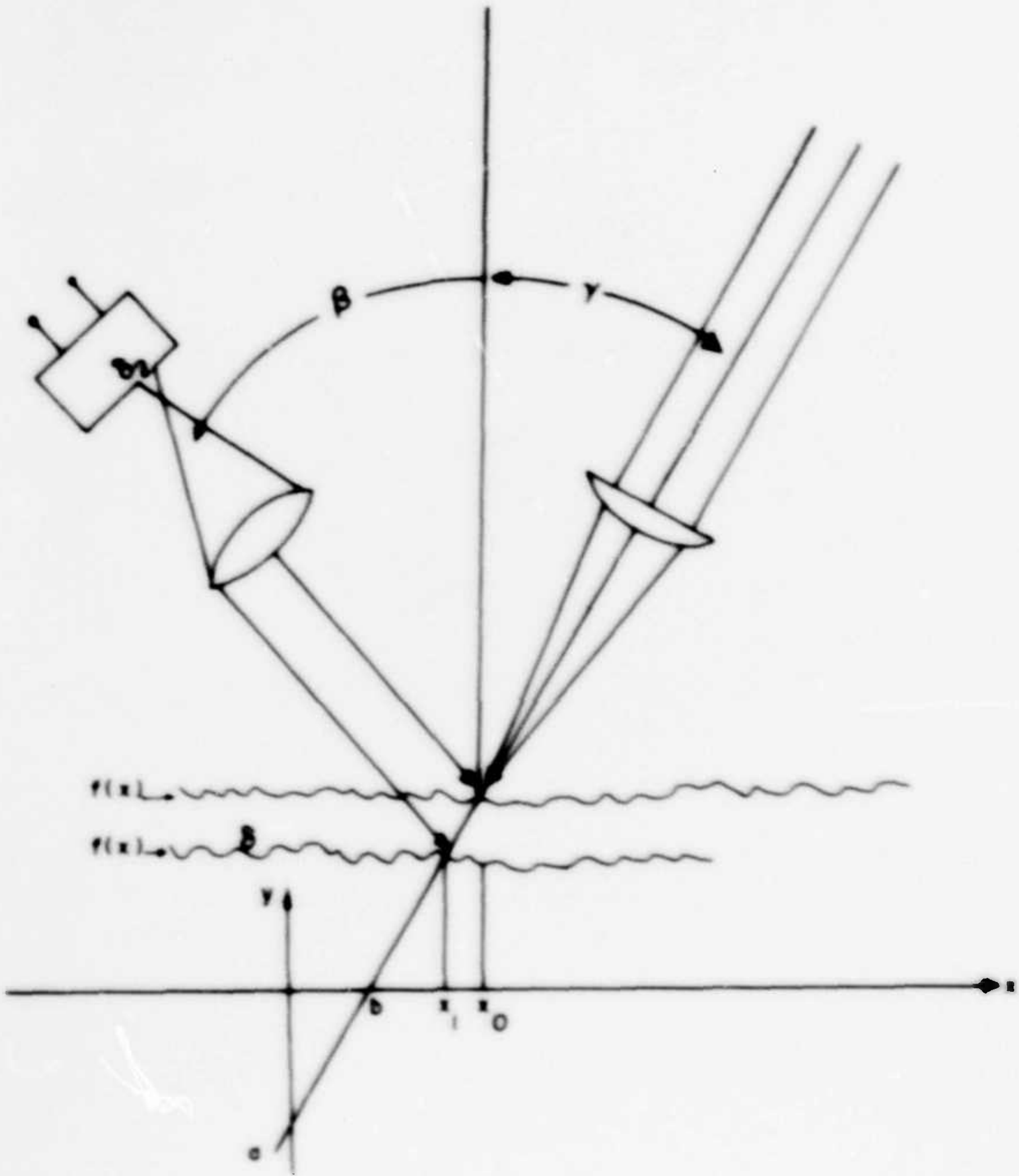

Figure A-2. Triangulation Parameters

$$f(x_1) = f(x_o) + \frac{f'(x_o)}{1}(x_1 - x_o) + \frac{f''(x_o)}{2}(x_1 - x_o)^2$$

Substitute this into the second intersection equation and subtracting the two gives

$$(x_1 - x_o)\tan(90 - \gamma) - \delta = f'(x_o)(x_1 - x_o) + \frac{f''(x_o)}{2}(x_1 - x_o)^2$$

which is solved to obtain,

$$(x_1 - x_o) = \frac{2\delta}{[f'(x_o) - \tan(90-\gamma)] \pm [f'(x_o) - \tan(90-x)]^2 - 2f''(x_o)\delta}$$

The image point is shofted by the component δ_2 normal to the axis of the imaging lens where,

$$\delta_2 = m\frac{\sin(\gamma + \beta)}{\sin\gamma} \cdot (x_1 - x_o)$$

The image motion can then be obtained as a function of the arrangement parameter (γ), the surface $f(x_o)$ and the surface displacement, (δ_1) by the equation

$$\delta_2 = m\,\delta_1\left(\frac{\sin(\gamma + \beta)}{\sin\gamma} \cdot \frac{2}{\left[\frac{\cos\gamma}{\sin\gamma} - f'(x_o)\right] \pm \left[\frac{\cos\gamma}{\sin\gamma} - f'(x_o)\right]^2 - 2f''(x_o)\delta}\right)$$

However, the pavement is rough on the scale of the focused spot on the runway. To eliminate the dependency on surface roughness, there are two alternatives. First, make the focused spot a focused line long enough that the effects of roughness are averaged to zero and second, reduce the angle between the pavement normal and input ray, γ, to zero. The image motion equation when $\gamma = 0$ reduces to

AD-A047 161 NONCONTACT NONDESTRUCTIVE DETERMINATION OF PAVEMENT DEFLECTION UNDER MOVING LOADS(U) PURDUE RESEARCH FOUNDATION LAFAYETTE IN M E HARR ET AL AUG 77 3/4

UNCLASSIFIED FAA-RD-77-127 DOT-FA73WAI-361 F/G 13/2 NL

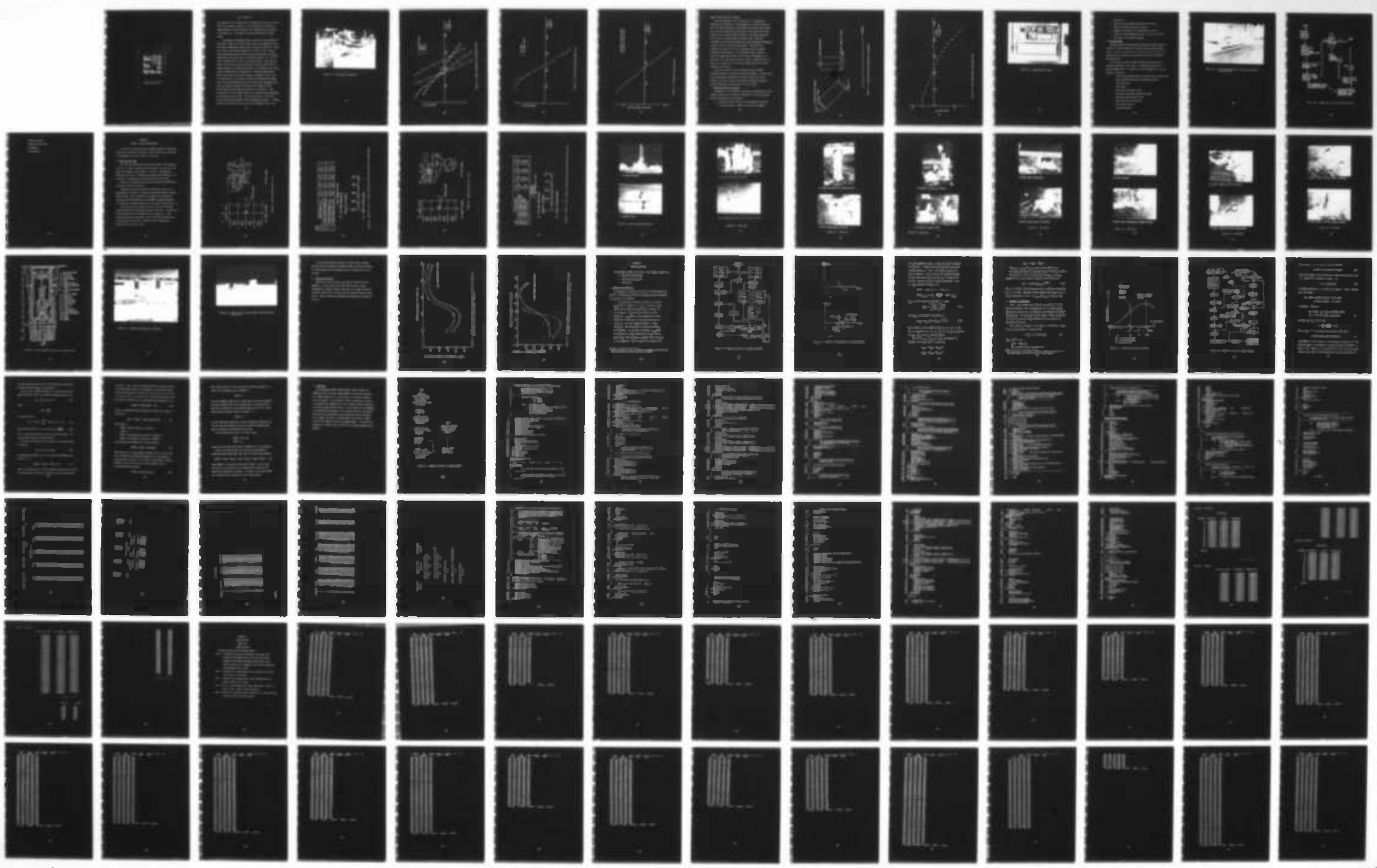

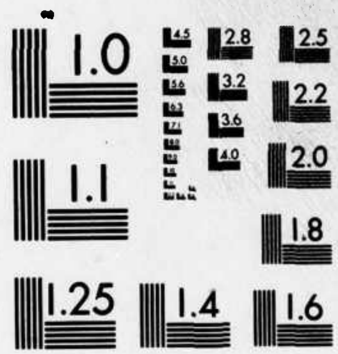

MICROCOPY RESOLUTION TEST CHART
NATIONAL BUREAU OF STANDARDS-1963-A

$$\delta_2 = m\,\delta \sin\beta$$

The sensitivity of the image motion is maximized when β goes to 90° but that is not physically possible. Also the collection of light for imaging depends on the solid angle of the imaging lens with respect to the pavement spot. The larger β forces the solid angle to smaller values.

A triangulation arrangement using a laser input was breadboarded and tested. Figure A-3 shows the laser setup in the laboratory at SAI. Some typical displacement signal curves are given in Figure A-4. These data are for four different samples and $\gamma = 23^{\circ}$, $\beta = 45^{\circ}$. Several other arrangements and the theory given above demonstrated that these calibration curves become smooth and repeatable when $\gamma = 0^{\circ}$, $\beta = 45^{\circ}$ using a cylinder lens to focus a line on the surface. Also shown in Figure A-5 is a curve which was obtained by using the sum of the two position signals as a normalization factor. An extension of the linear range is obtained with the normalization. Using the normalization method also yields a further more important advantage, that is, that the reflectivity of the surface is removed from affecting the signal. Figure A-6 shows normalized data for concrete and gray sandpaper which have the maximum and minimum reflectance of the sample set used. Their reflectance difference was greater than a factor of 2. The differences in the two signals appear in the regions where normalization has extended the linear range. The major contributor to this error was the inaccurate measurement of the normalization constant. If higher precision electronics had been used in this breadboard, most of the

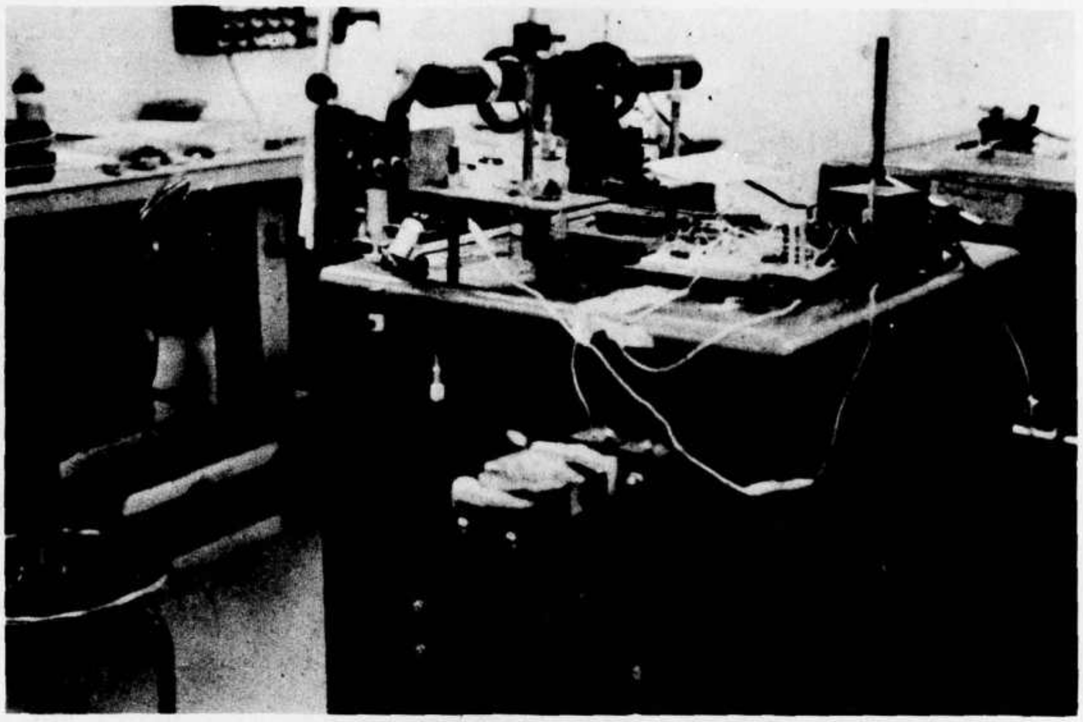

Figure A-3. Laser Setup in Laboratory

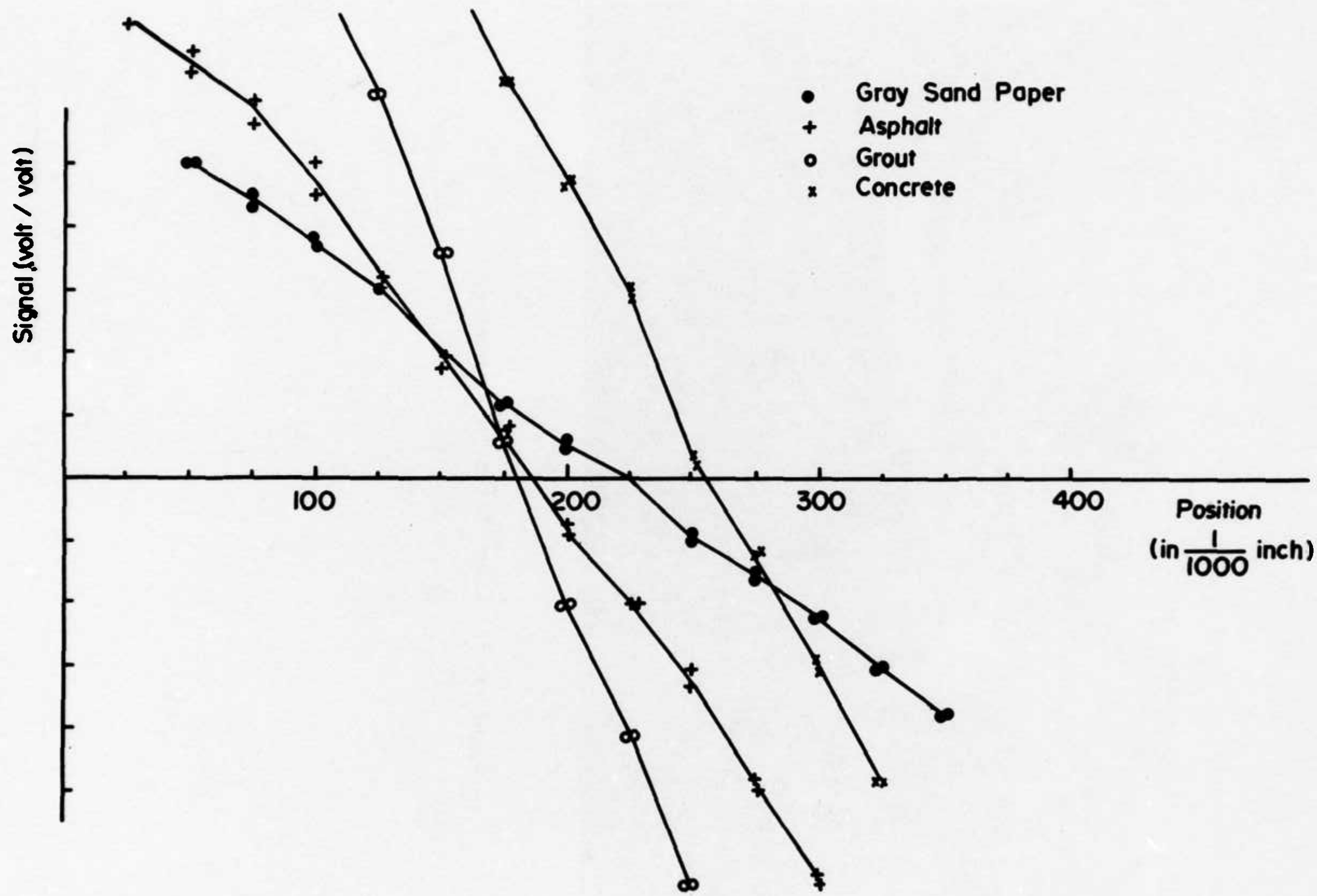

Figure A-4. Typical Triangulation Displacement Curves

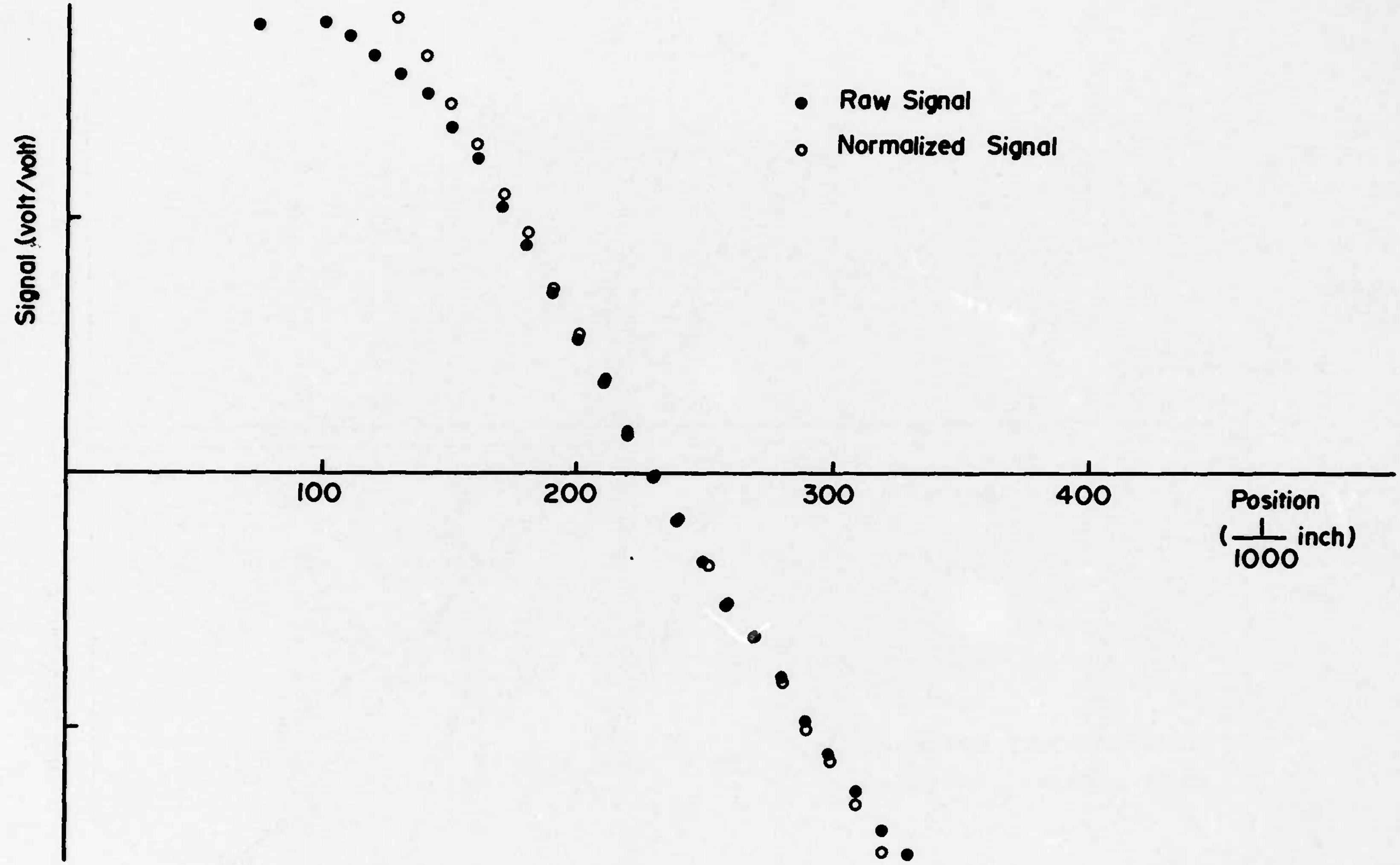

Figure A-5. Normal Incidence Displacement Curve

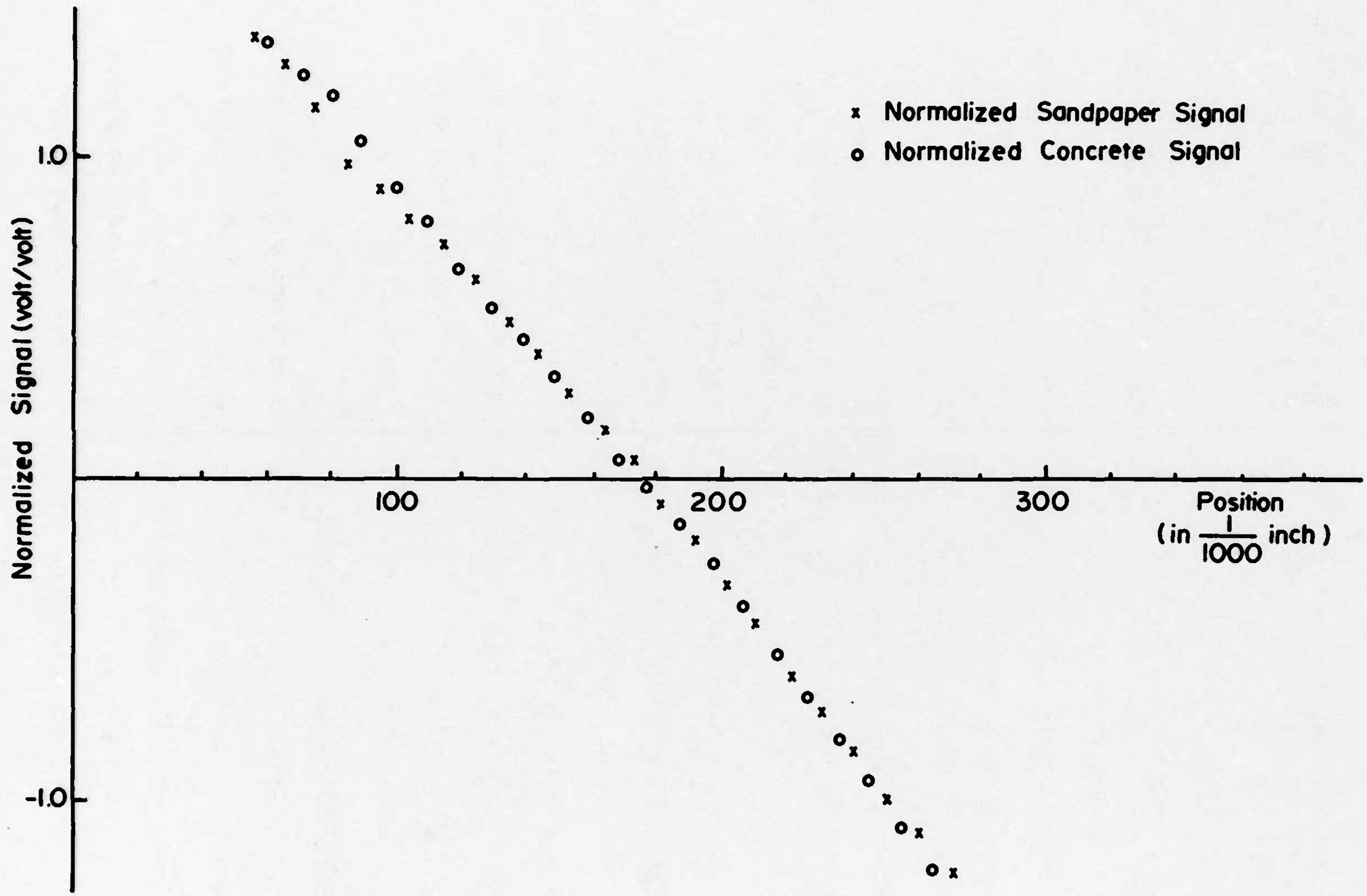

Figure A-6. Normalized Deflection Curves

signal differences would disappear.

The choice was made to use LED sources in a triangulation arrangement to deflections. This arrangement is shown in Figure A-7 and is the same triangulation arrangement as was tested before except that the light emitting diode replaces the input laser beam and the cylinder lens has been modified by adding a convex-plano spherical lens to form a composite spherical-cylinder lens. This lens arrangement was developed by mapping the three dimensional distribution of energy using an aperture and photodiode. The peak of the intensity was found for each lens arrangement until an optimum arrangement was determined. The displacement signal, shown in Figure A-8 demonstrates effects of the change in sharpness of the focal zone. The curve shows a change in slope in either side of the central focus region that is due to the larger area for the "line" focussed on the surface.

The basic optical principle as described herein remained unchanged throughout the course of system development. The electronics and the mechanical attachments were however modified to be more consistent with the concepts of the moving load-moving beam which evolved subsequent to the conclusions of SAI's effort.

b. Additional Work on LED System

Repackaging of the breadboard electronics and modification of the software supplied by SAI was done by personnel at Purdue University. This work consisted of the following:

1. Converting the basic wiring of the breadboard electronics to printed circuits. Figure A-9 shows the repackaged

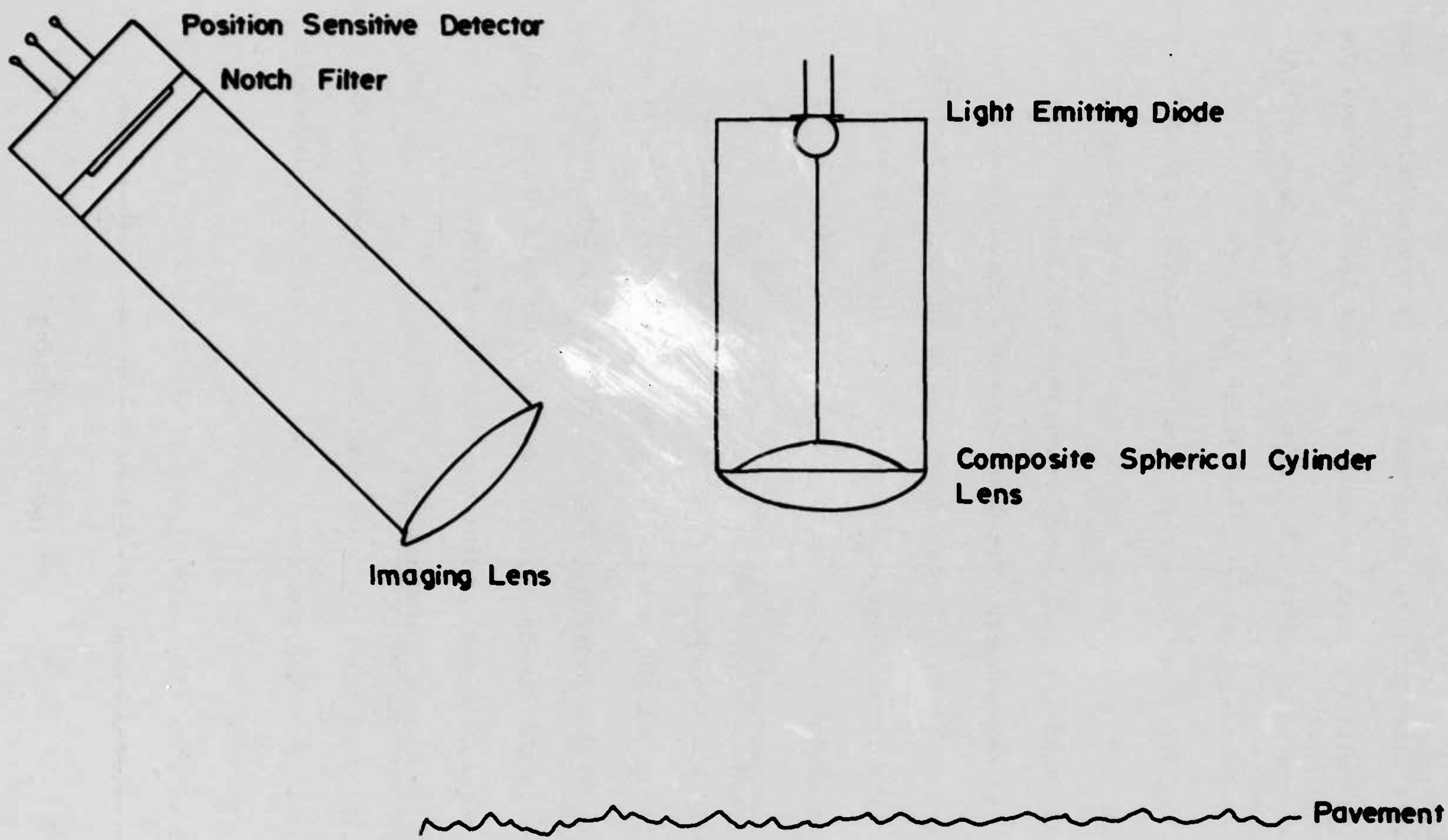

Figure A-7. Light Emitting Diode Triangulation Arrangement

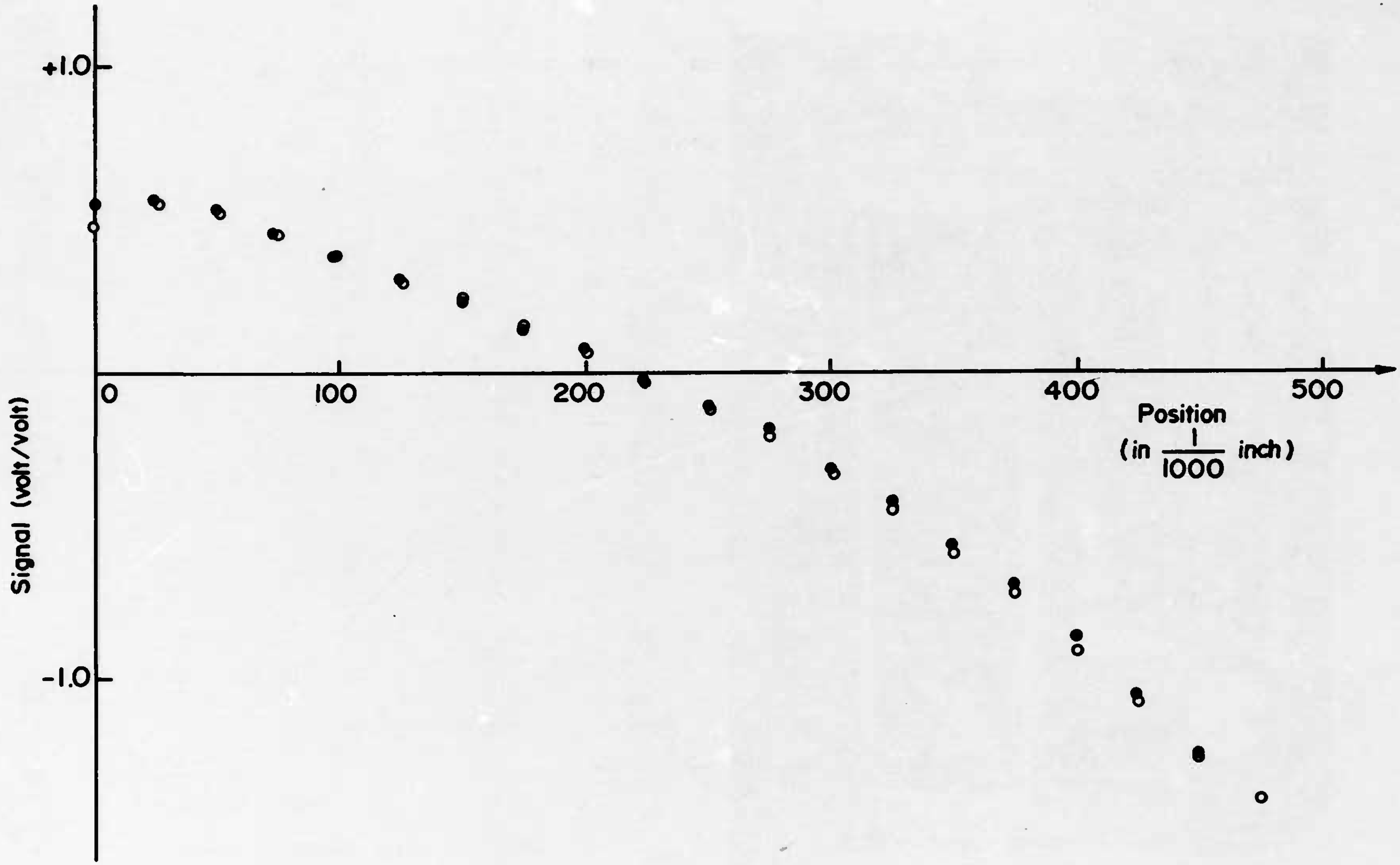

Figure A-8. Light Emitting Diode Displacement Curve

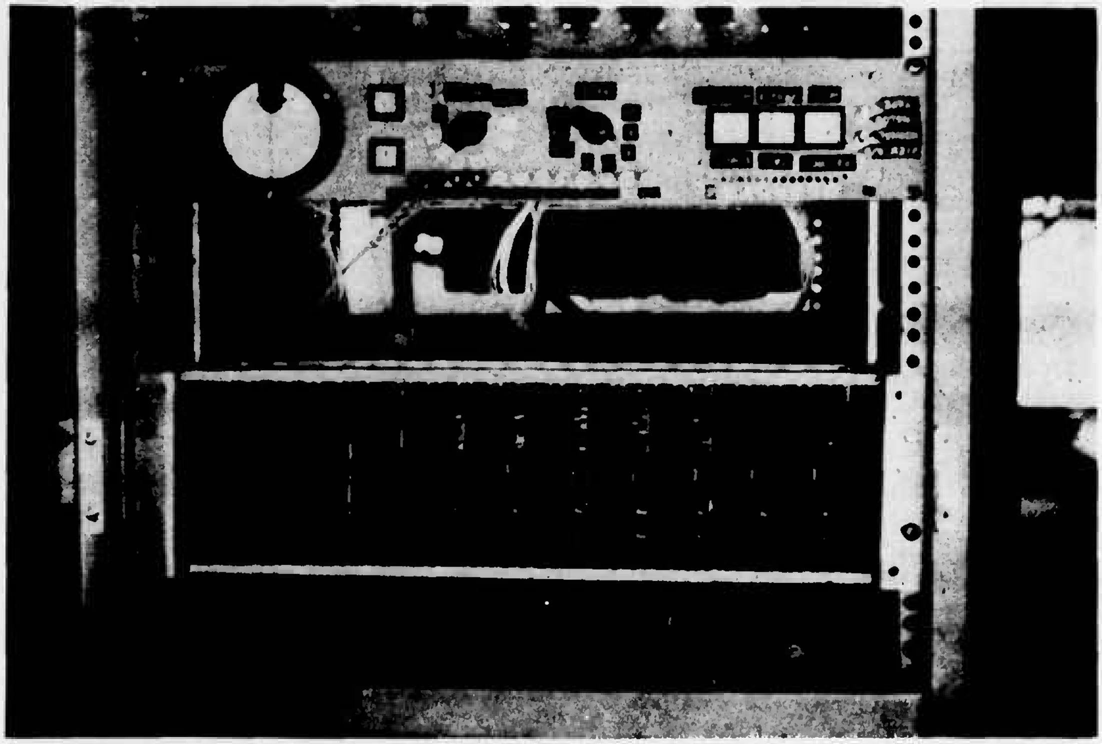

Figure A-9. Repackaged Electronics

electronics.

2. Testing the basic moving beam-moving load concept. Figure A-10 shows the basic test setup.

3. Changing the software to be compatible with the new concept of a moving beam-moving load. Figure A-11 shows a flow chart of the modified software.

c. <u>The LVDT System</u>

The LVDT system was designed and fabricated at Purdue University as part of a study sponsored by the Federal Highway Administration (FHWA). Because an overview of the system has already been presented previously in this repot only the details of the system components are present here.

The use of the system to measure response functions has been discussed previously in this report. For additional details see Baladi (Reference 52). A listing of the basic components of the LVDT system is as follows:

- Light Weight Aluminum I-beam, 80 inches long, 12 inches wide
- Linear Variable Differential Transformers (LVDTs)
- 2 Way Screw Jack
- Pipe (pivot)
- Small Screw Jacks under LVDTs
- 6-Channel Oscillograph Light Beam Recorder
- Kodak-2022-light Sensitive Paper
- Sears Electric Power Generator
- AC-DC Power Converter
- Micrometer-Caliper

Figure A-10. Test Setup Moving Beam - Moving Load Operation: Purdue University

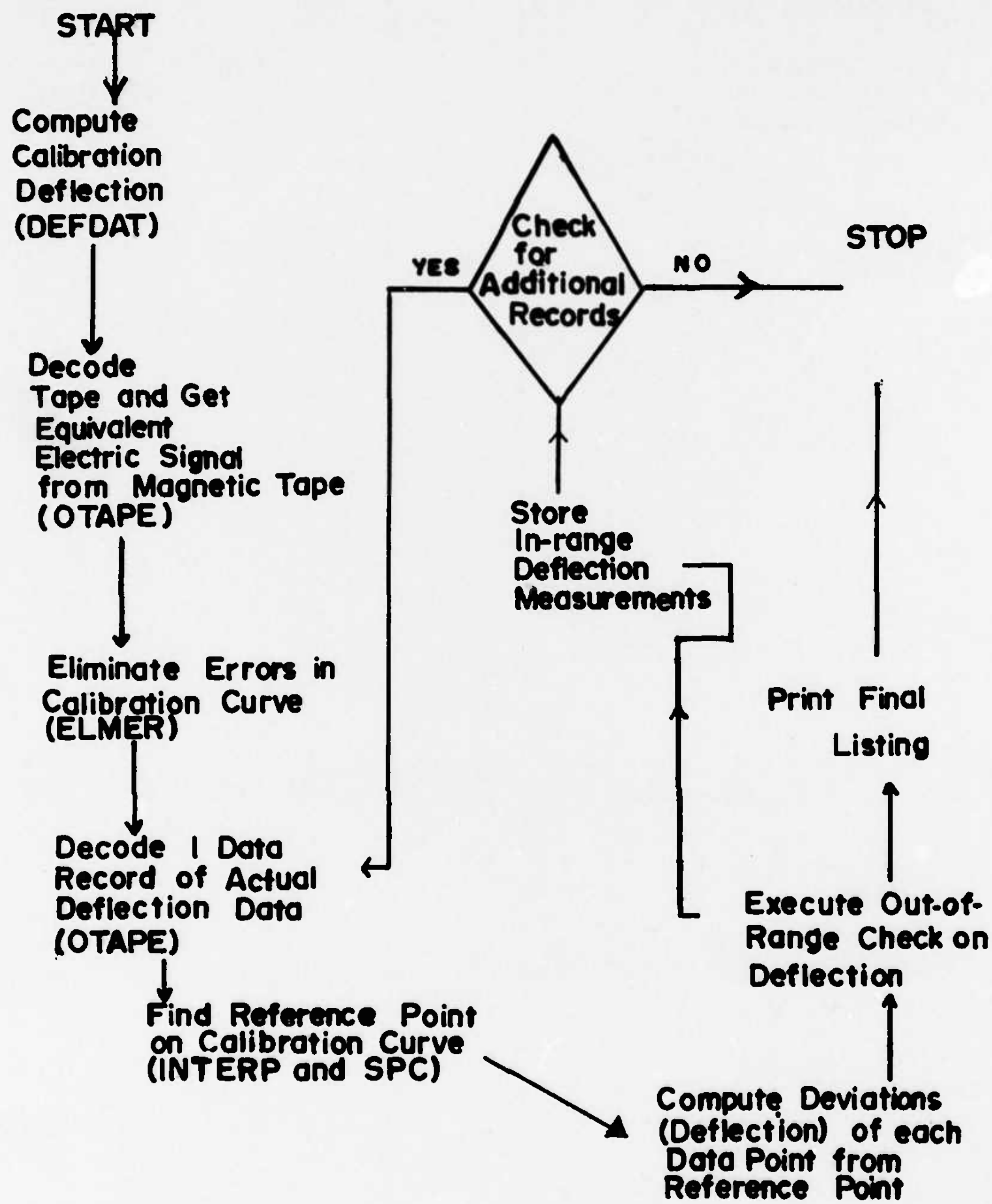

Figure A-11. Summary Flow Chart of LED System Software

- Hydraulic Scales
- Heavy Duty Silver Tape
- Thermometer
- Miscellaneous

APPENDIX B

SERIES A: FIELD INVESTIGATIONS

The Series A field investigation program consisted of conducting field tests at Eglin Air Force Base, Florida and Pease Air Force Base in New Hampshire during the period of this study.

a. Eglin Air Force Base

Two sites were selected at Eglin Air Force Base. The location of the sites is shown in Figures B-1(a) and B-3(a). At each site, LVDT gages were embedded in the pavement. At Site 1, five gages were installed and at site 2, four gages were placed in the pavement. The locations of the gages are shown in Figures B-1(b) and B-3(b).

Details of the boring locations and site profile characteristics are shown in Figures B-2 and B-4.

A summary of the gage installation procedure is shown in the photosequence in Figure B-5. Figure B-6 shows the details of typical installed gage. After installation, the gages were calibrated as discussed in Boyer (Reference 11), and pavement response functions were obtained as discussed previously in this report (see section 5.1).

Grids were laid out as shown in Figures B-1(b) and B-3(b) and response functions were determined using the LVDT beam. The gages were first calibrated using the equipment shown in Figure B-7. Then response functions were obtained at each of the grid locations shown in Figures B-1(b) and B-3(b). Figure B-8 shows a typical pass being made by the P-2 fire truck.

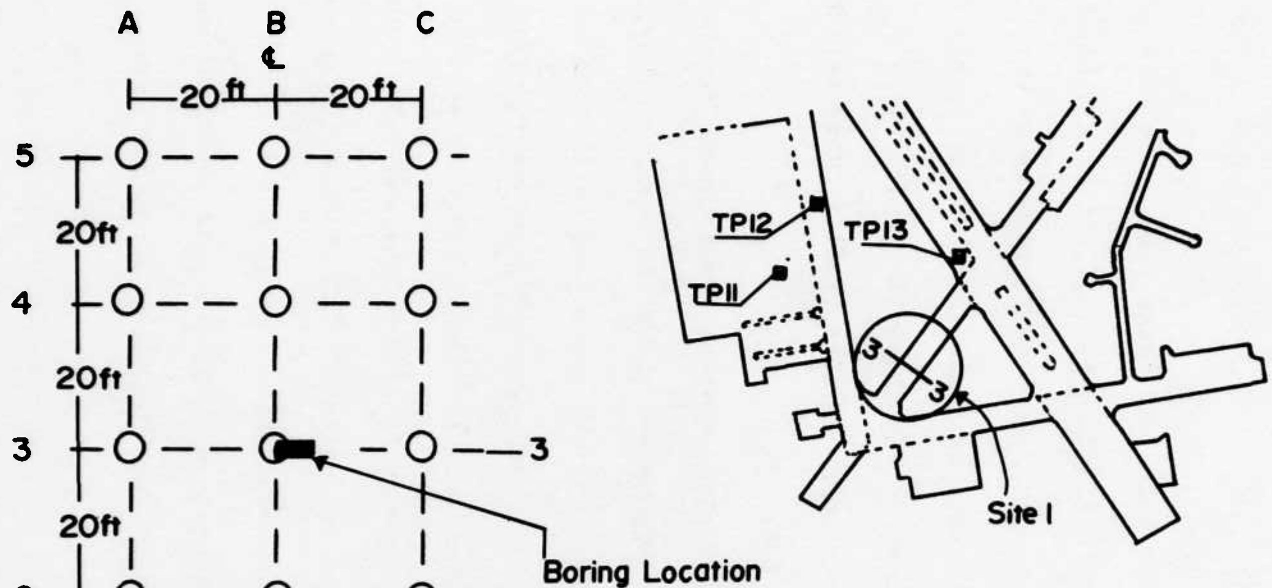

(b) Station Locations

(a) Site Location

Figure B-1. Eglin Air Force Base: Site 1

Layer

Layer	Boring Number	B 1	B 2	B 3	B 4	B 5
A	Layer-A-Asphalt Concrete	2.25 +	2.0	2.0	1.35	2.0
B	Layer-B-Sand Asphalt	7.0	7.5	7.0	7.0	7.0
C	Layer-C-Medium Sand	168	168	168	168	168

+ Layer Thickness in Inches

(a) Site Profile Characteristics

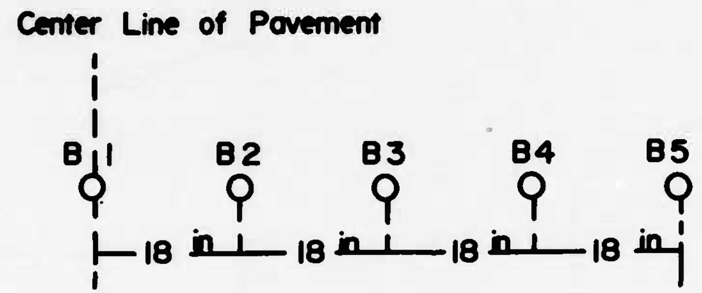

(b) Details of Boring Location

Figure B-2. Eglin AFB - Site 1: Details of Boring Location and Site Profile Characteristics

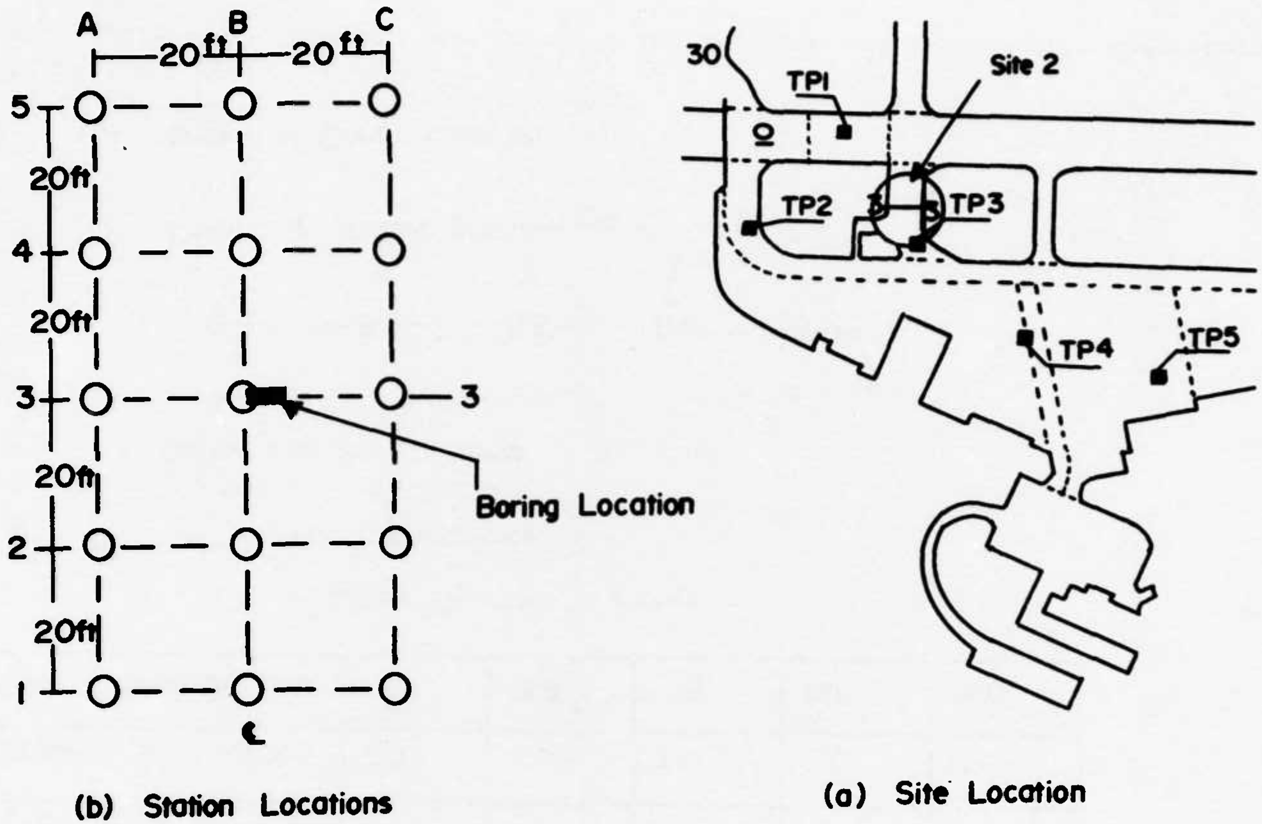

(b) Station Locations

(a) Site Location

Figure B-3. Eglin Air Force Base: Site 2

Layer	Boring Number	B 1	B 2	B 3	B 4
A	Layer A- Asphalt Concrete[1]	1.25+	1.125	1.25	1.25
B	Layer B-Asphalt Concrete[2]	3	3	3	3
C	Layer C-Sand Asphalt	14	13.5	11.5	12.0
D	Layer D-Medium Sand	132	132	132	132
E	Layer E-Silty Sand	48	48	48	48

1 Resurfacing
2 Old Surface
\+ Layer Thickness in inches

(a) Site Profile Characteristics

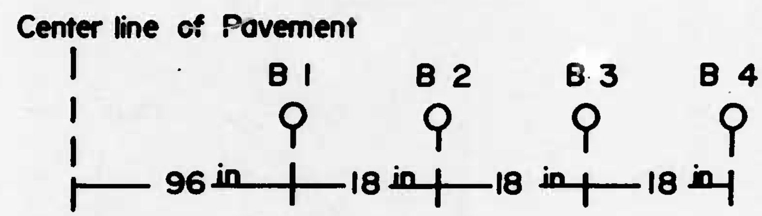

(b) Details of Boring Location

Figure B-4. Eglin - Site 2: Details of Boring Location and Site Profile Characteristics

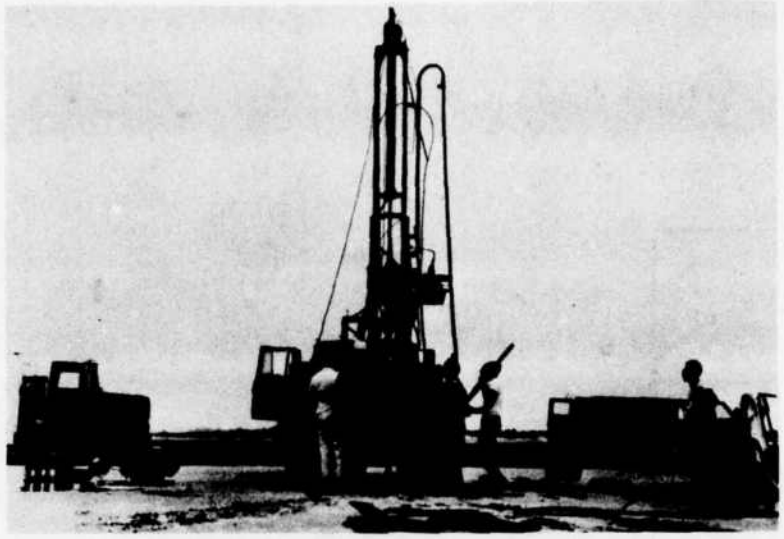

(a) Coring Pavement

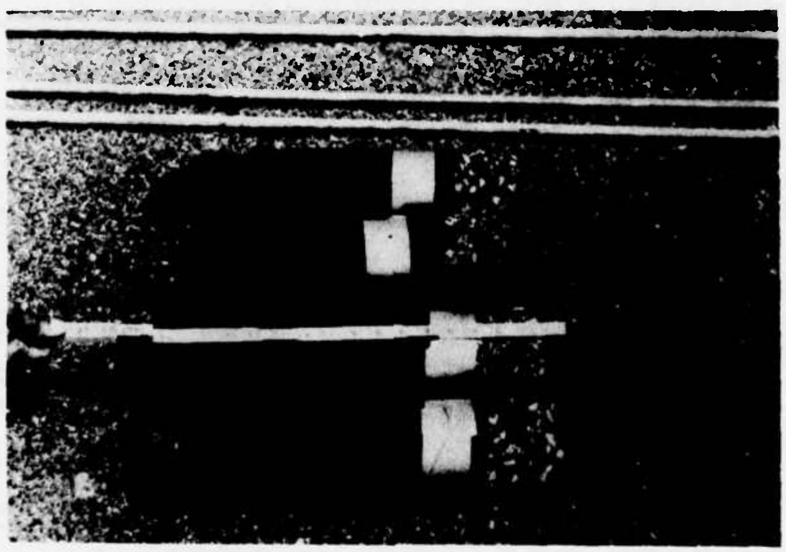

(b) Extract Cores

Figure B-5. Gage Installation Procedure

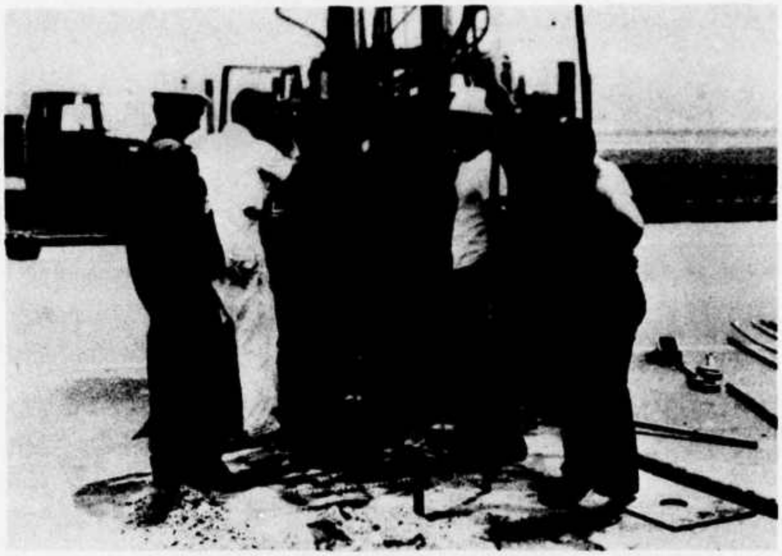

(c) Drill Hole to about 14 feet

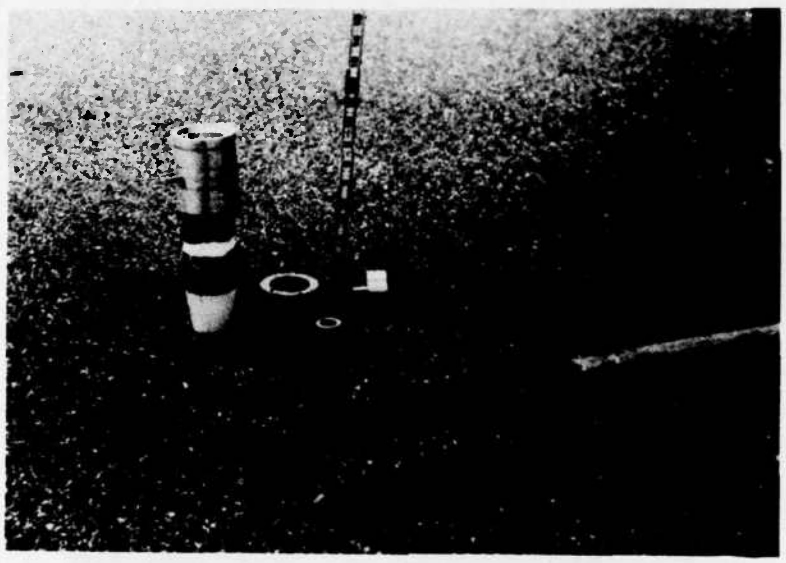

(d) Paraphernalia Ready for Installation in Hole

Figure B-5. (Continued)

(e) Lower Rod, Anchor and Casing into Hole

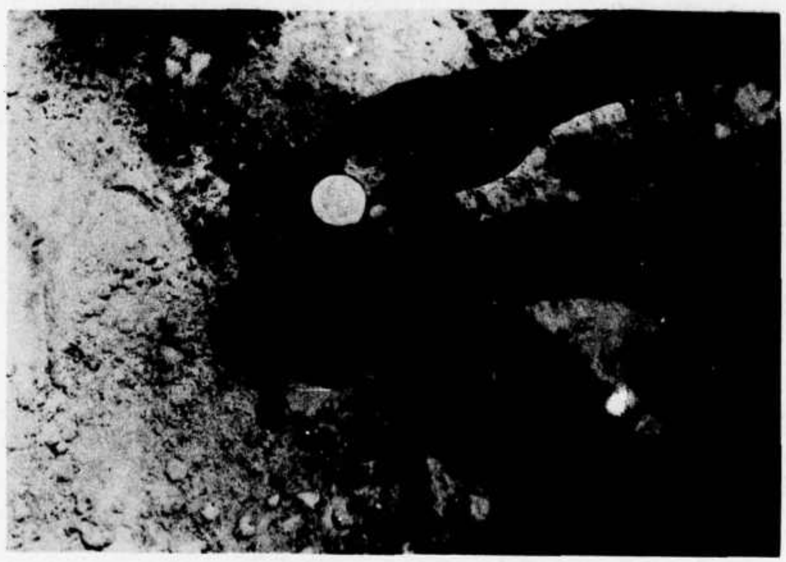

(f) Screw Impact Head to Inner Rod

Figure B-5. (Continued)

(g) Backfill with Sand and Compact

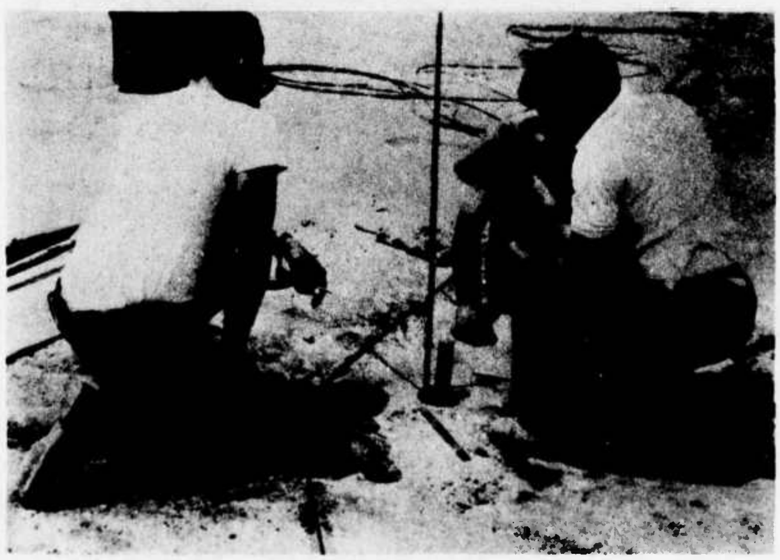

(h) Drive out Anchor Prongs

Figure B-5. (Continued)

(i) Position Upper Paraphernalia

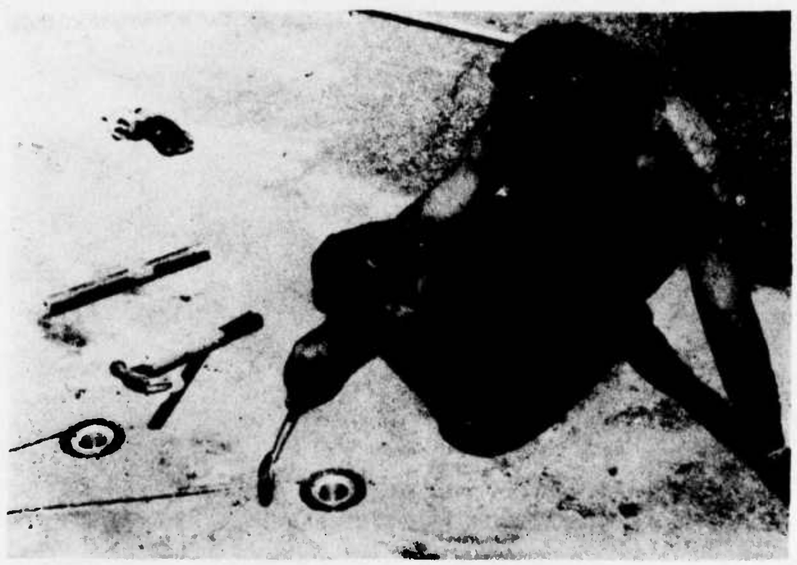

(j) Backfill Around Upper Paraphernalia

Figure B-5. (Continued)

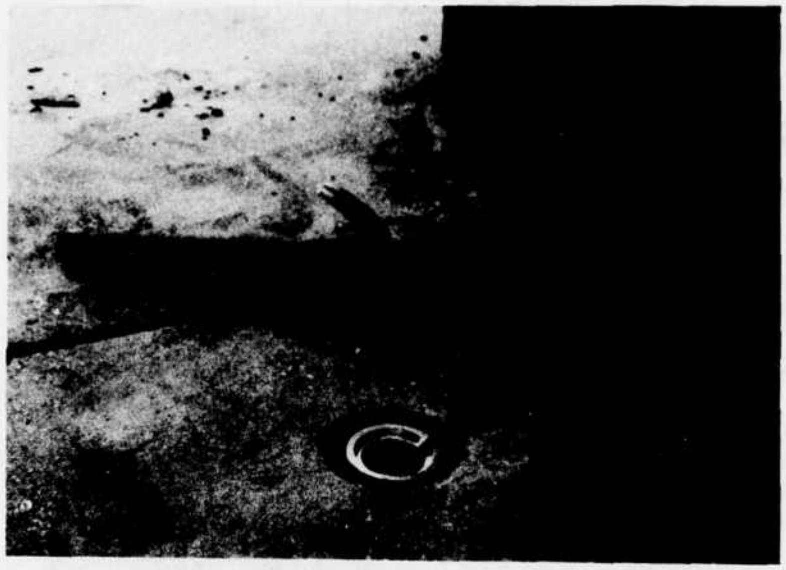

(k) Groove Pavement

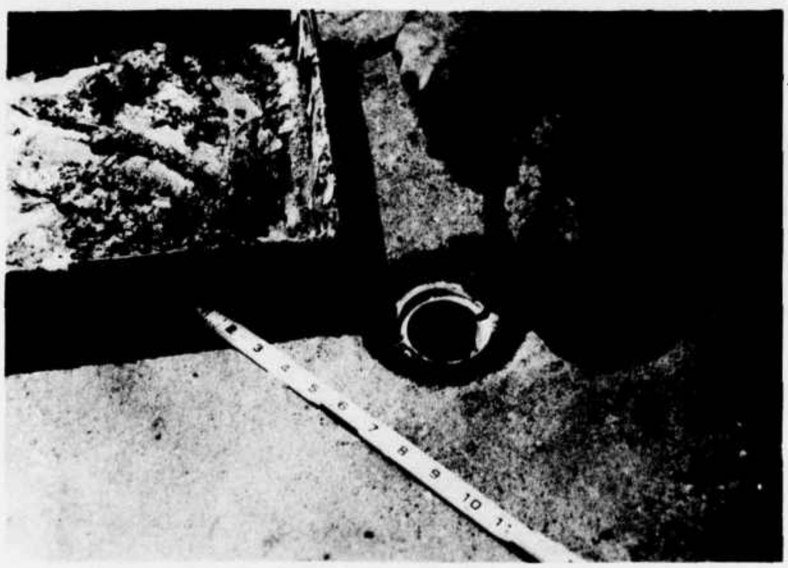

(l) Epoxy Upper Paraphernalia to Asphaltic Concrete

Figure B-5. (Continued)

(m) Epoxy Cables for LVDT into Groove

(n) Typical Installation-Partially Epoxied Cables

Figure B-5. (Continued)

(o) Epoxy Cable in Groove to Edge of Pavement

(p) Gages Ready for Element (Sensor) Installation

Figure B-5. (Concluded)

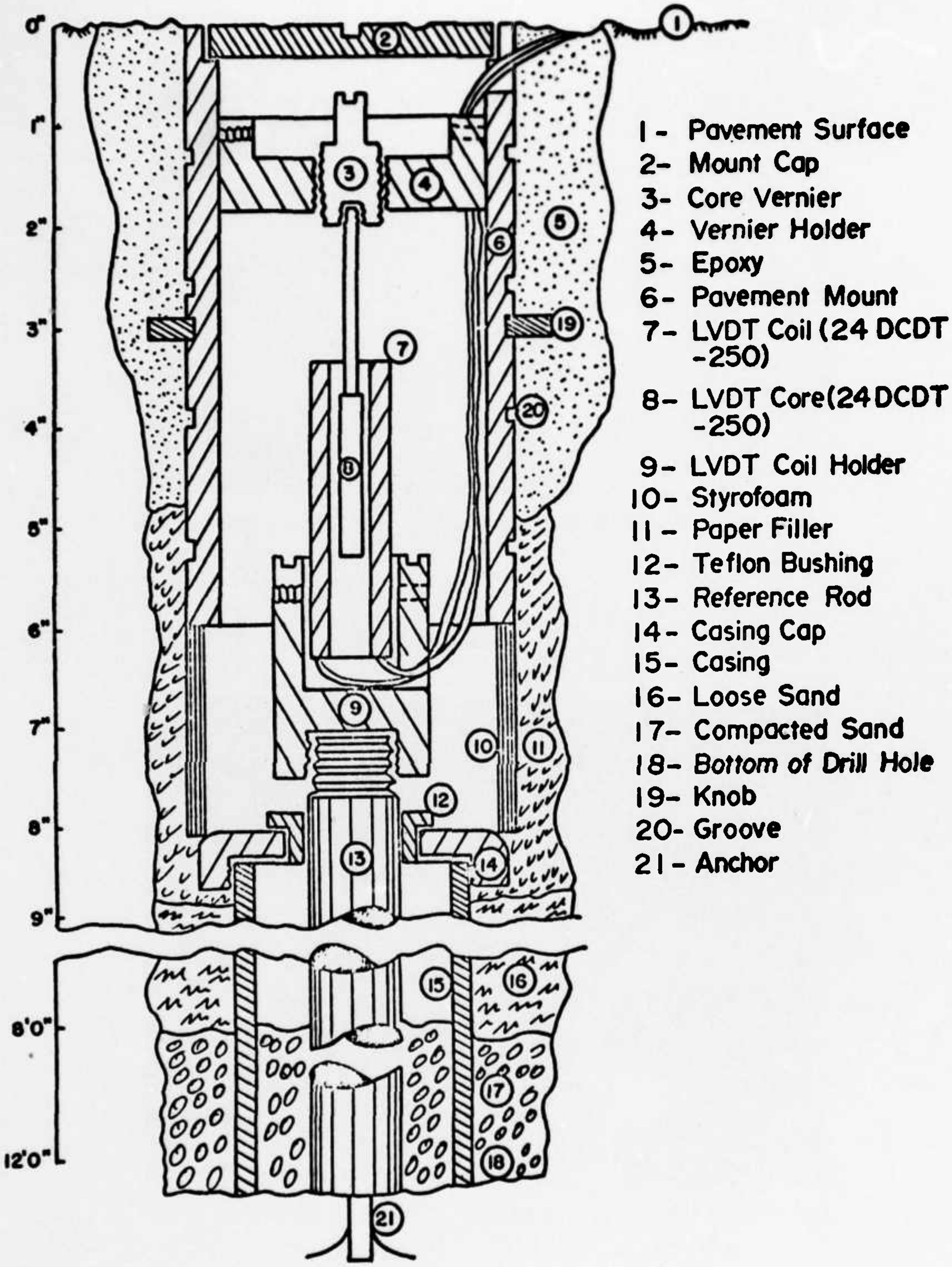

Figure B-6. Gage Installation (after Boyer [Reference 12])

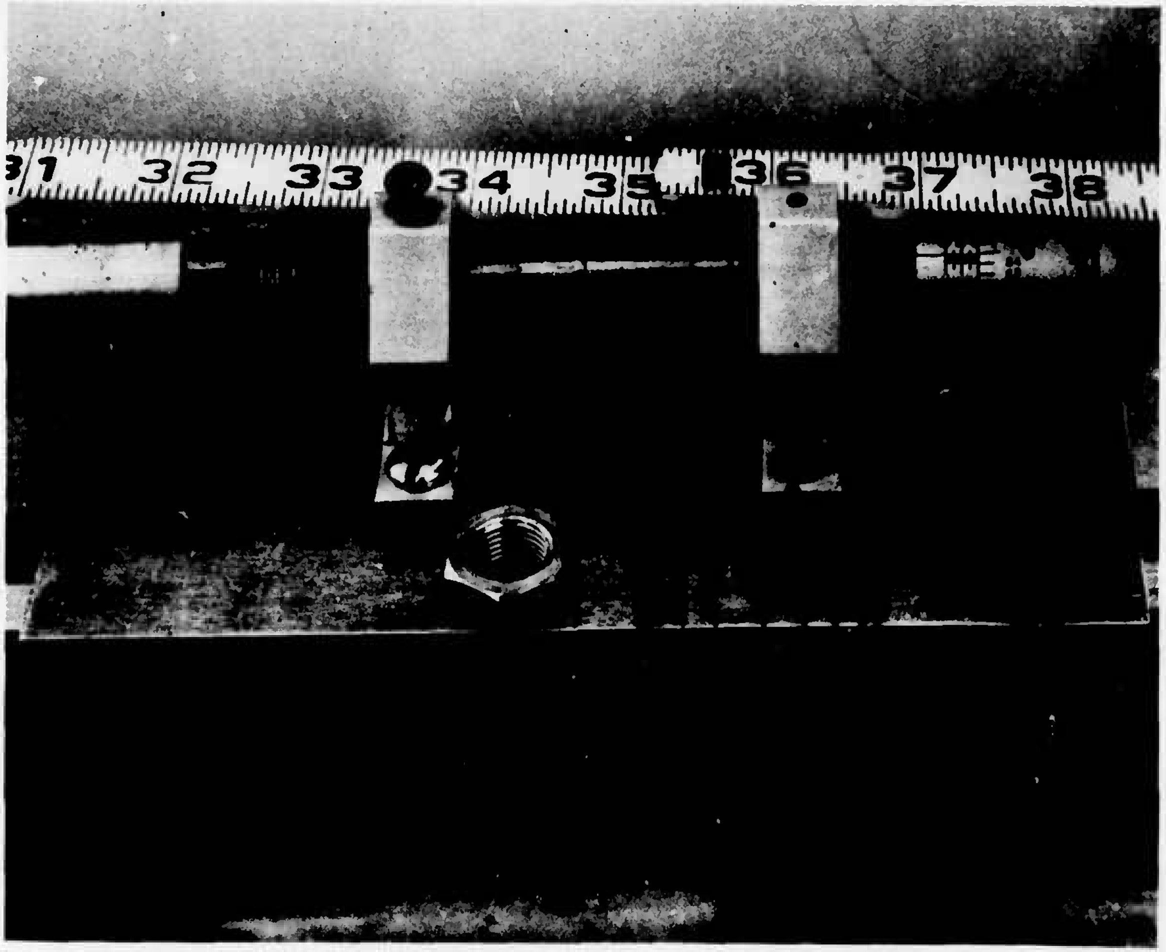

Figure B-7. Calibration Equipment for LVDT Gages

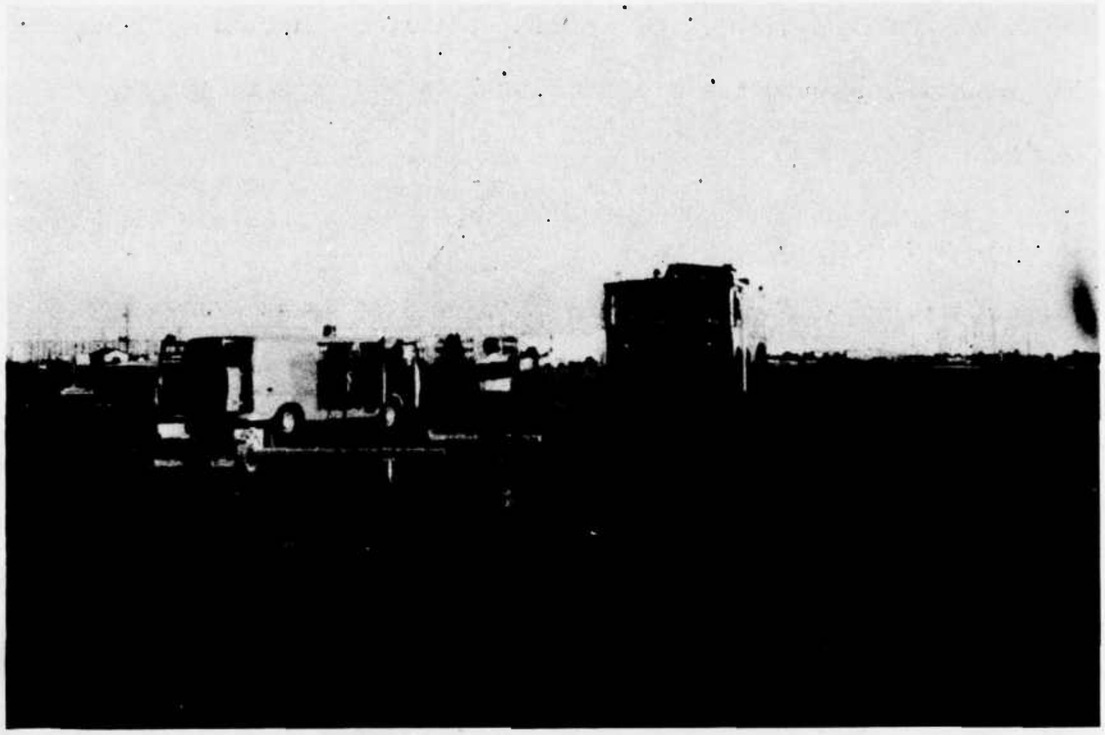

Figure B-8. Photo of P-2 Fire Truck Making a Pass During LVDT Beam Testing

At the locations shown in Figure B-1(b) and B-3(b), attempts were also made to estimate the pavement transfer function by dropping a 60 pound weight onto the pavement close to the gage at the tip of the beam.

b. <u>Pease Air Force Base</u>

One site, on the main runway, was tested at Pease AFB in New Hampshire. At this site only the LVDT beam was used to obtain measurements of pavement response functions in the manner previously described, using the P-2 fire truck and the KC-135A aircraft as prime movers. Typical deflection measurements are presented in Figures B-9 and B-10.

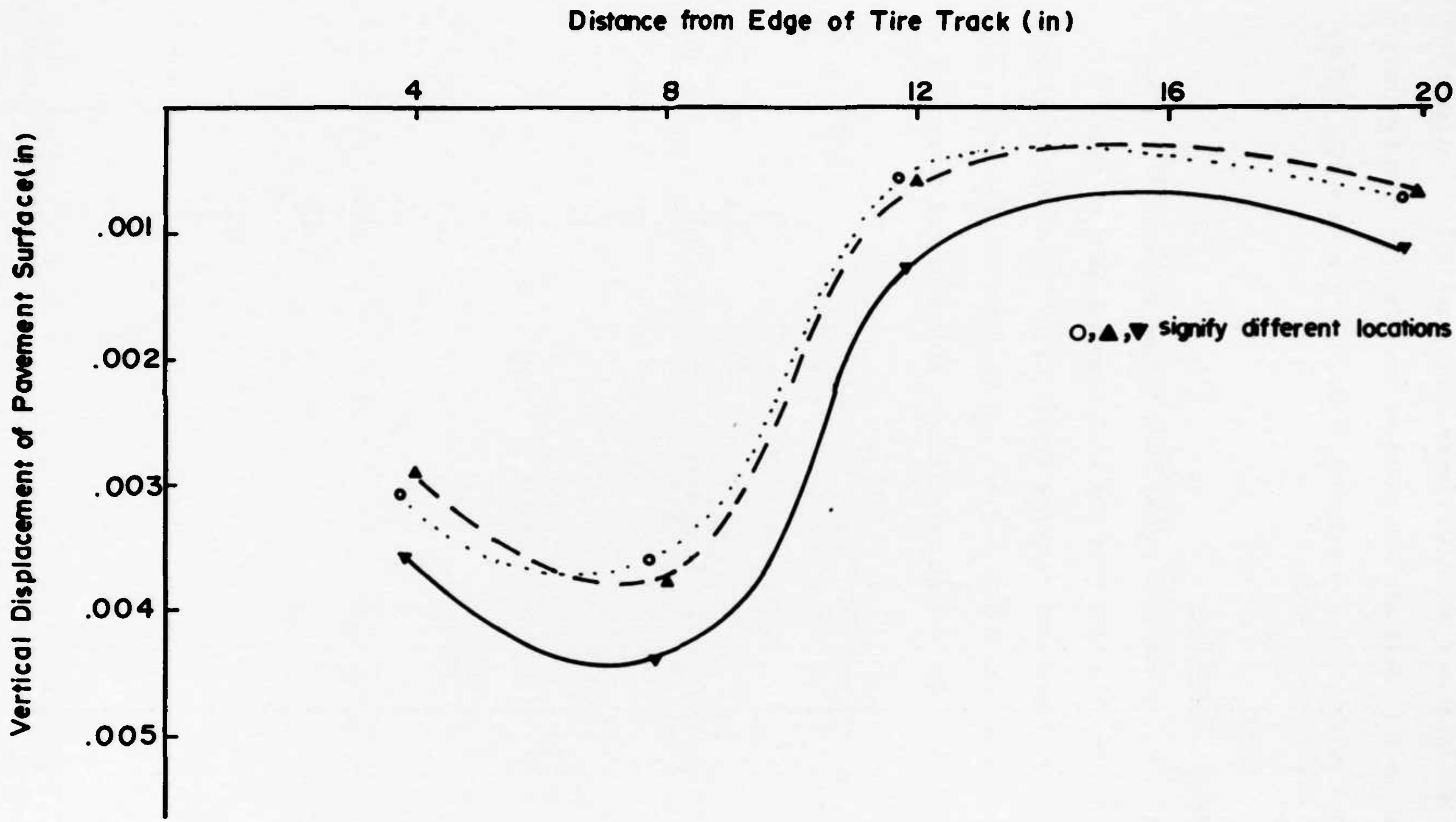

Figure B-9. Variability of Maximum Vertical Displacement of Pavement with Distance from Edge of Track of Tire Closest to Gage : KC-135 A

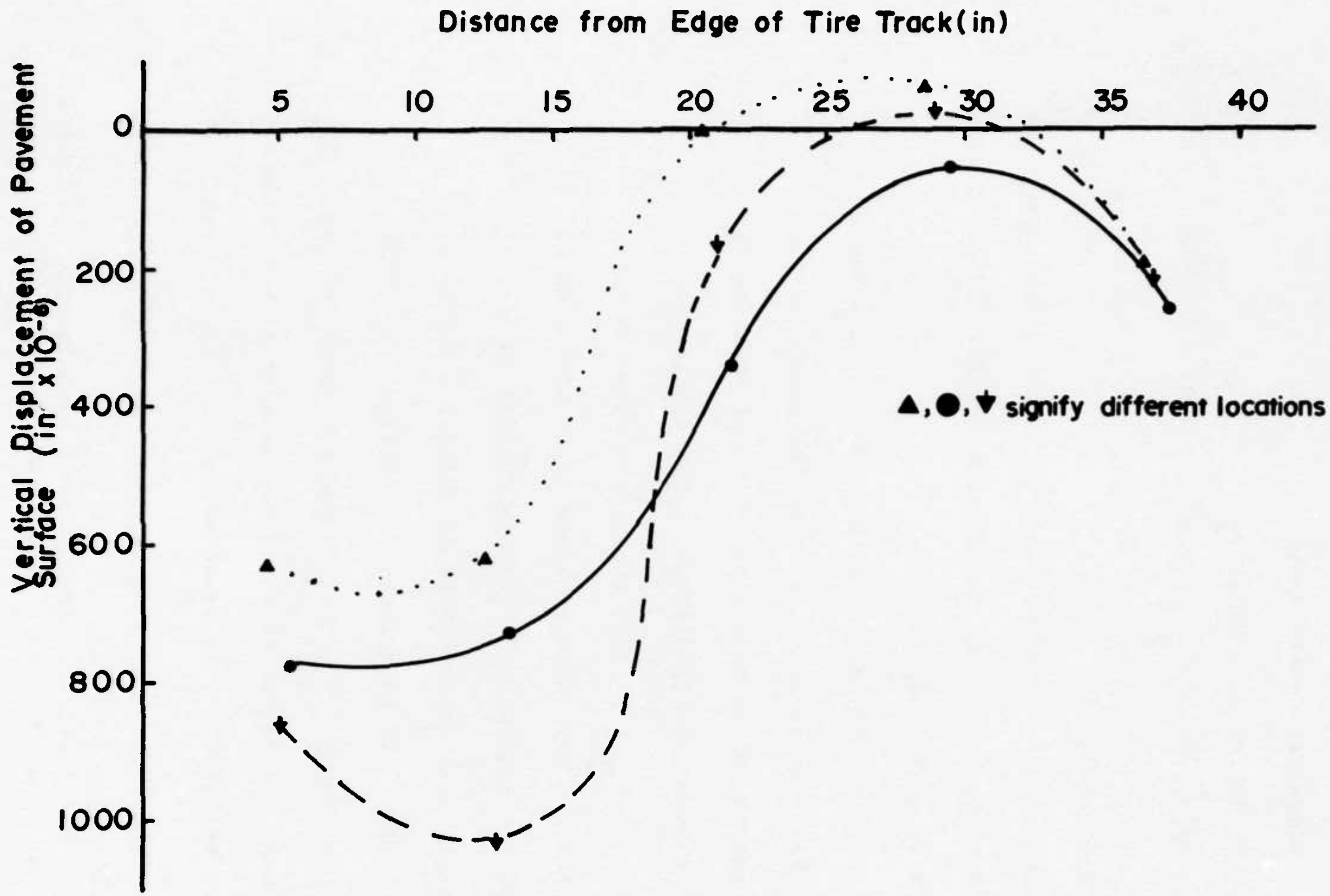

Figure B-10. Variability of Maximum Vertical Displacement of Pavement with Distance from Edge of Track of Tire Closest to Gage: P2 Fire Truck

APPENDIX C

COMPUTER PROGRAMS

This Appendix contains the details of the computer program for,

1. Signature determination
2. Parameter determination
3. Prediction

a. Signature Determination

The signature as defined in the text is calculated using the equations (3) through (10) and the subroutines EXACFIT and SIGNTR. The procedure is as follows:

With reference to Figures C-1 and C-2, a value of r_{peak}(FXP)[17] is assumed (0.2) then the left hand side (FLHS) and the right hand side (FRHS) of equation 5a are calculated. Their difference TVAL(1) is then calculated. r_{peak}(FXP) is then incremented by 0.0125 (DFXP) and the left hand side and right hand side of equation 5a, and their difference TVAL(2) is again calculated. The ratio (FDIF) of TVAL(2) and TVAL(1) is calculated. If this ratio is positive, r_{peak}(FXP) is incremented by 0.0125 (DFXP) and the ratio FDIF is again found. This procedure is repeated until the ratio is first negative. This is shown as S in Figure C-2a;

[17] Symbols in capital letters correspond to symbols used in the subroutine EXACFIT which performs the calculations.

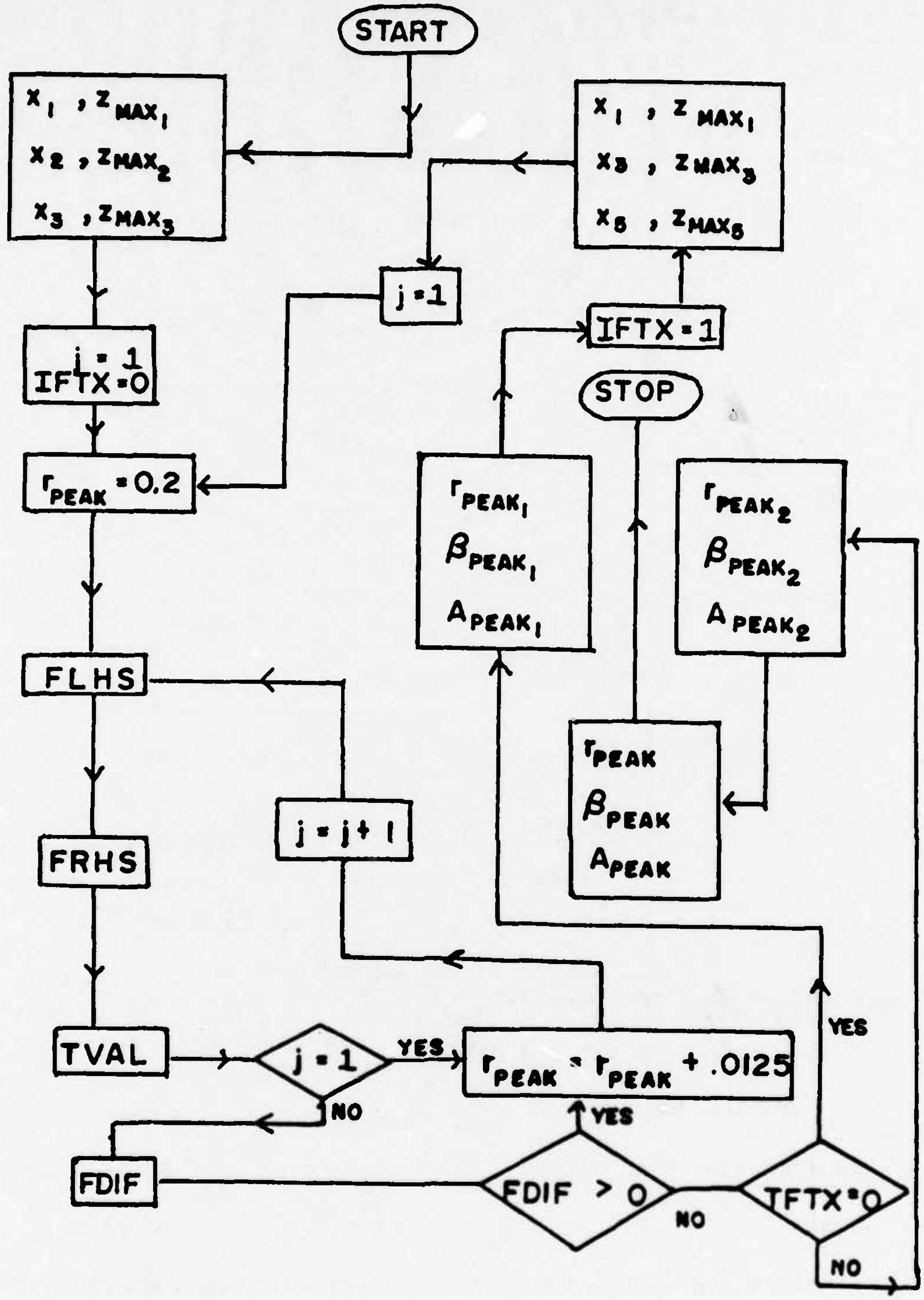

Figure C-1. Summary Flow Chart of Subroutine EXACFIT

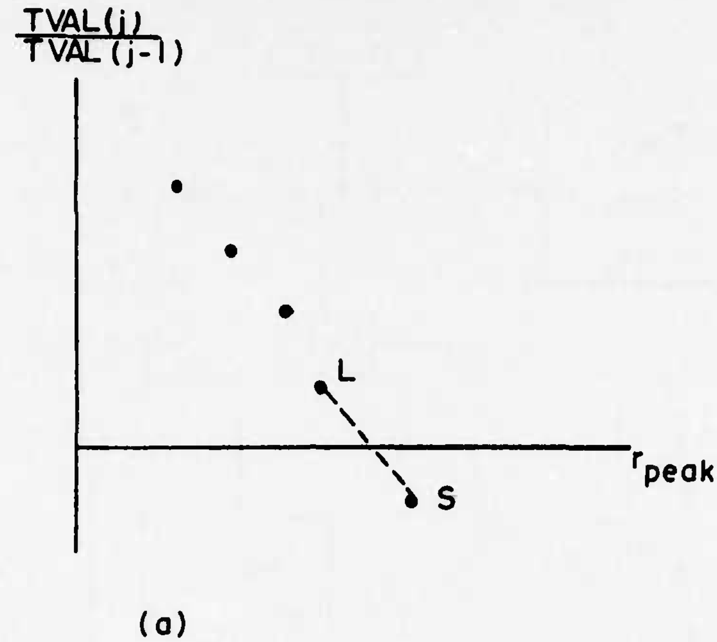

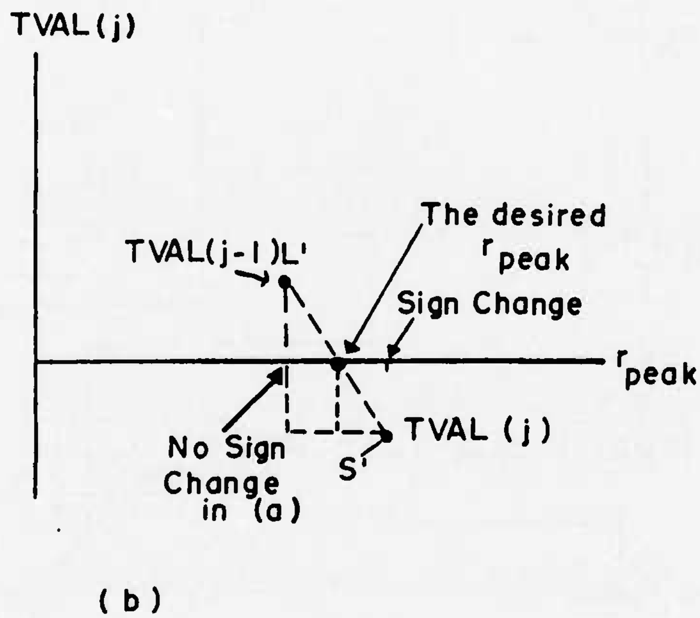

Figure C-2. Details of Interpolation in Subgrade EXACFIT

the point immediately before, at which the ratio is positive is labelled L. In Figure C-2b, the point before the ratio becomes negative is L' and S' is the point at which the ratio is negative. The point where the difference between the left hand side and the right hand side of equation 5a is zero is found by linearly interpolating between L' and S'. With reference to Figure C-2b

$$\mathrm{TFDIF} = |\,\mathrm{TVAL\ (J-1)}\,| + |\,\mathrm{TVAL\ (J)}\,|$$

$$\mathrm{FFXP}_{\mathrm{required}} = \mathrm{FXP}_j - \frac{\mathrm{TVAL(J)}}{\mathrm{TFDIF}} \cdot \mathrm{DFXP} = r'_{peak}$$

β'_{peak} is then calculated from equation 5 where

$$\beta'_{peak} = \frac{\ell n\ z_{max_1} - \ell n\ z_{max_3}}{x_1^{\,r'_{peak}} - x_2^{\,r'_{peak}}} \tag{5a}$$

and, A'_{peak} is calculated from equation 3a

$$A'_{peak} = z_{max_1} / [\exp\ (\beta'_{peak}\ x_1^{\,r_{peak}})] \tag{3a}$$

This procedure is then repeated using (x_1, z_1), (x_3, z_3) and (x_5, z_5) instead of (x_1, z_1), (x_2, z_2) and (x_3, z_3), and values of r''_{peak}, β''_{peak} and A_{peak} are calculated.

The desired r_{peak}, β_{peak} and A_{peak} are found as the average of the values using the equations,

$$r_{peak} = (r'_{peak} + r''_{peak})/2$$

$$\beta_{peak} = (\beta'_{peak} + \beta''_{peak})/2$$

$$A_{peak} = (A'_{peak} + A''_{peak})/2$$

The A_{peak}, r_{peak}, and β_{peak} values thus calculated are the parameters describing the maximum lateral deflection profile. The signature is then calculated using the r_{peak}, and β_{peak} parameter and the basic equation, equation 2a but in the form

$$A(t) = z(t)/\exp\left(\beta_{peak}\, x_1^{\,r_{peak}}\right) \quad (10)$$

where z(t) refers to the deflection at gate 1 (closest to the wheel), and t is the time. Subroutine SIGNTR performs these computations by direct substitution of z(t), x_1, r_{peak} and β_{peak} in equation (10).

b. Parameter Determination

The k, c and m parameters as defined by equation (1) in the text are calculated using the methodology, concepts and equations presented in Section III in the paragraph with subheading "Parameter Determination". The subroutines EXACT1, NWCONV, SIGNTR, and EXACFIT are called from the main program FNDPRM in order to perform the necessary computations.

With reference to Figure C-3 and Figure C-4, initially, a value of the spring constant k is assumed where

$$k = EQKA = AA1 \times PMAX/DMAX \quad (29)$$

where AA1[18] = 0.05

PMAX = 25000, and

DMAX = Maximum value of the signature.

[18]For convenience, the symbols in capitol letters in section (4) are the same symbols used in the computer program FNDPRM.

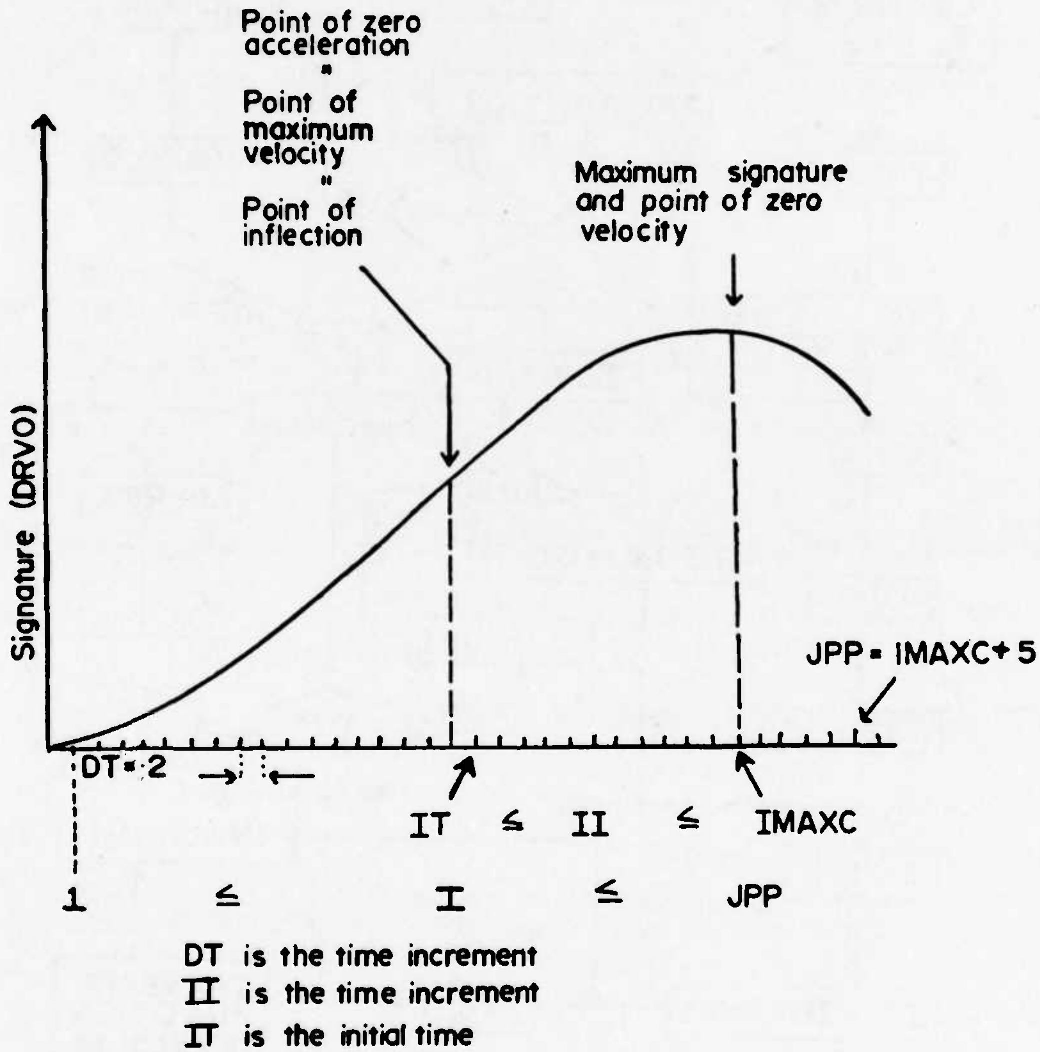

Figure C-3. Definition Sketch for Signature

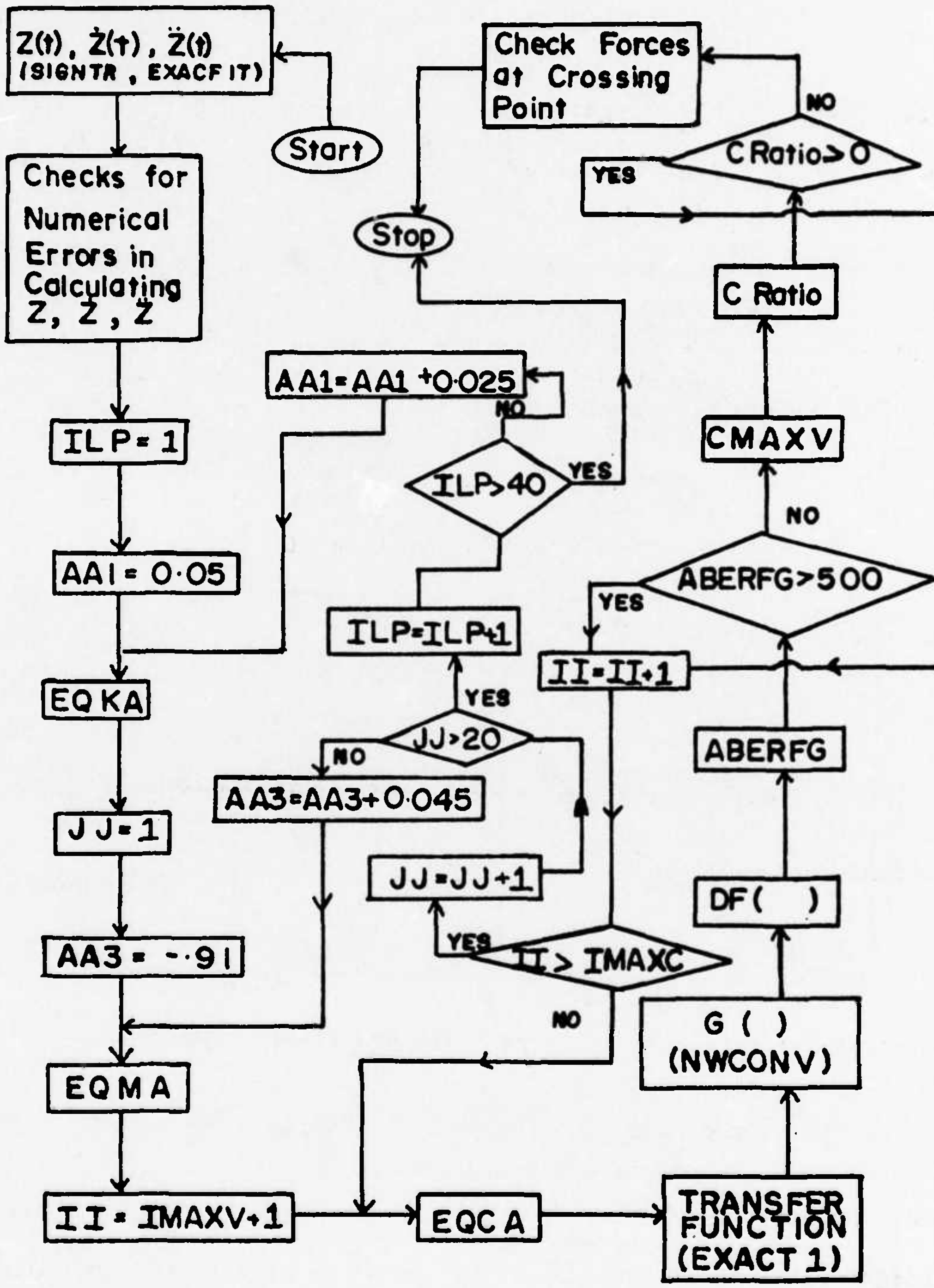

Figure C-4. Summary Flow Chart of Program FNDPRM

Then a value of m is calculated using the equation

$$m = EQMA = AA3 \times PMAX/DRV2\ (IMAXD) \tag{30}$$

where DRV2 (IMAXD) is the acceleration at maximum deflection and AA3 = .91. Equation 30 is derived as follows: Let

$$k = AA1 \times PMAX/DMAX \tag{29}$$

at maximum deflection, i.e., section (3), Figure 7. Using a constant AA2, the equation

$$\begin{aligned} AA2 \times PMAX &= EQMAXDRV2(IMAXD) + EQKA \times DMAX \\ &= EQMAXDRV2(IMAXD) + AA1 \times PMAX \end{aligned}$$

is obtained. Therefore

$$AA2 \times PMAX - AA1 \times PMAX = EQMAXDRV2(IMAXD)$$

$$(AA2 - AA1)PMAX = EQMA \times DRV2(IMAXD) \tag{31}$$

Letting, AA3 = AA2 - AA1 yields

$$m = \frac{AA3 \times PMAX}{DRV\ (IMAXD)} = EQMA$$

Next a value of c is calculated using equation (32) where

$$c = EQCA = EQMA \times DRV2(II)/DRV1(II) \tag{32}$$

where DRV1(II) is the velocity at time increment II (Figure C-3). The initial value of II corresponds to the point of zero acceleration + 1 (Figure C-3). Using the initial value of k, m and c calculated using equation (29), (30) and (32) respectively, the transfer function is

calculated using equation (11a) or (11b) whichever is applicable. Subroutine EXACT1 performs this computation.

Next the value of $\frac{F(t)}{m}$ (equation 33) is calculated using the discrete implicit form of the convolution integral equation (34)

$$O(t) = \int_{o}^{t} I(t-\tau)\cdot G(\tau)\, d\tau \qquad (33)$$

where

$$I(t) = \frac{F(t)}{m}$$

Its implicit form is

$$I(i) = O(i)/\Delta T - \sum_{m=1}^{k=i\ -1} G(\tilde{m})\cdot I\ (k + 2 - \tilde{m}) \qquad (34)$$

where the initial value of i is 2, and $I(1) = \frac{O(1)}{I(i)\cdot\Delta T}$ (34a)

$G(\tau)$ is the transfer function and ΔT is the time increment. Subroutine NWCONV performs these calculations.

Next F(t), the equivalent input function, is calculated using the equation

$$F(t) = m \times I(t) = DF(I) \qquad (34a)$$

The maximum value CPMAX of F(t), is then found and compared with 25,000 lbs. If

$$ABERFG = |CPMAX - 25000| > 500 \qquad (35)$$

then II is incremented by 1, and the procedure subsequent to that step is repeated using the DRV2(II) and DRV1(II) values corresponding to

the new II. ILP, JJ and II are counters which have maximum values of 40, 20 and IMAXC (Figure C-3) respectively. These counters ensure that the tested range of values for AA1 is from .05 to 1.05, for AA3 it is from -.91 to -.01, and for II it is from the first point after the point of inflection to the maximum deflection (Figure C-3). If

$$\text{ABERFG} = |\text{CPMAX}-25000| < 500 \qquad (35b)$$

then c is calculated using the equation for section (1), Figure 9, equation 36

$$\text{CMAXV} = (\text{ZVALUF} - \text{EQKA* ZVALVO})/\text{ZVALU1} \qquad (36)$$

where CMAXV = c

ZVALUF = force at section (1) (Figure 7)

EQKA = k

ZVALVO = the deflection at section (1) (Figure 7)

ZVALU1 = the velocity at section (1) (Figure 7)

The ratio given by equation (37) is next calculated

$$\text{CDIFFR} = (\text{CMAXV} - \text{EQCA})/\text{CMAXV} \qquad (37)$$

where EQCA is the c value computed in equation (32). For the first value of CDIFFR, the procedure increments II by 1 and repeats all the steps from that point. For the second and subsequent values of CDIFFR, the ratio of the current and the preceding value is calculated using the equation

$$\text{CRATIO} = \text{QC(ICC)/QC(ICC-1)} \qquad (38)$$

where QC(ICC) refers to the current ratio of CDIFFR, AND QC(ICC - 1) refers to the preceding ratio of CDIFFR. If

$$\text{CRATIO} > 0$$

then the difference between the c values computed from two independent equations, equation (32) at the crossing point, and equation (36) at the point of inflection, has not passed through zero, so II is incremented and the subsequent steps are repeated. If

$$\text{CRATIO} < 0$$

then the difference between the c values calculated by equations (32) and (36) has passed through zero and the c values calculated using these two equations are approximately the same.

It has been found that the two controls, namely,

$$\text{ABERFG} < 500\text{, and,}$$

$$\text{CRATIO} < 0$$

ensures that the conditions stated in paragraph 3.2.2, are satisfied.

Finally, the exact solution for the force is calculated by substitution EQCA, EQKA, EQMA, DRVO, DRV1, and DRV2 in the equation,

$$\text{CMPXX(I)} = \text{EQKA} \times \text{DRVO(I)} \times \text{EQMC} \times \text{DRV1(I)} + \text{EQMA} \times \text{DRV2(I)} \quad (39)$$

where CPMXX(I) is the force at each time increment I in the record. The force at the crossing point calculated by the convolution and substitution technique are computed. A listing of the program FNDPRM and a typical output is given at the end of this Appendix.

c. Prediction

The subroutines EXACFT, SIGNTR, NWCONV, EXACT 1, ERECT2, and MODPRM are used by the main program PREDCT to predict the signature of a vehicle (Vehicle A) at a site (site I) over which the vehicle has not traversed. It is required to know the signatures of vehicle A at another site (standard site), and a standard vehicle (vehicle B) at both the standard site and site I. Since details of the methodology for determining the parameters of the transfer function, the loading function, and the equivalency function has been detailed previously only a summary flow chart of program PREDCT is given here. Figure C-5 shows the summary flow chart of program PREDCT. A listing of the program and a typical output is given in the following pages of this Appendix.

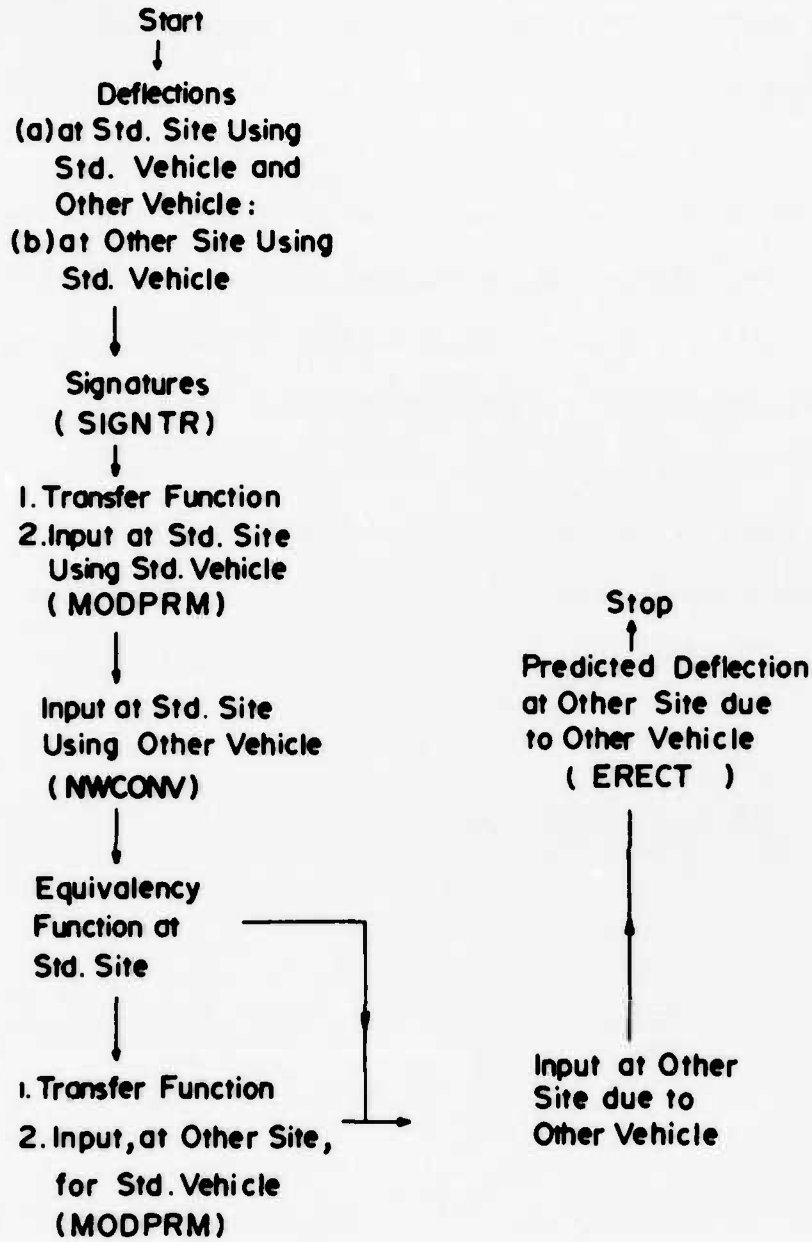

Figure C-5. Summary Flow Chart of Program PREDCT

```
      C-------------------------------------------------
            PROGRAM FNDPRM(INPUT,OUTPUT,TAPE5=INPUT,TAPE6=OUTPUT,PLOT)
      C
      C               THIS PROGRAM COMPUTES PARAMETERS OF THE
      C               REDUCED TRANSFER FUNCTION
      C               FROM DEFLECTIONS MEASURED AT 5 POSITIONS
      C               PERPENDICULAR TO THE DIRECTION OF TRAVEL
      C               OF THE LOAD VEHICLE
      C------------------------------------------------
      C
      C               SUBROUTINES REQUIRED
      C                           (1)  EXACT1
      C                           (2)  NWCONV
      C                           (3)  EXACFIT
      C                           (4)  SIGNTR
      C
      C               INPUT-    NR--NUMBER OF RECORDS
      C                         JM--NUMBER OF GAGES
      C                         AIN--DISTANCE OF GAGE FROM OUTER EDGE OF TIRE PR
      C                         NP-NUMBER OF DATA POINTS
      C                         PT--TIME INCREMENT IN SECONDS
      C                         WMAX--MAXIMUM WHEEL LOAD USED
      C                         INITX--DIGITIZED DATA
      C                         CALG--CALIBRATION DATA
      C
      C
      C
            DIMENSION FRESP(11,100,5),INITX(11,100,5),CALG(11,5),NP(11),PT(11)
           1,WMAX(11),DRV0(100),GMAX(11,5)
            DIMENSION VIPY(200),VISIG(200)
            DIMENSION AI(5),FI(5)
            DIMENSION AIN(5,11)
            DIMENSION QC(2000)
            DIMENSION APK(100),BT(100),TXPON(100)
            DIMENSION FR(10),DFY(10),FRR(10,6)
            DIMENSION DF(200)
            DIMENSION T(200)
            DIMENSION O(200),GG(200)
            DIMENSION V(200),G(200)
            DIMENSION IVEL(11,5)
            DIMENSION DRV1(200),DRV2(200),CPMXX(50)
      C
      C
            READ(5,804)NR,JM
            DO 810 K=1,NR
            READ(5,29)(AIN(J,K),J=1,JM)
            READ(5,801)NP(K),PT(K),WMAX(K)
            JP=NP(K)
            DO 800 I=1,JP
            READ(5,802)(INITX(K,I,J),J=1,5)
        800 CONTINUE
            READ(5,803)(CALG(K,J),J=1,5)
        810 CONTINUE
        801 FORMAT(I5,2F10.4)
        802 FORMAT(5(I4,2X))
        803 FORMAT(5F12.10)
        804 FORMAT(2I10)
         29 FORMAT(6F10.5)
      C
      C*************RECORDS RUN
      C**************
      C
      C   EGLIN     SITE 1    LOC B-4   LD. CT.   3.10.76   3.0  .2   46
      C
      C**************
      C**************
      C
      C               TOP OF MAIN LOOP THAT OPERATES ON ONE RECORD AT A TIME
      C
            DO 811 K=1,NR
      C
      C
      C               CALCULATES DEFLECTION RESPONSE FUNCTION FOR JM GAGES AND
      C               THE PEAK FOR EACH GAGE FOR THE K TH RECORD
      C
            DO 806 J=1,JM
```

```
      FI(J)=AIN(J,K)
      RMAX=0.0
      JP=NP(K)
      DO 807 I=2,JP
      FRESP(K,I-1,J)=FLOAT(INITX(K,I,J)-INITX(K,1,J))*CALG(K,J)/12.
      VIPY(I-1)=FRESP(K,I-1,2)
      IF(FRESP(K,I-1,J).LT.RMAX)GO TO 807
      RMAX=FRESP(K,I-1,J)
  807 CONTINUE
      GMAX(K,J)=RMAX
      FI(J)=GMAX(K,J)
  806 CONTINUE
C
C                     LISTS REDUCED DATA
C
      WRITE(6,833)
  833 FORMAT(1H1,40X,*NEW RECORD*//)
      WRITE(6,814)
  814 FORMAT(//1X,*NUMBER OF DATA POINTS      RECORD NUMBER        MAX. WH
     1EEL LOAD      TIME INCREMENT       NUMBER OF GAGES*/)
      WRITE(6,815)NP(K),K,WMAX(K),PT(K),JM
  815 FORMAT(10X,I4,19X,I4,18X,F6.0,19X,F4.2,18X,I2/)
      WRITE(6,816)
  816 FORMAT(//40X,*DEFLECTIONS IN FT*/)
      WRITE(6,817)
  817 FORMAT(13X,*GAGE 1            GAGE 2            GAGE 3            GAGE 4
     1           GAGE 5*/)
      DO 818 I=1,JP
      WRITE(6,819)(FRESP(K,I,J),J=1,JM)
  818 CONTINUE
  819 FORMAT(10X,5(F7.5,10X))
      WRITE(6,820)
  820 FORMAT(//40X,*PEAK DEFLECTIONS*/)
      WRITE(6,819)(GMAX(K,J),J=1,JM)
C------------------------------------------------------------------------
C                FIT MEASURED PEAK LATERAL DEFLECTION PROFILE TO
C                EQUATION USING SUBROUTINE EXACFIT
C------------------------------------------------------------------------
C
      CALL EXACFIT(FI,TFXP,TBETAF,FAF,AI)
C
      APK(K)=FAF
      BT(K)=TBETAF
      TXPON(K)=TFXP
C
      VBETA=TBETAF
      VRVAL=TFXP
      VIPX=AIN(2,K)
      NV=JP
C--------------------------------------------------------------
C                CALCULATE SIGNATURE OF PROTOTYPE USING
C                SUBROUTINE SIGNTR
C--------------------------------------------------------------
C
      CALL SIGNTR(VBETA,VRVAL,VIPX,VIPY,VISIG,NV)
C
C--------------------------------------------------------------
C                CALCULATE FIRST AND SECOND DERIVATIVES
C--------------------------------------------------------------
      DO 74 I=1,JP
      DRV0(I)=VISIG(I)
      TRM1=(VISIG(I)+VISIG(I+1))/2.
      IF(I.EQ.1)TRM2=VISIG(I)/2.
      TRM2=(VISIG(I)+VISIG(I-1))/2.
      DRV1(I)=(TRM1-TRM2)/PT(K)
   74 CONTINUE
      DO 75 I=1,JP
      TRN1=(DRV1(I+1)+DRV1(I))/2.
      IF(I.EQ.1)TRN2=DRV1(I)/2.
      TRN2=(DRV1(I)+DRV1(I-1))/2.
      DRV2(I)=(TRN1-TRN2)/PT(K)
   75 CONTINUE
C------------------------------------------------------------------------
C                IDENTIFY FIRST PEAK BY FINDING POINT WHERE FIRST
C                DERIVATIVE CHANGES SIGN
```

```
      C--------------------------------------------------------------
            BOTM=0.00000000001
            DO 726 I=1,JP
            HUMP1=DRV0(I+1)-DRV0(I)
            IF(HUMP1.GE.0.0)GO TO 726
            JPP=I+6
            GO TO 727
        726 CONTINUE
        727 CONTINUE
      C-----------------------------------------------------------------
      C              REPLACE ZEROES BY AVERAGING BEFORE AND AFTER POINTS
      C-----------------------------------------------------------------
            IMAXV=0
            DV1MX=0.0
            DO 315 I=1,JPP
            IF(DRV1(I).EQ.0.0)DRV1(I)=(DRV1(I+1)+DRV1(I-1))/2.
CAUTION - IS FLOATING POINT EQUALITY TO BE EXPECTED        *****************************
            IF(DRV1(I).EQ.0.0)DRV1(I)=(DRV1(I+2)+DRV1(I-2))/2.
CAUTION - IS FLOATING POINT EQUALITY TO BE EXPECTED        *****************************
            IF(ABS(DRV1(I)).LT.BOTM)DRV1(I)=(DRV1(I+1)+DRV1(I-1))/2.
            IF(ABS(DRV2(I)).LT.BOTM)DRV2(I)=(DRV2(I+1)+DRV2(I-1))/2.
            IF(DRV1(I).LT.DV1MX)GO TO 315
            DV1MX=DRV1(I)
            IMAXV=I
        315 CONTINUE
      C------------------------------------------
      C              FIND MAXIMUM VALUE OF SIGNATURE
      C------------------------------------------
            DMAX=DRV0(1)
            DO 53 I=2,JPP
            IF(DRV0(I).LT.DMAX)GO TO 53
            DMAX=DRV0(I)
            IMAXD=I
         53 CONTINUE
      C-----------------------------------------------------------
      C              REPLACE   ERRONEOUS ACCELERATIONS BY AVERAGING
      C              BEFORE AND AFTER POINTS
      C-----------------------------------------------------------
            IMAXV1=IMAXV-1
            DO 57 I=2,IMAXV1
            IF(DRV2(I).LE.0.0)DRV2(I)=(DRV2(I-1)+DRV2(I+1))/2.
            IF(DRV2(I).LE.0.0)DRV2(I)=(DRV2(I-2)+DRV2(I+2))/2.
         57 CONTINUE
            IMAXVA=IMAXV+1
            DO 109 I=IMAXVA,JPP
            IF(DRV2(I).GE.0.0)DRV2(I)=(DRV2(I-1)+DRV2(I+1))/2.
            IF(DRV2(I).GE.0.0)DRV2(I)=(DRV2(I-2)+DRV2(I+2))/2.
        109 CONTINUE
            DO 107 I=1,JPP
            IF(DRV1(I+1).EQ.DRV1(I))DRV1(I+1)=(DRV1(I+2)+DRV1(I))/2.
CAUTION - IS FLOATING POINT EQUALITY TO BE EXPECTED        *****************************
            IF(DRV2(I+1).EQ.DRV2(I))DRV2(I+1)=(DRV2(I+2)+DRV2(I))/2.
CAUTION - IS FLOATING POINT EQUALITY TO BE EXPECTED        *****************************
        107 CONTINUE
      C-----------------------------------------------------------
      C              FIND TIME INTERVAL WHERE VELOCITY CHANGES SIGN
      C              AND FRACTION OF VELOCITYTO ZERO BY
      C              LINEAR INTERPOLATION
      C-----------------------------------------------------------
            DO 789 IA=1,JPP
            DEROTS=DRV1(IA+1)/DRV1(IA)
            IF(DEROTS.GT.0.0)GO TO 789
            DZERO=DRV1(IA)-DRV1(IA+1)
            DDTZ=DRV1(IA)/DZERO
            NAFNL=IA
            GO TO 788
        789 CONTINUE
        788 CONTINUE
      C--------------------------------------------------------
      C              FIND INTERVAL AND TIME WHERE ACCELERATION IS
      C              ZERO AND THE CORRESPONDING DISPLACEMENT
      C              AND VELOCITY
      C--------------------------------------------------------
            DO 889 IA=1,JPP
            ZEROTS=DRV2(IA+1)/DRV2(IA)
```

```
      IF(ZEROTS.GT.0.0)GO TO 889
      TZERO=DRV2(IA)-DRV2(IA+1)
      FDTZ=DRV2(IA)/TZERO
      IAFNL=IA
      DRORNG=DRV0(IA+1)-DRV0(IA)
      ZVALU0=DRV0(IA)+FDTZ*DRORNG
      DR1RNG=DRV1(IA+1)-DRV1(IA)
      ZVALU1=DRV1(IA)+FDTZ*DR1RNG
      GO TO 888
  889 CONTINUE
  888 CONTINUE
C
C*********
      WRITE(6,99)
   99 FORMAT(/37X,*FOR SIGNATURE*/)
      WRITE(6,76)
   76 FORMAT(//7X,*     INCREMENT   SIGNATURE          VELOCITY      ACCEL
     1ERATION*/)
      WRITE(6,77)(I,DRV0(I),DRV1(I),DRV2(I),I=1,JPP)
   77 FORMAT(7X,I14,3E15.5)
      WRITE(6,1091)
 1091 FORMAT(//////////1X,*0*/)
      IMAXF=0
      PMAX=WMAX(K)
      AA1=0.05
      ICC=0
C--------------------------------------------
C              TOP OF LOOP INCREMENTING AA1
C--------------------------------------------
      DO 104 ILP=1,40
      EQKA=AA1*PMAX/DMAX
      AA3=-0.91
C--------------------------------------------
C              TOP OF LOOP INCREMENTING AA3
C--------------------------------------------
      DO 103 JJ=1,20
      IT=IMAXV
      EQMA=AA3*PMAX/DRV2(IMAXD)
      CPMAX=0.0
      AA2=AA1+AA3
      IF(AA2.LT.0.0)GO TO 1021
      IMAXC=IMAXD
      IT=IT+1
C-----------------------------------------------------------------
C              TOP OF LOOP VARYING TIME BETWEEN ZERO ACCELERATION
C              AND ZERO VELOCITY AND CALCULATING EQCA
C              FOR EACH INCREMENT
C-----------------------------------------------------------------
      DO 102 II=IT,IMAXC
      EQCA=EQMA*DRV2(II)/DRV1(II)
      EQCA=-EQCA
C
C
      EQVK=EQKA
      EQMASS=EQMA
      EQVC=EQCA
      MM=JPP
      DT=PT(K)
C-----------------------------------------------------------
C              CALCULATING REDUCED TRANSFER FUNCTION USING
C              SUBROUTINE EXACT1
C-----------------------------------------------------------
C
      CALL EXACT1(MM,DT,EQVK,EQMASS,T,GG,EQVC)
C
      DO 73 I=1,JPP
      D(I)=DRV0(I)
      V(I)=GG(I)
   73 CONTINUE
      N=JPP
C-----------------------------------------------------
C              CALCULATE I(T) USING SUBROUTINE NWCONV
C              BY IMPLICIT CONVOLUTION
C-----------------------------------------------------
C
```

```
      CALL NWCONV(N,V,G,O,DT)
C
C-----------------------------------------------------------------
C               CALCULATING EQUIVALENT FORCEAS PRODUCT OF
C               I(T) AND EQMASS
C-----------------------------------------------------------------
      DO 508 MP=1,JPP
      DF(MP)=G(MP)*EQMASS
  508 CONTINUE
      DO 509 MA=1,JPP
      DF(MA)=(DF(MA)+DF(MA+1))/2.
  509 CONTINUE
C--------------------------------------------------------------------------
C               AVERAGING AND FINDING MAXIMUM EQUIVALENT FORCE
C--------------------------------------------------------------------------
      CPMAX=0.
      DO 501 M=1,JPP
      DF(M)=(DF(M)+DF(M+1))/2.
      IF(DF(M).GT.CPMAX)GO TO 20
      GO TO 502
   20 CPMAX=DF(M)
      ICF=M
  502 CONTINUE
  501 CONTINUE
C------------------------------------------------------------------------------
C               EXECUTING FIRST CHECK TO ENSURE THAT THE
C               ABSOLUTE DIFFERENCE BETWEEN THE MAXIMUM COMPUTED
C               FORCE AND 25 KIPS IS LESS THAN 500 LBS
C------------------------------------------------------------------------------
      ERFCE=CPMAX-PMAX
      ABERFG=ABS(ERFCE)
      IF(ABERFG.GT.500.0)GO TO 102
C-------------------------------------------------------------------------------------
C               EXECUTING SECOND CHECK TO ENSURE THAT THE DIFFERENCE
C               BETWEEN THE C VALUES COMPUTED AT THE CROSSING POINT
C               AND THE POINT OF INFLECTION GOES THROUGH ZERO
C-------------------------------------------------------------------------------------
      ICC=ICC+1
      DFRNG=DF(IAFNL+1)-DF(IAFNL)
      ZVALUF=DF(IAFNL)+FDTZ*DFRNG
      CMAXV=(ZVALUF-EQKA*ZVALU0)/ZVALU1
      CDIFFR=(CMAXV-EQCA)/CMAXV
      ABCD=CDIFFR
      QC(ICC)=CDIFFR
      IF(ICC.EQ.1)GO TO 102
      CRATIO=QC(ICC)/QC(ICC-1)
      IF(CRATIO.GT.0.0)GO TO 102
C-------------------------------------------------------------------------
C               CALCULATING FORCE RATIOS COMPONENTS OF FORCE
C               AND TOTAL FORCE AT THE CROSSING POINT
C-------------------------------------------------------------------------
      FCHK=EQKA*DRV0(II)
      DIFCHK=FCHK-DF(II)
      DFCHKR=DIFCHK/FCHK
      FPFRAC=DF(II)/PMAX
      ICDPT=II
      TRMM=EQMA*DRV2(II)
      TRMC=EQCA*DRV1(II)
      TRMK=EQKA*DRV0(II)
      CPMXX(II)=TRMM+TRMC+TRMK
      WRITE(6,847)
  847 FORMAT(//10X,*GOOD RUN*//)
      GO TO 846
C**********
  102 CONTINUE
 1021 CONTINUE
      AA3=AA3+0.045
C*************
  103 CONTINUE
      AA1=AA1+0.025
C*******
  104 CONTINUE
 1000 FORMAT(/1X,*000*)
  845 FORMAT(6F15.4,10X,2I5,F10.3)
      WRITE(6,1002)
```

```
 1002 FORMAT(/10X,*OUTER LOOP COMPLETED*/)
      GO TO 94
  846 CONTINUE
      WRITE(6,1043)
 1043 FORMAT(//////////10X,*INCREMENT*,2X,*M-COMP.*,8X,*C-COMP.*,8X,*K-C
     1OMP.*,8X,*EXACT*,8X,*CONVOLUTION*,8X,*TDT FUNC*,8X,*SIGNATURE*/)
C------------------------------------------------------------------
C               CALCULATING COMPONENTS OF FORCE DUE TO INERTIAL
C               DAMPING AND STIFFNESS
C------------------------------------------------------------------
      JPN=JPP-3
      DO 106 I=1,JPN
      TMT=EQMA*DRV2(I)
      TCT=EQCA*DRV1(I)
      TKT=EQKA*DRV0(I)
      CPMXX(I)=TCT+TKT+TMT
      WRITE(6,1001)I,TMT,TCT,TKT,CPMXX(I),DF(I),GG(I),DRV0(I)
  106 CONTINUE
C------------------------------------------------------------------
C               CALCULATING FORCE RATIOS AT SECTIONS (1),(2),(3)
C------------------------------------------------------------------
      AFRNG=DF(NAFNL+1)-DF(NAFNL)
      DVALUF=DF(NAFNL)+DDTZ*AFRNG
C*****
      ZVALUR=ZVALUF/PMAX
C******
      DVALZD=DVALUF/PMAX
C*****
      FORTIO=ABERFG/PMAX
C------------------------------------------------------------------
C               CALCULATING TIME RATIOS AT SECTIONS(1),(2),(3)
C------------------------------------------------------------------
      DENOM=FLOAT(IMAXD)
      DENOM1=1.0
      TCRSPT=FLOAT(II)/DENOM
      TZROA=FLOAT(IAFNL)/DENOM
C*******
      WRITE(6,1041)
 1041 FORMAT(//////////10X,*EQUIV. MASS*,10X,*EQUIV. STIFFNESS*,9X,*EQUI
     1V. DAMPING*)
      WRITE(6,2041)
 2041 FORMAT(12X,*SLUGS*,16X,*LBS/FT*,20X,*LBS-SEC/FT*/)
      WRITE(6,1042)EQMA,EQKA,EQCA
 1042 FORMAT(10X,F10.2,15X,F10.2,12X,F10.1)
      WRITE(6,1044)
 1044 FORMAT(//20X,*     FORCE RATIOS(FORCE OVER 25000)*/)
      WRITE(6,1045)
 1045 FORMAT(25X,*SECTION(1) SECTION(2) SECTION(3)*/)
      WRITE(6,1046)ZVALUR,FPFRAC,DVALZD
 1046 FORMAT(23X,3F10.3)
      WRITE(6,1050)
 1050 FORMAT(///20X,*      TIME RATIOS(TIME OVER TIME TO MAX. DEF.)*/)
      DENOM1=1.
      WRITE(6,1045)
      WRITE(6,1046)TZROA,TCRSPT,DENOM1
      WRITE(6,1060)
 1060 FORMAT(///20X,*C-PARAMETER DIFFERENCE RATIO*/)
      WRITE(6,1061)CDIFFR
 1061 FORMAT(30X,F7.3)
      WRITE(6,1070)
 1070 FORMAT(///20X,*FORCE DIFFERENCE RATIO AT THE CROSSING POINT*/)
      WRITE(6,1061)DFCHKR
      WRITE(6,1080)
 1080 FORMAT(///20X,*MAXIMUM FORCE DIFFERENCE*/)
      WRITE(6,1061)ABERFG
 1001 FORMAT(10X,I5,7F15.5)
C------------------------------------------------------------------------
  811 CONTINUE
   94 CONTINUE
C
      STOP
      END
C
```

```
C------------------------------------------------------------------
      SUBROUTINE EXACFIT(FI,TFXP,TBETAF,FAF,AI)
C
C               THIS SUBROUTINE CALCULATES THE PARAMETERS OF THE
C               MAXIMUM LATERAL DEFLECTION PROFILE USING
C               THE DEVELOPED INTERPOLATION-ITERATION PROCEDURE
C------------------------------------------------------------------
C               INPUT-    FI--MEASURED DEFLECTIONS AT LOCATIONS LATERAL
C                             TO THE TIRE PRINT
C                         AI--LATERAL DISTANCES FROM EDGE OF TIRE PRINT
C                             CORRESPONDING TO FI
C               OUTPUT    TFXP--R PARAMETER
C                         TBETAF--BETA PARAMETER
C                         FAF--A PARAMETER
C
      DIMENSION FI(6),TBETA(3),TVAL(999),AI(5),FA(5),FFXP(5)
C$    TRACE SUBSCRIPTS
C$    TRACE ARITHMETIC
      M=1
      IFTX=0
      I=2
      IG=I+1
      IM=I+2
      ITRID=0
C
C***************************
C***************************
C
  710 CONTINUE
      FXP=0.2001
      DFXP=0.0125
      J=0
  771 CONTINUE
      J=J+1
      FXP=FXP+DFXP
      IFCHK=0
  772 CONTINUE
  776 CONTINUE
      CONS1=ALOG(FI(I))-ALOG(FI(IG))
      CONS2=ALOG(FI(I))-ALOG(FI(IM))
      CONF=CONS1/CONS2
      FLHS=CONF*((AI(I)**FXP)-(AI(IM)**FXP))
      FRHS=(AI(I)**FXP)-(AI(IG)**FXP)
      TVAL(J)=FLHS-FRHS
      IF(J.EQ.1)GO TO 771
      FDIF=TVAL(J)/TVAL(J-1)
      ABVAL=ABS(TVAL(J))
      IF(J.EQ.999)GO TO 726
      IF(FDIF.GT.0.0)GO TO 771
      TFDIF=ABS(TVAL(J-1))+ABS(TVAL(J))
      FFXP(M)=FXP-(TVAL(J)/TFDIF)*DFXP
  773 CONTINUE
C
      FBETA1=ALOG(FI(I))-ALOG(FI(IG))
      FBETA2=(AI(I)**FFXP(M))-(AI(IG)**FFXP(M))
      TBETA(M)=FBETA1/FBETA2
      FA1=TBETA(M)*(AI(1)**FFXP(M))
      FA(M)=FI(1)/EXP(FA1)
      GO TO 777
      IF(ITRID.EQ.1)GO TO 727
CAUTION - STATEMENT CANNOT BE EXECUTED - NO STATEMENT NUMBER        *******************
      IF(IFTX.EQ.1)GO TO 777
      M=M+1
      IG=IG+1
      IM=IM+2
      IFTX=1
      GO TO 710
  777 FAF=FA(M)
      TBETAF=TBETA(M)
      TFXP=FFXP(M)
      GO TO 728
C***************************
C**********
  726 CONTINUE
```

```
      ITRID=1
      M=M+1
      IG=IG+1
      IM=IM+2
      IFTX=1
      IF(IM.LE.5)GO TO 730
      WRITE(6,731)
  731 FORMAT(/20X,*DATA DOES NOT FIT--CHECK DATA*/)
      GO TO 720
  730 GO TO 710
  727 CONTINUE
C*************************************
      FAF=FA(2)
      TBETAF=TBETA(2)
      TFXP=FFXP(2)
  728 CONTINUE
      WRITE(6,775)
  775 FORMAT(/20X,*  A PARAMETER      BETA          EXPONENT R*/)
      WRITE(6,778)FAF,TBETAF,TFXP
  778 FORMAT(20X,3E15.5/)
      WRITE(6,750)
  750 FORMAT(/20X,*  CALCULATED Y    MEASURED Y      LATERAL DIST.*/)
      DO 701 M=1,5
      YY1=TBETAF*(AI(M)**TFXP)
      YY2=EXP(YY1)
      YY=FAF*YY2
      WRITE(6,20)YY,FI(M),AI(M)
  701 CONTINUE
  720 CONTINUE
   20 FORMAT(20X,3E15.5)
C
      RETURN
      END
C
C
C
C-----------------------------------------------------

      SUBROUTINE SIGNTR(VBETA,VRVAL,VIPX,VIPY,VISIG,NV)
C
C              THIS SUBROUTINE CALCULATES THE SIGNATURE BY
C              DIRECT SUBSTITUTION
C-----------------------------------------------------
C              INPUT-    VBETA--BETA PARAMETER
C                        VIPX--LATERAL DISTANCE OF GAGE FROM OUTER
C                              EDGE OF TIRE PRINT
C                        VIPY--NV VALUES OF MEASURED DEFLECTION
C                              AT VIPX FROM OUTER EDGE OF TIRE PRINT
C                        VRVAL--R PARAMETER
C
C              OUTPUT-   VISIG--NV VALUES OF THE SIGNATURE
C
      DIMENSION VIPY(200),VISIG(200)
      VTOP=VBETA*(VIPX**VRVAL)
      DO 40 I=1,NV
      VISIG(I)=VIPY(I)/EXP(VTOP)
   40 CONTINUE
      RETURN
      END
C
C-----------------------------------------------------

      SUBROUTINE NWCONV(N,V,G,O,DT)
C
C              THIS SUBROUTINE IMPLICITLY CONVOLUTES V(   ) AND O(   )TO
C              YIELD G(   ) AT N POINTS
C-----------------------------------------------------
C
C              INPUT-    V--N VALUES OF INPUT
C                        O--N VALUES OF OUTPUT
C                        DT--TIME INCREMENT
C
C              OUTPUT-   G--N VALUES OF THE IMPLICIT CONVOLUTION RESULT
C
C
C
```

```
      DIMENSION V(200),G(200),O(200)
      S=0.
      Q=0.0
      G(1)=O(1)/(V(1)*DT)
      DO 984 I=2,N
      K=I-1
      DO 985 M=1,K
      Q=Q+V(K+2-M)*G(M)
  985 CONTINUE
      S=Q
      G(I)=((O(I)/DT)-S)/V(1)
C
C
      Q=0.0
      S=0.0
  984 CONTINUE
      RETURN
      END
C
C
C-----------------------------------------------------------------------

      SUBROUTINE EXACT1(MM,DT,EQVK,EQMASS,T,GG,EQVC)
C
C             THIS SUBROUTINE CALCULATES THE REDUCED TRANSFER FUNCTION
C             BY DIRECT SUBSTITUTION
C-----------------------------------------------------------------------
C
C             INPUT-    EQVK--EQUIVALENT K PARAMETER
C                       EQMASS--EQUIVALENT MASS
C                       EQVC--EQUIVALENT C PARAMETER
C                       DT--TIME INCREMENT
C                       MM--NUMBER OF DATA POINTS
C
C             OUTPUT-   GG--MM VALUES OF THE TIME DEPENDENT TRANSFER FUN
C
      DIMENSION T(200),GG(200)
C$    TRACE ARITHMETIC
C
      DO 630 I=1,MM
      T(I)=FLOAT(I)*DT
      TIME=T(I)
C
C
      BB=SQRT(EQVK/EQMASS)
      AA=EQVC/(2.*EQMASS)
C
      TRI=BB*BB-AA*AA
      IF(TRI.LT.0.0)GO TO 3
C
      GE1=1./SQRT(TRI)
      GE2=1./EXP(AA*T(I))
      G3=SIN(SQRT(TRI)*T(I))
      GG(I)=GE1*GE2*G3
C
C
      GO TO 630
C
    3 CONTINUE
      PP=SQRT(ABS(TRI))
      P1=EXP(PP*T(I))
      P2=1./(EXP(PP*T(I)))
      P3=1./EXP(AA*T(I))
      P5=(P1-P2)/2.
      GG(I)=P3*P5/PP
C
  630 CONTINUE
C
      RETURN
      END
```

NEW RECORD

NUMBER OF DATA POINTS	RECORD NUMBER	MAX. WHEEL LOAD	TIME INCREMENT	NUMBER OF GAGES
46	1	25000.	.20	5

DEFLECTIONS IN FT

GAGE 1	GAGE 2	GAGE 3	GAGE 4	GAGE 5
.00001	0	.00001	.00001	-.00000
.00003	.00002	.00001	.00001	0
.00004	.00003	.00003	.00001	.00000
.00005	.00005	.00004	.00002	.00001
.00008	.00006	.00005	.00003	.00001
.00011	.00008	.00007	.00004	.00002
.00013	.00010	.00009	.00005	.00002
.00017	.00014	.00011	.00006	.00003
.00022	.00019	.00014	.00008	.00003
.00030	.00023	.00018	.00010	.00004
.00036	.00030	.00023	.00012	.00006
.00048	.00040	.00028	.00015	.00006
.00063	.00051	.00037	.00019	.00009
.00083	.00069	.00048	.00024	.00010
.00108	.00087	.00060	.00029	.00012
.00134	.00108	.00072	.00035	.00014
.00165	.00132	.00086	.00040	.00016
.00195	.00156	.00097	.00044	.00017
.00238	.00189	.00112	.00048	.00018
.00280	.00218	.00124	.00051	.00019
.00341	.00261	.00140	.00056	.00020
.00384	.00293	.00150	.00058	.00020
.00418	.00323	.00161	.00061	.00021
.00434	.00343	.00166	.00062	.00021
.00436	.00349	.00166	.00062	.00021
.00430	.00350	.00168	.00063	.00021
.00386	.00310	.00153	.00059	.00020
.00344	.00290	.00145	.00056	.00019
.00292	.00247	.00123	.00048	.00016
.00257	.00218	.00111	.00043	.00015
.00210	.00178	.00090	.00033	.00010
.00175	.00147	.00073	.00026	.00007
.00145	.00122	.00059	.00020	.00005
.00122	.00101	.00047	.00014	.00003
.00106	.00089	.00038	.00010	.00001
.00091	.00073	.00030	.00006	-.00001
.00082	.00065	.00026	.00004	-.00001
.00073	.00057	.00021	.00002	-.00002
.00067	.00051	.00018	.00001	-.00003

.00063	.00049	.00016	-.00000	-.00003
.00062	.00045	.00014	-.00001	-.00003
.00059	.00043	.00013	-.00001	-.00003
.00059	.00043	.00013	-.00002	-.00003
.00058	.00043	.00012	-.00002	-.00003
.00056	.00041	.00011	-.00002	-.00003
0	0	0	0	0

PEAK DEFLECTIONS

.00436	.00350	.00168	.00063	.00021

A PARAMETER	BETA	EXPONENT R
4.79864E-03	-6.02783E-01	1.31790E+00

CALCULATED Y	MEASURED Y	LATERAL DIST.
4.35510E-03	4.35510E-03	2.50000E-01
3.56827E-03	3.49750E-03	5.83330E-01
1.71561E-03	1.68158E-03	1.50000E+00
6.38773E-04	6.30420E-04	2.50000E+00
2.07310E-04	2.12980E-04	3.50000E+00

FOR SIGNATURE

INCREMENT	SIGNATURE	VELOCITY	ACCELERATION
1	0	7.83911E-05	2.93966E-04
2	3.13564E-05	1.17587E-04	9.79888E-05
3	4.70346E-05	7.83911E-05	9.79888E-05
4	6.27128E-05	7.83911E-05	1.46983E-04
5	7.83911E-05	1.17587E-04	1.95978E-04
6	1.09747E-04	1.56782E-04	1.95978E-04
7	1.41104E-04	1.95978E-04	2.93966E-04
8	1.88139E-04	2.74369E-04	2.93966E-04
9	2.50851E-04	3.13564E-04	2.93966E-04
10	3.13564E-04	3.91955E-04	5.87933E-04
11	4.07633E-04	5.48737E-04	7.83911E-04
12	5.33059E-04	7.05520E-04	1.07788E-03
13	6.89841E-04	9.79888E-04	1.27385E-03
14	9.25014E-04	1.21506E-03	8.81899E-04
15	1.17587E-03	1.33265E-03	6.85922E-04
16	1.45807E-03	1.48943E-03	6.85922E-04
17	1.77164E-03	1.60702E-03	1.07788E-03
18	2.10088E-03	1.92058E-03	1.17587E-03
19	2.53987E-03	2.07736E-03	1.27385E-03
20	2.93183E-03	2.43012E-03	1.07788E-03
21	3.51192E-03	2.50851E-03	-8.81899E-04
22	3.93523E-03	2.07736E-03	-2.05777E-03
23	4.34286E-03	1.68541E-03	-3.03765E-03
24	4.60939E-03	8.62302E-04	-3.62559E-03
25	4.68779E-03	2.35173E-04	-5.38939E-03
26	4.70346E-03	-1.29345E-03	-5.58536E-03
27	4.17040E-03	-1.99897E-03	-2.05777E-03
28	3.90387E-03	-2.11656E-03	-1.07788E-03
29	3.32378E-03	-2.43012E-03	-4.89944E-04
30	2.93183E-03	-2.31254E-03	5.38939E-04
31	2.39877E-03	-2.39093E-03	6.85922E-04
32	1.97545E-03	-1.88139E-03	1.00439E-03

300B RUN

INCREMENT	M-COMP.	C-COMP.	K-COMP.	EXACT	CONVOLUTION	TDT FUNC	SIGNATURE
1	72.36842	442.25146	0	514.61988	617.71209	.04052	0
2	24.12281	663.37719	95.83333	783.33333	675.91968	.03672	.00003
3	24.12281	442.25146	143.75000	610.12427	618.69802	.03287	.00005
4	36.18421	442.25146	191.66667	670.10234	788.48276	.02941	.00006
5	48.24561	663.37719	239.58333	951.20614	1087.28563	.02632	.00008
6	48.24561	884.50292	335.41667	1268.16520	1409.61497	.02355	.00011
7	72.36842	1105.62865	431.25000	1609.24708	1875.76839	.02108	.00014
8	72.36842	1547.88012	575.00000	2195.24854	2377.82005	.01886	.00019
9	72.36842	1769.00585	766.66667	2608.04094	2916.98704	.01688	.00025
10	144.73684	2211.25731	958.33333	3314.32749	3850.51099	.01511	.00031
11	192.98246	3095.76023	1245.83333	4534.57602	5092.77541	.01352	.00041
12	265.35088	3980.26316	1629.16667	5874.78070	6788.82147	.01210	.00053
13	313.59649	5528.14327	2108.33333	7950.07310	8855.46687	.01083	.00069
14	217.10526	6854.89766	2827.08333	9899.08626	10604.18900	.00969	.00093
15	168.85965	7518.27485	3593.75000	11280.88450	12230.96440	.00867	.00118
16	168.85965	8402.77778	4456.25000	13027.88743	13946.77641	.00776	.00146
17	265.35088	9066.15497	5414.58333	14746.08918	16225.51305	.00694	.00177
18	289.47368	10835.16082	6420.83333	17545.46784	18754.55138	.00621	.00210
19	313.59649	11719.66374	7762.50000	19795.76023	21549.91447	.00556	.00254
20	265.35088	13709.79532	8960.41667	22935.56287	24266.73247	.00498	.00293
21	-217.10526	14152.04678	10733.33333	24668.27485	24740.46330	.00445	.00351
22	-506.57895	11719.66374	12027.08333	23240.16813	23698.22351	.00399	.00394
23	-747.80702	9508.40643	13272.91667	22033.51608	21219.97611	.00357	.00434
24	-892.54386	4864.76608	14087.50000	18059.72222	17655.89134	.00319	.00461
25	-1326.75439	1326.75439	14327.08333	14327.08333	11497.90363	.00286	.00469
26	-1375.00000	-7297.14912	14375.00000	5702.85088	4443.21485	.00256	.00470
27	-506.57895	-11277.41228	12745.83333	961.84211	972.66864	.00229	.00417
28	-265.35088	-11940.78947	11931.25000	-274.89035	-1610.69484	.00205	.00390
29	-120.61404	-13709.79532	10158.33333	-3672.07602	-3627.83553	.00183	.00332

EQUIV. MASS SLUGS	EQUIV. STIFFNESS LBS/FT	EQUIV. DAMPING LBS-SEC/FT
246179.17	3056258.49	5641606.1

FORCE RATIOS(FORCE OVER 25000)

SECTION(1)	SECTION(2)	SECTION(3)
.981	.460	.417

TIME RATIOS(TIME OVER TIME TO MAX. DEF.)

SECTION(1)	SECTION(2)	SECTION(3)
.769	.962	1.000

C-PARAMETER DIFFERENCE RATIO

.044

FORCE DIFFERENCE RATIO AT THE CROSSING POINT

.197

MAXIMUM FORCE DIFFERENCE

259.537

```
      PROGRAM PREDCT (INPUT,OUTPUT,TAPE5=INPUT,TAPE6=OUTPUT,PLOT)
C
C----------------------------------------------------------------
C         THIS PROGRAM PREDICTS THE SIGNATURE AT AN UNTESTED SITE
C        DUE TO VEHICLE A,IF THE SIGNATURE OF A STANDARD VEHICLE
C        IS KNOWN AT THE UNTESTED SITE, AND THE SIGNATURE OF BOTH
C        THE STANDARD VEHICLE AND VEHICLE A ARE KNOWN AT A
C        STANDARD SITE
C-----------------------------------------------------------------
C
C-------------------------------
C        STANDARD VEHICLE AND SITE
C        C 131       SITE 1      47      SIGNATURE
C-------------------------------
C
C-------------------------------
C        C 131      SITE 3    47         BOYER     SIGNATURE
C        C-135 SITE 1     47  BOYER      SIGNATURE
C
C-----------------------------------------------------------------
C        INCLUDED ONLY FOR PURPOSES OF THIS EXAMPLE-THIS SIGNATURE
C        IS THE PREDICTED SIGNATURE
C     C 135   SITE 3       BOYER   SIGNATURE   47
C------------------------------------------------------------------
C------------------------------------------------------------------
C        INPUT-         SCR()     SIGNATURE DUE TO STANDARD VEHICLE
C                                 AT STANDARD SITE
C                       X( )      SIGNATURE DUE TO STANDARD VEHICLE
C                                 AT OTHER SITE
C                       DFCE( )   SIGNATURE DUE TO OTHER VEHICLE
C                                 AT STANDARD SITE
C                       COMPV( )  SIGNATURE DUE TO OTHER VEHICLE
C                                 AT OTHER SITE(FOR PURPOSES OF
C                                 THIS EXAMPLE ONLY)
C                       ALL INPUT SIGNATURES ARE IN INCHES
C        OUTPUT         DD( )     PREDICTED SIGNATURE IN FT.
C------------------------------------------------------------------
C        SUBROUTINES REQUIRED     (1)  EXACT1(      )
C                                 (2)  NWCONV(      )
C                                 (3)  ERECT2(      )
C                                 (4)  MODPRM(      )
C------------------------------------------------------------------
      DIMENSION SOUT1(200),SOUT2(200),VOUT1(200)
      DIMENSION ETINP(200),EQFNC(200)
      DIMENSION ET(200)
      DIMENSION VISIG(200)
      DIMENSION XT(6,200),XF(6,200),DTRK1(200),DF4(200),SFNC(200)
      DIMENSION PP(800),XG(800),DD(800)
      DIMENSION DRV0(100),DRV1(100),DRV2(100)
      DIMENSION DF(200),X(100),DFCE(100),DDEF(100)
      DIMENSION SCR(100),T(200),Y(200),D(200),G(200),GG(200)
      DIMENSION COMPV(200),VOUT2(200)
C$    TRACE ARITHMETIC
C
C
   50 FORMAT(//60X,20H--------------------//)
  498 FORMAT(29X,54HEQUIV INPUT IN LBS     TDT FUNCTION     RESPONSE IN
     1FT//)
  398 FORMAT(31X,E15.5,5X,E15.5,2X,E15.5)
C
      READ(5,100)(SCR(I),I=1,47)
      READ(5,100)(X(I),I=1,47)
      READ(5,100)(DFCE(I),I=1,47)
      READ(5,100)(COMPV(I),I=1,47)
  100 FORMAT(7F10.6)
C
C
      DO 496 I=1,47
      SOUT1(I)=SCR(I)/12.
      VOUT1(I)=DFCE(I)/12.
      SOUT2(I)=X(I)/12.
      VOUT2(I)=COMPV(I)/12.
  496 CONTINUE
C
C
```

```
C
      JP=47
      PMAX =20000.
      DT=0.04
      MM=47
      LL=47
      NT=47
C
      DO 74 I=1,NT
      VISIG(I)=SOUT1(I)
   74 CONTINUE
C
C
C
      WRITE(6,497)
  497 FORMAT(//2X,23HSITE ONE    STD VEHICLE//)
C
      CALL MODPRM(PMAX,JP,DT,VISIG,EQMASS,DF,GG)
C
C
C
C         COMPUTE EQUIV.   INPUT FOR VEHICLE 2     SITE 1
      DO 721 I=1,MM
      T(I)=FLOAT(I)*DT
      O(I)=VOUT1(I)
      V(I)=GG(I)
  721 CONTINUE
C
      N=47
C
      CALL NWCONV(N,V,G,O,DT)
C
      DO 722 I=1,MM
      ETINP(I)=G(I)*EQMASS
  722 CONTINUE
C
      WRITE(6,50)
      WRITE(6,495)
  495 FORMAT(//2X,21HSITE ONE    VEHICLF 2//)
      WRITE(6,498)
      WRITE(6,398)(ETINP(I),GG(I),O(I),I=1,MM)
C
C
C
C           COMPUTE EQUIVALENCY   FUNCTION
      DO 723 I=1,MM
      EQFNC(I)=ETINP(I)/DF(I)
  723 CONTINUE
C
C         COMPUTE TDT FUNCTION ,EQUIV. INPUT FOR NEXTSITE STD. VEHICLE
      WRITE(6,397)
  397 FORMAT(//2X,23HNEXT SITE   STD VEHICLE//)
C
C
      DO 724 I=1,MM
      VISIG(I)=SOUT2(I)
  724 CONTINUE
C
      CALL MODPRM(PMAX,JP,DT,VISIG,EQMASS,DF,GG)
C
C
C         COMPUTE EQUIV. INPUT NEXT SITE    VEHICLE 2
C
      DO 725 I=1,MM
      ET(I)=DF(I)*EQFNC(I)
  725 CONTINUE
C
C         COMPUTE OUTPUT FOR NEXT SITE VEHICLE 2
C
      DO 206 I=1,MM
      PP(I)=ET(I)/EQMASS
      XG(I)=GG(I)
  206 CONTINUE
C
C
```

```
      CALL ERECT2(MM,PP,XG,DT,OO)
C
C
      WRITE(6,50)
      WRITE(6,494)
  494 FORMAT(//2X,21HNEXT SITE   VEHICLE 2//)
      WRITE(6,498)
      WRITE(6,398)(ET(I),XG(I),OO(I),I=1,MM)
C
      WRITE(6,50)
      WRITE(6,2000)
 2000 FORMAT(//60X,*PREDICTED*,10X,*MEASURED*//)
      WRITE(6,1000)(OO(I),VOUT2(I),I=1,47)
 1000 FORMAT(52X,2F15.5)
C
      WRITE(6,50)
C
C
C
C
C
C
      STOP
      END
C
C
C
      SUBROUTINE NWCONV(N,V,G,O,DT)
      DIMENSION V(200),G(200),O(200)
      S=0.
      Q=0.0
C
C
      G(1)=O(1)/(V(1)*DT)
      DO 984 I=2,N
      K=I-1
      DO 985 M=1,K
      Q=Q+V(K+2-M)*G(M)
  985 CONTINUE
C
      S=Q
      G(I)=((O(I)/DT)-S)/V(1)
C
C
      Q=0.0
      S=0.0
  984 CONTINUE
      RETURN
      END
C
C
C
      SUBROUTINE ERECT2(MM,PP,XG,DT,OO)
      DIMENSION PP(800),XG(800),OO(800)
C
C
      PS2=0.0
      DO 331 I=2,MM
      K=I-1
      DO 332 M=1,K
      PS2=PP(K+1-M)*XG(M)+PS2
  332 CONTINUE
      OO(I-1)=PS2*DT
      PS2=0.0
  331 CONTINUE
      RETURN
      END
C
C
C
      SUBROUTINE EXACT (MM,DT,EQVK,EQMASS,T,GG,EQVC)
      DIMENSION T(200),GG(200)
```

```
C
C                 COMPUTING EXACT TRANSFER FUNCTION
      DO 630 I=1,MM
      T(I)=FLOAT(I)*DT
      TIME=T(I)
C
C
      BB=SQRT(EQVK/EQMASS)
      AA=EQVC/(2.*EQMASS)
C
      TRI=BB*BB-AA*AA
      IF(TRI.LT.0.0)GO TO 3
C
      GE1=1./SQRT(TRI)
      GE2=1./EXP(AA*T(I))
      G3=SIN(SQRT(TRI)*T(I))
      GG(I)=GE1*GE2*G3
C
C
      GO TO 630
C
    3 CONTINUE
      PP=SQRT(ABS(TRI))
      P1=EXP(PP*T(I))
      P2=1./(EXP(PP*T(I)))
      P3=1./EXP(AA*T(I))
      P5=(P1-P2)/2.
      GG(I)=P3*P5/PP
C
  630 CONTINUE
C
C
      RETURN
      END
C
      SUBROUTINE MODPRM(PMAX,JP,DT,VISIG,EQMASS,DF,GG)
      DIMENSION QC(100)
      DIMENSION DF(200)
      DIMENSION T(200)
      DIMENSION O(200),GG(200)
      DIMENSION V(200),G(200)
      DIMENSION IVEL(11,5)
      DIMENSION DRV1(200),DRV2(200),CPMXX(50),VISIG(200),DRV0(200)
C
C
      DO 74 I=1,JP
      DRV0(I)=VISIG(I)
      TRM1=(VISIG(I)+VISIG(I+1))/2.
      IF(I.GT.1)GO TO 744
      TRM2=VISIG(I)/2.
      GO TO 474
  744 CONTINUE
      TRM2=(VISIG(I)+VISIG(I-1))/2.
  474 CONTINUE
      DRV1(I)=(TRM1-TRM2)/DT
   74 CONTINUE
      DO 75 I=1,JP
      TRN1=(DRV1(I+1)+DRV1(I))/2.
      IF(I.GT.1)GO TO 755
      TRN2=DRV1(I)/2.
      GO TO 575
  755 CONTINUE
      TRN2=(DRV1(I)+DRV1(I-1))/2.
  575 CONTINUE
      DRV2(I)=(TRN1-TRN2)/DT
   75 CONTINUE
C
C
      BOTM=0.00000000001
C************
      DO 726 I=1,JP
      HUMP1=DRV0(I+1)-DRV0(I)
      IF(HUMP1.GE.0.0)GO TO 726
      JPP=I+6
```

```
      GO TO 727
  726 CONTINUE
  727 CONTINUE
C***********
C
      IMAXV=0
      DV1MX=0.0
      DO 315 I=1,JPP
      IF(DRV1(I).EQ.0.0)DRV1(I)=(DRV1(I+1)+DRV1(I-1))/2.
CAUTION - IS FLOATING POINT EQUALITY TO BE EXPECTED       ******************************
      IF(DRV1(I).EQ.0.0)DRV1(I)=(DRV1(I+2)+DRV1(I-2))/2.
CAUTION - IS FLOATING POINT EQUALITY TO BE EXPECTED       ******************************
      IF(ABS(DRV1(I)).LT.BOTM)DRV1(I)=(DRV1(I+1)+DRV1(I-1))/2.
      IF(ABS(DRV2(I)).LT.BOTM)DRV2(I)=(DRV2(I+1)+DRV2(I-1))/2.
      IF(DRV1(I).LT.DV1MX)GO TO 315
      DV1MX=DRV1(I)
      IMAXV=I
  315 CONTINUE
C
C
      DMAX=DRV0(1)
      DO 53 I=2,JPP
      IF(DRV0(I).LT.DMAX)GO TO 53
      DMAX=DRV0(I)
      IMAXD=I
   53 CONTINUE
C
C
      IMAXV1=IMAXV-1
      DO 57 I=2,IMAXV1
      IF(DRV2(I).LE.0.0)DRV2(I)=(DRV2(I-1)+DRV2(I+1))/2.
      IF(DRV2(I).LE.0.0)DRV2(I)=(DRV2(I-2)+DRV2(I+2))/2.
   57 CONTINUE
      IMAXVA=IMAXV+1
      DO 109 I=IMAXVA,JPP
      IF(DRV2(I).GE.0.0)DRV2(I)=(DRV2(I-1)+DRV2(I+1))/2.
      IF(DRV2(I).GE.0.0)DRV2(I)=(DRV2(I-2)+DRV2(I+2))/2.
  109 CONTINUE
      DO 107 I=1,JPP
      IF(DRV1(I+1).EQ.DRV1(I))DRV1(I+1)=(DRV1(I+2)+DRV1(I))/2.
CAUTION - IS FLOATING POINT EQUALITY TO BE EXPECTED       *****************************
      IF(DRV2(I+1).EQ.DRV2(I))DRV2(I+1)=(DRV2(I+2)+DRV2(I))/2.
CAUTION - IS FLOATING POINT EQUALITY TO BE EXPECTED       *****************************
  107 CONTINUE
C*******
      DO 789 IA=1,JPP
      DEROTS=DRV1(IA+1)/DRV1(IA)
      IF(DEROTS.GT.0.0)GO TO 789
      DZERO=DRV1(IA)-DRV1(IA+1)
      DDTZ=DRV1(IA)/DZERO
      NAFNL=IA
      GO TO 788
  789 CONTINUE
  788 CONTINUE
C**********
      DO 889 IA=1,JPP
      ZEROTS=DRV2(IA+1)/DRV2(IA)
      IF(ZEROTS.GT.0.0)GO TO 889
      TZERO=DRV2(IA)-DRV2(IA+1)
      FDTZ=DRV2(IA)/TZERO
      IAFNL=IA
      DRORNG=DRV0(IA+1)-DRV0(IA)
      ZVALU0=DRV0(IA)+FDTZ*DRORNG
      DR1RNG=DRV1(IA+1)-DRV1(IA)
      ZVALU1=DRV1(IA)+FDTZ*DR1RNG
      GO TO 888
  889 CONTINUE
  888 CONTINUE
C
C*********
C
C
      WRITE(6,99)
   99 FORMAT(/30X,*FOR SIGNATURE*/)
      WRITE(6,76)
```

```
   76 FORMAT(//1X,*      INCREMENT   DEFLECTION        VELOCITY     ACCEL
     1ERATION*/)
      WRITE(6,77)(I,DRV0(I),DRV1(I),DRV2(I),I=1,JPP)
   77 FORMAT(1X,I14,3E15.5)
   78 FORMAT(/15X,2I15/)
C******************
C********
      IDIFF=IMAXD-IMAXV
      IMAXF=0
      AA1=0.05
      ICC=0
C*********
      DO 104 ILP=1,40
C*******
      EQKA=AA1*PMAX/DMAX
      AA3=-0.91
C***
      DO 103 JJ=1,20
      IT=IMAXV
      EQMA=AA3*PMAX/DRV2(IMAXD)
      CPMAX=0.0
      AA2=AA1+AA3
      IF(AA2.LT.0.0)GO TO 1021
C****
      IMAXC=IMAXD
      IT=IT+1
      DO 102 II=IT,IMAXC
      EQCA=EQMA*DRV2(II)/DRV1(II)
      EQCA=-EQCA
C
C
      EQVK=EQKA
      EQMASS=EQMA
      EQVC=EQCA
      MM=JPP
      CALL EXACT1(MM,DT,EQVK,EQMASS,T,GG,EQVC)
C
C
C
      DO 73 I=1,JPP
      D(I)=DRV0(I)
      V(I)=GG(I)
   73 CONTINUE
C
      N=JPP
      CALL NWCONV(N,V,G,D,DT)
C
      DO 508 MP=1,JPP
      DF(MP)=G(MP)*EQMASS
  508 CONTINUE
      DO 509 MA=1,JPP
      DF(MA)=(DF(MA)+DF(MA+1))/2.
  509 CONTINUE
C
C
      CPMAX=0.
      DO 501 M=1,JPP
      DF(M)=(DF(M)+DF(M+1))/2.
      IF(DF(M).GT.CPMAX)GO TO 20
      GO TO 502
   20 CPMAX=DF(M)
      ICF=M
  502 CONTINUE
  501 CONTINUE
C
      ERFCE=CPMAX-PMAX
      ABERFG=ABS(ERFCE)
      IF(ABERFG.GT.500.0)GO TO 102
C
      ICC=ICC+1
C
      DFRNG=DF(IAFNL+1)-DF(IAFNL)
      ZVALUF=DF(IAFNL)+FDTZ*DFRNG
      CMAXV=(ZVALUF-EQKA*ZVALU0)/ZVALU1
      CDIFFR=(CMAXV-EQCA)/CMAXV
```

```
      ABCD=CDIFFR
      QC(ICC)=CDIFFR
      IF(ICC.EQ.1)GO TO 102
      CRATIO=QC(ICC)/QC(ICC-1)
      IF(CRATIO.GT.0.0)GO TO 102
C
C
C
      FCHK=EQKA*DRV0(II)
      DIFCHK=FCHK-DF(II)
      DFCHKR=DIFCHK/FCHK
      FPFRAC=DF(II)/PMAX
      ICDPT=II
      IBBB=IMAXD-ICDPT
      BB1=FLOAT(IBBB/IDIFF)
      TRMM=EQMA*DRV2(II)
      TRMC=EQCA*DRV1(II)
      TRMK=EQKA*DRV0(II)
      CPMXX(II)=TRMM+TRMC+TRMK
      WRITE(6,847)
  847 FORMAT(//10X,*GOOD RUN*//)
      GO TO 846
  102 CONTINUE
 1021 CONTINUE
      AA3=AA3+0.045
C************
  103 CONTINUE
      AA1=AA1+0.025
  104 CONTINUE
 1000 FORMAT(/1X,*000*)
  844 FORMAT(1X,7F10.2,3E15.5)
  845 FORMAT(6F15.4,10X,2I5,F10.3)
C*****************
C
      WRITE(6,1002)
 1002 FORMAT(/10X,*OUTER LOOP COMPLETED*/)
      GO TO 94
C
C
  846 CONTINUE
C
      WRITE(6,1000)
C********
      AFRNG=DF(NAFNL+1)-DF(NAFNL)
      DVALUF=DF(NAFNL)+DDTZ*AFRNG
C*****
      ZVALUR=ZVALUF/PMAX
C******
      DVALZD=DVALUF/PMAX
C*****
      FDRTIO=ABERFG/PMAX
C********
      DENOM=FLOAT(IMAXD)
      DENOM1=1.
      TCRSPT=FLOAT(II)/DENOM
      TZROA=FLOAT(IAFNL)/DENOM
C*******
 1199 FORMAT(/10X,11F11.3/)
 1001 FORMAT(10X,I5,7F15.5)
      CALL EXACT1(JP,DT,EQKA,EQMA,T,GG,EQCA)
      DO 733 I=1,JP
      O(I)=DRV0(I)
      V(I)=GG(I)
  733 CONTINUE
      N=JP
      CALL NWCONV(N,V,G,O,DT)
      DO 518 MP=1,JP
      DF(MP)=G(MP)*EQMA
  518 CONTINUE

C
   94 CONTINUE
      RETURN
      END
```

SITE ONE   STD VEHICLE

FOR SIGNATURE

INCREMENT	DEFLECTION	VELOCITY	ACCELERATION
1	1.27667E-04	1.92708E-03	9.93490E-03
2	1.54167E-04	7.94792E-04	8.31380E-03
3	1.91250E-04	1.03125E-03	6.69271E-03
4	2.36667E-04	1.33021E-03	1.03906E-02
5	2.97667E-04	1.86250E-03	1.57552E-02
6	3.85667E-04	2.59063E-03	2.10677E-02
7	5.04917E-04	3.54792E-03	2.91276E-02
8	6.69500E-04	4.92083E-03	3.62500E-02
9	8.98583E-04	6.44792E-03	4.09245E-02
10	1.18533E-03	8.19479E-03	4.38151E-02
11	1.55417E-03	9.95312E-03	3.51432E-02
12	1.98158E-03	1.10062E-02	9.81771E-03
13	2.43467E-03	1.07385E-02	-3.29948E-02
14	2.84067E-03	8.36667E-03	-8.32943E-02
15	3.10400E-03	4.07500E-03	-1.15703E-01
16	3.16667E-03	-8.89583E-04	-1.14401E-01
17	3.03283E-03	-5.07708E-03	-8.50130E-02
18	2.76050E-03	-7.69062E-03	-4.40234E-02
19	2.41758E-03	-8.59896E-03	-4.75260E-03
20	2.07258E-03	-8.07083E-03	-9.53125E-03
21	1.77192E-03	-6.89896E-03	7.39583E-03
22	1.52067E-03	-5.80104E-03	2.50000E-03

GOOD RUN

00

SITE ONE   VEHICLE 2

EQUIV INPUT IN LBS	TDT FUNCTION	RESPONSE IN FT
7.26622E+03	2.30853E-02	2.02000E-04
9.67190E+02	2.76124E-02	2.68500E-04
3.38946E+03	2.56125E-02	3.50500E-04
6.28019E+03	2.17664E-02	5.07583E-04
1.20998E+04	1.78084E-02	8.30917E-04
2.26201E+04	1.43096E-02	1.45967E-03
3.73522E+04	1.13959E-02	2.51742E-03
5.36091E+04	9.03463E-03	4.03258E-03
6.66077E+04	7.14611E-03	5.86650E-03
5.49146E+04	5.64567E-03	7.24833E-03
-4.40640E+03	4.45756E-03	6.66300E-03
-1.88870E+04	3.51838E-03	5.11650E-03
1.76576E+04	2.77663E-03	4.47067E-03
4.69750E+04	2.19108E-03	5.00992E-03
8.37103E+04	1.72893E-03	6.88358E-03
6.44724E+04	1.36424E-03	8.41667E-03
-1.57651E+04	1.07645E-03	7.41800E-03
-2.57654E+04	8.49373E-04	5.45308E-03
-5.79904E+03	6.70194E-04	3.97867E-03
-1.63126E+03	5.28813E-04	2.96208E-03
1.61962E+03	4.17257E-04	2.31008E-03
4.38986E+03	3.29234E-04	1.93375E-03
4.45170E+03	2.59780E-04	1.69475E-03

5.24889E+03	2.04977E-04	1.55192E-03
5.77634E+03	1.61736E-04	1.47250E-03
4.82121E+03	1.27617E-04	1.39683E-03
5.39067E+03	1.00695E-04	1.34767E-03
6.05333E+03	7.94527E-05	1.33158E-03
4.47763E+03	6.26916E-05	1.28433E-03
4.63410E+03	4.94664E-05	1.23733E-03
5.15415E+03	3.90311E-05	1.21075E-03
5.09242E+03	3.07972E-05	1.19233E-03
3.93199E+03	2.43003E-05	1.14658E-03
5.04313E+03	1.91740E-05	1.12867E-03
5.26145E+03	1.51291E-05	1.12800E-03
4.01299E+03	1.19375E-05	1.09825E-03
4.74872E+03	9.41922E-06	1.08333E-03
6.32678E+03	7.43217E-06	1.11892E-03
2.59107E+03	5.86430E-06	1.06242E-03
5.12136E+03	4.62719E-06	1.05375E-03
5.51294E+03	3.65105E-06	1.07242E-03
4.25295E+03	2.88083E-06	1.06250E-03
4.31075E+03	2.27310E-06	1.04625E-03
5.95350E+03	1.79358E-06	1.07567E-03
4.67396E+03	1.41521E-06	1.08050E-03
3.94255E+03	1.11666E-06	1.05650E-03
4.68328E+03	8.81093E-07	1.04683E-03

NEXT SITE STD VEHICLE

FOR SIGNATURE

INCREMENT	DEFLECTION	VELOCITY	ACCELERATION
1	9.95833E-05	1.52187E-03	7.77344E-03
2	1.21750E-04	6.21875E-04	6.71224E-03
3	1.49333E-04	8.09375E-04	5.65104E-03
4	1.86500E-04	1.07396E-03	6.19792E-03
5	2.35250E-04	1.30521E-03	5.92448E-03
6	2.90917E-04	1.54792E-03	7.12240E-03
7	3.59083E-04	1.87500E-03	8.54167E-03
8	4.40917E-04	2.23125E-03	9.60937E-03
9	5.37583E-04	2.64375E-03	1.25000E-02
10	6.52417E-04	3.23125E-03	1.47917E-02
11	7.96083E-04	3.82708E-03	1.32161E-02
12	9.58583E-04	4.28854E-03	7.79948E-03
13	1.13917E-03	4.45104E-03	-6.17187E-03
14	1.31467E-03	3.79479E-03	-2.66797E-02
15	1.44275E-03	2.31667E-03	-4.29948E-02
16	1.50000E-03	3.55208E-04	-4.88021E-02
17	1.47117E-03	-1.58750E-03	-3.80990E-02
18	1.37300E-03	-2.69271E-03	-1.61849E-02
19	1.25575E-03	-2.88229E-03	-1.82292E-03
20	1.14242E-03	-2.83854E-03	-5.88542E-03
21	1.02867E-03	-2.75000E-03	-7.35677E-04
22	9.22417E-04	-2.56146E-03	-7.16146E-04

GOOD RUN

00

NEXT SITE VEHICLE 2

EQUIV INPUT IN LBS	TDT FUNCTION	RESPONSE IN FT
2.39378E+04	2.79870E-02	1.57565E-04
-5.99763E+04	4.02600E-02	-1.68119E-04
6.45929E+03	4.45935E-02	-2.74326E-04
1.36858E+04	4.49856E-02	-2.24518E-04
2.55768E+04	4.34868E-02	-2.40447E-05
3.73268E+04	4.11442E-02	3.17975E-04
5.95647E+04	3.84877E-02	8.60932E-04
7.51046E+04	3.57813E-02	1.58148E-03
8.03293E+04	3.31525E-02	2.39395E-03
6.33737E+04	3.06592E-02	3.10814E-03
-4.96779E+03	2.83238E-02	3.29894E-03
-1.96412E+04	2.61510E-02	3.13688E-03
1.84098E+04	2.41370E-02	3.06340E-03
4.64276E+04	2.22741E-02	3.21925E-03
6.79205E+04	2.05529E-02	3.61990E-03
3.74124E+04	1.89636E-02	3.92125E-03
-3.11110E+01	1.74966E-02	3.91757E-03
2.12723E+04	1.61429E-02	3.90907E-03
5.20213E+03	1.48937E-02	3.79282E-03
1.06867E+03	1.37411E-02	3.60242E-03
-1.67619E+03	1.26777E-02	3.36579E-03
-3.75658E+03	1.16966E-02	3.10234E-03
-4.38155E+03	1.07913E-02	2.83187E-03
-6.42824E+03	9.95617E-03	2.55472E-03
-9.40418E+03	9.18563E-03	2.26518E-03
-6.84531E+03	8.47472E-03	1.99745E-03
-6.04811E+03	7.81883E-03	1.75536E-03
-7.78484E+03	7.21371E-03	1.52313E-03
-4.78390E+03	6.65541E-03	1.32403E-03
-2.34767E+03	6.14033E-03	1.16421E-03
-3.53550E+03	5.66511E-03	1.02124E-03
-8.24185E+02	5.22666E-03	9.09508E-04
3.66539E+03	4.82215E-03	8.46376E-04
5.42162E+03	4.44895E-03	8.20303E-04
-7.56887E+03	4.10463E-03	7.27339E-04
7.55546E+03	3.78696E-03	7.05572E-04
1.67329E+03	3.49387E-03	6.79791E-04
4.12036E+03	3.22347E-03	6.69173E-04
2.13777E+03	2.97399E-03	6.53120E-04
1.94469E+03	2.74383E-03	6.33810E-04
3.01993E+03	2.53147E-03	6.20752E-04
6.73974E+03	2.33555E-03	6.35642E-04
2.83888E+03	2.15480E-03	6.37603E-04
4.24396E+03	1.98803E-03	6.42583E-04
3.23174E+03	1.83417E-03	6.42152E-04
6.86666E+03	1.69222E-03	6.63086E-04
2.46450E+03	1.56125E-03	0

PREDICTED	MEASURED
.00016	.00018
-.00017	.00028
-.00027	.00044
-.00022	.00068
-.00002	.00107
.00032	.00165
.00086	.00252
.00158	.00357
.00239	.00404
.00311	.00367
.00330	.00318

.00314	.00289
.00306	.00284
.00322	.00314
.00362	.00382
.00392	.00433
.00392	.00399
.00391	.00320
.00379	.00244
.00360	.00178
.00337	.00128
.00310	.00091
.00283	.00067
.00255	.00051
.00227	.00041
.00200	.00035
.00176	.00032
.00152	.00029
.00132	.00027
.00116	.00025
.00102	.00014
.00091	.00012
.00085	.00012
.00082	.00012
.00073	.00012
.00071	.00012
.00068	.00011
.00067	.00012
.00065	.00011
.00063	.00011
.00062	.00011
.00064	.00011
.00064	.00011
.00064	.00011
.00064	.00011
.00066	.00011
0	.00011

APPENDIX D

DATA DIGITIZED

FROM LIGHT

SENSITIVE PAPER

The data listing has the following format

Card 1 - A comment card giving the base name, site number, grid location of measurement point, Load Cart data of test, distance from closest measurement gage to edge of tire track in inches, time increment at which data was digitized and estimated number of cards.

Card 2 - Distance (ft) of measurement point from edge of tire print where Gage 1 is the closest.

Card 3 - Number of cards actually read, time increment used, and weight of load cart (25 kips).

Card 4 to (n-1) - Data digitized and listed (from left to right) as, Gage 1, Gage 2, Gage 3, Gage 4, and Gage 5.

Card n (last card) - Calibration data for Gages 1 to 5 also listed from from left (Gage 1) to right (Gage 5).

[illegible] [illegible]IN SITE 1 LOC A-1 LD. CT. 3.11.76 7.25 .2 48

[illegible] .9375 1.6875 2.6875 3.6875

48 .200 25000.0

0027	0045	0071	0102	0134
0030	0048	0074	0106	0134
0034	0051	0078	0110	0136
0040	0058	0085	0117	0137
0049	0065	0094	0126	0141
0061	0078	0107	0138	0145
0077	0092	0122	0154	0151
0103	0115	0146	0175	0158
0130	0141	0172	0198	0165
0167	0174	0203	0223	0173
0210	0211	0234	0247	0181
0259	0254	0272	0277	0190
0307	0297	0306	0301	0195
0360	0340	0340	0324	0200
0414	0382	0371	0344	0206
0456	0420	0394	0358	0208
0487	0447	0411	0366	0209
0490	0456	0415	0367	0209
0483	0459	0419	0371	0209
0461	0451	0418	0375	0213
0427	0429	0403	0367	0212
0393	0402	0385	0354	0209
0359	0374	0363	0338	0204
0331	0349	0344	0324	0202
0302	0324	0320	0305	0194
0277	0301	0299	0288	0189
0248	0273	0273	0267	0182
0225	0250	0249	0247	0175
0198	0223	0223	0222	0167
0171	0196	0196	0196	0156
0141	0163	0163	0167	0147
0115	0137	0137	0143	0140
0096	0117	0117	0126	0136
0085	0105	0104	0117	0134
0076	0095	0095	0109	0133
0071	0089	0089	0103	0131
0067	0084	0084	0099	0131
0064	0080	0080	0096	0130
0060	0078	0078	0094	0129
0058	0074	0074	0092	0128
0057	0073	0073	0091	0128
0055	0072	0072	0090	0128
0055	0071	0072	0090	0128
0053	0070	0070	0089	0127
0053	0069	0069	0088	0128
0053	0069	0069	0087	0127
0051	0069	0069	0087	0128
0051	0069	0069	0087	0127

.00008065 .00006995 .00004052 .00002212 .00002778

C EGLIN SITE 1 LOC A-1 LD. CT. 3.11.76 7.00 53
.58333 .91666 1.83333 2.83333 3.83333
53 .200 25000.0

0023	0052	0075	0107	0137
0028	0057	0079	0108	0135
0034	0067	0090	0117	0136
0042	0077	0102	0127	0139
0052	0088	0115	0140	0143
0065	0104	0130	0156	0149
0080	0121	0150	0173	0153
0096	0138	0167	0189	0158
0113	0158	0185	0203	0164
0135	0180	0208	0222	0169
0160	0206	0229	0241	0174
0184	0231	0251	0259	0179
0211	0256	0271	0272	0183
0249	0292	0299	0291	0188
0288	0325	0321	0305	0191
0325	0357	0342	0316	0193
0364	0388	0359	0326	0195
0401	0414	0375	0333	0196
0433	0436	0388	0339	0198
0453	0447	0393	0340	0197
0473	0456	0400	0343	0197
0484	0460	0402	0342	0197
0488	0461	0402	0343	0198
0489	0461	0402	0344	0199
0487	0458	0403	0346	0201
0484	0453	0402	0346	0202
0475	0446	0397	0344	0202
0458	0430	0384	0334	0201
0437	0411	0370	0323	0198
0412	0389	0351	0308	0192
0386	0367	0331	0292	0187
0360	0344	0309	0273	0182
0330	0316	0284	0254	0176
0296	0288	0257	0232	0170
0267	0260	0232	0212	0164
0237	0233	0207	0192	0159
0213	0211	0187	0175	0154
0191	0191	0167	0159	0149
0168	0173	0149	0143	0144
0148	0154	0131	0127	0141
0129	0138	0115	0114	0136
0113	0123	0100	0101	0134
0100	0112	0089	0094	0131
0089	0102	0080	0086	0131
0081	0093	0073	0079	0127
0070	0085	0064	0072	0126
0062	0078	0059	0067	0125
0056	0073	0054	0064	0125
0051	0069	0051	0063	0124
0049	0066	0048	0059	0124
0048	0064	0047	0058	0123
0044	0063	0044	0057	0122
0042	0061	0043	0056	0121

.00008065 .00006995 .00004052 .00002212 .00002778

C EGLIN SITE 1 LOC A-2 LD. CT. 3.11.76 5.50 .2 38

.45833 .79167 1.70833 2.70833 3.70833

38 .200 25000.0

0042	0070	0100	0131	0148
0043	0070	0100	0132	0148
0044	0071	0101	0135	0149
0045	0072	0103	0138	0151
0046	0074	0106	0144	0153
0050	0077	0111	0155	0156
0054	0082	0116	0168	0162
0065	0092	0129	0193	0171
0083	0110	0149	0230	0183
0107	0131	0172	0273	0198
0138	0158	0199	0318	0211
0182	0197	0231	0366	0226
0245	0249	0269	0418	0238
0301	0293	0298	0451	0245
0318	0316	0311	0476	0255
0286	0301	0307	0480	0262
0238	0263	0281	0446	0254
0195	0225	0250	0395	0239
0160	0190	0218	0342	0222
0132	0161	0189	0290	0205
0111	0140	0167	0249	0192
0095	0124	0149	0216	0180
0086	0113	0137	0193	0173
0079	0105	0129	0178	0167
0074	0100	0123	0166	0163
0071	0097	0119	0158	0161
0069	0094	0116	0155	0159
0067	0092	0116	0151	0158
0066	0091	0114	0150	0157
0065	0090	0113	0148	0157
0065	0090	0113	0149	0158
0064	0089	0112	0148	0157
0063	0089	0113	0148	0158
0063	0088	0112	0148	0158
0061	0088	0112	0148	0158
0061	0088	0112	0148	0158
0061	0087	0111	0148	0158
0061	0087	0112	0149	[illegible]

.0001613 .0001399 [illegible] .00002212 .00002778

C EGLIN SITE 1 LOC A-2 LD. CT. 3.11.76 7.00 .2 45
.58333 .91666 1.83333 2.83333 3.83333
45 .200 25000.0

0026	0054	0083	0120	0145
0026	0055	0085	0124	0147
0027	0057	0088	0131	0150
0030	0059	0091	0139	0153
0032	0062	0096	0148	0156
0035	0067	0101	0159	0160
0041	0074	0109	0175	0166
0050	0084	0121	0198	0175
0062	0099	0137	0227	0185
0079	0116	0155	0261	0197
0099	0138	0175	0294	0207
0123	0160	0194	0323	0216
0153	0187	0214	0349	0222
0187	0217	0233	0374	0226
0223	0244	0249	0390	0228
0255	0266	0261	0403	0230
0277	0279	0270	0412	0230
0286	0280	0273	0415	0231
0281	0275	0273	0418	0232
0265	0261	0262	0403	0227
0237	0237	0245	0377	0218
0211	0215	0228	0351	0211
0181	0189	0205	0317	0200
0156	0167	0187	0287	0190
0134	0147	0169	0256	0180
0114	0129	0151	0225	0171
0097	0114	0137	0199	0163
0082	0101	0123	0176	0157
0073	0093	0114	0163	0153
0067	0086	0108	0152	0150
0060	0081	0102	0140	0146
0056	0076	0098	0133	0143
0050	0072	0094	0127	0142
0048	0070	0091	0122	0141
0045	0068	0089	0120	0141
0045	0067	0088	0118	0140
0043	0066	0087	0117	0139
0042	0064	0087	0116	0139
0041	0064	0086	0115	0139
0040	0062	0085	0115	0139
0038	0062	0084	0112	0138
0037	0060	0083	0110	0138
0036	0059	0082	0108	0138
0034	0058	0081	0107	0138
0034	0058	0081	0107	0138

.0001613 .0001399 .00008104 .00002212 .00002778

C EGLIN SITE 1 LOC A-3 LD. CT. 3.11.76 4.00 .2 37
.33333 .66666 1.58333 2.583333 3.583333
37 .200 25000.0

0048	0071	0094	0131	0148
0049	0071	0094	0131	0148
0050	0071	0095	0135	0149
0050	0073	0097	0137	0151
0052	0074	0099	0141	0152
0054	0075	0101	0149	0155
0058	0079	0105	0158	0161
0064	0082	0110	0172	0167
0072	0088	0118	0188	0173
0080	0098	0127	0202	0178
0092	0111	0139	0220	0182
0109	0125	0152	0242	0188
0146	0159	0182	0287	0202
0193	0197	0214	0330	0212
0261	0250	0252	0382	0223
0326	0298	0281	0414	0230
0366	0329	0297	0435	0235
0357	0333	0300	0446	0240
0312	0305	0282	0424	0234
0263	0268	0256	0386	0225
0220	0230	0226	0340	0211
0187	0198	0198	0298	0198
0157	0170	0170	0250	0183
0131	0143	0143	0204	0168
0116	0127	0126	0174	0158
0105	0116	0115	0152	0150
0098	0108	0108	0137	0145
0093	0102	0102	0128	0142
0091	0099	0099	0120	0139
0087	0096	0096	0116	0137
0085	0094	0094	0114	0136
0084	0093	0093	0110	0135
0083	0093	0093	0109	0135
0083	0092	0092	0109	0135
0082	0091	0091	0107	0134
0081	0091	0091	0107	0133
0081	0089	0089	0105	0133

.0001613 .0001399 .00008104 .0000221? .00002778

```
C   EGLIN     SITE 1    LOC A-3   LD. CT.   3.11.76   4.50 .2   45
    .375      .708     1.625     2.625     3.625
  45      .200 25000.0
0030  0049  0081  0100  0140
0029  0049  0081  0102  0140
0030  0049  0081  0103  0140
0030  0051  0083  0106  0142
0031  0052  0085  0111  0143
0034  0055  0088  0117  0145
0037  0058  0092  0126  0149
0040  0064  0098  0137  0152
0047  0070  0105  0151  0157
0054  0078  0114  0168  0163
0064  0089  0125  0188  0169
0079  0105  0140  0212  0176
0097  0123  0157  0242  0186
0120  0144  0176  0270  0193
0149  0170  0194  0293  0198
0186  0203  0215  0320  0204
0232  0239  0238  0349  0211
0278  0271  0255  0367  0214
0322  0298  0268  0378  0215
0345  0308  0272  0378  0214
0349  0308  0272  0378  0215
0334  0295  0265  0368  0211
0303  0269  0248  0339  0203
0270  0242  0227  0312  0196
0234  0211  0200  0271  0185
0203  0184  0176  0234  0174
0173  0159  0154  0199  0165
0153  0141  0138  0175  0159
0136  0126  0126  0153  0150
0124  0116  0115  0138  0147
0113  0108  0108  0126  0143
0105  0099  0101  0113  0139
0098  0094  0093  0102  0134
0092  0089  0088  0093  0131
0088  0086  0085  0086  0129
0083  0083  0082  0079  0126
0080  0080  0080  0074  0124
0079  0079  0079  0073  0124
0077  0077  0077  0070  0124
0075  0075  0075  0066  0121
0073  0073  0073  0063  0121
0072  0072  0072  0060  0119
0072  0072  0072  0060  0119
0070  0070  0070  0058  0118
0068  0069  0069  0056  0117
 .0001613   .0001399   .00008104   .00002212   .00002778
```

C   EGLIN   SITE 1   LOC A-4   LD. CT.   3.11.76   5.00 .2   53
.41667   .75   1.66667   2.66667   3.66667
53   .200 25000.0

0042	0069	0099	0134	0155
0045	0071	0101	0139	0157
0046	0074	0104	0147	0160
0048	0075	0107	0153	0163
0050	0078	0110	0160	0166
0053	0082	0114	0168	0169
0056	0086	0119	0178	0174
0061	0091	0125	0190	0178
0068	0098	0133	0205	0183
0076	0106	0143	0224	0190
0083	0116	0153	0240	0197
0093	0125	0164	0258	0203
0102	0135	0174	0275	0209
0115	0149	0188	0298	0215
0128	0163	0201	0315	0221
0148	0182	0217	0338	0227
0169	0203	0234	0361	0232
0195	0226	0252	0385	0238
0224	0252	0271	0409	0243
0255	0275	0287	0427	0247
0287	0299	0304	0444	0250
0317	0318	0316	0457	0252
0335	0329	0322	0463	0252
0341	0330	0322	0462	0251
0338	0326	0321	0462	0252
0323	0313	0310	0445	0249
0304	0295	0295	0426	0244
0281	0274	0277	0400	0236
0251	0248	0255	0368	0228
0225	0227	0238	0341	0221
0207	0212	0222	0317	0212
0189	0196	0207	0293	0205
0173	0181	0192	0269	0198
0158	0169	0180	0247	0191
0146	0157	0168	0227	0184
0137	0148	0158	0211	0178
0128	0141	0150	0196	0172
0121	0135	0144	0184	0169
0116	0130	0138	0174	0165
0111	0126	0134	0167	0164
0108	0124	0131	0162	0161
0107	0120	0128	0157	0158
0104	0119	0126	0152	0158
0102	0117	0124	0149	0156
0100	0116	0122	0146	0155
0099	0115	0121	0144	0155
0098	0114	0120	0142	0153
0097	0113	0119	0140	0153
0096	0112	0119	0139	0152
0095	0111	0119	0138	0151
0095	0111	0118	0137	0151
0095	0111	0118	0137	0151
0094	0110	0117	0136	0152

.0001613   .0001399   .00008104   .00002212   .00002778

```
C   EGLIN     SITE 1    LOC A-5   LD. CT.   3:11.76   5.00 .2   43
     .41667    .75       1.66667   2.66667   3.66667
   43     .200 25000.0
0036  0059  0083  0123  0141
0037  0061  0086  0128  0143
0040  0065  0090  0138  0147
0042  0068  0094  0148  0150
0045  0072  0100  0159  0157
0052  0079  0107  0174  0162
0057  0085  0114  0185  0166
0065  0093  0124  0202  0173
0074  0105  0136  0221  0180
0087  0118  0150  0244  0187
0104  0139  0168  0269  0196
0129  0161  0188  0294  0202
0161  0190  0210  0321  0209
0196  0220  0233  0344  0215
0233  0247  0251  0363  0219
0262  0266  0261  0370  0221
0279  0275  0264  0372  0219
0290  0279  0269  0376  0220
0286  0275  0268  0381  0223
0275  0265  0264  0381  0227
0252  0246  0248  0358  0219
0225  0225  0223  0328  0209
0198  0198  0204  0296  0198
0172  0174  0181  0261  0187
0149  0155  0162  0230  0179
0132  0138  0146  0202  0169
0116  0124  0131  0180  0162
0106  0115  0123  0166  0157
0098  0107  0114  0152  0152
0091  0101  0108  0143  0149
0084  0095  0103  0133  0145
0078  0090  0098  0123  0143
0073  0086  0093  0117  0139
0071  0082  0090  0110  0137
0066  0079  0087  0104  0135
0063  0077  0084  0099  0132
0062  0076  0083  0096  0132
0060  0074  0081  0093  0131
0059  0074  0081  0093  0132
0059  0073  0080  0092  0131
0059  0073  0080  0091  0131
0058  0073  0080  0091  0130
0058  0072  0080  0090  0130
 .0001613    .0001399    .00008104    .00002212    .00002778
```

```
C   EGLIN      SITE 1    LOC A-5   LD. CT.   3.11.76   6.00 .2   35
     .5          .83333   1.75       2.75        3.75
   35      .200 25000.0
0070  0082  0094  0122  0140
0071  0084  0096  0126  0142
0073  0086  0099  0132  0144
0075  0088  0101  0138  0147
0078  0092  0106  0148  0152
0084  0097  0112  0159  0156
0091  0104  0120  0176  0163
0104  0115  0132  0197  0171
0122  0132  0150  0227  0181
0142  0149  0167  0251  0188
0175  0179  0195  0293  0200
0209  0208  0217  0320  0208
0257  0250  0250  0359  0219
0294  0277  0266  0372  0218
0313  0296  0276  0380  0222
0305  0298  0279  0387  0226
0273  0275  0261  0365  0221
0238  0247  0240  0337  0213
0201  0214  0212  0298  0203
0176  0188  0188  0265  0191
0152  0165  0165  0226  0180
0135  0147  0147  0197  0169
0122  0132  0132  0171  0161
0113  0122  0122  0154  0154
0106  0114  0116  0142  0150
0103  0110  0110  0132  0147
0099  0109  0105  0125  0144
0096  0105  0102  0120  0142
0096  0103  0100  0116  0139
0094  0103  0100  0115  0140
0093  0102  0099  0113  0139
0092  0101  0098  0111  0138
0092  0100  0097  0111  0138
0091  0100  0096  0109  0137
0090  0099  0097  0110  0137
 .0001613    .0001399    .00008104    .00002212    .00002778
```

C EGLIN SITE 1 LOC C-1 LD.CT. 3.10.76 7.0 .2 40
.58333 .91667 1.83333 2.83333 3.83333
40 .200 25000.0

0018	0037	0054	0067	0102
0019	0037	0055	0069	0103
0020	0038	0056	0071	0103
0021	0040	0059	0075	0103
0024	0043	0060	0080	0103
0026	0045	0063	0085	0104
0029	0048	0068	0095	0103
0033	0053	0073	0104	0104
0039	0058	0079	0117	0105
0047	0065	0087	0132	0107
0059	0074	0096	0150	0111
0075	0085	0109	0170	0117
0097	0098	0123	0194	0124
0121	0113	0137	0216	0129
0149	0128	0153	0240	0153
0184	0145	0167	0258	0142
0222	0165	0183	0279	0145
0249	0183	0194	0289	0146
0263	0194	0201	0294	0146
0260	0196	0202	0295	0147
0250	0194	0202	0296	0148
0227	0183	0195	0287	0150
0202	0169	0183	0271	0147
0171	0149	0164	0242	0139
0144	0132	0148	0215	0131
0117	0113	0128	0182	0122
0096	0099	0113	0157	0116
0079	0083	0097	0128	0110
0064	0070	0083	0104	0105
0054	0060	0073	0085	0104
0046	0054	0065	0071	0104
0042	0048	0060	0061	0104
0038	0044	0055	0053	0104
0035	0042	0052	0047	0103
0035	0040	0050	0043	0103
0034	0039	0050	0042	0103
0034	0039	0050	0040	0103
0034	0039	0049	0040	0103
0034	0039	0049	0039	0103
0034	0038	0048	0038	0103

.0001613 .0001399 .00008104 .00002212 .00002778

```
C   EGLIN      SITE 1    LOC C-1   LD.CT.     3.10.76   7.0  .2   54
     .58333     .91667   1.83333   2.83333   3.83333
   54      .200 25000.0
0036  0055  0076  0095  0120
0037  0056  0077  0098  0120
0038  0057  0080  0101  0120
0039  0059  0081  0104  0121
0042  0061  0084  0108  0123
0044  0064  0087  0116  0124
0046  0067  0091  0121  0126
0049  0070  0095  0127  0127
0052  0075  0099  0134  0129
0057  0080  0105  0143  0132
0062  0084  0109  0150  0133
0070  0091  0115  0160  0136
0076  0098  0123  0170  0138
0087  0106  0131  0183  0142
0098  0114  0140  0195  0145
0112  0126  0150  0210  0149
0129  0137  0161  0226  0153
0148  0150  0170  0239  0155
0171  0164  0183  0255  0161
0196  0178  0193  0267  0162
0225  0191  0204  0284  0167
0251  0200  0211  0293  0170
0277  0211  0219  0304  0174
0291  0216  0222  0310  0177
0299  0217  0224  0314  0179
0299  0215  0226  0323  0184
0291  0207  0222  0319  0186
0276  0195  0213  0308  0185
0256  0181  0201  0293  0183
0235  0171  0191  0277  0181
0213  0159  0179  0258  0176
0191  0147  0168  0238  0171
0170  0134  0154  0215  0164
0152  0123  0141  0195  0157
0138  0113  0132  0179  0151
0127  0106  0122  0163  0146
0119  0098  0115  0148  0140
0112  0094  0108  0138  0137
0108  0090  0104  0128  0132
0104  0086  0099  0120  0130
0100  0083  0097  0114  0127
0097  0080  0093  0107  0125
0095  0079  0091  0102  0123
0093  0077  0088  0094  0121
0092  0075  0086  0092  0119
0090  0074  0085  0087  0118
0089  0073  0084  0084  0117
0089  0071  0083  0083  0116
0087  0071  0082  0081  0115
0087  0070  0081  0079  0114
0086  0070  0080  0077  0114
0085  0070  0080  0077  0113
0085  0069  0079  0074  0114
0084  0069  0078  0074  0113
 .0001613    .0001399    .00008104    .00002212    .00002778
```

C EGLIN SITE 1 LOC C-2 LD.CT. 3.10.76 4.5 .2 56
.375 .708 1.625 2.625 3.625
56 .200 25000.0

0035	0054	0074	0101	0117
0037	0055	0075	0103	0118
0038	0057	0078	0108	0119
0039	0059	0079	0113	0120
0041	0062	0083	0119	0121
0044	0065	0087	0127	0124
0047	0070	0093	0140	0127
0052	0076	0099	0151	0130
0056	0082	0107	0164	0133
0062	0087	0113	0179	0138
0068	0095	0122	0192	0142
0074	0102	0130	0208	0146
0082	0110	0139	0222	0150
0088	0119	0148	0240	0154
0096	0127	0157	0256	0157
0106	0137	0168	0275	0162
0114	0147	0178	0290	0167
0123	0155	0187	0305	0169
0133	0166	0197	0321	0173
0145	0178	0208	0337	0176
0160	0191	0220	0352	0178
0176	0206	0232	0368	0180
0191	0218	0241	0380	0180
0208	0230	0251	0390	0180
0225	0242	0261	0402	0180
0239	0251	0267	0409	0179
0247	0256	0271	0412	0178
0250	0256	0272	0412	0174
0250	0255	0273	0415	0174
0246	0251	0272	0415	0174
0236	0243	0264	0403	0171
0226	0233	0256	0390	0166
0212	0220	0244	0367	0158
0196	0206	0229	0343	0150
0179	0190	0211	0312	0141
0164	0176	0196	0281	0132
0150	0162	0180	0251	0124
0138	0149	0166	0225	0117
0129	0140	0156	0206	0114
0121	0133	0147	0188	0110
0115	0127	0140	0176	0110
0110	0122	0133	0165	0108
0105	0117	0129	0156	0108
0100	0113	0124	0147	0107
0098	0110	0121	0140	0106
0094	0108	0116	0133	0106
0091	0104	0113	0128	0105
0089	0102	0110	0122	0106
0086	0100	0109	0118	0106
0085	0098	0107	0115	0106
0082	0096	0104	0111	0107
0081	0095	0103	0108	0105
0081	0094	0102	0106	0105
0079	0093	0101	0105	0102
0079	0092	0100	0103	0102
0079	0092	0099	0102	0104

.0001613 .0001399 .00008104 .00002212 .00002778

C EGLIN SITE 1 LOC C-2 LD.CT. 3.10.76 4.5 .2 53

.375 .708 1.625 2.625 3.625

53 .200 25000.0

0017	0030	0043	0068	0106
0019	0031	0044	0070	0106
0019	0032	0045	0072	0105
0020	0033	0046	0075	0105
0022	0034	0048	0079	0105
0024	0036	0050	0082	0105
0025	0038	0052	0088	0106
0028	0041	0056	0094	0106
0032	0045	0060	0102	0106
0035	0050	0065	0113	0106
0041	0054	0070	0125	0106
0047	0061	0077	0138	0106
0054	0068	0086	0155	0106
0062	0076	0095	0172	0105
0071	0085	0105	0189	0106
0079	0093	0114	0205	0106
0091	0104	0127	0225	0106
0102	0114	0136	0240	0107
0114	0125	0147	0259	0109
0126	0136	0157	0271	0110
0143	0150	0170	0292	0113
0158	0164	0182	0308	0114
0174	0178	0192	0323	0116
0190	0191	0202	0333	0116
0203	0203	0211	0346	0119
0210	0210	0216	0352	0120
0212	0214	0219	0356	0120
0210	0216	0220	0362	0124
0205	0215	0221	0365	0126
0197	0210	0220	0365	0128
0185	0201	0213	0357	0127
0170	0189	0203	0343	0125
0158	0178	0193	0327	0121
0145	0166	0181	0307	0116
0134	0152	0168	0285	0111
0118	0139	0152	0258	0107
0105	0125	0137	0229	0106
0094	0113	0124	0202	0106
0083	0102	0110	0175	0105
0072	0090	0096	0148	0106
0066	0082	0087	0130	0106
0059	0075	0079	0114	0106
0054	0068	0072	0100	0106
0050	0063	0066	0088	0105
0046	0058	0061	0078	0105
0043	0054	0057	0069	0105
0041	0051	0054	0063	0106
0038	0049	0051	0056	0106
0036	0047	0047	0052	0105
0034	0047	0047	0048	0105
0033	0045	0045	0046	0105
0034	0044	0044	0045	0106
0032	0044	0044	0044	0105

.0001613 .0001399 .00008104 .00002212 .00002778

C EGLIN SITE 1 LOC C-3 LB.CT. 3.10.76 4.5 .2 60

.375 .708 1.625 2.625 3.625

60 .200 25000.0

0037	0060	0084	0118	0131
0038	0061	0086	0121	0133
0039	0062	0089	0127	0136
0041	0065	0091	0134	0139
0043	0067	0094	0140	0140
0044	0068	0097	0145	0144
0046	0071	0100	0153	0148
0049	0074	0104	0163	0151
0052	0078	0109	0177	0158
0055	0082	0113	0186	0162
0058	0086	0120	0198	0167
0063	0091	0126	0212	0172
0069	0099	0135	0230	0180
0075	0106	0143	0245	0186
0084	0115	0154	0268	0194
0094	0126	0167	0295	0204
0103	0136	0178	0317	0213
0113	0147	0190	0340	0222
0124	0158	0203	0362	0230
0136	0170	0217	0386	0238
0148	0182	0229	0407	0245
0161	0197	0242	0428	0252
0174	0210	0255	0450	0258
0189	0224	0268	0472	0265
0203	0235	0277	0485	0268
0218	0248	0288	0501	0274
0234	0259	0295	0513	0276
0245	0265	0299	0520	0279
0247	0264	0300	0521	0280
0242	0259	0298	0521	0279
0232	0248	0289	0503	0273
0217	0237	0278	0482	0264
0203	0222	0264	0454	0254
0189	0209	0251	0426	0242
0176	0196	0237	0399	0231
0164	0183	0222	0370	0218
0154	0173	0209	0343	0206
0142	0163	0197	0315	0195
0134	0153	0186	0295	0185
0125	0145	0175	0271	0176
0118	0138	0167	0252	0167
0111	0130	0158	0233	0159
0106	0126	0153	0221	0153
0101	0121	0147	0208	0148
0098	0118	0142	0198	0145
0094	0114	0138	0190	0142
0091	0111	0134	0181	0138
0088	0108	0131	0175	0136
0086	0107	0128	0171	0134
0085	0105	0126	0166	0133
0083	0103	0124	0163	0131
0082	0102	0124	0159	0131
0081	0100	0121	0157	0130
0079	0099	0121	0154	0129
0078	0099	0120	0153	0129
0078	0098	0119	0152	0129
0078	0098	0118	0151	0129
0077	0097	0119	0150	0129
0077	0097	0118	0150	0128
0077	0097	0118	0149	0128

.0001613 .0001[illegible] .00008104 .00002212 .00002778

C EGLIN SITE 1 LOC C-3 LD.CT. 3.10.76 4.0 .2 50
.33333 .66667 1.58333 2.58333 3.58333
50 .200 25000.0

0036	0059	0080	0108	0126
0038	0061	0083	0115	0129
0041	0064	0086	0123	0132
0044	0066	0091	0133	0136
0048	0071	0096	0145	0142
0052	0076	0102	0159	0148
0056	0080	0108	0172	0153
0063	0086	0116	0188	0160
0068	0092	0122	0202	0166
0075	0098	0131	0220	0174
0083	0106	0140	0237	0181
0091	0115	0151	0258	0189
0101	0126	0162	0280	0198
0114	0137	0175	0304	0208
0127	0151	0188	0328	0217
0144	0166	0203	0354	0228
0160	0181	0218	0380	0237
0177	0197	0232	0402	0245
0195	0211	0244	0425	0252
0210	0225	0256	0441	0259
0224	0238	0268	0464	0265
0233	0247	0275	0476	0268
0238	0255	0283	0490	0273
0232	0255	0287	0498	0275
0220	0248	0284	0497	0275
0204	0235	0273	0475	0269
0186	0218	0257	0448	0259
0169	0201	0241	0415	0246
0152	0183	0221	0375	0229
0135	0165	0199	0328	0210
0120	0149	0178	0289	0192
0107	0136	0163	0255	0179
0098	0125	0150	0226	0167
0089	0115	0137	0198	0153
0081	0106	0125	0169	0141
0075	0098	0116	0150	0132
0068	0091	0106	0129	0125
0064	0087	0102	0118	0120
0061	0083	0098	0109	0117
0057	0080	0095	0102	0115
0055	0078	0092	0098	0113
0054	0076	0090	0093	0111
0053	0075	0088	0091	0111
0052	0074	0088	0089	0111
0052	0074	0088	0089	0111
0051	0073	0087	0087	0111
0050	0072	0087	0087	0111
0050	0072	0088	0087	0111
0050	0072	0087	0087	0110
0050	0072	0087	0087	0111

.0001613 .0001399 .00008104 .00002212 .00002778

C EGLIN SITE 1 LOC C-4 LD.CT. 3.10.76 4.0 .2 61
.33333 .66667 1.58333 2.58333 3.58333
61 .200 25000.0

0034	0054	0075	0107	0117
0036	0055	0076	0111	0119
0037	0057	0077	0115	0120
0037	0058	0079	0120	0122
0039	0060	0080	0125	0124
0041	0062	0084	0131	0126
0044	0066	0088	0139	0129
0046	0069	0091	0147	0132
0049	0072	0096	0156	0135
0051	0075	0100	0165	0138
0055	0079	0103	0172	0140
0058	0083	0107	0181	0144
0061	0087	0112	0191	0147
0066	0092	0118	0203	0150
0071	0098	0123	0214	0155
0076	0103	0130	0226	0159
0081	0109	0136	0237	0161
0088	0116	0143	0250	0166
0094	0124	0149	0263	0170
0101	0132	0157	0277	0175
0110	0140	0166	0292	0178
0120	0151	0176	0309	0184
0130	0161	0185	0326	0188
0141	0172	0195	0343	0192
0153	0184	0206	0359	0197
0169	0199	0218	0378	0203
0185	0212	0228	0389	0205
0204	0227	0238	0400	0207
0224	0242	0248	0411	0209
0243	0255	0255	0419	0211
0258	0263	0263	0427	0213
0266	0266	0266	0428	0213
0266	0266	0266	0430	0213
0262	0265	0268	0436	0218
0256	0261	0266	0436	0218
0247	0254	0265	0432	0218
0234	0242	0255	0416	0213
0221	0230	0243	0393	0206
0204	0214	0228	0361	0192
0187	0199	0211	0325	0177
0170	0181	0194	0292	0163
0156	0168	0178	0259	0150
0142	0155	0163	0226	0136
0132	0144	0151	0202	0128
0122	0136	0142	0183	0122
0116	0130	0137	0171	0119
0112	0125	0132	0162	0117
0108	0121	0127	0155	0115
0105	0118	0124	0149	0115
0102	0116	0122	0144	0112
0099	0113	0119	0140	0112
0098	0112	0117	0136	0111
0097	0111	0116	0134	0110
0095	0110	0115	0132	0110
0094	0110	0115	0130	0111
0093	0108	0113	0129	0111
0091	0107	0112	0128	0110
0091	0105	0111	0127	0112
0090	0105	0110	0127	0112
0090	0104	0111	0126	0111
0089	0104	0111	0126	0111

.0001613 .0001399 .00008104 .00002212 .00002778

C EGLIN SITE 1 . LOC C-4 LD.CT. 3.10.76 4.5 .2 38
.375 .708 1.625 2.625 3.625
38 .200 25000.0

0025	0041	0061	0080	0104
0026	0042	0062	0081	0104
0027	0043	0063	0082	0103
0030	0045	0064	0086	0104
0034	0050	0071	0100	0104
0042	0058	0079	0121	0108
0051	0066	0090	0144	0115
0060	0076	0100	0166	0124
0070	0086	0110	0188	0131
0084	0100	0126	0217	0142
0099	0114	0139	0243	0152
0117	0133	0156	0274	0164
0137	0151	0173	0303	0173
0161	0173	0191	0332	0183
0186	0194	0207	0358	0191
0210	0213	0220	0376	0197
0227	0229	0230	0390	0200
0232	0234	0236	0394	0200
0229	0236	0237	0401	0203
0218	0232	0239	0408	0208
0202	0222	0236	0409	0210
0184	0204	0222	0386	0204
0166	0188	0207	0356	0194
0148	0172	0189	0321	0181
0131	0154	0172	0285	0167
0115	0138	0155	0249	0152
0102	0124	0139	0216	0140
0092	0111	0126	0186	0129
0081	0100	0113	0157	0119
0073	0091	0103	0136	0111
0068	0085	0095	0118	0107
0063	0078	0089	0104	0104
0057	0073	0082	0091	0103
0055	0070	0080	0084	0103
0053	0068	0077	0080	0103
0052	0066	0076	0078	0103
0050	0064	0075	0075	0103
0049	0064	0074	0075	0103

.0001613 .0001399 .00008104 .00002212 .00002778

C EGLIN SITE 1 LDC C-5 LD.CT. 3.10.76 4.5 .2 52
.375 .708 1.625 2.625 3.625
52 .200 25000.0

0036	0058	0087	0124	0141
0037	0059	0089	0130	0143
0040	0062	0092	0139	0148
0041	0065	0096	0148	0152
0044	0068	0101	0161	0159
0047	0072	0107	0175	0167
0052	0077	0113	0189	0175
0057	0085	0121	0209	0183
0068	0097	0136	0238	0196
0081	0112	0154	0273	0209
0092	0126	0169	0303	0221
0106	0141	0186	0335	0235
0121	0158	0204	0369	0245
0142	0181	0227	0408	0260
0164	0202	0246	0438	0269
0190	0228	0269	0472	0278
0214	0250	0288	0497	0285
0244	0277	0310	0531	0295
0270	0295	0323	0545	0297
0295	0312	0336	0561	0303
0313	0321	0340	0567	0306
0318	0322	0343	0566	0309
0313	0318	0345	0568	0314
0296	0304	0335	0568	0312
0279	0288	0322	0549	0307
0257	0267	0303	0514	0295
0238	0250	0286	0483	0282
0220	0233	0268	0447	0268
0204	0218	0253	0418	0258
0190	0204	0237	0390	0246
0178	0192	0223	0361	0234
0166	0181	0210	0333	0223
0156	0171	0197	0309	0210
0146	0161	0188	0289	0201
0138	0155	0178	0269	0193
0132	0148	0172	0253	0184
0127	0142	0164	0240	0178
0123	0139	0160	0231	0174
0118	0134	0156	0221	0170
0115	0132	0152	0212	0165
0112	0129	0148	0204	0161
0109	0127	0146	0199	0159
0108	0124	0144	0194	0156
0105	0123	0142	0189	0155
0104	0121	0141	0186	0153
0103	0121	0139	0184	0152
0102	0120	0139	0182	0152
0101	0119	0138	0181	0151
0101	0119	0138	0181	0151
0100	0119	0137	0180	0151
0101	0118	0137	0180	0152
0100	0117	0137	0180	0152

.0001613 .0001399 .00008104 .00002212 .00002778

```
C   EGLIN      SITE 1 .  LOC C-5   LD.CT.    3.10.76   5.0  .2   38
     .41667     .75      1.66667   2.66667   3.66667
   38      .200 25000.0
0033  0041  0056  0072  0160
0034  0044  0057  0075  0163
0036  0044  0059  0080  0165
0037  0046  0062  0088  0168
0040  0049  0065  0095  0172
0045  0054  0071  0108  0178
0049  0059  0077  0121  0183
0055  0065  0085  0138  0192
0065  0074  0095  0158  0201
0074  0084  0107  0181  0211
0088  0096  0122  0210  0223
0102  0110  0137  0241  0233
0122  0130  0156  0276  0246
0148  0153  0178  0313  0261
0175  0179  0202  0352  0275
0206  0206  0225  0386  0285
0238  0233  0245  0415  0294
0266  0256  0262  0436  0299
0282  0271  0273  0449  0302
0283  0279  0279  0461  0306
0272  0276  0282  0466  0309
0250  0263  0274  0458  0309
0226  0240  0254  0425  0300
0201  0217  0232  0388  0285
0175  0190  0207  0336  0265
0153  0168  0180  0284  0243
0128  0141  0151  0224  0220
0110  0120  0127  0181  0200
0098  0107  0112  0151  0185
0089  0098  0101  0125  0173
0081  0090  0092  0106  0164
0077  0085  0087  0094  0159
0075  0082  0084  0087  0156
0072  0080  0081  0083  0154
0071  0078  0079  0079  0152
0070  0077  0077  0077  0151
0069  0076  0076  0075  0149
0068  0075  0076  0073  0149
 .0001613    .0001399    .00008104   .00002212   .00002778
```

C EGLIN SITE 1 LOC A-4 LD. CT. 3.11.76 5.00 .2 41
.41667 .75 1.66667 2.66667 3.66667
41 .200 25000.0

0108	0126	0139	0159	0175
0110	0127	0139	0159	0175
0110	0128	0140	0162	0177
0111	0128	0142	0165	0178
0112	0129	0143	0169	0180
0113	0130	0146	0173	0182
0116	0133	0148	0179	0185
0117	0134	0150	0185	0187
0121	0137	0154	0194	0191
0124	0141	0159	0202	0195
0128	0144	0163	0212	0198
0132	0148	0168	0222	0202
0139	0154	0175	0234	0207
0146	0161	0182	0247	0211
0155	0169	0191	0263	0216
0166	0180	0202	0279	0221
0181	0193	0216	0302	0227
0200	0210	0232	0328	0235
0230	0235	0253	0355	0242
0267	0267	0278	0387	0249
0302	0295	0302	0414	0254
0338	0322	0323	0439	0260
0374	0354	0343	0463	0265
0391	0371	0354	0474	0267
0387	0375	0358	0480	0271
0363	0361	0349	0471	0268
0327	0333	0327	0439	0260
0290	0300	0300	0400	0249
0254	0267	0267	0349	0234
0222	0236	0236	0298	0215
0196	0210	0208	0244	0196
0178	0185	0190	0206	0182
0164	0171	0176	0176	0171
0157	0165	0168	0159	0166
0147	0157	0150	0141	0158
0145	0155	0147	0137	0158
0143	0154	0147	0136	0158
0142	0153	0146	0134	0157
0142	0152	0146	0134	0158
0142	0152	0145	0134	0158
0141	0150	0145	0135	0158

.0001613 .0001399 .00008104 .00002212 .00002778

```
C   EGLIN      SITE 2    LOC A-1   LD.CT.     3.11.76   3.0  .2    70
    .25        .58333    1.5        2.5        3.5
   70       .200 25000.0
0023  0055  0079  0104  0125
0027  0060  0082  0108  0129
0032  0067  0087  0115  0135
0038  0073  0092  0120  0140
0044  0079  0096  0125  0144
0051  0086  0100  0131  0150
0057  0094  0106  0136  0154
0065  0101  0111  0144  0160
0072  0111  0117  0150  0166
0082  0120  0123  0157  0173
0092  0130  0129  0165  0178
0102  0141  0136  0172  0185
0113  0152  0143  0179  0191
0125  0163  0150  0186  0196
0138  0175  0157  0194  0204
0151  0187  0164  0201  0209
0163  0198  0170  0208  0215
0176  0209  0176  0214  0220
0191  0221  0183  0221  0227
0202  0230  0188  0226  0230
0212  0239  0193  0230  0234
0220  0245  0198  0235  0238
0225  0251  0201  0237  0241
0227  0253  0202  0239  0244
0228  0254  0204  0241  0246
0229  0256  0205  0244  0248
0228  0255  0206  0246  0252
0227  0254  0208  0250  0260
0226  0253  0208  0252  0264
0225  0252  0202  0239  0244
0224  0251  0208  0253  0267
0220  0246  0205  0251  0268
0213  0240  0202  0248  0266
0206  0233  0198  0244  0264
0200  0228  0195  0241  0263
0193  0220  0190  0236  0259
0187  0214  0187  0232  0256
0181  0208  0183  0228  0253
0175  0203  0179  0224  0250
0170  0197  0175  0220  0246
0165  0192  0172  0217  0246
0160  0187  0169  0213  0243
0154  0181  0165  0208  0237
0146  0173  0160  0202  0231
0140  0167  0155  0196  0227
0133  0159  0150  0189  0220
0126  0153  0145  0184  0215
0119  0146  0140  0177  0209
0114  0140  0136  0173  0204
0108  0135  0131  0166  0197
0102  0129  0127  0161  0191
0098  0123  0123  0157  0184
0093  0119  0119  0152  0180
0090  0116  0116  0149  0177
0086  0114  0112  0144  0173
0083  0112  0111  0142  0171
0080  0109  0107  0140  0167
0079  0102  0108  0136  0162
0076  0102  0106  0134  0160
0075  0098  0104  0131  0156
0073  0097  0103  0131  0155
0071  0096  0102  0130  0154
0070  0095  0101  0127  0153
0069  0094  0100  0127  0152
0068  0092  0098  0125  0149
0066  0090  0097  0123  0147
0066  0089  0096  0122  0145
0065  0088  0095  0120  0142
0065  0086  0095  0119  0141
0064  0085  0094  0118  0141
 .000040325  .000034965  .00004052  .00002212  .00001111
```

```
[illegible]    N    SITE 2    LDC A-2    LD.CT.    3.11.76    4.5    .2    72
    [illegible]75    .708    1.625    2.625    3.625
    68    .200 25000.0
```

[illegible]	0154	0165	0190	0207
0141	0155	0166	0192	0208
0142	0155	0166	0193	0209
0144	0157	0167	0194	0211
0146	0158	0168	0195	0213
0146	0159	0169	0196	0215
0147	0160	0170	0197	0216
0150	0163	0172	0201	0219
0153	0165	0174	0203	0224
0155	0168	0176	0206	0227
0159	0172	0179	0210	0232
0163	0175	0182	0215	0237
0167	0180	0186	0219	0243
0174	0187	0190	0227	0252
0180	0193	0195	0233	0260
0189	0201	0201	0241	0271
0198	0211	0209	0250	0280
0209	0221	0217	0260	0292
0221	0232	0224	0269	0303
0235	0246	0234	0282	0315
0252	0261	0245	0294	0327
0269	0276	0255	0307	0340
0290	0295	0268	0321	0354
0310	0314	0280	0334	0367
0335	0336	0293	0348	0382
0357	0356	0305	0361	0392
0382	0377	0319	0373	0405
0399	0393	0328	0382	0412
0409	0406	0337	0391	0419
0416	0415	0342	0397	0425
0421	0416	0345	0401	0430
0425	0415	0350	0408	0438
0424	0412	0351	0412	0444
0412	0397	0348	0409	0444
0396	0376	0335	0398	0435
0376	0355	0323	0385	0424
0355	0331	0308	0367	0407
0334	0312	0295	0351	0390
0313	0291	0281	0333	0371
0295	0274	0268	0316	0351
0277	0259	0255	0299	0331
0261	0244	0244	0284	0313
0248	0232	0232	0269	0295
0236	0224	0222	0258	0279
0226	0217	0213	0247	0266
0218	0211	0206	0239	0256
0211	0205	0202	0232	0247
0205	0195	0201	0227	0241
0201	0191	0198	0222	0234
0197	0189	0196	0217	0229
0192	0186	0192	0214	0226
0189	0182	0190	0213	0223
0188	0180	0188	0210	0220
0187	0179	0187	0209	0219
0185	0177	0186	0208	0218
0183	0175	0185	0207	0217
0184	0181	0173	0206	0216

0184	0181	0173	0204	0214
0184	0180	0173	0204	0214
0183	0180	0171	0204	0214
0182	0179	0170	0204	0214
0182	0178	0170	0202	0213
0181	0178	0170	0203	0212
0182	0178	0169	0202	0212
0181	0177	0168	0202	0211
0180	0176	0167	0202	0212
0180	0176	0165	0202	0211
0180	0175	0164	0201	0211
.000040325	.000034965	.00004052	.00002212	.00001111

```
C   EGLIN      SITE-2    LOC C-1   LD.CT.    3.11.76   4.5  .2   70
     .375       .708     1.625     2.625     3.625
  70       .200 25000.0
0041  0057  0117  0141  0192
0041  0058  0117  0142  0194
0042  0059  0118  0142  0194
0043  0060  0118  0142  0194
0044  0060  0119  0144  0195
0045  0062  0119  0145  0197
0047  0062  0120  0146  0197
0049  0065  0121  0149  0200
0052  0067  0123  0150  0202
0054  0069  0125  0152  0204
0056  0072  0127  0156  0207
0060  0074  0130  0159  0210
0063  0079  0132  0162  0213
0067  0082  0134  0166  0217
0072  0087  0138  0169  0220
0078  0093  0142  0175  0225
0085  0099  0146  0179  0229
0092  0106  0151  0186  0235
0101  0113  0155  0190  0239
0111  0121  0162  0197  0244
0122  0131  0169  0203  0249
0136  0145  0177  0212  0257
0152  0159  0186  0220  0263
0171  0176  0196  0230  0271
0193  0195  0208  0239  0278
0220  0218  0220  0251  0286
0250  0243  0236  0261  0293
0284  0271  0251  0271  0299
0315  0295  0263  0278  0305
0348  0320  0277  0284  0306
0376  0341  0285  0288  0308
0402  0362  0294  0293  0308
0419  0378  0301  0296  0308
0427  0390  0307  0299  0311
0426  0398  0312  0304  0315
0418  0400  0313  0309  0320
0401  0391  0311  0309  0325
0368  0365  0297  0298  0320
0327  0330  0280  0284  0313
0297  0305  0267  0273  0306
0268  0279  0252  0260  0298
0242  0255  0238  0247  0289
0215  0229  0223  0234  0277
0193  0207  0210  0222  0268
0173  0189  0199  0210  0259
0159  0173  0188  0201  0249
0145  0159  0179  0191  0242
0134  0147  0171  0183  0234
0125  0137  0164  0175  0227
0115  0127  0157  0168  0220
0110  0120  0152  0163  0215
0103  0114  0147  0157  0210
0099  0108  0143  0153  0206
0095  0104  0139  0150  0204
0092  0101  0138  0148  0202
0088  0098  0135  0146  0200
0087  0096  0134  0145  0199
0085  0095  0134  0144  0199
0083  0093  0132  0143  0198
0083  0092  0132  0143  0198
0082  0091  0132  0142  0198
0080  0089  0132  0142  0198
0080  0089  0131  0142  0198
0079  0089  0130  0142  0198
0079  0087  0130  0141  0197
0079  0087  0130  0141  0197
0079  0087  0130  0141  0198
0077  0087  0130  0141  0197
0077  0087  0130  0142  0197
0076  0087  0130  0142  0198
 .000040325  .000034965  .00004052   .00002212   .00001111
```

```
C   EGLIN     SITE-2    LOC C-2   LD.CT.    3.11.76   4.0  .2   60
     .33333    .66667   1.58333   2.58333   3.58333
   60      .200 25000.0
0071  0087  0105  0130  0157
0073  0088  0106  0132  0160
0076  0090  0107  0132  0162
0077  0092  0109  0134  0163
0079  0094  0110  0136  0165
0081  0097  0112  0139  0168
0085  0100  0114  0141  0171
0089  0103  0117  0143  0173
0094  0109  0121  0148  0178
0100  0114  0124  0152  0181
0109  0122  0130  0158  0187
0117  0130  0136  0163  0192
0129  0142  0142  0170  0198
0140  0154  0152  0177  0205
0158  0169  0163  0187  0214
0174  0183  0172  0192  0218
0195  0203  0184  0202  0226
0216  0222  0197  0208  0232
0242  0247  0211  0218  0239
0269  0269  0225  0224  0244
0301  0297  0241  0232  0250
0330  0320  0253  0235  0251
0364  0345  0266  0240  0254
0390  0364  0276  0242  0256
0415  0384  0287  0246  0259
0429  0398  0292  0248  0262
0435  0407  0297  0251  0263
0428  0409  0299  0255  0268
0409  0400  0294  0257  0271
0382  0382  0283  0255  0270
0352  0357  0270  0251  0267
0320  0330  0253  0243  0260
0290  0301  0236  0235  0253
0264  0278  0219  0226  0246
0239  0250  0203  0216  0237
0212  0226  0186  0205  0228
0188  0199  0167  0193  0216
0168  0179  0154  0183  0208
0155  0167  0146  0175  0199
0148  0157  0140  0169  0194
0142  0151  0137  0163  0188
0137  0145  0133  0160  0184
0133  0142  0130  0157  0181
0131  0139  0129  0154  0178
0128  0136  0128  0152  0176
0126  0133  0126  0150  0174
0126  0133  0125  0150  0172
0125  0132  0125  0150  0172
0124  0130  0124  0148  0170
0124  0129  0123  0148  0169
0122  0129  0122  0146  0169
0121  0127  0121  0146  0168
0121  0127  0121  0145  0168
0121  0126  0120  0145  0167
0119  0126  0121  0145  0167
0118  0125  0121  0145  0167
0118  0125  0121  0145  0166
0117  0124  0121  0145  0166
0117  0125  0121  0144  0167
0117  0124  0121  0144  0166
 .000040325  .000034965  .00004052   .00002212   .00001111
```

AD-A047 161 NONCONTACT NONDESTRUCTIVE DETERMINATION OF PAVEMENT 4/4
DEFLECTION UNDER MOVING LOADS(U) PURDUE RESEARCH
FOUNDATION LAFAYETTE IN M E HARR ET AL AUG 77
UNCLASSIFIED FAA-RD-77-127 DOT-FA73WAI-361 F/G 13/2 NL

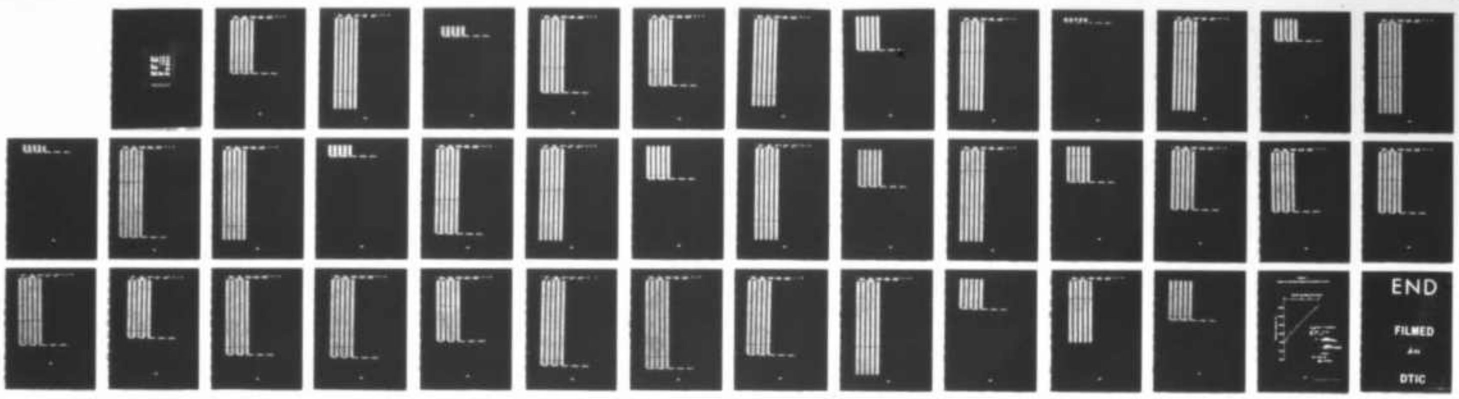

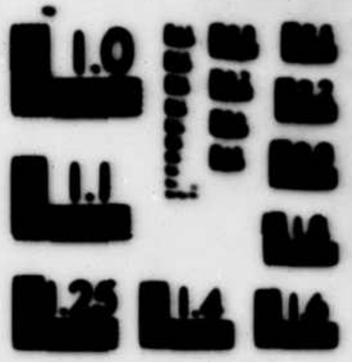

MICROCOPY RESOLUTION TEST CHART
NATIONAL BUREAU OF STANDARDS-1963-A

[illegible]

[illegible]

C [illegible] [illegible] [illegible] [illegible] [illegible] 4.0 .0 [illegible]

[illegible]

[illegible]

[illegible]

[illegible]

[illegible]

[illegible]

[illegible]

[illegible]

[illegible]

6 [illegible] [illegible] [illegible] [illegible] [illegible] 4.0 [illegible] 70

[illegible]

C [illegible] SITE 8 [illegible] [illegible] [illegible] [illegible] .2 [illegible]

[illegible]

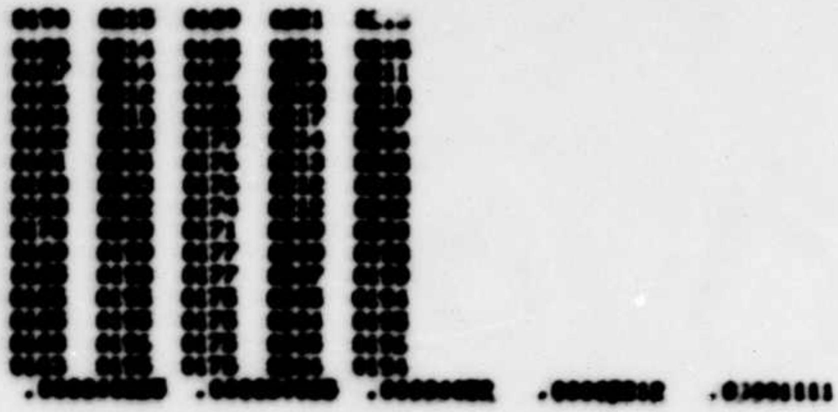

C EBL.1N SITE 2 LEC 0-8 LB.CT. 3.11.76 3.0 .2 73
.41667 .75 1.66667 2.66667 3.66667
73 .000 20000.0

[illegible]	0165	[illegible]	[illegible]	0167
[illegible]	[illegible]	[illegible]	[illegible]	0169
[illegible]	[illegible]	[illegible]	[illegible]	[illegible]
[illegible]	0165	[illegible]	[illegible]	0170
[illegible]	0167	[illegible]	[illegible]	0171
[illegible]	[illegible]	[illegible]	0147	0175
[illegible]	0110	[illegible]	0147	0177
[illegible]	0111	[illegible]	[illegible]	[illegible]
[illegible]	0113	[illegible]	[illegible]	[illegible]
[illegible]	0117	[illegible]	[illegible]	[illegible]
[illegible]	[illegible]	[illegible]	0164	[illegible]
[illegible]	[illegible]	[illegible]	0166	[illegible]
0113	[illegible]	[illegible]	0170	[illegible]
0119	0127	[illegible]	0177	[illegible]
[illegible]	[illegible]	[illegible]	[illegible]	[illegible]
[illegible]	[illegible]	[illegible]	[illegible]	[illegible]
[illegible]	[illegible]	0163	[illegible]	[illegible]
0151	[illegible]	[illegible]	[illegible]	[illegible]
[illegible]	0181	0179	[illegible]	[illegible]
0170	[illegible]	[illegible]	[illegible]	0271
[illegible]	0210	[illegible]	[illegible]	[illegible]
[illegible]	[illegible]	[illegible]	[illegible]	[illegible]
[illegible]	[illegible]	[illegible]	[illegible]	[illegible]
[illegible]	0270	[illegible]	[illegible]	[illegible]
[illegible]	0291	[illegible]	[illegible]	0301
0319	0310	[illegible]	[illegible]	[illegible]
[illegible]	[illegible]	[illegible]	0310	[illegible]
[illegible]	[illegible]	[illegible]	[illegible]	[illegible]
[illegible]	0381	[illegible]	[illegible]	[illegible]
[illegible]	[illegible]	[illegible]	[illegible]	[illegible]
[illegible]	0411	[illegible]	[illegible]	[illegible]
[illegible]	[illegible]	[illegible]	[illegible]	[illegible]
[illegible]	[illegible]	[illegible]	0441	[illegible]
[illegible]	[illegible]	[illegible]	[illegible]	[illegible]
[illegible]	[illegible]	[illegible]	[illegible]	[illegible]
[illegible]	[illegible]	[illegible]	[illegible]	[illegible]
[illegible]	[illegible]	[illegible]	[illegible]	[illegible]
[illegible]	0391	[illegible]	[illegible]	[illegible]
[illegible]	[illegible]	[illegible]	[illegible]	[illegible]
[illegible]	[illegible]	[illegible]	0310	0310
[illegible]	[illegible]	0272	[illegible]	[illegible]
0277	0311	[illegible]	[illegible]	[illegible]
[illegible]	[illegible]	[illegible]	0273	[illegible]
[illegible]	[illegible]	[illegible]	[illegible]	[illegible]
0219	[illegible]	0217	0241	[illegible]
0201	[illegible]	[illegible]	0227	[illegible]
[illegible]	0215	[illegible]	0211	[illegible]
0173	0201	[illegible]	0201	[illegible]
[illegible]	[illegible]	0174	0191	[illegible]
[illegible]	[illegible]	0167	[illegible]	0170
[illegible]	[illegible]	[illegible]	0172	0173
[illegible]	[illegible]	[illegible]	[illegible]	[illegible]
[illegible]	0157	[illegible]	0164	0167
[illegible]	[illegible]	[illegible]	[illegible]	0163
[illegible]	[illegible]	[illegible]	[illegible]	0164
[illegible]	0144	[illegible]	[illegible]	0161
[illegible]	[illegible]	[illegible]	[illegible]	[illegible]
0119	[illegible]	[illegible]	0151	0164
0118	[illegible]	[illegible]	[illegible]	0161
0117	[illegible]	[illegible]	[illegible]	[illegible]
0115	[illegible]	[illegible]	[illegible]	[illegible]
0114	[illegible]	[illegible]	[illegible]	[illegible]
0113	[illegible]	[illegible]	[illegible]	[illegible]
0111	[illegible]	[illegible]	0147	0161
0111	0131	[illegible]	[illegible]	[illegible]
[illegible]	0131	[illegible]	[illegible]	[illegible]
0110	[illegible]	[illegible]	[illegible]	[illegible]
[illegible]	[illegible]	[illegible]	[illegible]	[illegible]

[illegible]

C [illegible] [illegible] [illegible] [illegible] [illegible] 4.0 .8 [illegible]

[illegible]

.[illegible] .[illegible] .[illegible] .[illegible] .[illegible]111

C [illegible] [illegible] [illegible] [illegible] [illegible] 4.3 .8 70

[illegible]

[illegible]

[illegible]	[illegible]	[illegible]	[illegible]	[illegible]

[illegible]

[illegible]

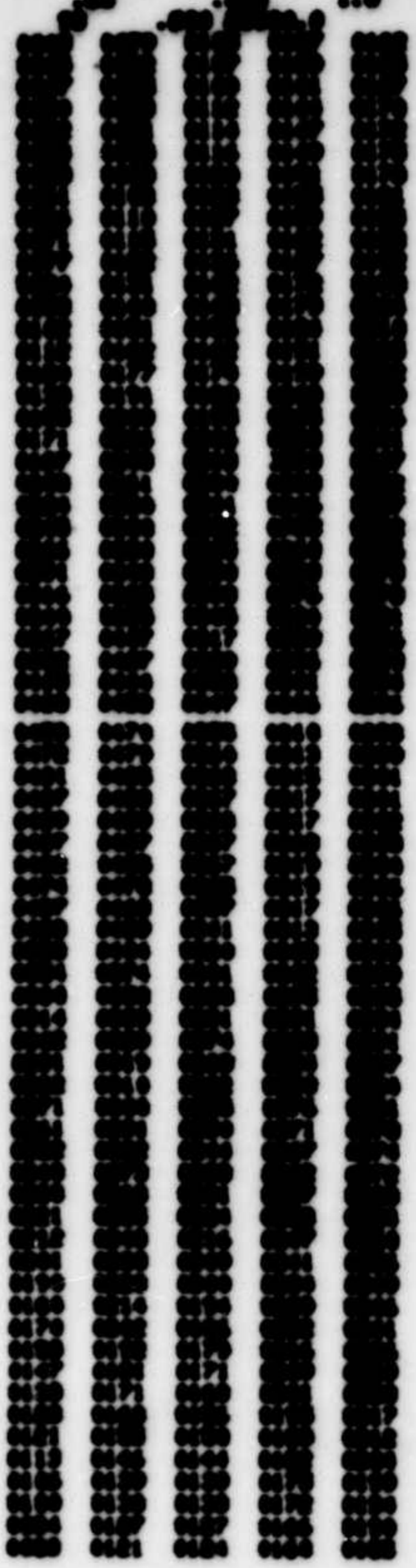

[illegible]

[illegible]

[illegible]

[illegible]

C [illegible] [illegible] [illegible] [illegible] [illegible] 4.0 .8 90

[illegible] 1.[illegible] 2.[illegible] 3.[illegible]

[illegible]

[illegible]	[illegible]	[illegible]	[illegible]	[illegible]

[illegible] [illegible] [illegible] [illegible] [illegible]

C [illegible]

[illegible]

C [illegible] SITE 1 [illegible] [illegible] [illegible] 7.0 .8 [illegible]

[illegible]

.[illegible]613 .[illegible] .[illegible] .[illegible] .[illegible]

C [illegible] SITE 1 [illegible] [illegible] CT. [illegible] 6.5 .8 48
[illegible] [illegible] [illegible] [illegible] [illegible]
[illegible] [illegible] [illegible]

[illegible]

.[illegible]613 .[illegible] .[illegible] .[illegible] .[illegible]

C [illegible].IN SITE 1 [illegible] LB. CT. [illegible] [illegible] .[illegible] [illegible]
.[illegible] .[illegible] 1.7[illegible] [illegible] [illegible]
[illegible] .[illegible] [illegible]

[illegible]	[illegible]	[illegible]	0113	[illegible]
[illegible]	[illegible]	[illegible]	0110	[illegible]
[illegible]	[illegible]	[illegible]	[illegible]	[illegible]
[illegible]	[illegible]	[illegible]	[illegible]	[illegible]
[illegible]	[illegible]	[illegible]	[illegible]	[illegible]
[illegible]	[illegible]	[illegible]	[illegible]	[illegible]
[illegible]	[illegible]	0101	[illegible]	0147
[illegible]	[illegible]	0107	0171	[illegible]
[illegible]	[illegible]	0114	[illegible]	[illegible]
[illegible]	[illegible]	[illegible]	[illegible]	0161
[illegible]	[illegible]	[illegible]	[illegible]	[illegible]
[illegible]	0116	[illegible]	[illegible]	[illegible]
[illegible]	[illegible]	[illegible]	[illegible]	[illegible]
[illegible]	[illegible]	[illegible]	[illegible]	[illegible]
[illegible]	0167	[illegible]	[illegible]	[illegible]
[illegible]	0191	[illegible]	[illegible]	[illegible]
[illegible]	[illegible]	[illegible]	[illegible]	[illegible]
[illegible]	[illegible]	[illegible]	[illegible]	[illegible]
[illegible]	[illegible]	[illegible]	[illegible]	[illegible]
[illegible]	[illegible]	[illegible]	[illegible]	[illegible]
0011	0013	[illegible]	[illegible]	[illegible]
[illegible]	[illegible]	[illegible]	[illegible]	[illegible]
[illegible]	[illegible]	[illegible]	[illegible]	[illegible]
[illegible]	[illegible]	[illegible]	[illegible]	[illegible]
[illegible]	[illegible]	[illegible]	[illegible]	[illegible]
[illegible]	[illegible]	[illegible]	0171	[illegible]
[illegible]	[illegible]	[illegible]	[illegible]	[illegible]
[illegible]	[illegible]	[illegible]	[illegible]	[illegible]
[illegible]	[illegible]	[illegible]	[illegible]	[illegible]
[illegible]	[illegible]	[illegible]	[illegible]	[illegible]
[illegible]	[illegible]	[illegible]	[illegible]	[illegible]
[illegible]	[illegible]	[illegible]	[illegible]	0194
[illegible]	[illegible]	[illegible]	[illegible]	[illegible]
0177	[illegible]	0181	[illegible]	[illegible]
[illegible]	[illegible]	[illegible]	[illegible]	[illegible]
[illegible]	[illegible]	[illegible]	[illegible]	[illegible]
[illegible]	[illegible]	[illegible]	[illegible]	[illegible]
[illegible]	0141	[illegible]	[illegible]	[illegible]
0131	[illegible]	[illegible]	[illegible]	[illegible]
[illegible]	[illegible]	0131	0101	0144
[illegible]	0130	[illegible]	[illegible]	[illegible]
0119	[illegible]	[illegible]	[illegible]	[illegible]
0117	[illegible]	[illegible]	[illegible]	[illegible]
0114	[illegible]	[illegible]	[illegible]	[illegible]
0113	[illegible]	0110	[illegible]	[illegible]
0111	0110	0116	[illegible]	[illegible]
[illegible]	0117	[illegible]	[illegible]	[illegible]
[illegible]	0116	0114	[illegible]	[illegible]
[illegible]	0115	0114	[illegible]	0131
[illegible]	0115	0113	[illegible]	0131

.[illegible]613 .[illegible] .[illegible] .[illegible] .[illegible]

C [illegible] [illegible] [illegible] [illegible] CT. [illegible] [illegible] [illegible] [illegible]

[illegible]

C [illegible] [illegible] [illegible] [illegible] [illegible] [illegible] [illegible] [illegible]

[illegible]

.[illegible] .[illegible] .[illegible] .[illegible] .[illegible]

C [illegible]

[illegible]

.[illegible]613 .[illegible] .[illegible] .[illegible] .[illegible]

[illegible]

C [illegible] [illegible] [illegible] [illegible] [illegible] [illegible] [illegible] [illegible]

[illegible]

[illegible] [illegible] [illegible] [illegible] [illegible]

C [illegible] [illegible] [illegible] [illegible] [illegible] [illegible] 0.0 [illegible]
[illegible] .000 [illegible]

[illegible]	[illegible]	[illegible]	[illegible]	[illegible]

.[illegible] .[illegible] .[illegible] .[illegible] .[illegible]

C [illegible] SITE [illegible] [illegible] [illegible] [illegible] 4.0 .8 [illegible]
.[illegible] .[illegible] 1.[illegible] 2.[illegible] 3.[illegible]

[illegible]	[illegible]	[illegible]	[illegible]	[illegible]

.[illegible] .[illegible] .[illegible] .[illegible] .[illegible]

[illegible]

[illegible]	[illegible]	[illegible]	[illegible]	[illegible]

C [illegible] [illegible] [illegible] [illegible] [illegible] 4.0 .8 [illegible]

[illegible]

[illegible]

C [illegible] [illegible] [illegible] [illegible] [illegible] [illegible] [illegible] [illegible]

[illegible]

[illegible]	[illegible]	[illegible]	[illegible]	[illegible]
[illegible]	[illegible]	[illegible]	[illegible]	[illegible]
[illegible]	[illegible]	[illegible]	[illegible]	[illegible]
[illegible]	[illegible]	[illegible]	[illegible]	[illegible]
[illegible]	[illegible]	[illegible]	[illegible]	[illegible]
[illegible]	0191	[illegible]	[illegible]	[illegible]
[illegible]	0177	[illegible]	[illegible]	[illegible]
[illegible]	[illegible]	[illegible]	[illegible]	[illegible]
[illegible]	[illegible]	[illegible]	[illegible]	[illegible]
[illegible]	[illegible]	[illegible]	0177	[illegible]
[illegible]	0141	[illegible]	[illegible]	[illegible]
0121	0137	[illegible]	0169	[illegible]
0117	[illegible]	[illegible]	0167	[illegible]
0114	[illegible]	0141	[illegible]	[illegible]
[illegible]	[illegible]	[illegible]	0164	[illegible]
[illegible]	[illegible]	[illegible]	0164	[illegible]
[illegible]	[illegible]	[illegible]	0163	[illegible]
[illegible]	[illegible]	[illegible]	0163	[illegible]
[illegible]	[illegible]	[illegible]	0163	[illegible]
[illegible]	[illegible]	[illegible]	0163	[illegible]
[illegible]	[illegible]	0137	0163	[illegible]
[illegible]	[illegible]	0137	0163	[illegible]
[illegible]	0121	0137	0163	[illegible]
[illegible]	0121	0137	[illegible]	[illegible]
[illegible]	0121	0137	[illegible]	[illegible]
[illegible]	[illegible]	[illegible]	[illegible]	[illegible]
0101	[illegible]	[illegible]	0161	[illegible]
0101	0119	[illegible]	[illegible]	[illegible]
[illegible]	0119	[illegible]	[illegible]	[illegible]
.[illegible]	.[illegible]	.[illegible]	.[illegible]	.[illegible]

APPENDIX E

EXAMPLE OF SIMPLIFIED PROCEDURE FOR ESTIMATING $\bar{E}$ AND CBR

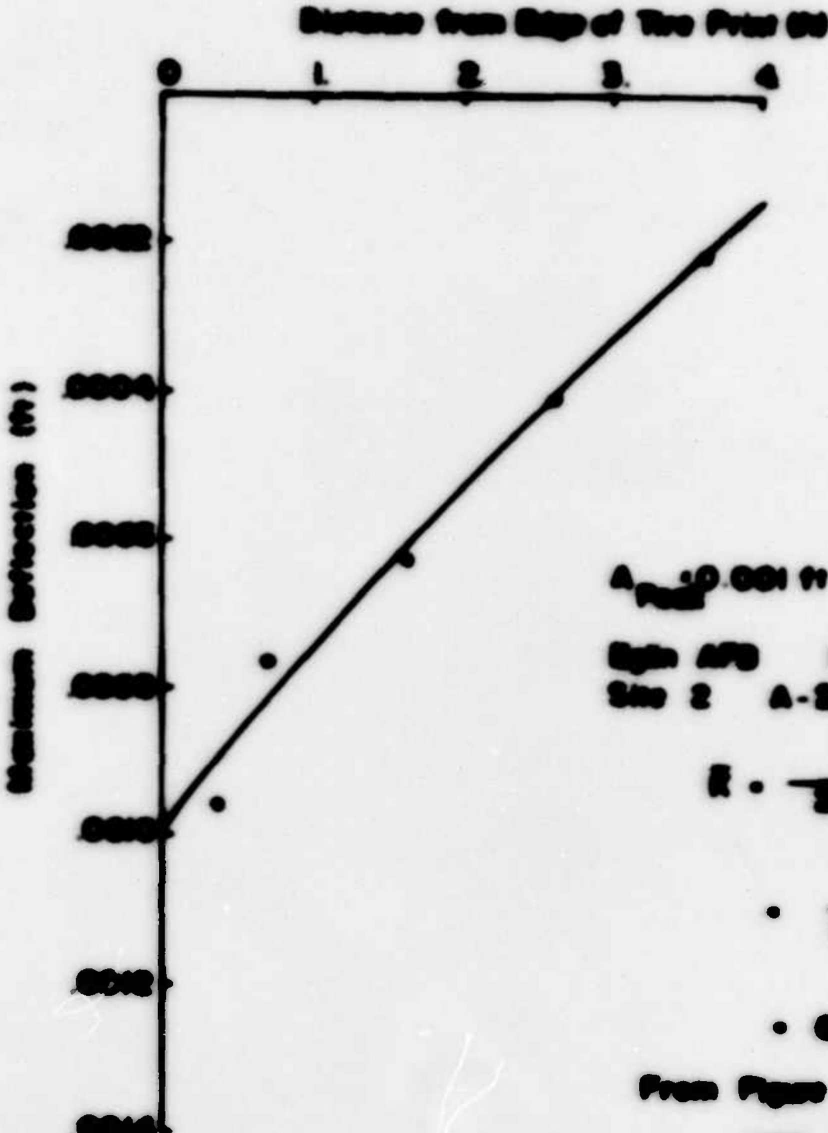

A_{Peak} = 0.001 ft = 0.01200 in

Eglin AFB D = 17 in

Site 2 A-2

$\bar{E}$ = [illegible]

= [illegible] / [illegible] + 177 [illegible] (0.[illegible])

= 646 psi

From Figure 60

CBR = 72 percent

U.S. GOVERNMENT PRINTING OFFICE [illegible]

END

FILMED

2-86

DTIC